Modulation of human macrophage activity by mRNA-mediated genetic engineering

Hanieh Moradian

Kumulative Dissertation

zur Erlangung des akademischen Grades
"Doktor der Naturwissenschaften"
(Dr. rer. nat.)
in der Wissenschaftsdisziplin
"Materialien in den Lebenswissenschaften"

eingereicht an der
Mathematisch-Naturwissenschaftlichen Fakultät
Institut für Biochemie und Biologie
der Universität Potsdam
und
Institut für aktive Polymere
Helmholtz-Zentrum Hereon, Teltow

Hauptbetreuer:	Prof. Dr. Andreas Lendlein *Universität Potsdam*
Zweitbetreuerin:	Prof. Dr. Katja Hanack *Universität Potsdam*
Mentor:	Dr. Manfred Gossen *Helmholtz Zentrum Hereon*
Gutachter:	Prof. Dr. Andreas Lendlein *Universität Potsdam* Prof. Dr. Martina Seifert *Charité – Universitätsmedizin Berlin- Institute of Medical Immunology* Dr. Rainer Glauben *Charité - Universitätsmedizin Berlin*

Ort und Tag der Disputation: Potsdam, 11.03.2022

Statement of Authenticity

I, Hanieh Moradian, formally submit the cumulative dissertation entitled "**Modulation of human macrophage activity by mRNA-mediated genetic engineering**" to the Institute of Biochemistry and Biology, Faculty of Science of the University of Potsdam, Germany, for the acquirement of the academic degree of Doctor of Natural Sciences (Dr. ret. nat.) in the discipline "Materials in Life Sciences".

I hereby declare that this cumulative thesis is my own original work based on the research performed at *Helmholtz-Zentrum Hereon, Institute of Active polymers* in Teltow, Germany, from July 2016 to September 2021 under the supervision of Prof. Dr. Andreas Lendlein and Prof. Dr. Katja Hanack. To the best of my knowledge and belief, this dissertation contains no previously published material by another person, except where due reference is made in thesis itself. No other section of this thesis has been previously submitted in the support of any other degree to another university or institute. Any contribution made by other colleagues to this research is explicitly acknowledged in the dissertation.

Hanieh Moradian

Acknowledgements

Table of contents

List of figures

Abbreviations and symbols

ARCA	Anti-reverse cap analogs
CleanCap (AG)	Clean Cap structure starting with Adenosine and Guanosine
DCs	Dendritic cells
DEPC	Diethyl pyrocarbonate
dsRNA	Double strand RNA
EDTA	Ethylenediaminetetraacetic acid
FBR	Foreign body reaction
FBGCs	Foreign body giant cells
GOI	Gene of interest
HPLC	High-performance liquid chromatography
IL-6	Interleukin-6
IFN	Interferon
IRF	Interferon regulatory factor
IVT-mRNA	In vitro transcribed mRNA
iPCs	Induced pluripotent stem cells
LipoMM	Lipofectamine messenger max
MDA-5	Melanoma differentiation-associated protein 5
MCs	Monocytes
MΦs	Macrophages
ORF	Open reading frame
pDNA	Plasmid DNA
PCR	Polymerase chain reaction
PKR	Protein kinase R
PRRs	Pattern recognition receptors
RIG-I	Retinoic acid-inducible gene I
rNTPs	Ribonucleotides
ROS	Reactive oxygen species
T7RNAP	T7 RNA polymerase
TNF-α	Tumor necrotic factor-α
UTR	Untranslated region
Ψ	Pseudouridine
5meC	5-methylcytidine
5moU	5-methoxyurdine
me^{1}Ψ	N1-methyl-pseudouridine
VLE	Very low endotoxin

Abstract

Macrophages play an integral role for the innate immune system. It is critically important for basic research and therapeutic applications to find approaches to potentially modulate their function as the first line of defense. Transient genetic engineering via delivery of synthetic mRNA can serve for such purposes as a robust, reliable and safe technology to modulate macrophage functions. However, a major drawback particularly in the transfection of sensitive immune cells such as macrophages is the immunogenicity of exogenous IVT-mRNAs. Consequently, the direct modulation of human macrophage activity by mRNA-mediated genetic engineering was the aim of this work. The synthetic mRNA can instruct macrophages to synthesize specific target proteins, which can steer macrophage activity in a tailored fashion. Thus, the focus of this dissertation was to identify parameters triggering unwanted immune activation of macrophages, and to find approaches to minimize such effects. When comparing different carrier types as well as mRNA chemistries, the latter had unequivocally a more pronounced impact on activation of human macrophages and monocytes. Exploratory investigations revealed that the choice of nucleoside chemistry, particularly of modified uridine, plays a crucial role for IVT-mRNA-induced immune activation, in a dose-dependent fashion. Additionally, the contribution of the various 5' cap structures tested was only minor. Moreover, to address the technical aspects of the delivery of multiple genes as often mandatory for advanced gene delivery studies, two different strategies of payload design were investigated, namely "bicistronic" delivery and "monocistronic" co-delivery. The side-by-side comparison of mRNA co-delivery via a bicistronic design (two genes, one mRNA) with a monocistronic design (two gene, two mRNAs) unexpectedly revealed that, despite the intrinsic equimolar nature of the bicistronic approach, it was outperformed by the monocistronic approach in terms of reliable co-expression when quantified on the single cell level. Overall, the incorporation of chemical modifications into IVT-mRNA by using respective building blocks, primarily with the aim to minimize immune activation as exemplified in this thesis, has the potential to facilitate the selection of the proper mRNA chemistry to address specific biological and clinical challenges. The technological aspects of gene delivery evaluated and validated by the quantitative methods allowed us to shed light on crucial process parameters and mRNA design criteria, required for reliable co-expression schemes of IVT-mRNA delivery.

Zusammenfassung

Makrophagen spielen eine wesentliche Rolle für das angeborene (innate) Immunsystem. Sowohl für die Grundlagenforschung sowie als auch für therapeutische Anwendungen ist es von größter Wichtigkeit, Möglichkeiten zu finden, die Funktion von Makrophagen als erstem Abwehrmechanismus des Immunsystems zu modulieren. Transientes Genetic Engineering mittels synthetischer mRNA kann hierbei als robuste, zuverlässige und sichere Technologie zur Modulation des Zellverhaltens zu dienen. Eine besondere Herausforderung ist jedoch die Immunogenität exogener IVT-mRNAs, insbesondere für sensitive Immunzellen wie Makrophagen. Die direkte Modulation der Zellaktivität von humanen Makrophagen durch mRNA-vermitteltes Genetic Engineering ist das Ziel dieser Arbeit. Mit synthetischer mRNA lassen sich Makrophagen so instruieren, dass sie spezifische Zielproteine produzieren, um die Zellaktivität bedarfsgerecht zu steuern. Der Hauptfokus dieser Dissertation war die Identifikation der Parameter, die eine aus dem IVT-mRNA Transfer resultierende, unerwünschten Zellaktivierung bei Makrophagen auslösen und Ansätze zu finden, um diese zu minimieren. Beim Vergleich verschiedener Transfektionsagenzien und Nukleinsäurekompositionen der mRNA zeigte sich, dass letztere einen weitaus eindeutigeren Effekt auf die Zellaktivierung von humanen Makrophagen und Monozyten haben. Explorative Untersuchungen ergaben, dass die Wahl der Nukleosidchemie, insbesondere des modifizierten Uridins, eine entscheidende Rolle für diese dosisabhängige Immunaktivierung durch IVT-mRNA spielt. Im Vergleich dazu war der Einfluss der verschiedenen getesteten 5'-Cap-Strukturen nur geringfügig. Der Transfer mehrerer Gene in Zellen ist für komplexe Studien und Anwendungen oft zwingend erforderlich. Hierzu wurden die technischen Aspekte von zwei verschiedenen Strategien untersucht, nämlich die "bicistronische" Transfektion und die "monocistronische" Co-Transfektion. Der direkte Vergleich von mRNA-Co-Transfer über ein bicistronisches Design (zwei Gene, eine mRNA) mit einem monocistronischen Design (zwei Gene, zwei mRNAs) ergab überraschenderweise, dass trotz der intrinsischen äquimolaren Natur des bicistronischen Ansatzes dieser dem monocistronische Ansatz in Bezug auf eine zuverlässige Koexpression bei der Quantifizierung auf Einzelzellebene unterlegen war. Wie in dieser Arbeit gezeigt kann die Einbeziehung geeigneter chemischer Modifikationen in IVT-mRNA durch die Verwendung der entsprechenden Bausteine bei der Synthese zur Bewältigung spezifischer biologischer und klinischer Herausforderungen beitragen, in erster Linie durch die Minimierung der Immunaktivierung. Die Evaluation und Validierung technologischer Aspekte des Gentransfers durch quantitative Methoden ermöglichten uns auch entscheidende Prozessparameter und Kriterien für das mRNA-Design zu identifizieren, die für eine zuverlässige Co-Expression von Genen nach IVT-mRNA Transfektion erforderlich sind.

Chapter 1: Introduction

An overview of the scientific background of the thesis is presented in this chapter, organized in the two main parts. First part describes the immunomodulation by macrophages, which was the primary motivation of this study. The second part elaborates genetic engineering by *in vitro* transcribed messenger RNA (IVT-mRNA) as the envisaged scientific concept of this work in more detail.

1.1 Immunomodulation by macrophages

1.1.1 Distinct features of macrophages desired for immunomodulation

Innate and adaptive immunity are two arms of the immune system to protect the organism against exogenous pathogens, and potential endogenous malfunctions [1]. Innate immunity responds promptly, and is nonspecifically directed against a broad range of pathogens. However, adaptive immunity has more versatile and complex means, which can theoretically adapt and specifically respond to any danger signal or invading pathogens[2]. Despite the innate immune system is often incapable of complete eradication of an infection, it has crucial roles in initiation and regulation of adaptive immunity [3, 4]. Moreover, in some cases cells of the innate immune system are recruited as effector means by activated lymphocytes, such as T helper cells, to eradicate the source of infection, e.g. by phagocytosis [5]. Therefore, the immune homeostasis is maintained by active interplay of both innate and adaptive immune responses [6]. Among the different innate immune cells, macrophages and neutrophils are the first line of defense, which encounter the pathogens and immediately initiate the immune response [5]. Compared to neutrophils, which have a short half-life of a few hours, macrophages can live days to weeks after activation, or even permanently reside in tissues in case of tissue macrophages[7-9]. Besides maintaining homeostasis by clearance of senescent or dead cells in sterile inflammation [10], tissue resident macrophages present antigens and release chemokines and cytokines to attract other leukocytes from bloodstream to the site of infection upon pathogen recognition [11]. Examples for tissue macrophages are microglial cells in brain tissue, Kupffer cells in liver, alveolar cells in lung, and Langerhans cells in skin tissue [12]. While tissue macrophages originate from fetal precursor cells, hematopoietic-derived circulating monocytes differentiate to macrophages "on-demand", after recruitment/migration to the site of infection by inflammatory chemokines [11]. They play a key role both in further development of immune response and at later stages to resolve the immune response and promote healing process and

tissue repair [9]. To accommodate this wide range of functions, macrophages develop distinct phenotypes depending on microenvironmental stimuli, each delineated by unique sets of surface markers and secretome characteristics [13-15]. This phenotypical and also morphological heterogeneity is a prominent feature of macrophages, which appears not only progressively over different stages of development, but is also visible within a single population at a given time [13, 16-18] (Figure 1.1). Moreover, given that macrophages are not terminally differentiated, they can dynamically respond to microenvironmental cues, a feature known as plasticity [19]. Exploiting this character in immunomodulation studies, macrophages can be deliberately polarized to an intended phenotype by providing the corresponding milieu or stimuli [17, 20].
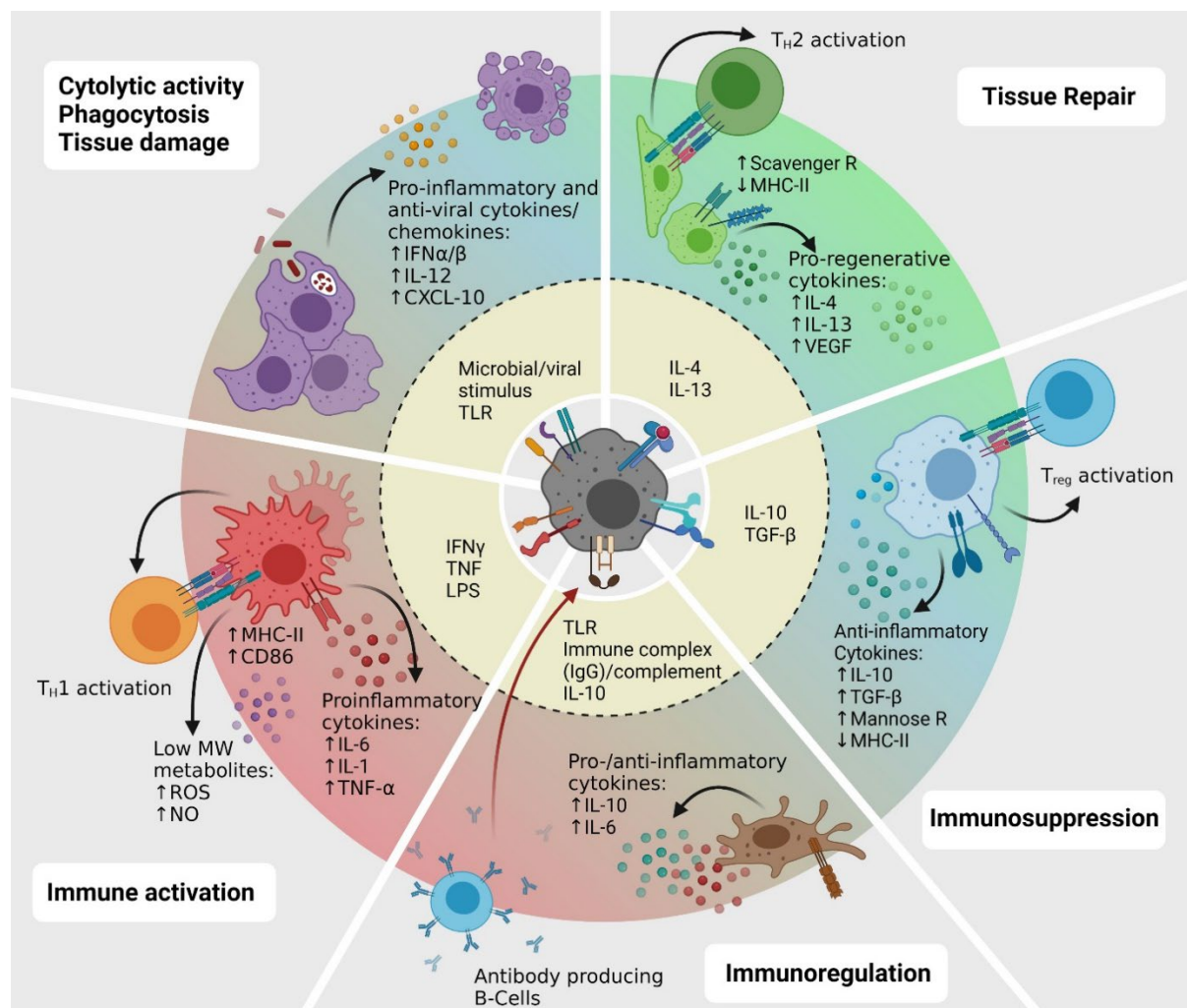
Figure 1.1. Different features and functions of macrophages

The spectrum of macrophages features and functions are illustrated. M0 macrophage are equipped with different sorts of receptors enabling them to response to different microenvironmental cues, shown in dark gray color in the center. The second circle illustrates various stimulation factors, which direct macrophage response to the specific pattern, i.e. unique pattern of cytokine, chemokine and biological marker production. The ultimate function for each phenotype is written in the white box in the outermost rectangle. These versatile functions enable macrophages to play a key role in many biological processes such as FBR to biomaterials; see text for more details.

1.1.2 Macrophage polarization for regulation of foreign body response

The macrophage polarization paradigm was traditionally defined by two main phenotypes, including classically activated macrophages, and alternatively activated macrophages, referred to as M1 and M2 phenotypes, respectively [16]. While M1 macrophages promote inflammation by producing pro-inflammatory surface markers, cytokines and chemokines, as well as proteolytic enzymes and reactive oxygen species (ROS), M2 macrophages reduce inflammation and promote tissue remodeling and healing processes [16, 17, 21, 22]. Despite being initially accepted by researchers in the immunology field, soon it became evident that macrophages versatility is beyond the two defined phenotypes, and instead a continuum spectrum of subtypes, identified by distinct sets of features and functions, which present macrophages heterogeneity more precisely [23-25]. However, the M1/M2 model was taken up by numerous studies in other fields, as a simplified classification to investigate macrophages phenotype switching, i.e., polarization, in response to different stimulation methods. One prominent example is studying the effect of macrophage polarization, i.e. M1/M2 balance, on foreign body reaction (FBR) to biomaterials [26-28], which is elaborated on in more detail in the following.

The foreign body reaction consists of five main phases, including protein absorption, acute inflammation, chronic inflammation, formation of foreign body giant cells (FBGCs) and fibrous capsule formation [29-32]. In the first phase, a provisional matrix composed of fibrin, complement proteins, and platelets are deposited on surface of biomaterial. The complement proteins, e.g. C3a, and C5a play as strong chemoattractant for phagocytic cells. Mast cells and poly-morphnuclear leukocyte are recruited to the implant interface during acute inflammation phase, which usually lasts hours to few days [31]. Next, monocytes migrate to the site of injury and differentiate to macrophages, and play the major role in chronic inflammation phase. The macrophage phenotype depends on the type of cytokines secreted by other leukocytes nested on surface of implant. For instance, IL-4 and IL-13 cytokines secreted by mast cells can differentiate macrophages to M2 phenotype. Subsequently, anti-inflammatory macrophages promote tissue remodeling and later the vascularization by production of matrix metalloproteinase enzymes (MMPs) and secretion of pro-angiogenic cytokines such as VEGF[33, 34]. In contrast, pro-inflammatory macrophage can cause degradation of biomaterial by release of degradative enzymes and/or reactive oxygen species (ROS) at biomaterial interface [30]. The chronic inflammation takes 2-5 weeks in context of implants. If macrophages fail to phagocyte the implant biomaterial, they tend to fuse together and form multinucleated giant cells, referred to as foreign body giant cells (FBGS). These cellular structures can be up to several hundred µm large encompassing dozens of nuclei, adhering to implant surface. The formation of fibrous

capsule is the ultimate phase in FBR, which involves fibrotic collagenous capsule around the biomaterial isolating it from the rest of host microenvironment [29, 31] (Figure 1.2)
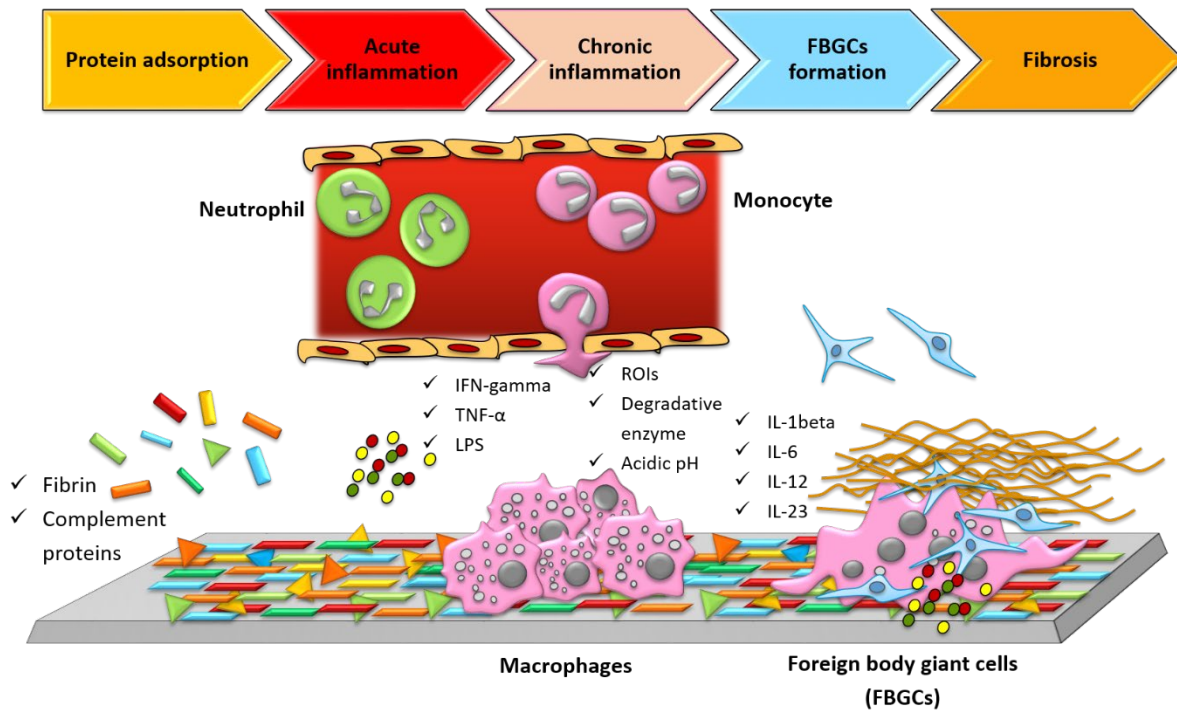
Figure 1.2 Schematic representation of the five phases in foreign body response to implants
The gray substrate is a simplified illustration of a biomaterial surface.

Given that macrophages are the predominant and key cell type orchestrating FBR [35], approaches to induce anti-inflammatory functions are of utmost importance for modulation of immune response to support host-implant integration [36]. Of note, the goal of such studies is not necessarily to completely avoid the pro-inflammatory phenotype, but to induce to the anti-inflammatory capacities at proper time, and to have the best pro/anti-inflammatory balance supporting the healing and remodeling process [30]. For instance, Brown et al. evaluated the FBR to several scaffolds from natural ECM, and found more constructive remodeling for samples with higher M2 to M1 ratio [37].

By exploiting the active interplay between implant and host microenvironment, the modulation of macrophage polarization by changing the physical or chemical properties at biomaterials-tissue interface has been studied [36, 38-42]. For physical features such as surface topography, mechanical properties, porosity, and wettability, effects on macrophage responses have been shown [27, 43, 44]. For instance, it was reported that surface topography had an influence on macrophages morphology and cytokine secretion *in vitro* and cell adhesion *in vivo* [45]. By

evaluation of poly(ε-caprolactone) (PCL), polylactide (PLA) and poly(dimethyl siloxane) (PDMS) substrates with imprinted rectangular patterns of different dimensions, Chen and colleagues found reduced macrophage adhesion on 2 µm grating compared to planar controls [26, 45]. Likewise, surface chemistry [46], e.g. type and density of functional groups [47], functionalization with specific ligands [48], growth factors [49] or other signaling molecules [50, 51] affect foreign body response. More precisely, they can affect the primary protein absorption on the surface, the macrophage polarization and consequently the type of immune response, i.e. pro-inflammatory vs. pro-regenerative response. For example, hydrophilic biomaterials such as polyesthers, e.g. poly(ethylene glycol) (PEG), and polyhydroxyethylmethacrylate (poly(HEMA)) [52], were presumed to reduce protein absorption [53] and dampen the immune activation by production of an aqueous layer on biomaterials surface [54]. The *in vivo* evaluation, however, invalidated this assumption, and macrophages, as main player of inflammatory response, were found to secrete higher level of pro-inflammatory cytokines in contact with neutral or hydrophilic surfaces compared to hydrophobic or charged surfaces[55]. Sustained release of anti-inflammatory cytokines such as IL-4 [56], and IL-10 [57] from biomaterials is another possibility for immunomodulation mediated by macrophages [38]. Given the dynamics of host-implant interaction and the progressive changes in both biomaterial's properties and biological milieu, finding robust biomaterial-based strategies to regulate macrophages phenotype and function and eventual immune response is challenging [38]. Alternatively, also to complement those approaches, biological tools such as genetic engineering can be harnessed to modulate macrophages response, as elaborated in the next section.

1.1.3 Modulation of macrophage response by genetic engineering

Macrophages can polarize to pro-inflammatory or anti-inflammatory phenotypes in response to the corresponding stimuli [11]. While the anti-inflammatory features are preferred for organ transplantation [58], modulation of FBR and autoimmune diseases, the pro-inflammatory capacities are useful in tumor microenvironments mediating tumor rejection [59, 60] or for vaccination approaches serving as adjuvant. The biological cues to shift the macrophages to either direction can be provided either by soluble mediators such as cytokines [57], alternatively cells can be instructed to produce their own stimulatory factors [61]. The latter is realized by introduction of genetic material to cells to transfer the information required for synthesis of intended proteins, by genetic engineering tools, such as virus, plasmid DNA, or mRNA. Since synthetic mRNA was used as tool for genetic engineering in this study, the details including

comparison of these tools as well as advantages of gene delivery versus protein delivery are described in details in the next sections.

1.2 Genetic engineering by *in vitro* transcribed messenger RNA

1.2.1 Gradual development of IVT-mRNA in gene delivery field

The emergence of *in vitro* transcribed mRNA (IVT-mRNA) technology was primarily spurred by demands for more versatile therapeutics [62]. Indeed, traditionally developed small molecule drugs are only beneficial for a fraction of diseases, and the vast majority of diseases is attributed to malfunctioning proteins, which are often not "druggable" with small molecules (only 3000 out of 20 000 human proteins are druggable) [63]. Therefore, the hope is that a next generation of biomolecular-based drugs might fill up this gap. In particular, nucleic acid (NA)-based drugs used in gene therapy enabled treatment of both hereditary as well as acquired diseases. In a broader perspective for infectious diseases, beside drugs for treatment, preventive vaccines were also of high interest [64]. Among various nucleic acid types for gene therapy, including virus-based DNA, pDNA, siRNA/microRNA, antisense oligos, and RNA aptamers, IVT-mRNA has become into spotlight particularly in recent years [65-67]. While initially established in 1961, it took almost three decades for IVT-mRNA to be first administrated in mice in 1990 by Wolff et al. [68] and to successfully result in protein expression [62]. Subsequently, it took another three decades, until IVT-mRNA reached its full momentum in pharmaceutical industry in 2020, upon SARS-CoV-2 mRNA vaccines received the FDA approval and were globally administrated, in response to the Covid-19 pandemic [69-71].

The major drawback, which impeded the initial development of mRNA was low stability and susceptibility to prevalent RNA degradation enzymes, namely RNases [72]. These primary well-known issues could be addressed with further improvements of *in vitro* transcription technology to synthesize mRNA with structural features resembling the endogenous mRNA molecules [64]. Overcoming issues like stability opened up new horizons for mRNA-based therapeutics, with the potential to surpass other established biomacromolecules [63].

1.2.2 IVT-mRNA as an alternative to other bioactive molecules

While recombinant protein-based drugs face the challenge of a highly individualized multi-step manufacturing and purification process, large-scale mRNA production can be performed in a single-step process, with high efficiency and relatively low costs [63]. Moreover, a protein production pipeline has to be re-established for every new product, whereas IVT-mRNA synthesis process is essentially universal, with little impact of a given sequence [72]. The

6

sequence-independent IVT technology facilitated the adaptable and tailor-made production of IVT-mRNA, simply by customizing the template DNA sequence [62]. This well-defined production pipeline is suited for complying with good manufacturing practice (GMP) regulations, required for pharmaceutical and therapeutic applications [64].

Biological activity of IVT-mRNA is largely determined by its intact primary structure, and upon delivery, IVT-mRNA harnesses the host cell machinery to produce protein of interest with proper folding and post-translational modifications, e.g., glycosylation [63]. In contrast, protein products are highly susceptible to lose their desired 3D structure due to misfolding or misglycosylation during the production process and prior to or during administration. Besides impaired functionality, a misfolded protein can be immunogenic, and elicits unintended side effects [63].

As an alternative to viral vectors and non-viral plasmid DNA (pDNA), IVT-mRNA presents the following advantages. First, IVT-mRNA is instantly translated to proteins after cellular uptake and transfer to the cytoplasm[67, 73]. By contrast, for DNA-based NAs to reach the cell nucleus for transcription they have to breach an extra barrier, the nuclear membrane. This has to be overcome either actively or passively, during mitosis, when the nuclear membrane temporarily dissolves. The latter option is difficult to realize for non- or poorly-proliferative cells, such as the majority of primary cells [67]. The lack of genotoxicity is the other prominent advantage of using IVT-mRNA compared to pDNA and viral DNA [74], because mRNA is unable to integrate with genome and cause mutation [67].

Next, IVT-mRNA expression is transient, which is sufficient for many – but not all – biological and therapeutic applications. In consequence, IVT-mRNA does not leave biological signature corresponding to the protein products after a given time period [75]. By contrast, pDNA and viral gene expression could result in long-term if not permanent expression of proteins, i.e. in case of genomic integration, which might be detrimental in many cases such a vaccines, where a temporary expression of an antigen is sufficient and desired to induce an immune response and immunize a person [67]. Transient expression might also be beneficial for potential modulation of immune cells such as macrophages, which might affect the foreign body response to biomaterials [76].

1.2.3 Structural features of mRNA realized by IVT technology

The IVT-mRNA technology has been improved over time to more and more resemble the structure and chemical identity of endogenous mRNA, encompassing the following elements from 5' to 3' end (Figure 1.3):
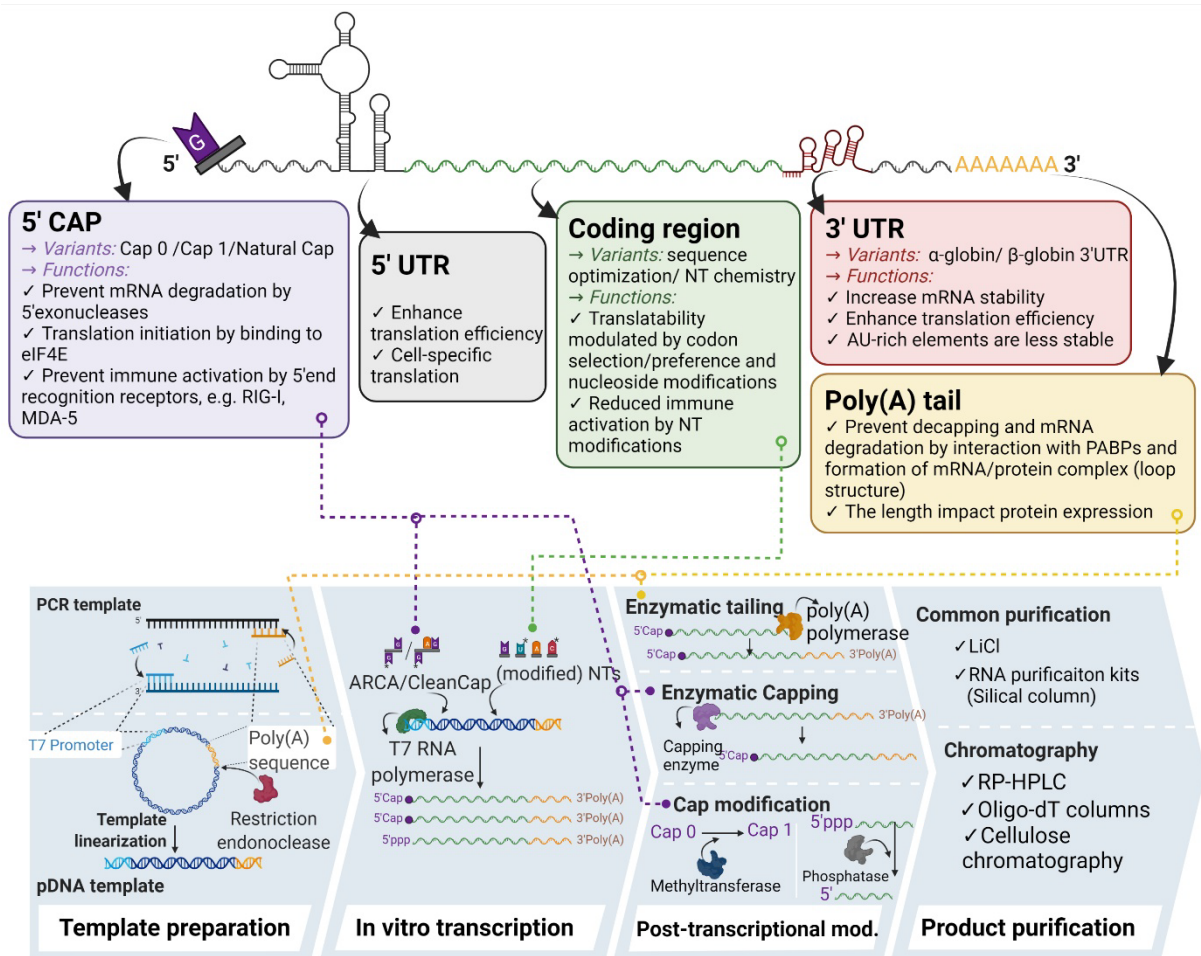
Figure 1.3 mRNA features and functions substantiated by in vitro transcription process

The structure of an exemplary mRNA molecule including its prominent features and their corresponding functions is illustrated in the upper panel. The different main as well as optional steps in the production of *in vitro* transcribed mRNA are presented in the lower panel. The several options to implement the same feature are indicated with color-coded dashed lines connected the upper panel with lower panel.

5'cap structure; a phosphate-phosphate linkage of 7-Methylguanosine (N^7-methyl guanosine or m^7G) to the Guanidine (G) in the 5'end of mRNA, resulting in formation of m^7GpppG. The cap structure increases the mRNA stability by inhibiting degradation by exonuclease enzymes [62]. Moreover, translation initiation can be facilitated by formation of a loop structure in mRNA, made by its interaction with cap-binding proteins and other intermediate eukaryotic initiation factors[77]. In synthetic RNA, other cap structures, namely anti-reverse cap analogues, are usually incorporated to the RNA molecules due to technical reasons [78], explained in an upcoming section; "*Structural features of mRNA realized by IVT technology: Capping*".

5'untranslated region (5' UTR); a non-coding sequence regulating the specificity and enhances the level of translation efficiency [79].

Coding region; the sequence, which determines the protein product.

3' UTR; another non-coding region, which involves in regulation of expression, increasing the mRNA stability and translation efficiency [62].

Poly(A) tail; a homopolymeric stretch of adenine, which is also regulating the level of protein expression depending on its length, and increases the stability by formation of loop complex together with poly(A) binding protein and cap binding proteins, by preventing the decapping and degradation of mRNA [62].

In order to synthesize fully functional mRNA molecules, comprising all the above-mentioned features, *in vitro* transcription technology was developed based on phage RNA polymerases [76]. While eukaryotic and prokaryotic RNA polymerases are highly complex holoenzymes, including multiple protein subunits, each specified for a distinct function, phage polymerases perform transcription as comparably simple, monomeric proteins, which makes it more feasible to control and reproduce such reaction in an in vitro experimental set up [80]. Among various available phage RNA polymerases, including SP6, T3, and T7, the latter was most extensively used, and thus commercialized by biotech supply companies. The process of mRNA synthesis by *in vitro* transcription is described step-by-step in the following; at each step, options available to realize the corresponding properties are elaborated. An overview of the in vitro transcription process is illustrated in Figure 1.3.

DNA template should encompass a promoter sequence specific to the RNA polymerase to support initiation of transcription. This sequence can be either integrated upstream of the gene of interest (GOI) in a pDNA vector, or incorporated via a polymerase chain reaction (PCR) and proper primers containing the phage promoter sequence. In the former case, pDNA must be linearized with a restriction endonuclease downstream of GOI to avoid production of transcripts with heterogeneous size distributions, as there is often no transcription termination sequence presented in the vector. Of note, experimental evidences suggested that only blunt-end or 5'overhang have to be realized by the use of appropriate restriction endonucleases for pDNA linearization to prevent any unpredicted T7RNAP activity [81]. The resulting DNA template should be purified upon enzymatic reaction (i.e. PCR or digestion) and before proceeding with *in vitro* transcription, with either phenol/chloroform, salt (sodium acetate, EDTA and ethanol), or silica columns.

In vitro transcription reaction is assembled by mixing rNTPs, a buffer containing magnesium ion (Mg^{2+}), DNA template, and the RNA polymerase in RNase free DEPC treated water. When rNTPs are provided separately, modifications can readily be incorporated to transcripts, by partial or complete substitution of chemically modified rNTPs with non-modified ones, as desired [62].

Capping of transcripts is achieved co-transcriptional or post-transcriptional, depending on the type cap structure to be incorporated. To ensure unidirectional incorporation of cap structure to the 5'ends of transcripts in co-transcriptional reaction, the cap structure (i.e. m^7GpppG) is modified by substitution of the 3'-OH with a 3'-O-methyl group, resulting in formation of $m^{7,3'O}GpppG$ or so-called *anti-reverse cap analog* (ARCA) [78]. Other cap analog variants include CleanCap structures with distinct first two nucleotides (CleanCap AG, AU, GG), all of which are known as Cap 1 structures due to methylation of the first nucleotide at the 2' position. Implementing CleanCap structures requires introducing changes to the T7 promoter sequence [82].

While "one pot" co-transcriptional reaction omits the need for additional purification steps, which is in particular beneficial in large-scale production of mRNA by avoiding loss of transcripts, there will always be a fraction of transcripts left uncapped [83]. The post-transcriptional enzymatic reaction, however, results in almost 100 % capping efficiency with the cap structure identical to naturally occurring cap. The Vaccinia virus Capping Enzyme (VCE) modifies the 5'end of transcripts with Cap 0 structure, i.e. m^7GpppG. This can be converted to Cap 1, with extra treatments explained in the following [83]. Noteworthy, both co-transcriptional and post-transcriptional reactions are actively used for capping mRNA transcripts not only in research scale, but also in large-scale production of IVT-mRNA in pharma industry, with each method having distinct advantages and limitations compared to the other.

Tailing/Polyadenylation of 3'ends of transcripts is conceivable via two different approaches, including co-transcriptional and post-transcriptional tailing reactions. The former harnesses a 60-130 stretch of adenine incorporated with DNA template to synthesize poly(A) tail, whereas in the latter approach utilizes the *E.coli* poly(A)-polymerase to introduce the homopolymeric adenine sequence at 3'end of RNA after completion of transcription reaction. Similar to the T7RNAP promoter, in the co-transcriptional reaction the poly(A) tail can be added to the GOI using PCR reaction and oligo(dT) primers, or alternatively the pDNA template encodes the poly(A) sequence [62]. Aside from requirements for additional purification steps, as mentioned for post-transcriptional polyadenylation, the major drawback of this method is the undefined and heterogeneous size distribution of poly(A) tail in transcripts, which is the bottleneck for production of mRNA with intended therapeutic applications. Moreover, omitting an extra enzymatic reaction facilitates the process of GMP approval required for large-scale production of mRNA-based therapeutics in pharmaceutical companies [75].

Post-transcriptional modification of 5'ends are optional post-transcriptional treatments, to reduce the mRNA immunogenicity, if necessary. In this section, however, the two most common treatments including dephosphorelation and methylation of 5'end are described. As mentioned above, the capping process is not 100% efficient, particularly when performing a co-transcriptional reaction [83]. Thus, the fraction of uncapped transcripts presenting a triphosphate group at their 5'ends, which is removed by treatment with phosphatase enzyme [84]. Further, a methylation reaction can convert the Cap 0 to a Cap 1 structure, relevant for transcripts capped enzymatically or co-transcriptional using ARCA cap structures. The mRNA cap 2′-O-methyltransferase (MTase) and S-Adenosylmethionin (SAM) are incubated with purified transcripts in a subsequent reaction to methylate the 2'-OH of the first nucleotide, which is essential character of Cap 1 structure [85, 86].

Purification of transcripts is performed to remove impurities including free rNTPs, proteins used for transcription and potential subsequent reactions, salts and buffers supplied with enzymatic reaction, as well as potential RNA contaminations. The conventional approach for purification of mRNA transcript is precipitation of mRNA using LiCl, or silica-membrane purification provided commercially in form of spin column, both of which are capable of removing non-RNA impurities. However, in order to remove RNA impurities such as dsRNA, high performance chromatography (HPLC) was successfully implemented as reported by Kariko et al. [87]. Oligo(dT) affinity chromatography purification is also commonly used for purification of mRNAs with poly(A) tail [88]. Other alternative purification methods based on oligo(dT) hybridization include magnetic beads covalently attached to oligo(dT) [89], either imbedded on the 96-/384-well plate or combined with spin-column separation, as well as oligo(dT) cellulose columns [90]. More recently, an approach only based on cellulose purification has been reported to be effective for removal of dsRNA byproducts [91].

Understanding the mechanisms involved in *in vitro* transcription technology facilitates the design of a workflow, by careful selection of the proper process parameters regarding each individual step, in order to achieve the synthesis mRNAs with defined properties.

1.2.4 Therapeutic applications of IVT-mRNA

Facile production of mRNA using *in vitro* transcription technology motivated its application in a wide range of research from basic biomedical and biotechnological areas to therapeutic and clinical studies [92, 93]. Being able to produce any given protein using the host cell machinery, mRNA became an intriguingly versatile tool, which can be exploited for many different purposes [63]. The applications of IVT-mRNA in different fields are explained in the following.

Applications of IVT-mRNA in biotechnology research include genetic circuits, biosensors, and studies, where the function of a single protein can be identified or studied by its upregulation [94]. IVT-mRNA can also be used as a tool for genome editing, by inducing the expression of Cas9 protein in CRISPR/Cas-mediated genome editing approaches [82, 95], or epigenetic modifications of cells using dead Cas9 (dCas9) [96]. Generation of induced pluripotent stem cells by transfection with mRNAs coding for the reprogramming transcription factors required for dedifferentiation of cells is another prominent application, more and more replacing viral transductions [76].

The therapeutic applications of mRNA is presented here in three main categories: (i) immunotherapy [97], (ii) protein replacement therapy [98], and (iii) regenerative medicine [93].

Firstly, IVT-mRNA coding an antigen is employed to elicit immune response either to immunize against infectious diseases, or tumors, referred to as RNA Vaccine therapies [99, 100]. Vaccines against flu [101], HIV [102], Zika virus [103], HBV infection [104], and SARS-Cov-2 [70, 105] are examples of using mRNA for prevention from infectious diseases. The immunotherapy of leukemia as well as solid tumors is currently addressed by RNA vaccines [106, 107], some of which are currently in clinical trial phases[105, 108]. Anti-tumor mRNA vaccines can be customized on an individual basis, presenting them as a platform for personalized medicine [92, 106]. By collection and bioinformatics analysis of the gene mutation data from patients, the predominant target tumor antigen can be identified and targeted. (Pre)clinical studies reported remarkable efficacy of mRNA tumor vaccines in eradication of some tumors, also for residing metastatic cancers at late stages [109].

Secondly, IVT-mRNA can also encode a functional protein (i.e., not restricted to its immunogenic potential), in order to reduce the symptom of a disease rather than omitting the cause [98]. This is in line with classical gene therapy approaches, except that IVT- mRNA expression is transient [67]. The production of cytokines for immune modulation, erythropoietin (EPO) in treatment of anemia, Foxp3, TLR1/2, and TLR2/6 for treatment of asthma, Bcl-2 for prevention of liver damage and Neprilysin for clearance for beta amyloid are some examples of protein replacement therapy. IVT-mRNA-mediated production of antibodies against both tumor and infectious diseases for passive immunization has also been reported [110, 111].

The third major application of IVT-mRNA is promoting damaged tissue repair. Production of growth factors and/or the proteins facilitating tissue regeneration by host cells is the strategy behind using mRNA in regenerative medicine. BMP-2 and BMP-9 expression for bone regeneration, IGF1, Fstl1, Pkm2-for cardiac tissue regeneration upon myocardial infarction, HGF for liver regeneration are examples, where mRNA successfully promoted tissue

regeneration [93]. Given that most of these proteins are secretory and have both autocrine and paracrine effects, all cells transfected with mRNA serve as a source for production target proteins, supplying the adjacent cells and tissues with their induced signaling factors.

1.2.5 Challenges of using IVT-mRNA for genetic engineering

Employing mRNA as a tool for gene delivery was suggested at the same time as for pDNA three decades ago [100]. However, only the latter was initially perused in gene therapy applications. This was partially because of overestimated issue of lack of RNA stability, which further delayed the progress of mRNA compared to pDNA [73]. The stability issue, however, was addressed upon advances in *in vitro* transcription technology and production of IVT-mRNA with features mimicking the naturally occurring mRNA, as explained in the previous sections. While the half-life time of mRNA was remarkably increased, susceptibility to RNases, prevalently exists both *in vitro* and to a higher extend *in vivo*, which can ultimately impede RNA transfer to cells [112]. Developing different types of lipid- and polymeric-based delivery systems solved this issue by protecting mRNA molecules from degradative enzymes in extracellular microenvironment [113]. This, however, is only one of the many functions envisaged for a carrier system to fulfill.

Transient expression was another challenge, which hindered widespread use of mRNA-based genetic engineering within the first decades upon its discovery. This is in part due to the intrinsic nature of mRNA, an entity acting as a blueprint of pDNA in cytoplasm, and ultimately degradation but also out-dilution for proliferating cells is inevitable. However, mRNA pharmacokinetic is currently adaptable to match many biological demands, by altering its structural elements such as 5'and 3' untranslated regions (UTRs), nucleotides chemistry and 5'Cap structures [114]. Repeated transfection over time with negligible influence on cells viability, as well as sustained release of mRNA from an advanced carrier system are other approaches to extend mRNA expression lifespan, even by so-called RNA-replicons [115]. It is important to take into account, that there are many applications were the transient expression is preferred, and therefore using mRNA per se without extra modifications is indeed advantageous.

Unintended immunogenicity is the third major issue, and the most challenging of all, which hindered mRNA research, as soon as it was administrated *in vivo* [116]. Despite being advantageous in some therapeutic applications such as vaccines, in most cases such as protein replacement therapy and other biotechnological applications, immune stimulation is usually undesirable. Therefore, understanding the underlying reasons for mRNA immunogenicity

facilitates tackling this issue. In the following, it is explained how and why mRNA is causing immune stimulation. IVT-mRNAs immunogenicity is attributed to either intrinsic features of an "ideal IVT-mRNA molecule", or to unintended features of an "imperfect structure" both are explained in the following. Here, an ideal mRNA molecule is defined as the structure, which encompasses all designed features, with no impurities or unintended addition or elimination of a feature. Interestingly, regardless of being the identical entity as endogenous mRNA, this ideal mRNA molecule is still able to elicit immune response. This is in part due to the fact that they have different transport routes [116]. Endogenous mRNA is transcribed within the nucleus and is subsequently transported to the cytoplasm, whereas the IVT-mRNA has to enter the cell from extracellular space, often through endosomal pathways. If it escapes the endosome prior to its merging with the lysosome, it enters the cytosolic space, where it is translated to proteins. Therefore, IVT-mRNA encounters endosomal receptors leading to immune stimulation. These are indeed the pathways, which cells have developed primarily as defense mechanisms against RNA-based virus infections [117]. Examples for such endosomal receptors are Toll-like receptors (TLRs), with TLR-7 and -8 particular known to be activated by single strand mRNA molecule within the endosome [118].

Next, the imperfect synthesis of mRNA results in production of transcripts either lacking one or the other key features such as 5'Cap, or containing RNA impurities and byproducts. In both cases, i.e. the free 5'-triphosphate ends and the dsRNA byproducts, mRNA can trigger an immune response. In particular, RNA byproducts can form long dsRNA structures, which is recognized by both endosomal receptors, TLR3, and cytosolic receptors including retinoic acid-inducible gene-I (RIG-I), RIG-like receptors (RLRs), melanoma differentiation-associated protein-5 (MDA-5), protein kinase R (PKR), and RNA interference receptors [119]. Activation of these receptors leads to expression of inflammation and antiviral response cytokines, such as IL-6, TNF-α, as well as type I interferons (IFN-α, and IFN-β), which further stimulates immune response not only in transfected cells but also potentially in adjacent cells by a paracrine effect [116]. However, activated PKR inhibits translation by phosphorylation of eukaryotic initiation factor 2α (eIF2α), hampering the formation of translation initiation complex, which results in global suppression of protein synthesis and eventually induction of cell death [120]. In the RNA interference pathway, the expression is suppressed by cleavage of partial RNA duplexes, as a result of annealing of short RNA oligoes, i.e. the short RNA byproducts, with complementary sequence in single strand mRNA molecules [119]. Noteworthy, immune stimulation is not only from mRNA, but can also be initiated from a carrier, such as poly(ethylene glycol) moiety of lipid nanoparticles (LNPs), which recently was found to cause allergic reaction when tested in

clinical applications in patients [121]. It was recently reported that surface modification of nanoparticles with PEG conjugates to prolong their blood circulation can result in production of anti-PEG antibodies, when administrated in patients. Consequently, the acquired anti-PEG antibodies might result in accelerated blood clearance, hypersensitivity and in severe cases dire side effect [122].

1.2.6 Strategies to ameliorate IVT-mRNA modalities

In this section, an overview of already existing solutions to some of the mentioned challenges of IVT-mRNA is provided, with particular focus immunogenicity, as a key aspect of this thesis. In the following, approaches to reduce immunogenicity and other confounding issues are explained.

Chemical modifications of nucleotides were initially suggested to decrease immune response. The idea of incorporating naturally occurring chemical modifications of nucleotides was spurred by a study, where different fractions of mammalian and *E.coli* RNA were evaluated *in vivo* and the corresponding immune response to each fraction was determined by measuring TNF-α concentration. By comparing total RNA with nuclear, cytoplasmic, polyA$^+$ mRNA, mitochondrial and tRNA, Kariko and colleagues found that the tRNA fraction elicited almost no inflammatory response [123]. Incorporation of these chemical modifications of nucleotides to the mRNA structure proved to reduce the immune response significantly, both *in vitro* by evaluation of dendritic cells cytokine production[123] and later tested in an *in vivo* mouse model [124].

Cap modifications can also have a considerable effect on reducing the immune response to IVT-mRNA spurring the use of Cap variants mimicking Cap 0 or Cap 1. Previous reports suggested reduced immunogenicity of mRNA modified with Cap 1 compared to Cap 0 [82]. However, the differences were marginal and thus there is no consensus in necessity of using Cap 1 versus Cap 0. Besides, in case of co-transcriptional capping, extra treatment with phosphatase enzyme to remove the 5'triphosphage group was also performed in some reports to reduce immune response [82].

Extra purification steps using HPLC or cellulose column can reduce or even abrogate immune response to IVT-mRNA by removing dsRNA impurities [87]. The efficiency of these methods can be evaluated by dot plot technique using J2 anti-dsRNA antibody, which measures the dsRNA content of each sample prior to and upon purification. Both approaches were successful in eliminating dsRNA and thus the immune response to purified mRNA as measured by type I interferon response [87].

Sequence optimization might increase translation efficiency, and by avoiding formation of secondary structure also to some extend reduce immune response. Replacing rare-codons with preferred codons of the target species can also remarkably increase the level of mRNA expression. Besides, reduction of uridine content in mRNA sequence, also referred to as "uridine depletion", was reported to remarkably reduce immune responses to the corresponding mRNA transfection [82]. The underlying reason is not yet clear, however, some researchers suggest that it is due to a higher tendency of uridine to interact with single strand RNA receptors TLR7 and TLR8.

The scientific concept and precise goals of this thesis founded on the above background is elaborated in the next chapter.

Chapter 2: Aims and Strategy

Given the pivotal role of macrophages in orchestrating immune responses, reliable approaches to modulate their behavior are instrumental. Particularly, polarization of macrophages to anti-inflammatory phenotype could abolish foreign body reaction to implants, and thus improve the implant-host integration and long-term performance. Addressing the technological demands, the primary goal of the thesis was to regulate macrophages response by genetic engineering with *in vitro* transcribed mRNA.

IVT-mRNA shall provide macrophages with the instruction to synthesize the target proteins, as biological entities delineating their phenotypes and functions. Despite being an appealing and potentially reliable tool for modulation of the cell behavior, IVT-mRNA delivery to macrophages can lead to unintended cell stress and immune activation. Thus, the aim of the thesis was to explore an IVT-mRNA-based technology for genetic engineering of macrophages with minimum to ideally no side effects.

Four consecutive steps to perceive this concept were defined. The first step was dedicated to identify whether the transfection-induced immune activation of human monocytes and macrophages is primarily influenced by carrier formula or the payload chemistry. Second, to minimize or abrogate immune responses, various 5'end or internal chemical modifications of IVT-mRNA were explored. Next, the methodological aspects required for co-expression of multiple genes was addressed, investigated in terms of payload design and process parameters. The following strategies were conceived to substantiate the above concepts.

1. Transfection of primary human monocytes and macrophages with different carrier formula, lipid- and polymeric-based, and payload chemistries, i.e. non-modified and Ψ/5meC modified IVT-mRNA, could reveal the extent, to which each element of a the IVT-mRNA/carrier complex affects transfection efficiency and cell stress. Moreover, the pattern of mRNA dose-response provides a more conclusive scheme, when compared between different transfection conditions and cell types.

2. By exploring different 5'end and internal modifications of IVT-mRNA, the optimal chemistry for reduction and potentially ablation of immune response in human macrophages should be identified. In case, the extra purification step would not be required, thus omitting the potential source of variations.

3. Comparison of different payload designs, i.e. bicistronic versus monocistronic, could reveal the ideal method to achieve co-expression of several genes, which is required for many advanced gene delivery studies.

4. Quantitative evaluation of process parameters in NA co-delivery as well as successive delivery could provide a clear methodological scheme to consolidate the results, by preventing the arbitrary selection of experimental setup.

Measurement of cell stress is quintessential to evaluate the effectivity of gene transfer to immune cells, in particular macrophages, in addition to common readouts such as transfection efficiency. Here, assessment of human macrophage responses to IVT-mRNA delivery was as follows. First, transgene expression was measured both qualitatively by fluorescent imaging and quantitatively by flow cytometry, after transfection of cells with marker genes coding for fluorescent reporter proteins, such as EGFP and mCherry. Consequently, the transfection efficiency and the level of IVT-mRNA expression were defined as percent of EGFP positive cells and mean fluorescent intensity. The integrity of synthesized proteins was evaluated by immunoblotting.

Cells viability and immune activation were measured to investigate the transfection-induced cell stress. Cell viability was quantified by flow cytometry and defined as percent of DAPI-negative cells. The inflammatory surface marker expression, CD80, and cytokine secretion were measured as parameters indicating the immune response. The proinflammatory cytokines, TNF-α, and IL-6, and antiviral cytokine type I interferon, IFN-β, were quantified by a multiplex immunoassay.

Attributing the immune response to distinct chemical modifications requires investigation of IVT-mRNA quality, such as integrity and dsRNA content. The integrity of transcripts was measured by agarose gel electrophoresis, whereas the dsRNA content was assessed by dot-blot immunoblotting method. Of note, to avoid induction of immune response in macrophages during the isolation and differentiation process, endotoxin-free reagents were used throughout. Further, at least two different mRNA doses were implemented side-by-side mainly to compare the level of expression at low dose and level of immune activation at high dose of mRNA.

Chapter 3: Organization of the Thesis

This cumulative thesis aims to explore a reliable and robust technology based on IVT-mRNA for genetic engineering of primary human macrophages without causing an interfering cell response. The methodological aspects required for co-delivery of two genes were also systematically addressed. The content of comprising chapters is outlined as follows.

Chapter 1 titled "Introduction" provides the scientific background of this dissertation, covering different aspects experimentally investigated in chapters 4-7, considered as pillars of this research.

Chapter 2 titled "Aims and Strategy" presents the motivations, aims, hypothesis, strategies and outline of methodologies implemented in this thesis.

Chapter 3 titled "Organization of the Thesis" describes the structure of the thesis.

Chapter 4 titled "mRNA transfection-induced activation of primary human monocytes and macrophages: dependence on carrier system and nucleotide modification" refers to the systematic evaluation of different carrier types and two payload chemistries. The original article is presented in Appendix I.

Chapter 5 titled "Chemical modification of uridine modulates mRNA-mediated proinflammatory and antiviral response in primary human macrophages" refers to the explorative study of various 5'end and internal modifications to the cell activation potential of synthetic mRNA. The original submitted manuscript is presented in Appendix II.

Chapter 6 titled "Co-delivery of genes can be confounded by bicistronic vector design" refers to study of payload design and its influence on co-expression of multiple genes. The original submitted is presented in Appendix III.

Chapter 7 titled "Strategies for simultaneous and successive delivery of RNA" refers to the methodological investigation of co-delivery, and the remarkable role of process parameters on the co-expression pattern, quantified at single cell level. The original article is presented in Appendix IV.

Chapter 8 titled "Discussion" places the outcomes of this thesis into a more general perspective, in context of recent state of the art.

Chapter 9 titled "Summary and Outlook" presents an overview of the key findings, and envisioned future prospects.
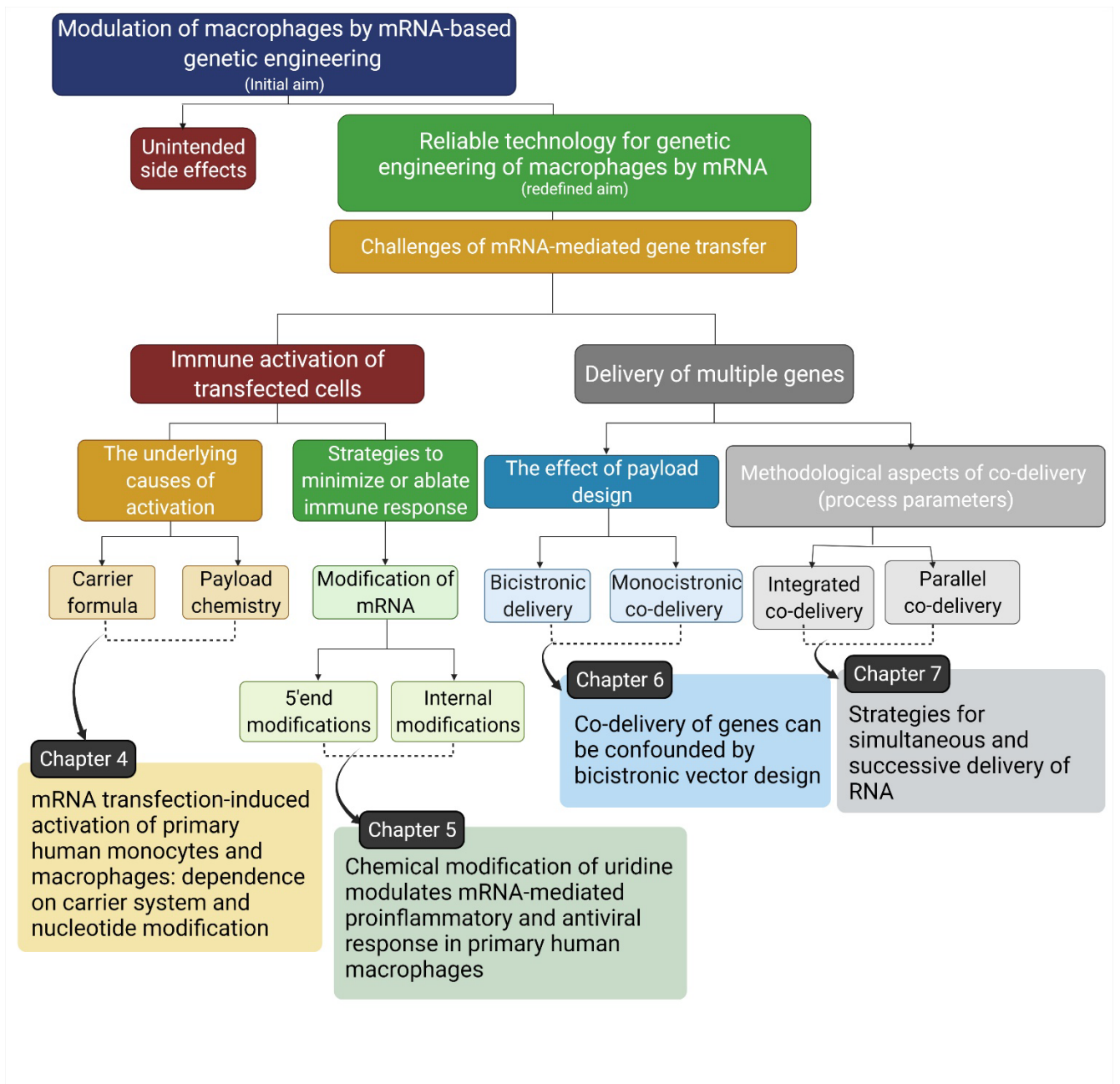
Figure 3.1. Organization of thesis

The diagram shows various scientific perspectives addressed in this dissertation and how each chapter is related to the main storyline.

Chapter 4: mRNA transfection-induced activation of primary human monocytes and macrophages: dependence on carrier system and nucleotide modification

Summary

In this publication, we investigated the primary human monocytes (MCs) and monocyte-derived macrophages (MΦs) response to IVT-mRNA delivery. In a systematic study, the effect of mRNA dose, mRNA modifications as well as the carrier type on cells viability, gene transfer efficacy and immune response patterns was evaluated. By increasing mRNA doses the transfection efficiency and the intensity of target gene expression within population of positive cells were increased. However, it was at expense of substantial decrease in viability and high level of macrophage activation, quantified by inflammatory surface molecule expression and cytokines secretion. IVT-mRNA modified with pseudouridine (Ψ) and 5-methyl-cytidine (5meC) elicited lower level of immune activation in both MCs and MΦs, when compared with non-modified IVT-mRNA. The findings also indicate that between three types of commercially available carrier systems, including both polymer- and lipid-based reagents, one lipid-based formula consistently resulted in the highest transfection efficiencies. The outcomes of this study highlight the crucial impact of both carrier and payload on the overall performance of the carrier system in terms of gene transfer and unintended cell response, particularly crucial for innate immune cells, which are exceedingly sensitive to external interventions.
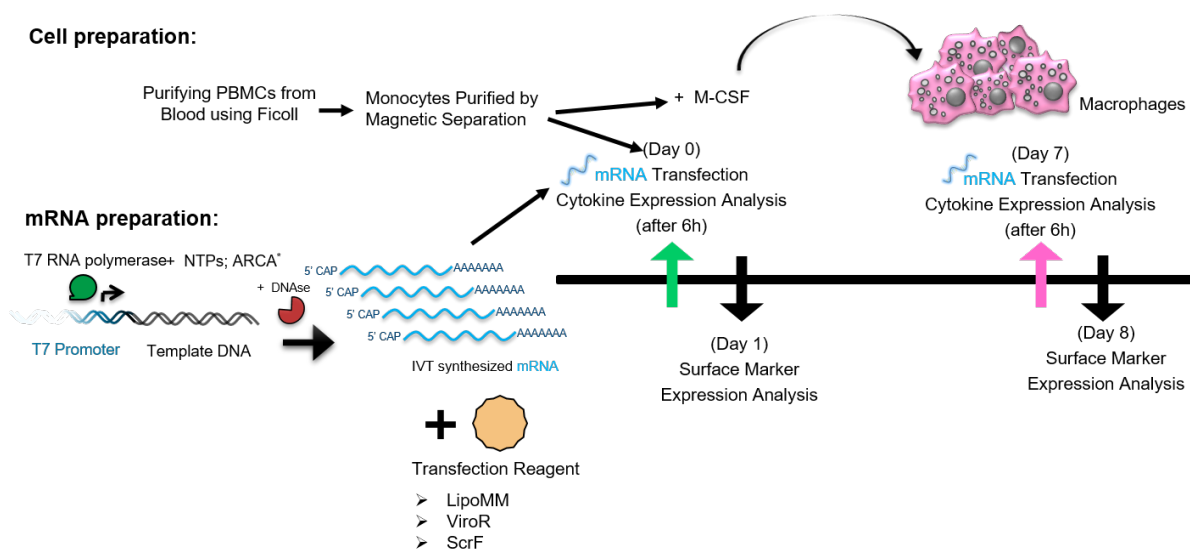
Figure 4.1. Graphical representation of the study concept, derived from the publication[125]

Contribution to the publication

Literature review

- Advantages of gene delivery using IVT-mRNA as payload versus other nucleic acid entities, e.g. pDNA
- Essential role of monocytes and macrophages in innate immunity
- Advantages of IVT-mRNA delivery to hard-to-transfect cells such as monocytes and macrophages, versus the challenges due to the potential activation of macrophages

Study design[1]

- Selection of different mRNA transfection reagents to cover both polymeric and lipid-based carrier systems
- Choice of cell type, also suitable for elucidation of immune response, i.e. MCs, and MΦs differentiated from them
- Readouts for measurement of cell response including viability, mRNA transfer rate, inflammatory surface molecules, as well as inflammatory and antiviral cytokine secretion
- Selection of another marker protein for comparison to rule-out potential sequence-specific effect

Experimental work

- Synthesis and characterization of *in vitro* transcribed mRNA
- Isolation of MCs from buffy coats, and establishment of differentiation to MΦs
- Transfection of MCs and MΦs with different reagents
- Morphological study of cells upon transfection via phase-contrast and fluorescent microscopy
- Quantification of cells viability, transfection efficiency and surface molecule expression at single cell level using flow cytometry
- Measurement of cytokine secretion via a multiplex immunoassay

Analysis and interpretation of the data

- Evaluation of microscopic cell images for influence of transfection of cells morphology and comparison of mRNA expression intensity between different samples

---

[1] Study design was performed in discussion with co-authors.

- Analysis and representation of flow cytometry data in form of dot plots, histograms and bar graphs
- Calculation of total cytokine secretion in samples using the corresponding standard curves
- Statistical analysis of data sets to identify the significance of mRNA transfection condition impact on measured parameters

Manuscript preparation

- Preparation of the manuscript outline, refined by discussion with the co-authors
- Writing the first draft of the manuscript. Manuscript revision and finalization of text for submission according to comments from the co-authors
- Revision of the manuscript based on additional data, which were incorporated to address reviewers comments and finalizing the revised manuscript together with the co-authors

Publication – Appendix I

H. Moradian, T. Roch, A. Lendlein and M. Gossen: mRNA Transfection-Induced Activation of Primary Human Monocytes and Macrophages: Dependence on Carrier System and Nucleotide Modification. *Scientific reports* 10, 4181 (2020). doi: 10.1038/s41598-020-60506-4.

Chapter 5: Chemical modification of uridine modulates mRNA-mediated proinflammatory and antiviral response in primary human macrophages

Summary

The impact of IVT-mRNA chemistry on immune cells response was the subject of this study. By incorporation of chemical modifications to transcripts either at the 5'end or internally by substitution of nucleosides, we comprehensively evaluated the quality of run-off products at the molecular level, i.e. dsRNA content, the transgene expression and distinct schemes of immune response. The latter was measured in terms of both proinflammatory and antiviral responses triggered by mRNA transfection in immune cells. Being relevant for both basic research as well as therapeutic applications, study of primary human macrophages was the major focus. A side-by-side comparison of different mRNA modifications revealed nucleotide chemistry to have a remarkable impact compared to various tested 5' cap structures on both gene expression and immune activation. The outcomes suggested uridine chemistry to have the utmost influence both at molecular and cellular level, as the highest dsRNA content was observed for the Ψ sample, whereas the minimum level of dsRNA was identified for mRNA modified with 5-methoxy-uridine, which was found to be directly correlated with the immune response level. The predictable immune response pattern corresponding to distinct mRNA chemistry according to the empirical evidences presented in this study can be harnessed as a reference to select mRNA chemistry depending on intended biological applications. Thus, the study clarifies key technological demands for genetic engineering of macrophages as the primary goal of this thesis.
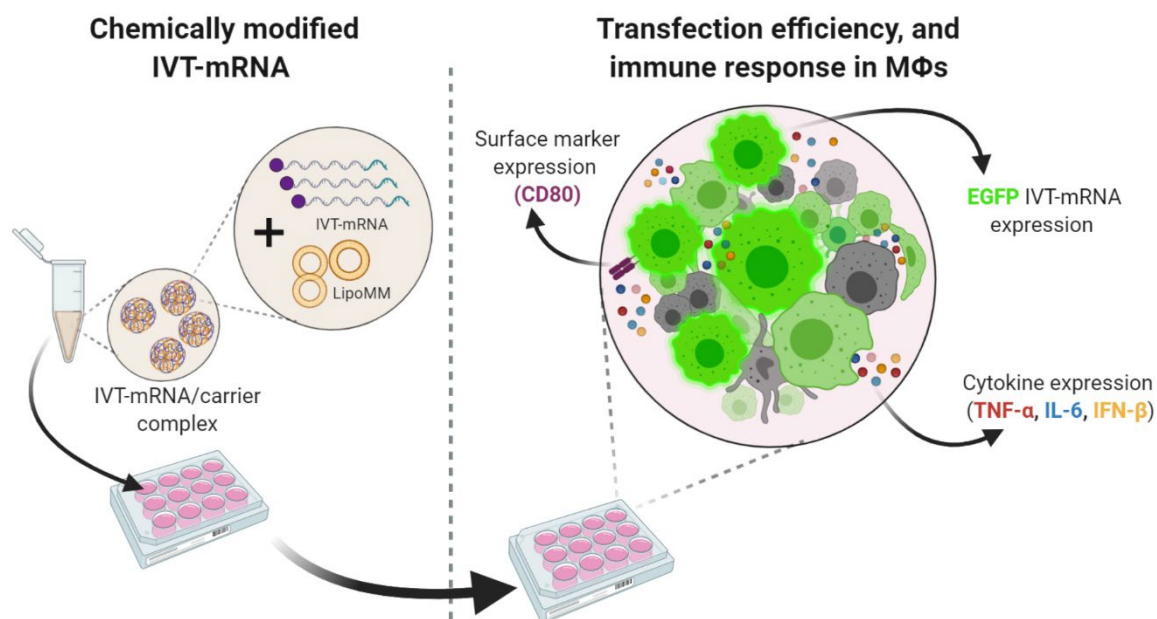
Figure 5.1. Summary of transfection of primary human macrophages and the subsequent cellular response analysis

The transfection efficiency as well as immune response as key readouts. This figure was obtained from the graphical abstract of the manuscript.

Contribution to the manuscript

Literature review

- Therapeutic applications of IVT-mRNA
- The vital role of macrophages as primary line of defense in innate immune response with potential therapeutic relevance
- Molecular mechanisms of immune response to IVT-mRNA
- Strategies to minimize unintended immune response to IVT-mRNA based on altering mRNA chemistry

Study design[1]

- Selection of IVT-mRNA modification schemes, including 5'end modifications and nucleotide modifications
- Evaluation of IVT-mRNA performance at the molecular level, including integrity and dsRNA content of run-off transcripts

---

[1] Study design was performed in discussion with co-authors.

- Assessment of IVT-mRNA performance at the cellular level, including macrophage transfection efficiency and patterns of innate immune activation, by evaluation of both inflammatory and anti-viral response

Experimental procedure

- IVT-mRNA synthesis with different chemical modifications, including post-transcriptional treatments for cap modifications
- Measurement of dsRNA content of transcripts by immunoblotting
- Preparation of primary human macrophages from buffy coats followed by transfection with IVT-mRNA with distinct chemistry
- Qualitative evaluation of cells morphology and transgene expression level, i.e. fluorescent marker protein by microscopic methods
- Quantification of viability, transgene expression and immune activation surface marker, e.g., CD80, at single cell level by flow cytometry
- Validation of protein production using western immunoblotting
- Quantitative evaluation of proinflammatory and antiviral cytokines secretion at different time points post-transfection by Bioplex multiplex immunoassay

Analysis and interpretation of the data

- Evaluation of microscopic images and intensity of mRNA expression after cell transfection
- Analysis of flow cytometry data, interpretation of data, and representation of data in form of various types of graphs including concatenated dot-plots, bar graphs, and histograms
- Calculation of net protein, i.e. cytokine concentration of different samples by curve fitting using values from standard series, and plotting the data in form of bar graphs
- Statistical analysis of data to compare different conditions and identify potential correlations

Manuscript preparation

- Preparation of the manuscript outline, refined by discussion with the co-authors
- Writing the first draft of the manuscript, and manuscript revision and finalization for submission according to comments from the co-authors

Publication – Appendix II

H. Moradian, T. Roch, A. Anthofer, A. Lendlein and M. Gossen: Chemical modification of uridine modulates mRNA-mediated proinflammatory and antiviral response in primary human macrophages. Molecular Therapy: Nucleic Acids 27, 854-869 (2022), doi: https://doi.org/10.1016/j.omtn.2022.01.004.

Chapter 6: Co-delivery of genes can be confounded by bicistronic vector design

Summary

Two co-delivery methods differing in terms of payload design were investigated in this manuscript. In a comparative study, we performed a series of side-by-side experiments to identify the most reliable and robust method for co-delivery of two genes, which is demanded in numerous biological studies. The two genes were either integrated within a single open reading frame, to be separated via a 2A self-cleavage peptide sequence, or co-delivered as two separate expression units, referred to as "bicistronic delivery" and "monocistronic co-delivery", respectively. While we initially envisaged the bicistronic method to result in homogeneous co-expression of the two genes, due to inherent equimolar delivery, the empirical observations proved otherwise. The co-delivery method, in contrast, consistently lead to uniform pattern of co-expression. Moreover, the potential role of size ratio of the two genes, dependence on nucleic acid entity, as well as the cell type were examined, none of which found to have a clear influence on the co-expression outcomes. Overall, our findings suggested that co-expression can be confounded by bicistronic delivery, in contrast to the co-delivery method, which reliably resulted in uniform patterns of co-expression.
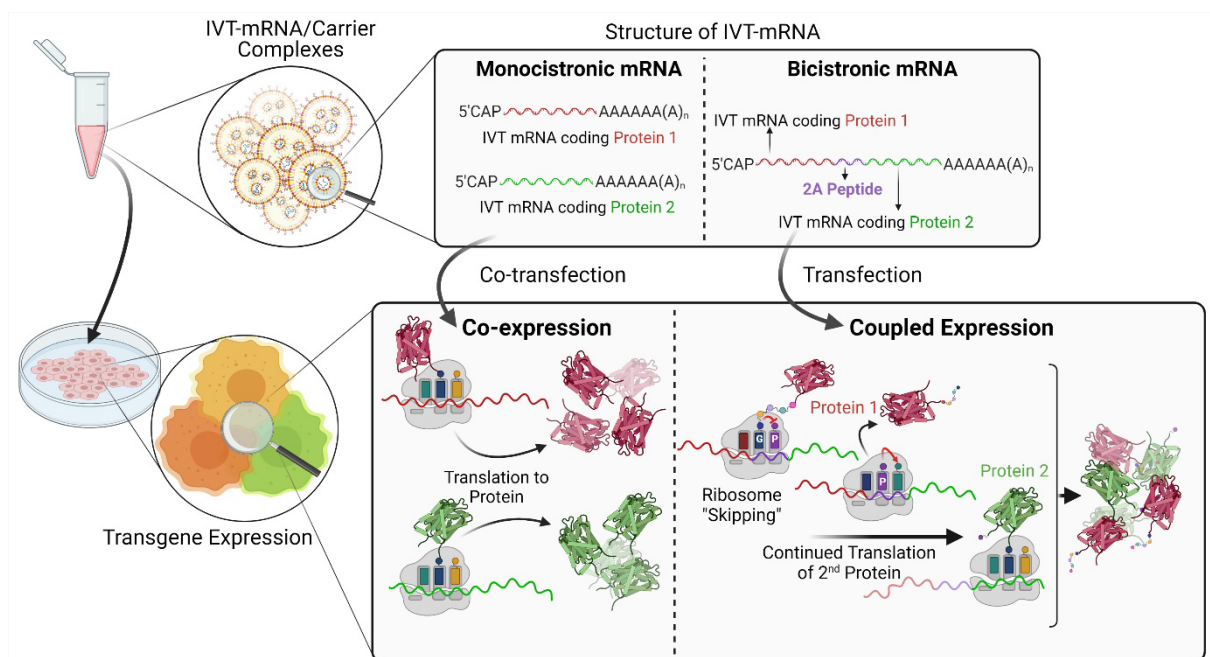
Figure 6.1. Schematic representation of the study design

Approaches to achieve mRNA-directed co- production of target proteins in individual cells, derived from the graphical abstract of the manuscript.

Contribution to the manuscript

Literature review

- Biological demands for induced co-expression of multiple genes
- Various approaches for co-expression of multiple genes and their advantages and disadvantages
- Bicistronic delivery and 2A peptide-mediated co-expression

Study design[1]

- Sequence design to prepare a bicistronic cassette, including 2A peptide sequence
- Potential interfering variables including size ratio of the two genes, NA entity, e.g. IVT-mRNA and pDNA, and cell type
- Investigation of equimolar versus equimass delivery of mRNA

Experimental procedure

- Molecular cloning of bicistronic genes into a T7 promoter-based, poly(A) tail-encoding vector
- (Co)-transfection experiments of IVT-mRNA
- (Co)-transfection experiments of pDNA
- Qualitative measurement of cells by microscopic evaluation of transfected cells
- Quantitative measurement of gene (co)-expression by flow cytometry
- Immunocytochemistry for detection of non-fluorescent proteins

Analysis and interpretation of the data

- Evaluation and comparison of fluorescent protein expression from microscopic images
- Analysis and interpretation of flow cytometry data, and summarizing data in different forms of graphs
- Calculation of precise molecular weight of each NA type, including IVT-mRNA, pDNA, both for bicistronic and monocistronic vector designs

Manuscript preparation

- Preparation of the manuscript outline, refined by discussion with the co-authors
- Writing the first draft of the manuscript; manuscript revision and finalization according to comments from the co-authors

---

[1] Study design was performed in discussion with co-authors.

Publication – Appendix III

H. Moradian, M. Gossen and A. Lendlein: Co-delivery of genes can be confounded by bicistronic vector design. MRS Communications 18:1-9 (2022), doi: 10.1557/s43579-021-00128-7.

Chapter 7: Strategies for simultaneous and successive delivery of RNA

Summary

In this publication, we evaluated different methods for concurrent or successive delivery of two nucleic acid (NA) entities, with the main focus on IVT-mRNA. Two strategies for simultaneous delivery were conceptualized and experimentally investigated, including "integrated co-transfection" and "parallel co-transfection". The former refers to the condition where different NA payloads were mixed prior to complexation with the carrier, whereas the NA complexes were prepared separately in the latter method. The mRNA dose, carrier type as well as cell type were three process parameters systematically examined in side-by-side experiments for the two approaches. The co-expression rate of the two marker genes was quantified on a single cell level, as the key readout. The outcomes suggested a distinct pattern of co-expression corresponding to each method. While the integrated co-transfection resulted in uniform, largely dose-independent distribution of co-transfected cells, the parallel co-transfection method lead to heterogeneous, dose-dependent co-expression of the two marker genes. Similar patterns were consistently observed for polymeric and lipid carrier types and different cell types. By successive transfection of mRNA, we found out that cells are less prone to uptake the mRNA/carrier complexes in the second round of transfection. However, time-delayed multi-step transfections would be instrumental for NA entities with kinetically distinct peaks, e.g. IVT-mRNA and siRNA, aimed to be delivered to the same cell. The discrete patterns of co-delivery, revealed by single cell quantification, emphasizes the importance of process parameters to be precisely selected according to the particular experimental requirements. The quantification scheme provided by the experimental framework defined by us in this study addressed the technological aspects of co-delivery, in line with the strategies envisaged in the thesis.
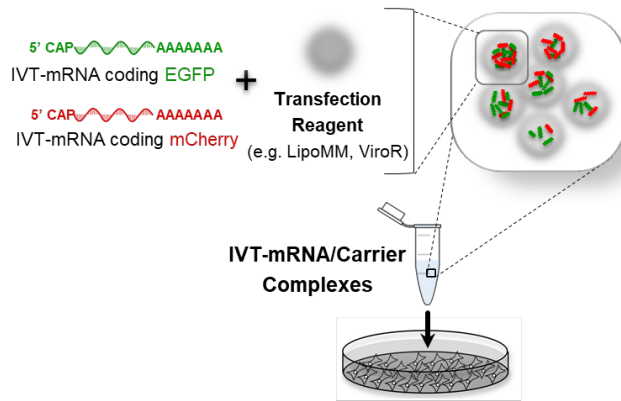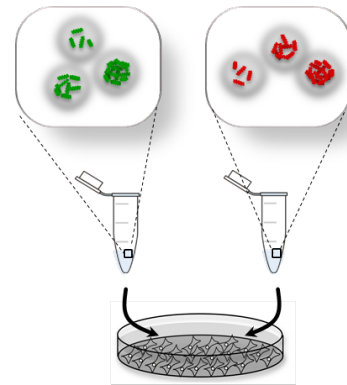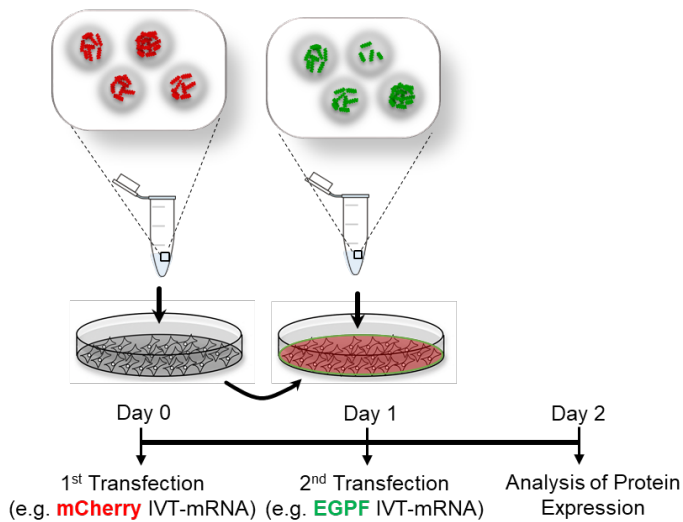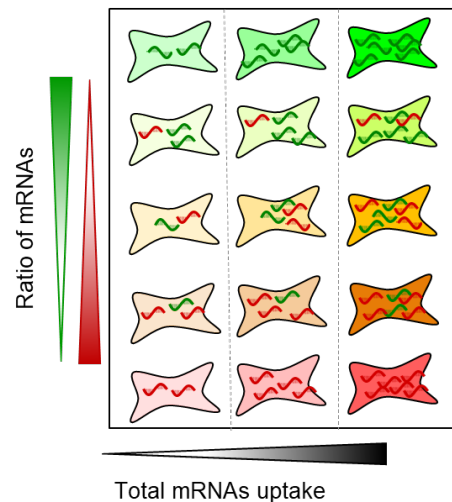
Figure 7.1. Schematic overview of various methods for co-/successive delivery of IVT-mRNA

Graphic was btained from the publication [126]

Contribution to the publication

Literature review

- Demands for establishment of co-delivery methods
- Co-delivery of multiple NA entities, as well as different types of NAs
- Successive delivery of genes, including benefits and necessity of such strategies
- Importance of quantification of genes co-expression at single cell level

Study design[1]

- Definition of two co-transfection methods: integrated versus parallel co-transfection
- Successive transection of IVT-mRNA using two fluorescent marker genes
- Simultaneous versus successive transfection of mRNA and siRNA as two distinct entities with different action mechanisms and peak performance time points
- Covering both polymeric and lipid-based carriers as transfection reagents
- Dose-dependence of co-expression both for IVT-mRNA and pDNA co-delivery methods

Experimental procedure

- IVT-mRNA synthesis coding for two different fluorescent proteins
- Co-transfection of cells with different methods using different types of carriers
- Isolation of monocytes from buffy coat and differentiation to human macrophages and co-transfection according to established condition
- Microscopic evaluation of transfected cells
- Quantitative measurement of genes co-expression/ expression and knock-down on single cell level using flow cytometry
- Quantitative measurement of encapsulation efficiency using RiboGreen assay

Analysis and interpretation of the data

- Analysis of microscopic images for comparison of genes co-expression patterns
- Analysis of flow cytometry data and creating different types of graphs to represent and compare data sets
- Statistical evaluation and comparison between different groups
- Quantification of encapsulation efficiency

Manuscript preparation

- Preparation of the manuscript outline, refined by discussion with the co-authors
- Writing the first draft of the manuscript; manuscript revision and finalization for first submission according to comments from the co-authors
- Revision of the manuscript based on additional data, incorporated to address reviewers comments and finalizing the revised manuscript together with the co-authors

---

[1] Study design was performed in discussion with co-authors.

Publication – Appendix IV

H. Moradian, A. Lendlein and M. Gossen: Strategies for simultaneous and successive delivery of RNA. *Journal of Molecular Medicine* 98, 1767 (2020). doi: 10.1007/s00109-020-01956-1.

Chapter 8: Discussion

In this chapter, the collective findings presented in chapters 4-7 are discussed in context of the recent state of the art. With the IVT-mRNA technology as the central focus of the studies, two subtopics are addressed: (i) IVT-mRNA as a tool for genetic engineering of macrophages, and (ii) strategies for IVT-mRNA co-delivery. The findings discussed in the first subtopic are presented in chapters 4 and 5. The second part, is dedicated to the methodological aspect relates to the data, which are presented in chapters 6 and 7.

8.1 IVT-mRNA as a tool for genetic engineering of macrophages

8.1.1 Challenges of macrophage immunomodulation via genetic engineering

As part of the innate immunsystem, macrophages play a pivotal role as stimulator of (adaptive) immune response by antigen presentation or cytokine secretion, and as the effector cell type, by phagocytosis of pathogens and damaged cells [9, 10, 127, 128]. Macrophages are able to differentiate to versatile phenotypes to accommodate these wide ranges of functions [13, 16, 22, 129, 130]. Given that macrophages are not terminally differentiated, they can respond to microenvironmental cues [14, 17, 18, 131, 132], as elaborated in details in previous chapters (see *Chapter 1 Introduction: 1.1Immunomodulation by macrophages*). This plasticity in the form of dynamic phenotypical changes and diversification in function, makes macrophages a unique and appealing candidate for immune modulation studies [19, 133]. Noteworthy, shifting macrophages activity to either end of pro-/anti-inflammatory spectrum could be of utmost interest, from basic studies to clinical applications [134, 135]. One prominent example is the activation of macrophages toward pro-inflammatory phenotype in immunosuppressive tumor microenvironment, also known as CAR-macrophage, as an immunotherapeutic strategy for cancer treatment [59, 136, 137]. On the contrary, numerous studies investigated the differentiation of macrophages to anti-inflammatory phenotype, which is of relevance in treatment of autoimmune diseases [138], as well as avoiding rejection of biomaterial implants [139-141] or organ transplants [58], due to local overstimulation of immune response. In both scenarios, finding approaches to change macrophages activity is the key to exploit them to orchestrate the immune response toward the desired direction [60].

Among the different approaches to polarize macrophages to the desired activity status [43, 142-145], genetic engineering methods are of particular interest [146-148]. Cues to modulate macrophages are often applied exogenously [149], and thereby might be subjected to uncontrollable changes

potentially influencing the response of macrophages. By contrast, genetic engineering provides cells with the instruction to produce their own modulatory factors [150-153]. However, successful gene transfer to macrophages has its own drawbacks, which might require extensive process adjustments for individual experiments. Limited cell proliferation impairs the successful use of pDNA as a nucleic acid entity for gene delivery to primary human macrophages, due to difficulties in overcoming the barrier of nucleus membrane and reaching the nucleus space, the target destination of pDNA, without transient nuclear envelop breakdown during mitosis [62]. Besides, viral gene delivery methods are facing the issue of safety and genotoxicity, a particular concern in therapeutic application and translational research [62]. Thus, IVT-mRNA was suggested as an alternative to the former methods for gene delivery, facing a less complex path for delivery, as mRNA is immediately translated to protein upon cytoplasmic delivery [67]. However, recognition of IVT-mRNA via numerous endosomal and cytosolic receptors and subsequent activation of immune response is the major restriction in mRNA-mediate genetic engineering of macrophages. Our initial attempt to transfect macrophages with IVT-mRNA also proved this notion [125]. While our original motivation was to reduce innate immune response in macrophages to support host-implant integration, the primary experimental evidences revealed macrophages polarizing to the opposite direction. Thus, the aim was redefined by raising the following scientific questions:

1. *Why are macrophages activated upon mRNA delivery? Is the induced immune response mainly triggered by carrier formula or the payload (mRNA) chemistry – or by both in combination?*
2. *What are the meaningful readouts to measure the immune activation of macrophages upon transfection?*
3. *How to address the issue of unintended immune activation?*

The systematic and explorative studies were designed to answer the above questions, which led us to establishment of both IVT-mRNA technology and efficient gene transfer to macrophages with minimal to negligible side effects, e.g. reduced viability and/or immune activation. The use of primary human monocytes and monocyte-derived macrophages was a centerpiece of this study. While numerous studies about monocytes and macrophages were performed *in vivo* using mouse models, the findings are of limited relevance for potential therapeutic applications, due to the substantial differences between immune system of mouse versus human [154]. Macrophage cell lines such as murine RAW 264.7 [155] and human THP-1 [156]were also commonly employed in gene delivery studies. Considering cell proliferation as a determining factor in

gene transfection, studying these immortalized cells with infinite proliferation capability is restricted in fully predicting the behavior of non-dividing primary cells. Thus, having more relevance for therapeutic applications, the primary human macrophages were implemented as an *in vitro* model throughout all our studies, the results of which are discussed in detail in the next sections.

8.1.2 The role of carrier formula and payload chemistry in transfection-induced immune response in macrophages

As the first line of response against invading pathogens as well as malfunctioning host cells, macrophages are equipped with numerous surface, endoplasmic and cytosolic receptors. While essential for keeping the homeostasis, the intricate network of pattern recognition receptors (PRRs) and subsequent signaling pathways in macrophages might restrict interventions based on gene delivery approaches, due to potential recognition of NAs as foreign intrusion [157]. Despite being a highly similar biomolecule to natural mRNA, IVT-mRNA can be recognized by the PRRs and thereby initiate the immune response [116, 119]. This can be attributed to the advanced defense mechanisms developed by cells in discriminating self- mRNAs from non-self viral RNAs [117]. First, the intracellular transport pathways and localization of these mRNAs are different. While endogenous mRNA is transcribed in the nucleus and transported to the cytoplasm to be harnessed as a blueprint for protein production, the IVT-mRNA is transported from the extracellular space primarily to the endosome and, upon endosomal escape, to the cytosol. Endosomal localization of mRNA is highly uncommon for cells, and can be recognized as a viral attack, sensed by numerous PRRs located in the endosomal membrane[116]. Macrophages can also recognize the free 5'phosphate-end and long double stranded structure in mRNA molecules as non-self viral RNA, involving a set of cytosolic receptors [158].

Transporting IVT-mRNA as a large polyanionic biomolecule through the hydrophobic membrane lining around any living cell requires a carrier system. Protection from extracellular nucleases, facilitating the intracellular transport, endosomal escape, and payload unpacking and release in the cytosol are some of the essential requirements for a carrier system [73, 113, 159]. Besides accommodating these functions in a most efficient manner, an ideal carrier system should minimize potential side effects, such as cytotoxicity or immunogenicity, caused by the carrier substance itself. The physicochemical properties of the carrier/payload complexes, such as size, shape, surface charge and colloidal stability determine the interaction of cells with carrier systems and the subsequent cell response [160]. The carrier can also interact with the microenvironmental cues both extra- and intracellularly such as pH, and redox condition [161].

This mutual interplay can be exploited to facilitate the stimuli-responsive delivery, or otherwise, when not envisaged thoroughly, result in degradation or destabilization of the carrier, and subsequent release of degradation products. The latter can cause cell stress, immune activation, and ultimately cytotoxic effects.

Two lipid-based and one polymeric-based carrier were investigated to evaluate the potential influence of carrier formula on immune response of transfected monocytes and macrophages. Our findings suggested LipoMM to outperform the polymeric ViroR in terms of viability, transfection efficiency and immunogenicity. These differences could be attributed to the intrinsic different nature of these lipoplexes and polyplexes, as they differ in physicochemical characteristics and thus their interaction with nucleic acids. Lipid-based carriers are composed of a hydrophilic cationic head group and a hydrophobic tail. The former accommodates the particles with capacity to complex the negatively charged nucleic acid molecules via electrostatic interaction, often in micellar, vesicle-like bilayer or multilamellar shape [162]. However, polyplexes might form complexes with branched spherical shape, or tubular structure. The molecular weight, geometry of the cationic polymer, and number of primary amines available at polymer surface are determining factors [163]. Surface charge, is another aspect, which might vary depending on carrier type [164]. While lipoplexes are known to have overall positive charge, also upon NA complexation [165], polyplexes such as ViroR/NA complexes, were reported to have neutral surface charge due to the special chemical structure of the polymeric carrier (information provided by supplier). Eventually, the endosomal release mechanism as a crucial step for a successful gene transfection varies in the two types of carriers. Lipoplexes might escape endosome and release their cargo into the cytosolic space by fusion to the endosomal membrane via their hydrophobic tail [163]. Polyplexes, on the other hand, have complete different mechanism known as proton sponge effect, which can be influenced by polymers physicochemical properties, such as surface charge and degree of ionization [163].

Despite the overall differences observed between the three carrier formulas were modest, chemical modification of mRNA found to have a pronounced effect, particularly on immune activation of transfected macrophages. In this regard, , the IFN-β secretion was reduced by up to two-orders of magnitude in macrophages transfected with Ψ/5meC modified compared to non-modified IVT-mRNA. These modifications were initially introduced by Kariko et al., who found reduced immune activation when transfected in primary human dendritic cells *in vitro* [123], and later when administrated *in vivo* [124, 166]. The level of modified IVT-mRNA expression was notably lower than for non-modified mRNA, consistently for all doses tested. These

findings emphasized the demand for seeking other nucleotide modifications with more optimal translation concomitant with less stimulation of immune response. Of note, the effect of IVT-mRNA transfection on cell viability, transfection efficiency, and immune activation proved to be dose-dependent, with more pronounced effects in monocytes compared to macrophages. Overall, these results indicated that it is well possible to strike a balance between maximizing gene transfer efficiency and minimizing pleiotropic effects triggered by the experimental manipulation of cells.

8.1.3 Parameters defining the IVT-mRNA performance in macrophages

Viability and transfection efficiency are commonly measured as key readouts in gene delivery studies. However, when transfecting immune cells, particularly cells of innate immunity, these two parameters are not sufficient to describe the cells response and effectiveness of the gene transfer. Multiple readouts were set to describe different aspects of cell response to explore a reliable and robust method for genetic engineering of macrophages with minimal side effects, elaborated as follows.

i) Translatability

The transgene expression was defined by percent of transfected cells as well as the intensity of protein production within each cell. Our data showed that these two parameters do not always change in the same direction, i.e., a higher level of expression was not always correlated to a higher transfection efficiency (Appendix I, Figure 3). Thus, it is crucial to identify the correlation between the process parameters and both transfection efficiency and level of transgene expression.

ii) Immunogenicity

Immune activation must be taken into account as the utmost important parameter, when studying gene transfer to macrophages. The immune response was evaluated by quantification of co-stimulatory surface molecule expression, i.e. CD80, as well as TNF-α and IL-6 proinflammatory cytokines, as well as IFN-β antiviral cytokine secretion. Measurements of surface molecules by flow cytometry provide information at single cell level, which can be correlated to the transgene expression for individual cells, whereas secretion of cytokines is measured for a pool of cells within each condition. The systematic side-by-side experiments revealed that the difference in cytokine secretion between macrophages transfected with various mRNA chemistries, was more pronounced than the CD80 expression (Appendix 5, Figure 5-7). This was in line with previous studies, in which quantification of type I interferons were

used as the key readout for measurement of antiviral immune response to mRNA transfection, also correlated to dsRNA content of samples in that case [87]. The higher resolution of differences in patterns of immune response makes cytokine secretion both a sensitive and conclusive readout, which is favorable for comparison of conditions with rather no recognizable difference in surface molecule expression [167].

iii) Viability

Viability was also measured as a critical output, which was often inversely correlated with immune activation of cells. In other words, conditions resulting in high levels of immune responses were found to have poor viability. Viability of transfected monocytes and macrophages varied in a dose-dependent way, where higher doses of mRNA resulted in the lower cell survival, particularly noticeable for monocytes with a more negative slope of viability curve (Appendix I, Figure 2).

8.1.4 Strategies to reduce undesired immune responses to IVT-mRNA transfection

Immune cells can recognize IVT-mRNA and thereby trigger immune responses mainly by three types of receptors; i) receptors recognizing ssRNA such as endosomal TLR-7/8 [123], ii) dsRNA sensors such as endosomal TLR-3 [168], and cytosolic RIG-I, MDA-5, PKR, AOS [119], and iii) receptors binding to uncapped 5'triphosphate (ds)mRNA, such as cytosolic RIG-I [169]. While having different downstream molecular mechanisms in activation of immune response, they ultimately result in the nuclear translocation of transcription factors such as NF-κB, IRF-3/7, and subsequent upregulation of proinflammatory cytokines such as IL1β, IL-6, TNF-α, and antiviral cytokines such as type I interferons, IFN-α and IFN-β [116, 167]. The latter binds to the interferon receptors on cells surfaces, triggering a secondary signaling pathway known as JAK/STAT cascade, which further upregulates expression of proinflammatory genes [116]. Once secreted to the extracellular milieu, interferons stimulate both autocrine and paracrine signaling pathways, which can result in propagation of immune activation to adjacent untransfected cells.

By understanding the three above-mentioned mechanisms, various strategies can be implemented to prevent immune activation caused by IVT-mRNA transfection, an issue recognized shortly after the first administration of IVT-mRNA in the early 2000s [170]. Of note, given the interconnected network of immune signaling pathways, modifications to inhibit one cascade might also be beneficial for blocking others. In the following, the approaches implemented in different studies to address the immunogenicity of IVT-mRNA are discussed, particularly in context of what was examined in this thesis and found to be effective in our

defined experimental set-up. These strategies are classified in three categories, corresponding to the above-mentioned mechanisms of immune response.

i) Strategies to reduce the activation by ssRNA

Initial efforts to address immunogenicity of IVT-mRNA mainly focused on altering mRNA chemistry by incorporation of modified nucleotides. In a systematic investigation, the immune response of dendritic cells (DC) transfected with naturally occurring RNA samples, derived from *E.coli* as well as total and fractionated mammalian RNAs, including nuclear, cytoplasmic, mitochondrial RNA, polyA-containing mRNA, and tRNA, were measured side-by-side [123]. Spurred by the pronounced abrogation of TNF-α secretion in DC transfected with tRNA samples containing nucleosides with versatile chemistry, Kariko et al. suggested that incorporation of similar modified nucleosides might reduce immune activation of IVT-mRNA. This notion was supported by experimental evidence, where they reported less immunogenicity for IVT-mRNAs transfected in human DCs. By exploiting TLR overexpressing cell lines, the effect of nucleoside modification was subsequently attributed to the TLR7/8 mediated immune response [123], and later to reduced PKR activation [120], and increased resistance to RNase L cleavage [171]. Another study examined various modified IVT-mRNA in an *in vivo* mouse model and found the combination of 2-thiouridine and 5-methylcytidine modifications to be beneficial in circumventing immune response [166]. In a more recent study by Vaidyanathan et al. a series of nucleoside and 5'Cap modifications were investigated. The performance of various modified IVT-mRNAs were measured both *in vitro* by transfection of THP-1 cells and *in vivo* by Cas9-mediated <u>in</u>sertion or <u>del</u>etion (indel) in the genome in a mouse model [82]. Noteworthy, the bottleneck for practical implementation of many chemically modified nucleosides is the inability of T7 RNA polymerase (T7RNAP) to accept these nucleosides as substrate for mRNA synthesis[80]. Moreover, synthetic non-natural nucleosides, such as fluorine-based modifications were also investigated both *in vitro* and *in vivo*. Despite successfully passing the preclinical studies in rodents, "Fialuridine" proved fatal in the first clinical trial due to hepatic and pancreatic toxicity [172]. This discrepancy of preclinical and clinical trial outcomes was later attributed to expression of a functional protein in mitochondrial membrane of human, called human equilibrative nucleo-side transporter 1 (hENT1), which does not exist in rodents [173]. In consequence the use of these and similar nucleotides was not further pursued for clinical applications.

In line with previous reports, our initial data revealed significant reduction in immune response of monocytes and macrophages transfected with 5meC/Ψ modified IVT-mRNA compared to

non-modified mRNA. However, two problems persisted. First, the immune response was not entirely abrogated, particularly for higher doses of IVT-mRNA. Second, the expression levels following modified IVT-mRNA transfection were remarkably lower than for non-modified IVT-mRNA. Thus, the aim was to address both issues, by performing an explorative study, where the IVT-mRNAs with various 5'Cap and nucleoside modifications were examined. Our findings revealed that uridine modifications play the crucial role in immunostimulatory potential of IVT-mRNA, especially compared with Cap modifications with no obvious influence on immune response. The importance of uridine modification can be attributed to interaction of modified RNA with TLR7/8 receptors. By elucidating the crystal structures of human TLR7/8, it was revealed that uridine has a binding site at dimerization interface, which was revealed to be essential for activation of these receptors and stimulation of the downstream signaling pathway [174, 175]. This observation inspired another strategies to circumvent immune activation, based on sequence optimization to decrease uridine content, and thereby TLR activation. Upon empirical evaluation, "uridine depletion" proved to be effective in the ablation of immune responses, especially when combined with the modification of IVT-mRNA with 5moU [82].

Altering the cellular uptake and intracellular trafficking pathways to avoid endosomal localization of IVT-mRNA is another strategy to escape mRNA recognition by TLR7/8 receptors and thus circumvent the immune stimulation caused by ssRNA. Most of the currently used lipid- and polymeric based carrier systems are taken up by cells via endocytosis, and thus end up in endosomes upon entering cells [176]Manzanares, 2020 #290}. Demands for carrier systems which could support active transport through cellular membrane independent of endocytosis is therefore of utmost interest. One example is the recently developed lipid formula, which was claimed to fuse to the cell membrane and release its content directly to the cytosolic space [177]. Harnessing physical methods for gene transfer such as electroporation is another method to directly reach the cytoplasm, through temporary pores within the cell membrane created by cells exposure to electrical field [178].

ii) Strategies to inhibit immune activation by dsRNA

There are multiple distinct sources of dsRNA with the potential to trigger immune activation. First, long dsRNA molecules, also referred to as "dsRNA contamination", formed by interaction of two reverse complement strands of ssRNA, one of which is unintended byproduct of mRNA synthesis by T7RNAP. Discussion of the underlying mechanisms of the unexpected activities of T7RNAP is beyond the scope of this study, but explicitly explained elsewhere [179-

[181]. Second, partial RNA duplexes, which are formed due to the interaction of intramolecular complementary sequences, also known as "secondary structure" of mRNA molecules [182]. Next, various strategies, envisaged and examined by previous studies to either prevent formation of RNA duplex or remove the dsRNA contamination, as the main source of IVT-mRNA immunogenicity are discussed. Of note, since the methods commonly used for recognition of dsRNA, such as immunoblotting, are incapable of distinction between the two types of dsRNA, here both are addressed as "dsRNA content" throughout the text.

Sequence optimization is an approach to tailor the stability, translatability, specificity of expression, as well as immunostimulatory effect of IVT-mRNA, depending on the segment to which changes are incorporated. Given that most often the specificity and stability of mRNA is modulated by 5'UTR and 3'UTR sequences, respectively, the corresponding highly stable secondary structures in these untranslated regions should be avoided, due to the potential influence on immunogenicity of mRNA. Likewise, the coding region sequence can be optimized to prevent formation of stable stem-loop secondary structures [183]. Besides, the sequence at 3'end region should be designed to prevent the spurious activity of T7RNAP, which can result in formation of long RNA molecules by extension of transcripts 3'end [81]. In such cases, the complementary sequences of the run-off products folds back and form a RNA molecule encompassing a long duplex structure [81]. Addition of polyA to the DNA template is one of the approaches, inhibiting the 3'end extension by T7RNAP [81], which was also taken up in this study.

Process parameters can determine the quality of the T7RNAP transcripts, and thereby the formation of dsRNA byproducts. Parameters such as magnesium concentration, as a co-factor for T7 enzyme [184], the molar ratio of NTPs [88], as well as the temperature of the reaction [185] were previously investigated. The latter refers to the high-temperature *in vitro* transcription using a thermostable T7RNAP, which was reported to be beneficial for reducing immunogenicity by preventing antisense RNA synthesis, and formation of the consequent long dsRNA [185]. The potential allosteric effect of UTP on T7RNAP can increase the affinity of T7RNAP to use the newly synthesized RNA molecules as template for transcription [186], and thus synthesis of antisense RNA as an unintended byproduct. The concentration of magnesium can have a crucial impact on proper activity of T7RNAP, resulting in reduced immunostimulatory properties as measured via MDA5 activation by the dsRNA [184].

Our findings revealed that the chemical modification of nucleosides can have a direct impact on the dsRNA content of the run-off transcripts (Appendix II, figure 3), which can be explained

43

from two different perspectives. First, some nucleoside modifications might render RNA duplexes less stable and thereby prevent formation of dsRNA of different sorts (i.e. internal secondary structure and long dsRNA). This notion was experimentally proved in a previous study, where the thermodynamic stability of RNA duplexes and hairpins were diminished, due to incorporation of modified adenosines, e.g. N^6-alkyladenosines, to RNA molecules [182]. Second, chemically modified nucleotides might interact differently with T7RNAP, which might influence its (unwanted) activities and the consequent quality of run-off transcripts. In this sense, further scrutiny is required to attribute the differences in dsRNA content of different mRNA chemistries, in particular uridine, to its above-mentioned allosteric effects on T7RNAP.

The majority of the above-mentioned approaches are useful strategies to prospectively avoid formation of dsRNA. However, purification of the transcripts facilitates removal of dsRNA byproducts as a post-transcriptional strategy. As elaborated previously, there are multiple purification methods used in different studies such as HPLC purification [87], cellulose purification [91], as well as using oligo(dT) columns [88]. The HPLC purification of mRNA was first suggested by Kariko et al., who reported a successful reduction in dsRNA content. By transfection of primary dendritic cells, they found significant less IFN-α production for HPLC-purified mRNA samples compared to non-purified, measured as prove of concept [87].

iii) Strategies to circumvent the activation by 5'triphosphate uncapped mRNAs

Recognition of the free 5'end containing a triphosphate group of long RNA molecules is one of the strategies, by which cells distinguish self- from non-self mRNA molecules. The 5'end of T7 transcripts are modified with a cap structure to resemble the endogenous mRNA and avoid recognition by receptors such as RIG-I [187]. In our study, two types of caps known as Cap 0 and Cap 1 structures, namely ARCA and CleanCap AG were investigated. Another Cap1 formula was also synthesized and investigated side-by-side, by post-transcriptional treatment of ARCA-capped IVT-mRNA with a methyl transferase enzyme. The differences between immunogenicity of the Cap 0 and the two Cap 1-modified IVT-mRNAs were modest and in some cases confounded. This was in line with a previous study by Vaidyanathan et al, where they found no significant difference between Cap 0 and Cap 1 modified mRNA investigated in vitro. While they reported Cap 1 to be less immunogenic than Cap 0, these differences were not statistically significant [82]. Of note, the effectiveness of Cap1 modified-RNA in reduction of RIG-I activation compared to Cap 0 was primarily reported for dsRNA structures, but not ssRNA [187].

As previously mentioned, the co-transcriptional capping is not 100% efficient, and part of transcripts carry a triphosphate group on their 5'end. Thus, dephosphorylation of mRNA was

suggested in some protocols to reduce the resulting immune activation. Our experimental results back that notion, in particular for high doses of mRNA, consistently for all three above-mentioned examined caps. However, the extent to which the immune response was reduced, was consistently higher for CleanCap. Since most of studies used CleanCap modification in combination with phosphatase treatment, there is no clear reference point to compare our findings against the literature. Nevertheless, the overall patterns of differences support the concept of implementing IVT-mRNA dephosphorelation for reduction of immune response.

8.1.5 Modulation of IVT-mRNA expression

Production of the encoded protein of interest is the ultimate aim of mRNA transfections, and is quantified and assessed by different methods as a key readout. In the course of the pilot study of IVT-mRNA, a substantial reduction in immunogenicity of Ψ/5meC modified IVT-mRNA was identified. However, the intensity of protein production was lower compared to non-modified IVT-mRNA (Appendix I, Fig. 3). Therefore, concomitant reduction or even abrogation of immune responses, with increasing the level of mRNA expression by modifying chemistry of IVT-mRNA was investigated.

By exploring different nucleoside modifications, 5moU modified IVT-mRNA was found to outperform other samples both in terms of a higher level of protein production and ablated immune response, when administrated in low those (Appendix II, Fig 4, and 7). This could be attributed to translation capacity of mRNAs with different chemistries. This notion is in line with a previous study by Svitkin et al. They found that me$^1\Psi$ modified mRNA has higher translatability compared to non-modified mRNA. This was then attributed toto the higher rates of ribosome recruitment and recycling in modified mRNA, measured by exploiting a cell-free system [188].

8.2 Strategies for IVT-mRNA co-delivery

Delivery of multiple NA entities to the same cell is essential for many advanced biological and also biotechnological studies. Examples are identification of non-florescent target protein production coupled with a reporter protein useful for live cell imaging [189], production of large multisubunit proteins [190], e.g. antibodies, and expression of enzyme complexes [191]. Moreover, expression of multiple genes coding for transcription factors [192], which can reprogram cell fate, such as dedifferentiation of somatic cells into iPSCs [193], are other prominent examples. To address the corresponding methodological demands, series of studies were performed aiming to find a reliable and robust co-delivery approach. First, to induce simultaneous overexpression

of two genes, a bicistronic approach to encode both genes separated co-translationally by a 2A peptide sequence was examined in comparison with a co-delivery of two monocistronic genes. Despite the equimolar nature of the bicistronic genes, between constructs with different genes positioned 5' to the 2A sequence, the expression level of the (common) 3' gene varied remarkably. Previous studies also suggested similar confounded pattern of co-expression, also when using different types of 2A peptides [194, 195].

Process parameters playing a major role in the outcomes of co-delivery studies could be identified. By quantifying the co-expression distinct patterns was identified for cells transfected with particles containing premixed (i.e., "integrated") nucleic acids, compared to cells transfected with mixtures of two types of particles, each complexed with either of the two marker genes (i. e., "parallel") (Figure 7.1). These conditions were examined both using IVT-mRNA as well as pDNA. While integrated co-transfection resulted in homogeneous co-expression of genes within each cell, the parallel co-transfection rendered cells expressing genes with heterogeneous patterns. Identifying such distinct co-expression schemes, independent of cell type, carrier type, and even NA type is beneficial in selecting a suitable method according to the experimental demands. For instance, it is critically important to have a reliable co-transfection method, which enables isolation of cells producing a non-fluorescent target protein coupled with fluorescent reporter protein by cell sorting methods[196].

Chapter 9: Summary and Outlook

Growing demands for advanced cell-based therapies draw more attention to reliable approaches to modulate cells response. Among those genetic engineering based methods are of ultimate importance. In this dissertation, an IVT-mRNA-based genetic engineering approach was established for primary human macrophages. Our findings suggested that mRNA chemistry affected transfection efficiency and more remarkably immune activation of macrophages. However, the differences among the three types of carriers examined in our defined experimental framework was moderate. The explorative study of IVT-mRNA chemistry revealed that nucleotide modifications play a pivotal role in translatability and immunostimulatory properties of transcripts, whereas the impact of the 5'end modifications was modest. Uridine modifications, in particular, lead to spectral differences in IVT-mRNA features and performance, as evidenced for pseudouridine versus 5-methoxyuridine modified IVT-mRNAs. Findings of this work is anticipated to provide direct guidance for advancing strategies to produce IVT-mRNA with minimal immunogenicity by the right choice of nucleotide chemistry, eliminating the need for subsequent purification steps. Despite the fact that purification can alleviate immune responses to transfected transcripts, addition of an extra step, such as chromatographic purification, e.g. HPLC, in the IVT-mRNA production pipeline can be a source of potential variations in the final mRNA products. This is of relevance for therapeutic applications of IVT-mRNA, when batch-to-batch differences of the products due to extra processing, e.g. mRNA integrity after recovery and potential residue of purification solvents must be prevented.

The versatility of IVT-mRNA applications and the corresponding required features underscores the demand for developing technologies to synthesis of mRNA with tailorable features. For instance, while lack of immune stimulation is quintessential for the majority of therapeutic applications such as protein replacement therapies, it might be beneficial for other applications, such as the adjuvant effect demanded for RNA vaccines. In this regard, our findings could serve future research by providing a scheme, where immunogenicity as well as transgene expression corresponding to the given modifications can be investigated in an *in vitro* experimental setup using primary human macrophages.

Predictive modeling of the gene transfer process to immune cells requires more than evaluation of the transfection efficiency, as the observed cell stress and immune stimulation were in part substantial, potentially interfering with the intended application. As it was evidenced in this

study, the unintended immune response to mRNA transfection hindered our primary attempt to polarize macrophages to anti-inflammatory cells, and moved our focus to establish the IVT technology to minimize these side effects. In this sense, two distinct perspectives can be defined in gene delivery to macrophages. First, to employ mRNA as a tool to modulate phenotype and function of macrophages as target cells, i.e. the primary motivation of this study. Second, to implement macrophages, the key cell type in innate immune response, as a tool to measure the immunogenicity of differently modified IVT-mRNAs. Thus, the scope of this part of the study extends well beyond macrophages with relevance to a much broader range of human cells, e.g. mesenchymal stem cells and endothelial cells. Noteworthy, the choice of primary human monocyte-derived macrophages was one of the defining unique features of this study, because it is more relevant for therapeutic applications compared to *in vivo* mouse models with different immune system. Further scrutiny might be carried out using macrophage models derived from induced pluripotent stem (iPS) cells [197], as an alternative to study and predict immune response. This might not only open, for example, new avenues of modulation of foreign body response to biomaterials, but also provide the starting point for implementing stratified or even personalized approaches to innate immune reactions in mRNA-based therapies.

In addressing methodological aspects for the combined expression of multiple genes, series of studies were performed based on different payload designs, and variations of process parameters. The quantitative scheme of co-expression at single cell level identified for each method provides a guideline for future studies to select the experimental setup consolidating their intended requirements, by eliminating the risk of random methodological choices. For instance, the homogeneous expression is essential for detection of a target gene expression via co-expression with a marker gene. In contrast, in some biotechnological studies, e.g. genetic circuits, heterogeneous pattern of co-expression is of interest [198]. Of note, these data also emphasize the necessity of empirical evaluation of envisaged strategies, because the results are not always in line with theoretical assumptions. For example, despite the intrinsic equimolar composition of two genes in bicistronic NA constructs, it was found that the co-expression patterns were often confounded, which might depend on the sequence of the first gene.

The future perspectives for this research technology-oriented studies, which could further advance the synthetic mRNA-mediated genetic engineering, and in application-oriented studies, which can turn the current findings into practical applications, by employing the IVT-mRNA as a tool to substantiate their intended function.

Technology-oriented studies might continue to further improve *in vitro* transcription process, IVT-mRNA features, and delivery systems to consolidate IVT-mRNA genetic engineering and breach the existing barriers. Modifying the mRNA synthesis pipeline by rational selection of template, precursors, i.e. nucleosides, reaction conditions, and enzymes could improve the quality of transcripts to prevent production of unintended byproducts, and thus eliminate the need for extra purification steps, as described previously. Specificity and stability of transcripts can be customized, by implementing mRNA structural features such as 5' and 3'UTRs. In this regards, the high-throughput screening of UTR libraries for different cell types would be beneficial [79]. Despite the transient nature of mRNA expression, this period can be prolonged using self-replicating mRNAs, which trigger cell activation patterns identical to those described here in the early phase upon delivery. Self-amplifying RNAs originated from alphaviruses can be replicated within cytoplasm upon delivery and increase the lifespan of RNA to more than a month. In case the sustained production of protein in low dose is sufficient to fulfill the defined function, self-amplifying RNA could be delivered without the need for a carrier system. For instance, a type of self-amplifying RNA encoding influenza hemagglutinin antigen was evaluated *in vivo*. The findings suggested that due to the self-amplification of RNA in cytoplasm, the initial low amounts of this RNA was adequate to elicit neutralizing antibody production and activate the protective immune response [199]. Alternatively, the transgene expression can be extended by repeated transfections of mRNA in given intervals. However, this method is not preferred due to transfection-induced cell stress, which is a bottleneck for sensitive primary cells. In this case controlled delivery systems could provide a solution by extending the release patterns of NAs. Further strategies remain to be tested to further develop and address potential safety issues of self-amplifying RNAs, which would be beneficial to expand the range of mRNA applications.

Design of delivery systems to protect mRNAs from degradation and support their sustained release is helpful in paving the way for therapeutic application of mRNA. In this sense, chemical and physical selection criteria might be considered for "on-demand" as well as "targeted" mRNA delivery using "multifunctional" carrier systems. The former is beneficial when timely delayed delivery of mRNA is intended, whereas the latter would facilitate delivery of mRNA to a specific cell type, where it is aimed to perform its function. Moreover, by enabling the active transmembrane transport and thus prohibiting mRNA to encounter endosomal receptors, future delivery systems might help to reduce the potential immune stimulation of cells.

Application-oriented studies might also benefit from the mRNA-based genetic engineering approach established in this study. These findings can pave the way for transfection of other sensitive primary human cells such as endothelial cells and mesenchymal stem cells, both relevant for therapeutic applications. Moreover, the current experimental framework in macrophages can be followed by studies to modulate macrophages immune response. This is of utmost interest for controlling the foreign body response to implants. Further, the incorporation of mRNA/carrier complex to porous scaffolds, also known as transcript activated matrixes (TAMs) [200] could lead to formation of the next generation of highly specific immunomodulatory biomaterials.

References

1. S.E. Turvey and D.H. Broide: Innate immunity. *Journal of Allergy and Clinical Immunology* **125**, S24 (2010).
2. S.R. Paludan, T. Pradeu, S.L. Masters and T.H. Mogensen: Constitutive immune mechanisms: mediators of host defence and immune regulation. *Nature Reviews Immunology* **21**, 137 (2021).
3. A. Iwasaki and R. Medzhitov: Control of adaptive immunity by the innate immune system. *Nature Immunology* **16**, 343 (2015).
4. R. Medzhitov: Origin and physiological roles of inflammation. *Nature* **454**, 428 (2008).
5. E. Vivier and B. Malissen: Innate and adaptive immunity: specificities and signaling hierarchies revisited. *Nature Immunology* **6**, 17 (2005).
6. A. Liston and S.L. Masters: Homeostasis-altering molecular processes as mechanisms of inflammasome activation. *Nature Reviews Immunology* **17**, 208 (2017).
7. P.J. Murray and T.A. Wynn: Protective and pathogenic functions of macrophage subsets. *Nature Reviews Immunology* **11**, 723 (2011).
8. M. De Santis, M. Locati and C. Selmi: The elegance of a macrophage. *Cellular & Molecular Immunology* **15**, 196 (2018).
9. S. Gordon and L. Martinez-Pomares: Physiological roles of macrophages. *Pflügers Archiv - European Journal of Physiology* **469**, 365 (2017).
10. X. Zhang and D.M. Mosser: Macrophage activation by endogenous danger signals. *The Journal of pathology* **214**, 161 (2008).
11. G. Sreejit, A.J. Fleetwood, A.J. Murphy and P.R. Nagareddy: Origins and diversity of macrophages in health and disease. *Clinical & translational immunology* **9**, e1222 (2020).
12. L.C. Davies, S.J. Jenkins, J.E. Allen and P.R. Taylor: Tissue-resident macrophages. *Nature Immunology* **14**, 986 (2013).
13. S. Gordon and P.R. Taylor: Monocyte and macrophage heterogeneity. *Nature Reviews Immunology* **5**, 953 (2005).
14. F. Geissmann, S. Gordon, D.A. Hume, A.M. Mowat and G.J. Randolph: Unravelling mononuclear phagocyte heterogeneity. *Nature Reviews Immunology* **10**, 453 (2010).
15. A.R. Muñoz-Rojas, I. Kelsey, J.L. Pappalardo, M. Chen and K. Miller-Jensen: Co-stimulation with opposing macrophage polarization cues leads to orthogonal secretion programs in individual cells. *Nature communications* **12** (2021).
16. S. Gordon: Alternative activation of macrophages. *Nature Reviews Immunology* **3**, 23 (2003).
17. F.O. Martinez, A. Sica, A. Mantovani and M. Locati: Macrophage activation and polarization. *Frontiers in bioscience : a journal and virtual library* **13**, 453 (2008).
18. D.M. Mosser and J.P. Edwards: Exploring the full spectrum of macrophage activation. *Nature reviews. Immunology* **8**, 958 (2008).
19. S.K. Biswas and A. Mantovani: Macrophage plasticity and interaction with lymphocyte subsets: cancer as a paradigm. *Nature Immunology* **11**, 889 (2010).
20. R. Medzhitov and T. Horng: Transcriptional control of the inflammatory response. *Nature Reviews Immunology* **9**, 692 (2009).
21. M. Orecchioni, Y. Ghosheh, A.B. Pramod and K. Ley: Macrophage Polarization: Different Gene Signatures in M1(LPS+) vs. Classically and M2(LPS–) vs. Alternatively Activated Macrophages. *Frontiers in immunology* **10** (2019).
22. D.M. Mosser: The many faces of macrophage activation. *Journal of leukocyte biology* **73**, 209 (2003).

23. J. Xue, Susanne V. Schmidt, J. Sander, A. Draffehn, W. Krebs, I. Quester, D. De Nardo, Trupti D. Gohel, M. Emde, L. Schmidleithner, H. Ganesan, A. Nino-Castro, Michael R. Mallmann, L. Labzin, H. Theis, M. Kraut, M. Beyer, E. Latz, Tom C. Freeman, T. Ulas and Joachim L. Schultze: Transcriptome-Based Network Analysis Reveals a Spectrum Model of Human Macrophage Activation. *Immunity* **40**, 274 (2014).

24. F. Ginhoux, J.L. Schultze, P.J. Murray, J. Ochando and S.K. Biswas: New insights into the multidimensional concept of macrophage ontogeny, activation and function. *Nature Immunology* **17**, 34 (2016).

25. S. Arlauckas, N. Oh, R. Li, R. Weissleder and M.A. Miller: Macrophage imaging and subset analysis using single-cell RNA sequencing. *Nanotheranostics* **5**, 36 (2021).

26. R. Sridharan, A.R. Cameron, D.J. Kelly, C.J. Kearney and F.J. O'Brien: Biomaterial based modulation of macrophage polarization: a review and suggested design principles. *Materials Today* **18**, 313 (2015).

27. J.K. Antonios, Z. Yao, C. Li, A.J. Rao and S.B. Goodman: Macrophage polarization in response to wear particles in vitro. *Cellular & Molecular Immunology* **10**, 471 (2013).

28. T.B. Vijaya Bhaskar, N. Ma, A. Lendlein and T. Roch: The interaction of human macrophage subsets with silicone as a biomaterial. *Clinical hemorheology and microcirculation* **61**, 119 (2015).

29. J.M. Anderson, A. Rodriguez and D.T. Chang: Foreign body reaction to biomaterials. *Seminars in Immunology* **20**, 86 (2008).

30. D. Williams: Essential Biomaterials Science, (Cambridge University Press, Cambridge, 2014).

31. R. Klopfleisch and F. Jung: The pathology of the foreign body reaction against biomaterials. *Journal of Biomedical Materials Research Part A* **105**, 927 (2017).

32. D.W. Grainger: All charged up about implanted biomaterials. *Nature Biotechnology* **31**, 507 (2013).

33. R. Klopfleisch and F. Jung: The pathology of the foreign body reaction against biomaterials. *Journal of biomedical materials research. Part A* **105**, 927 (2017).

34. Y. Wang, Y. Fan and H. Liu: Macrophage Polarization in Response to Biomaterials for Vascularization. *Annals of biomedical engineering* (2021).

35. R. Klopfleisch: Macrophage reaction against biomaterials in the mouse model - Phenotypes, functions and markers. *Acta biomaterialia* **43**, 3 (2016).

36. J.M. Morais, F. Papadimitrakopoulos and D.J. Burgess: Biomaterials/tissue interactions: possible solutions to overcome foreign body response. *The AAPS journal* **12**, 188 (2010).

37. B.N. Brown, J.E. Valentin, A.M. Stewart-Akers, G.P. McCabe and S.F. Badylak: Macrophage phenotype and remodeling outcomes in response to biologic scaffolds with and without a cellular component. *Biomaterials* **30**, 1482 (2009).

38. Y.K. Kim, E.Y. Chen and W.F. Liu: Biomolecular strategies to modulate the macrophage response to implanted materials. *Journal of Materials Chemistry B* **4**, 1600 (2016).

39. L. Davenport Huyer, S. Pascual-Gil, Y. Wang, S. Mandla, B. Yee and M. Radisic: Advanced Strategies for Modulation of the Material–Macrophage Interface. *Advanced Functional Materials* **30**, 1909331 (2020).

40. C. Chu, L. Liu, S. Rung, Y. Wang, Y. Ma, C. Hu, X. Zhao, Y. Man and Y. Qu: Modulation of foreign body reaction and macrophage phenotypes concerning microenvironment. *Journal of biomedical materials research. Part A* **108**, 127 (2020).

41. L.S. Saleh and S.J. Bryant: The Host Response in Tissue Engineering: Crosstalk Between Immune cells and Cell-laden Scaffolds. *Current opinion in biomedical engineering* **6**, 58 (2018).

42. Y. Liu and T. Segura: Biomaterials-Mediated Regulation of Macrophage Cell Fate. *Frontiers in bioengineering and biotechnology* **8** (2020).

43. M.J. Vassey, G.P. Figueredo, D.J. Scurr, A.S. Vasilevich, S. Vermeulen, A. Carlier, J. Luckett, N.R.M. Beijer, P. Williams, D.A. Winkler, J. de Boer, A.M. Ghaemmaghami and M.R. Alexander: Immune Modulation by Design: Using Topography to Control Human Monocyte Attachment and Macrophage Differentiation. *Advanced science (Weinheim, Baden-Wurttemberg, Germany)* **7**, 1903392 (2020).

44. F.Y. McWhorter, C.T. Davis and W.F. Liu: Physical and mechanical regulation of macrophage phenotype and function. *Cellular and Molecular Life Sciences* **72**, 1303 (2015).

45. S. Chen, J.A. Jones, Y. Xu, H.-Y. Low, J.M. Anderson and K.W. Leong: Characterization of topographical effects on macrophage behavior in a foreign body response model. *Biomaterials* **31**, 3479 (2010).

46. Y. Luan, H.C. Van Der Mei, M. Dijk, G.I. Geertsema-Doornbusch, J. Atema-Smit, Y. Ren, H. Chen and H.J. Busscher: Polarization of Macrophages, Cellular Adhesion, and Spreading on Bacterially Contaminated Gold Nanoparticle-Coatings in Vitro. *ACS Biomaterials Science & Engineering* **6**, 933 (2020).

47. D.F. Moyano, Y. Liu, D. Peer and V.M. Rotello: Modulation of Immune Response Using Engineered Nanoparticle Surfaces. *Small (Weinheim an der Bergstrasse, Germany)* **12**, 76 (2016).

48. P.A. Alvarado-Vazquez, L. Bernal, C.A. Paige, R.L. Grosick, C. Moracho Vilrriales, D.W. Ferreira, C. Ulecia-Morón and E.A. Romero-Sandoval: Macrophage-specific nanotechnology-driven CD163 overexpression in human macrophages results in an M2 phenotype under inflammatory conditions. *Immunobiology* **222**, 900 (2017).

49. J.E. Glim, F.B. Niessen, V. Everts, M. van Egmond and R.H. Beelen: Platelet derived growth factor-CC secreted by M2 macrophages induces alpha-smooth muscle actin expression by dermal and gingival fibroblasts. *Immunobiology* **218**, 924 (2013).

50. N. Mokarram, A. Merchant, V. Mukhatyar, G. Patel and R.V. Bellamkonda: Effect of modulating macrophage phenotype on peripheral nerve repair. *Biomaterials* **33**, 8793 (2012).

51. L. Li, D.S.W. Ng, W.C. Mah, F.F. Almeida, S.A. Rahmat, V.K. Rao, S.C. Leow, F. Laudisi, M.T. Peh, A.M. Goh, J.S.Y. Lim, G.D. Wright, A. Mortellaro, R. Taneja, F. Ginhoux, C.G. Lee, P.K. Moore and D.P. Lane: A unique role for p53 in the regulation of M2 macrophage polarization. *Cell Death & Differentiation* **22**, 1081 (2015).

52. C. Wang, B. Yu, B. Knudsen, J. Harmon, F. Moussy and Y. Moussy: Synthesis and performance of novel hydrogels coatings for implantable glucose sensors. *Biomacromolecules* **9**, 561 (2008).

53. D. Grafahrend, K.H. Heffels, M.V. Beer, P. Gasteier, M. Möller, G. Boehm, P.D. Dalton and J. Groll: Degradable polyester scaffolds with controlled surface chemistry combining minimal protein adsorption with specific bioactivation. *Nature materials* **10**, 67 (2011).

54. S. Jiang and Z. Cao: Ultralow-fouling, functionalizable, and hydrolyzable zwitterionic materials and their derivatives for biological applications. *Advanced materials (Deerfield Beach, Fla.)* **22**, 920 (2010).

55. A.D. Lynn, A.K. Blakney, T.R. Kyriakides and S.J. Bryant: Temporal progression of the host response to implanted poly(ethylene glycol)-based hydrogels. *Journal of biomedical materials research. Part A* **96**, 621 (2011).

56. S. Minardi, B. Corradetti, F. Taraballi, J.H. Byun, F. Cabrera, X. Liu, M. Ferrari, B.K. Weiner and E. Tasciotti: IL-4 Release from a Biomimetic Scaffold for the Temporally Controlled Modulation of Macrophage Response. *Annals of biomedical engineering* **44**, 2008 (2016).

57.   M.C.P. Sok, N. Baker, C. McClain, H.S. Lim, T. Turner, L. Hymel, M. Ogle, C. Olingy, J.I. Palacios, J.R. Garcia, K. Srithar, A.J. García, P. Qiu and E.A. Botchwey: Dual delivery of IL-10 and AT-RvD1 from PEG hydrogels polarize immune cells towards pro-regenerative phenotypes. *Biomaterials* **268**, 120475 (2021).

58.   F. Ordikhani, V. Pothula, R. Sanchez-Tarjuelo, S. Jordan and J. Ochando: Macrophages in Organ Transplantation. *Frontiers in immunology* **11** (2020).

59.   D. Cortés-Selva, B. Dasgupta, S. Singh and I.S. Grewal: Innate and Innate-Like Cells: The Future of Chimeric Antigen Receptor (CAR) Cell Therapy. *Trends in pharmacological sciences* **42**, 45 (2021).

60.   E. Mass and N. Lachmann: From macrophage biology to macrophage-based cellular immunotherapies. *Gene Therapy* (2021).

61.   R.M. Gower, R.M. Boehler, S.M. Azarin, C.F. Ricci, J.N. Leonard and L.D. Shea: Modulation of leukocyte infiltration and phenotype in microporous tissue engineering scaffolds via vector induced IL-10 expression. *Biomaterials* **35**, 2024 (2014).

62.   U. Sahin, K. Karikó and Ö. Türeci: mRNA-based therapeutics — developing a new class of drugs. *Nature Reviews Drug Discovery* **13**, 759 (2014).

63.   N. Dammes and D. Peer: Paving the Road for RNA Therapeutics. *Trends in pharmacological sciences* **41**, 755 (2020).

64.   N. Pardi, M.J. Hogan, F.W. Porter and D. Weissman: mRNA vaccines — a new era in vaccinology. *Nature Reviews Drug Discovery* **17**, 261 (2018).

65.   T.R. Damase, R. Sukhovershin, C. Boada, F. Taraballi, R.I. Pettigrew and J.P. Cooke: The Limitless Future of RNA Therapeutics. *Frontiers in bioengineering and biotechnology* **9** (2021).

66.   M.F. Coutinho, L. Matos, J.I. Santos and S. Alves: RNA Therapeutics: How Far Have We Gone?, (Springer International Publishing2019), pp. 133.

67.   I. Tombácz, D. Weissman and N. Pardi: Vaccination with Messenger RNA: A Promising Alternative to DNA Vaccination, (Springer US2021), pp. 13.

68.   J.A. Wolff, R.W. Malone, P. Williams, W. Chong, G. Acsadi, A. Jani and P.L. Felgner: Direct gene transfer into mouse muscle in vivo. *Science (New York, N.Y.)* **247**, 1465 (1990).

69.   A. Choi, M. Koch, K. Wu, L. Chu, L. Ma, A. Hill, N. Nunna, W. Huang, J. Oestreicher, T. Colpitts, H. Bennett, H. Legault, Y. Paila, B. Nestorova, B. Ding, D. Montefiori, R. Pajon, J.M. Miller, B. Leav, A. Carfi, R. McPhee and D.K. Edwards: Safety and immunogenicity of SARS-CoV-2 variant mRNA vaccine boosters in healthy adults: an interim analysis. *Nature Medicine* (2021).

70.   J.S. Turner, J.A. O'Halloran, E. Kalaidina, W. Kim, A.J. Schmitz, J.Q. Zhou, T. Lei, M. Thapa, R.E. Chen, J.B. Case, F. Amanat, A.M. Rauseo, A. Haile, X. Xie, M.K. Klebert, T. Suessen, W.D. Middleton, P.-Y. Shi, F. Krammer, S.A. Teefey, M.S. Diamond, R.M. Presti and A.H. Ellebedy: SARS-CoV-2 mRNA vaccines induce persistent human germinal centre responses. *Nature* **596**, 109 (2021).

71.   Z. Wang, F. Schmidt, Y. Weisblum, F. Muecksch, C.O. Barnes, S. Finkin, D. Schaefer-Babajew, M. Cipolla, C. Gaebler, J.A. Lieberman, T.Y. Oliveira, Z. Yang, M.E. Abernathy, K.E. Huey-Tubman, A. Hurley, M. Turroja, K.A. West, K. Gordon, K.G. Millard, V. Ramos, J. Da Silva, J. Xu, R.A. Colbert, R. Patel, J. Dizon, C. Unson-O'Brien, I. Shimeliovich, A. Gazumyan, M. Caskey, P.J. Bjorkman, R. Casellas, T. Hatziioannou, P.D. Bieniasz and M.C. Nussenzweig: mRNA vaccine-elicited antibodies to SARS-CoV-2 and circulating variants. *Nature* **592**, 616 (2021).

72.   S.S. Rosa, D.M.F. Prazeres, A.M. Azevedo and M.P.C. Marques: mRNA vaccines manufacturing: Challenges and bottlenecks. *Vaccine* **39**, 2190 (2021).

73.   A. Wadhwa, A. Aljabbari, A. Lokras, C. Foged and A. Thakur: Opportunities and Challenges in the Delivery of mRNA-Based Vaccines. *Pharmaceutics* **12**, 102 (2020).

74. S. Hacein-Bey-Abina, A. Garrigue, G.P. Wang, J. Soulier, A. Lim, E. Morillon, E. Clappier, L. Caccavelli, E. Delabesse, K. Beldjord, V. Asnafi, E. MacIntyre, L. Dal Cortivo, I. Radford, N. Brousse, F. Sigaux, D. Moshous, J. Hauer, A. Borkhardt, B.H. Belohradsky, U. Wintergerst, M.C. Velez, L. Leiva, R. Sorensen, N. Wulffraat, S. Blanche, F.D. Bushman, A. Fischer and M. Cavazzana-Calvo: Insertional oncogenesis in 4 patients after retrovirus-mediated gene therapy of SCID-X1. *J Clin Invest* **118**, 3132 (2008).

75. Z. Meng, J. O'Keeffe-Ahern, J. Lyu, L. Pierucci, D. Zhou and W. Wang: A new developing class of gene delivery: messenger RNA-based therapeutics. *Biomaterials Science* **5**, 2381 (2017).

76. H. Steinle, A. Behring, C. Schlensak, H.P. Wendel and M. Avci-Adali: Concise Review: Application of In Vitro Transcribed Messenger RNA for Cellular Engineering and Reprogramming: Progress and Challenges. *Stem cells (Dayton, Ohio)* **35**, 68 (2017).

77. K.Y. Paek, K.Y. Hong, I. Ryu, S.M. Park, S.J. Keum, O.S. Kwon and S.K. Jang: Translation initiation mediated by RNA looping. *Proceedings of the National Academy of Sciences* **112**, 1041 (2015).

78. I. Kocmik, K. Piecyk, M. Rudzinska, A. Niedzwiecka, E. Darzynkiewicz, R. Grzela and M. Jankowska-Anyszka: Modified ARCA analogs providing enhanced translational properties of capped mRNAs. *Cell Cycle* **17**, 1624 (2018).

79. P.J. Sample, B. Wang, D.W. Reid, V. Presnyak, I.J. McFadyen, D.R. Morris and G. Seelig: Human 5′ UTR design and variant effect prediction from a massively parallel translation assay. *Nature Biotechnology* **37**, 803 (2019).

80. N. Milisavljevič, P. Perlíková, R. Pohl and M. Hocek: Enzymatic synthesis of base-modified RNA by T7 RNA polymerase. A systematic study and comparison of 5-substituted pyrimidine and 7-substituted 7-deazapurine nucleoside triphosphates as substrates. *Organic & Biomolecular Chemistry* **16**, 5800 (2018).

81. Y. Gholamalipour, Aruni and C.T. Martin: 3′ end additions by T7 RNA polymerase are RNA self-templated, distributive and diverse in character—RNA-Seq analyses. *Nucleic Acids Research* **46**, 9253 (2018).

82. S. Vaidyanathan, K.T. Azizian, A.K.M.A. Haque, J.M. Henderson, A. Hendel, S. Shore, J.S. Antony, R.I. Hogrefe, M.S.D. Kormann, M.H. Porteus and A.P. McCaffrey: Uridine Depletion and Chemical Modification Increase Cas9 mRNA Activity and Reduce Immunogenicity without HPLC Purification. *Molecular Therapy - Nucleic Acids* **12**, 530 (2018).

83. A.-L. Fuchs, A. Neu and R. Sprangers: A general method for rapid and cost-efficient large-scale production of 5' capped RNA. *RNA (New York, N.Y.)* **22**, 1454 (2016).

84. M. Avci-Adali, A. Behring, H. Steinle, T. Keller, S. Krajeweski, C. Schlensak and H.P. Wendel: In vitro synthesis of modified mRNA for induction of protein expression in human cells. *J Vis Exp*, e51943 (2014).

85. M. Strenkowska, R. Grzela, M. Majewski, K. Wnek, J. Kowalska, M. Lukaszewicz, J. Zuberek, E. Darzynkiewicz, A.N. Kuhn, U. Sahin and J. Jemielity: Cap analogs modified with 1,2-dithiodiphosphate moiety protect mRNA from decapping and enhance its translational potential. *Nucleic Acids Res* **44**, 9578 (2016).

86. P.J. Sikorski, M. Warminski, D. Kubacka, T. Ratajczak, D. Nowis, J. Kowalska and J. Jemielity: The identity and methylation status of the first transcribed nucleotide in eukaryotic mRNA 5′ cap modulates protein expression in living cells. *Nucleic Acids Research* **48**, 1607 (2020).

87. K. Karikó, H. Muramatsu, J. Ludwig and D. Weissman: Generating the optimal mRNA for therapy: HPLC purification eliminates immune activation and improves

translation of nucleoside-modified, protein-encoding mRNA. *Nucleic Acids Research* **39**, e142 (2011).

88. J. Nelson, E.W. Sorensen, S. Mintri, A.E. Rabideau, W. Zheng, G. Besin, N. Khatwani, S.V. Su, E.J. Miracco, W.J. Issa, S. Hoge, M.G. Stanton and J.L. Joyal: Impact of mRNA chemistry and manufacturing process on innate immune activation. *Science Advances* **6**, eaaz6893 (2020).

89. M.R. Green and J. Sambrook: Isolation of Poly(A)(+) Messenger RNA Using Magnetic Oligo(dT) Beads. *Cold Spring Harbor protocols* **2019** (2019).

90. V. Iadevaia, A.M. Matia-González and A.P. Gerber: An Oligonucleotide-based Tandem RNA Isolation Procedure to Recover Eukaryotic mRNA-Protein Complexes. *J Vis Exp*, 58223 (2018).

91. M. Baiersdörfer, G. Boros, H. Muramatsu, A. Mahiny, I. Vlatkovic, U. Sahin and K. Karikó: A Facile Method for the Removal of dsRNA Contaminant from In Vitro-Transcribed mRNA. *Molecular Therapy - Nucleic Acids* **15**, 26 (2019).

92. A. Heine, S. Juranek and P. Brossart: Clinical and immunological effects of mRNA vaccines in malignant diseases. *Molecular cancer* **20**, 52 (2021).

93. S. Patel, A. Athirasala, P.P. Menezes, N. Ashwanikumar, T. Zou, G. Sahay and L.E. Bertassoni: Messenger RNA Delivery for Tissue Engineering and Regenerative Medicine Applications. *Tissue engineering. Part A* **25**, 91 (2019).

94. S. Kawasaki, Y. Fujita, T. Nagaike, K. Tomita and H. Saito: Synthetic mRNA devices that detect endogenous proteins and distinguish mammalian cells. *Nucleic Acids Res* **45**, e117 (2017).

95. H.X. Zhang, Y. Zhang and H. Yin: Genome Editing with mRNA Encoding ZFN, TALEN, and Cas9. *Molecular therapy : the journal of the American Society of Gene Therapy* **27**, 735 (2019).

96. D.-D. Wu, J. Song, S. Bartel, S. Krauss-Etschmann, M.G. Rots and M.N. Hylkema: The potential for targeted rewriting of epigenetic marks in COPD as a new therapeutic approach. *Pharmacology & therapeutics* **182**, 1 (2018).

97. L. Van Hoecke, R. Verbeke, H. Dewitte, I. Lentacker, K. Vermaelen, K. Breckpot and S. Van Lint: mRNA in cancer immunotherapy: beyond a source of antigen. *Molecular cancer* **20** (2021).

98. I. Sahu, A.K.M.A. Haque, B. Weidensee, P. Weinmann and M.S.D. Kormann: Recent Developments in mRNA-Based Protein Supplementation Therapy to Target Lung Diseases. *Molecular Therapy* **27**, 803 (2019).

99. A. Esprit, W. de Mey, R. Bahadur Shahi, K. Thielemans, L. Franceschini and K. Breckpot: Neo-Antigen mRNA Vaccines. *Vaccines* **8** (2020).

100. R. Verbeke, I. Lentacker, S.C. De Smedt and H. Dewitte: Three decades of messenger RNA vaccine development. *Nano Today* **28**, 100766 (2019).

101. N. Pardi, K. Parkhouse, E. Kirkpatrick, M. McMahon, S.J. Zost, B.L. Mui, Y.K. Tam, K. Karikó, C.J. Barbosa, T.D. Madden, M.J. Hope, F. Krammer, S.E. Hensley and D. Weissman: Nucleoside-modified mRNA immunization elicits influenza virus hemagglutinin stalk-specific antibodies. *Nature communications* **9** (2018).

102. B.F. Haynes: SARS-CoV-2 and HIV-1 — a tale of two vaccines. *Nature Reviews Immunology* **21**, 543 (2021).

103. A. Pattnaik, B.R. Sahoo and A.K. Pattnaik: Current Status of Zika Virus Vaccines: Successes and Challenges. *Vaccines* **8**, 266 (2020).

104. A. Ely, P. Singh, T.S. Smith and P. Arbuthnot: In vitro transcribed mRNA for expression of designer nucleases: Advantages as a novel therapeutic for the management of chronic HBV infection. *Advanced drug delivery reviews* **168**, 134 (2021).

105. K.S. Corbett, D.K. Edwards, S.R. Leist, O.M. Abiona, S. Boyoglu-Barnum, R.A. Gillespie, S. Himansu, A. Schäfer, C.T. Ziwawo, A.T. DiPiazza, K.H. Dinnon, S.M. Elbashir, C.A. Shaw, A. Woods, E.J. Fritch, D.R. Martinez, K.W. Bock, M. Minai, B.M. Nagata, G.B. Hutchinson, K. Wu, C. Henry, K. Bahl, D. Garcia-Dominguez, L. Ma, I. Renzi, W.P. Kong, S.D. Schmidt, L. Wang, Y. Zhang, E. Phung, L.A. Chang, R.J. Loomis, N.E. Altaras, E. Narayanan, M. Metkar, V. Presnyak, C. Liu, M.K. Louder, W. Shi, K. Leung, E.S. Yang, A. West, K.L. Gully, L.J. Stevens, N. Wang, D. Wrapp, N.A. Doria-Rose, G. Stewart-Jones, H. Bennett, G.S. Alvarado, M.C. Nason, T.J. Ruckwardt, J.S. McLellan, M.R. Denison, J.D. Chappell, I.N. Moore, K.M. Morabito, J.R. Mascola, R.S. Baric, A. Carfi and B.S. Graham: SARS-CoV-2 mRNA vaccine design enabled by prototype pathogen preparedness. *Nature* **586**, 567 (2020).
106. L. Van Hoecke, R. Verbeke, H. Dewitte, I. Lentacker, K. Vermaelen, K. Breckpot and S. Van Lint: mRNA in cancer immunotherapy: beyond a source of antigen. *Molecular cancer* **20**, 48 (2021).
107. T. Soundara Rajan, A. Gugliandolo, P. Bramanti and E. Mazzon: In Vitro-Transcribed mRNA Chimeric Antigen Receptor T Cell (IVT mRNA CAR T) Therapy in Hematologic and Solid Tumor Management: A Preclinical Update. *International journal of molecular sciences* **21**, 6514 (2020).
108. U. Sahin, A. Muik, E. Derhovanessian, I. Vogler, L.M. Kranz, M. Vormehr, A. Baum, K. Pascal, J. Quandt, D. Maurus, S. Brachtendorf, V. Lörks, J. Sikorski, R. Hilker, D. Becker, A.K. Eller, J. Grützner, C. Boesler, C. Rosenbaum, M.C. Kühnle, U. Luxemburger, A. Kemmer-Brück, D. Langer, M. Bexon, S. Bolte, K. Karikó, T. Palanche, B. Fischer, A. Schultz, P.Y. Shi, C. Fontes-Garfias, J.L. Perez, K.A. Swanson, J. Loschko, I.L. Scully, M. Cutler, W. Kalina, C.A. Kyratsous, D. Cooper, P.R. Dormitzer, K.U. Jansen and Ö. Türeci: COVID-19 vaccine BNT162b1 elicits human antibody and T(H)1 T cell responses. *Nature* **586**, 594 (2020).
109. C.S. Shemesh, J.C. Hsu, I. Hosseini, B.Q. Shen, A. Rotte, P. Twomey, S. Girish and B. Wu: Personalized Cancer Vaccines: Clinical Landscape, Challenges, and Opportunities. *Molecular therapy : the journal of the American Society of Gene Therapy* **29**, 555 (2021).
110. T. Schlake, M. Thran, K. Fiedler, R. Heidenreich, B. Petsch and M. Fotin-Mleczek: mRNA: A Novel Avenue to Antibody Therapy? *Molecular therapy : the journal of the American Society of Gene Therapy* **27**, 773 (2019).
111. T. Schlake, A. Thess, M. Thran and I. Jordan: mRNA as novel technology for passive immunotherapy. *Cellular and Molecular Life Sciences* **76**, 301 (2019).
112. I. Gómez-Aguado, J. Rodríguez-Castejón, M. Vicente-Pascual, A. Rodríguez-Gascón, M. Solinís and A. Del Pozo-Rodríguez: Nanomedicines to Deliver mRNA: State of the Art and Future Perspectives. *Nanomaterials (Basel, Switzerland)* **10** (2020).
113. M.D. Buschmann, M.J. Carrasco, S. Alishetty, M. Paige, M.G. Alameh and D. Weissman: Nanomaterial Delivery Systems for mRNA Vaccines. *Vaccines* **9**, 65 (2021).
114. M. Tusup, L.E. French, M. De Matos, D. Gatfield, T. Kundig and S. Pascolo: Design of in vitro Transcribed mRNA Vectors for Research and Therapy. *CHIMIA International Journal for Chemistry* **73**, 391 (2019).
115. A.B. Vogel, L. Lambert, E. Kinnear, D. Busse, S. Erbar, K.C. Reuter, L. Wicke, M. Perkovic, T. Beissert, H. Haas, S.T. Reece, U. Sahin and J.S. Tregoning: Self-Amplifying RNA Vaccines Give Equivalent Protection against Influenza to mRNA Vaccines but at Much Lower Doses. *Molecular Therapy* **26**, 446 (2018).
116. J. Devoldere, H. Dewitte, S.C. De Smedt and K. Remaut: Evading innate immunity in nonviral mRNA delivery: don't shoot the messenger. *Drug discovery today* **21**, 11 (2016).

117. Q. Xu, Y. Tang and G. Huang: Innate immune responses in RNA viral infection. *Frontiers of medicine*, 1 (2020).
118. G.P. Amarante-Mendes, S. Adjemian, L.M. Branco, L.C. Zanetti, R. Weinlich and K.R. Bortoluci: Pattern Recognition Receptors and the Host Cell Death Molecular Machinery. *Frontiers in immunology* **9** (2018).
119. S. Hur: Double-Stranded RNA Sensors and Modulators in Innate Immunity. *Annual Review of Immunology* **37**, 349 (2019).
120. B.R. Anderson, H. Muramatsu, S.R. Nallagatla, P.C. Bevilacqua, L.H. Sansing, D. Weissman and K. Karikó: Incorporation of pseudouridine into mRNA enhances translation by diminishing PKR activation. *Nucleic Acids Research* **38**, 5884 (2010).
121. R. Shavit, R. Maoz-Segal, M. Iancovici-Kidon, I. Offengenden, S. Haj Yahia, D. Machnes Maayan, Y. Lifshitz-Tunitsky, S. Niznik, S. Frizinsky, M. Deutch, E. Elbaz, H. Genaim, G. Rahav, I. Levy, A. Belkin, G. Regev-Yochay, A. Afek and N. Agmon-Levin: Prevalence of Allergic Reactions After Pfizer-BioNTech COVID-19 Vaccination Among Adults With High Allergy Risk. *JAMA Network Open* **4**, e2122255 (2021).
122. T.T. Hoang Thi, E.H. Pilkington, D.H. Nguyen, J.S. Lee, K.D. Park and N.P. Truong: The Importance of Poly(ethylene glycol) Alternatives for Overcoming PEG Immunogenicity in Drug Delivery and Bioconjugation. *Polymers* **12** (2020).
123. K. Karikó, M. Buckstein, H. Ni and D. Weissman: Suppression of RNA Recognition by Toll-like Receptors: The Impact of Nucleoside Modification and the Evolutionary Origin of RNA. *Immunity* **23**, 165 (2005).
124. K. Karikó, H. Muramatsu, F.A. Welsh, J. Ludwig, H. Kato, S. Akira and D. Weissman: Incorporation of Pseudouridine Into mRNA Yields Superior Nonimmunogenic Vector With Increased Translational Capacity and Biological Stability. *Molecular Therapy* **16**, 1833 (2008).
125. H. Moradian, T. Roch, A. Lendlein and M. Gossen: mRNA Transfection-Induced Activation of Primary Human Monocytes and Macrophages: Dependence on Carrier System and Nucleotide Modification. *Scientific reports* **10** (2020).
126. H. Moradian, A. Lendlein and M. Gossen: Strategies for simultaneous and successive delivery of RNA. *Journal of Molecular Medicine* **98**, 1767 (2020).
127. S. Gordon: The macrophage: past, present and future. *European journal of immunology* **37 Suppl 1**, S9 (2007).
128. T.A. Wynn, A. Chawla and J.W. Pollard: Macrophage biology in development, homeostasis and disease. *Nature* **496**, 445 (2013).
129. J.P. Edwards, X. Zhang, K.A. Frauwirth and D.M. Mosser: Biochemical and functional characterization of three activated macrophage populations. *Journal of leukocyte biology* **80**, 1298 (2006).
130. D. Dang, S. Taheri, S. Das, P. Ghosh, L.S. Prince and D. Sahoo: Computational Approach to Identifying Universal Macrophage Biomarkers. *Frontiers in physiology* **11**, 275 (2020).
131. M. Chambers, A. Rees, J.G. Cronin, M. Nair, N. Jones and C.A. Thornton: Macrophage Plasticity in Reproduction and Environmental Influences on Their Function. *Frontiers in immunology* **11**, 607328 (2020).
132. C.D. Buckley, C. Ospelt, S. Gay and K.S. Midwood: Location, location, location: how the tissue microenvironment affects inflammation in RA. *Nature Reviews Rheumatology* (2021).
133. K. Liddiard and P.R. Taylor: Understanding Local Macrophage Phenotypes In Disease: Shape-shifting macrophages. *Nature Medicine* **21**, 119 (2015).
134. V.M.T. Bart, R.J. Pickering, P.R. Taylor and N. Ipseiz: Macrophage reprogramming for therapy. *Immunology* **163**, 128 (2021).

135. L. Yang and Y. Zhang: Tumor-associated macrophages: from basic research to clinical application. *Journal of hematology & oncology* **10** (2017).
136. L. Zhang, L. Tian, X. Dai, H. Yu, J. Wang, A. Lei, M. Zhu, J. Xu, W. Zhao, Y. Zhu, Z. Sun, H. Zhang, Y. Hu, Y. Wang, Y. Xu, G.M. Church, H. Huang, Q. Weng and J. Zhang: Pluripotent stem cell-derived CAR-macrophage cells with antigen-dependent anti-cancer cell functions. *Journal of hematology & oncology* **13**, 153 (2020).
137. Z. Niu, G. Chen, W. Chang, P. Sun, Z. Luo, H. Zhang, L. Zhi, C. Guo, H. Chen, M. Yin and W. Zhu: Chimeric antigen receptor-modified macrophages trigger systemic anti-tumour immunity. *The Journal of pathology* **253**, 247 (2021).
138. S.C. Funes, M. Rios, J. Escobar-Vera and A.M. Kalergis: Implications of macrophage polarization in autoimmunity. *Immunology* **154**, 186 (2018).
139. K. Sadtler, K. Estrellas, B.W. Allen, M.T. Wolf, H. Fan, A.J. Tam, C.H. Patel, B.S. Luber, H. Wang, K.R. Wagner, J.D. Powell, F. Housseau, D.M. Pardoll and J.H. Elisseeff: Developing a pro-regenerative biomaterial scaffold microenvironment requires T helper 2 cells. *Science (New York, N.Y.)* **352**, 366 (2016).
140. A. Vishwakarma, N.S. Bhise, M.B. Evangelista, J. Rouwkema, M.R. Dokmeci, A.M. Ghaemmaghami, N.E. Vrana and A. Khademhosseini: Engineering Immunomodulatory Biomaterials To Tune the Inflammatory Response. *Trends in biotechnology* **34**, 470 (2016).
141. S. Franz, S. Rammelt, D. Scharnweber and J.C. Simon: Immune responses to implants – A review of the implications for the design of immunomodulatory biomaterials. *Biomaterials* **32**, 6692 (2011).
142. T. Lawrence and G. Natoli: Transcriptional regulation of macrophage polarization: enabling diversity with identity. *Nature Reviews Immunology* **11**, 750 (2011).
143. G. Natoli and S. Monticelli: Macrophage activation: glancing into diversity. *Immunity* **40**, 175 (2014).
144. I. Amit, D.R. Winter and S. Jung: The role of the local environment and epigenetics in shaping macrophage identity and their effect on tissue homeostasis. *Nature Immunology* **17**, 18 (2016).
145. Y. Liu and T. Segura: Biomaterials-Mediated Regulation of Macrophage Cell Fate. *Frontiers in bioengineering and biotechnology* **8**, 609297 (2020).
146. F. Zhang, N.N. Parayath, C.I. Ene, S.B. Stephan, A.L. Koehne, M.E. Coon, E.C. Holland and M.T. Stephan: Genetic programming of macrophages to perform anti-tumor functions using targeted mRNA nanocarriers. *Nature communications* **10** (2019).
147. J.D. Smith: Human Macrophage Genetic Engineering. *Arteriosclerosis, Thrombosis, and Vascular Biology* **36**, 2 (2016).
148. K.W. Moyes, N.A. Lieberman, S.A. Kreuser, H. Chinn, C. Winter, G. Deutsch, V. Hoglund, R. Watson and C.A. Crane: Genetically Engineered Macrophages: A Potential Platform for Cancer Immunotherapy. *Human gene therapy* **28**, 200 (2017).
149. D. Hachim, S.T. Lopresti, C.C. Yates and B.N. Brown: Shifts in macrophage phenotype at the biomaterial interface via IL-4 eluting coatings are associated with improved implant integration. *Biomaterials* **112**, 95 (2017).
150. M. Herb, A. Farid, A. Gluschko, M. Krönke and M. Schramm: Highly Efficient Transfection of Primary Macrophages with In Vitro Transcribed mRNA. *Journal of Visualized Experiments* (2019).
151. A.S. Poltavets, P.A. Vishnyakova, A.V. Elchaninov, G.T. Sukhikh and T.K. Fatkhudinov: Macrophage Modification Strategies for Efficient Cell Therapy. *Cells* **9**, 1535 (2020).
152. M. Poorebrahim, M.F. Abazari, S. Sadeghi, R. Mahmoudi, A. Kheirollahi, H. Askari, S.L. Wickström, V. Poortahmasebi, A. Lundqvist, R. Kiessling and A. Cid-Arregui:

Genetically modified immune cells targeting tumor antigens. *Pharmacology & therapeutics* **214**, 107603 (2020).

153. Y. Xu, L. Huang, J.L. Kirschman, D.A. Vanover, P.M. Tiwari, P.J. Santangelo, X. Shen and D.G. Russell: Exploitation of Synthetic mRNA To Drive Immune Effector Cell Recruitment and Functional Reprogramming In Vivo. *The Journal of Immunology* **202**, 608 (2019).

154. M. Schneemann and G. Schoeden: Macrophage biology and immunology: man is not a mouse. *Journal of leukocyte biology* **81**, 579 (2007).

155. R. Lv, Q. Bao and Y. Li: Regulation of M1-type and M2-type macrophage polarization in RAW264.7 cells by Galectin-9. *Molecular Medicine Reports* **16**, 9111 (2017).

156. A. Madhvi, H. Mishra, G.R. Leisching, P.Z. Mahlobo and B. Baker: Comparison of human monocyte derived macrophages and THP1-like macrophages as in vitro models for M. tuberculosis infection. *Comparative Immunology, Microbiology and Infectious Diseases* **67**, 101355 (2019).

157. O. Takeuchi and S. Akira: Pattern Recognition Receptors and Inflammation. *Cell* **140**, 805 (2010).

158. S.A. Safran, D.M. Eckert, E.A. Leslie and B.L. Bass: PKR activation by noncanonical ligands: a 5′-triphosphate requirement versus antisense contamination. *RNA* **25**, 1192 (2019).

159. P.S. Kowalski, A. Rudra, L. Miao and D.G. Anderson: Delivering the Messenger: Advances in Technologies for Therapeutic mRNA Delivery. *Molecular Therapy* **27**, 710 (2019).

160. J.C. Kaczmarek, P.S. Kowalski and D.G. Anderson: Advances in the delivery of RNA therapeutics: from concept to clinical reality. *Genome medicine* **9** (2017).

161. C. Yu, L. Li, P. Hu, Y. Yang, W. Wei, X. Deng, L. Wang, F.R. Tay and J. Ma: Recent Advances in Stimulus-Responsive Nanocarriers for Gene Therapy. *Advanced Science* **8**, 2100540 (2021).

162. C. Tros de Ilarduya, Y. Sun and N. Düzgüneş: Gene delivery by lipoplexes and polyplexes. *European Journal of Pharmaceutical Sciences* **40**, 159 (2010).

163. P. Shende, N. Ture, R.S. Gaud and F. Trotta: Lipid- and polymer-based plexes as therapeutic carriers for bioactive molecules. *International Journal of Pharmaceutics* **558**, 250 (2019).

164. K. Kettler, K. Veltman, D. Van De Meent, A. Van Wezel and A.J. Hendriks: Cellular uptake of nanoparticles as determined by particle properties, experimental conditions, and cell type. *Environmental Toxicology and Chemistry* **33**, 481 (2014).

165. Z.U. Rehman, D. Hoekstra and I.S. Zuhorn: Mechanism of Polyplex- and Lipoplex-Mediated Delivery of Nucleic Acids: Real-Time Visualization of Transient Membrane Destabilization without Endosomal Lysis. *ACS Nano* **7**, 3767 (2013).

166. M.S.D. Kormann, G. Hasenpusch, M.K. Aneja, G. Nica, A.W. Flemmer, S. Herber-Jonat, M. Huppmann, L.E. Mays, M. Illenyi, A. Schams, M. Griese, I. Bittmann, R. Handgretinger, D. Hartl, J. Rosenecker and C. Rudolph: Expression of therapeutic proteins after delivery of chemically modified mRNA in mice. *Nature Biotechnology* **29**, 154 (2011).

167. S. Uchida, K. Kataoka and K. Itaka: Screening of mRNA Chemical Modification to Maximize Protein Expression with Reduced Immunogenicity. *Pharmaceutics* **7**, 137 (2015).

168. K. Karikó, H. Ni, J. Capodici, M. Lamphier and D. Weissman: mRNA Is an Endogenous Ligand for Toll-like Receptor 3. *Journal of Biological Chemistry* **279**, 12542 (2004).

169. V. Hornung, J. Ellegast, S. Kim, K. Brzózka, A. Jung, H. Kato, H. Poeck, S. Akira, K.K. Conzelmann, M. Schlee, S. Endres and G. Hartmann: 5'-Triphosphate RNA is the ligand for RIG-I. *Science (New York, N.Y.)* **314**, 994 (2006).

170. D. Weissman, H. Ni, D. Scales, A. Dude, J. Capodici, K. McGibney, A. Abdool, S.N. Isaacs, G. Cannon and K. Karikó: HIV Gag mRNA Transfection of Dendritic Cells (DC) Delivers Encoded Antigen to MHC Class I and II Molecules, Causes DC Maturation, and Induces a Potent Human In Vitro Primary Immune Response. *The Journal of Immunology* **165**, 4710 (2000).

171. B.R. Anderson, H. Muramatsu, B.K. Jha, R.H. Silverman, D. Weissman and K. Kariko: Nucleoside modifications in RNA limit activation of 2'-5'-oligoadenylate synthetase and increase resistance to cleavage by RNase L. *Nucleic Acids Research* **39**, 9329 (2011).

172. T. Institute of Medicine Committee to Review the Fialuridine Clinical: in Review of the Fialuridine (FIAU) Clinical Trials, edited by F. J. Manning and M. Swartz

173. E.-W. Lee, Y. Lai, H. Zhang and J.D. Unadkat: Identification of the Mitochondrial Targeting Signal of the Human Equilibrative Nucleoside Transporter 1 (hENT1). *Journal of Biological Chemistry* **281**, 16700 (2006).

174. H. Tanji, U. Ohto, T. Shibata, M. Taoka, Y. Yamauchi, T. Isobe, K. Miyake and T. Shimizu: Toll-like receptor 8 senses degradation products of single-stranded RNA. *Nature Structural & Molecular Biology* **22**, 109 (2015).

175. Z. Zhang, U. Ohto, T. Shibata, E. Krayukhina, M. Taoka, Y. Yamauchi, H. Tanji, T. Isobe, S. Uchiyama, K. Miyake and T. Shimizu: Structural Analysis Reveals that Toll-like Receptor 7 Is a Dual Receptor for Guanosine and Single-Stranded RNA. *Immunity* **45**, 737 (2016).

176. P. Foroozandeh and A.A. Aziz: Insight into Cellular Uptake and Intracellular Trafficking of Nanoparticles. *Nanoscale Research Letters* **13**, 339 (2018).

177. F.-i. mRNA.

178. D. Campillo-Davo, M. De Laere, G. Roex, M. Versteven, D. Flumens, Z.N. Berneman, V.F.I. Van Tendeloo, S. Anguille and E. Lion: The Ins and Outs of Messenger RNA Electroporation for Physical Gene Delivery in Immune Cell-Based Therapy. *Pharmaceutics* **13**, 396 (2021).

179. H.S. Zaher and P.J. Unrau: T7 RNA Polymerase Mediates Fast Promoter-Independent Extension of Unstable Nucleic Acid Complexes. *Biochemistry* **43**, 7873 (2004).

180. G.A. Nacheva and A. Berzal-Herranz: Preventing nondesired RNA-primed RNA extension catalyzed by T7 RNA polymerase. *European Journal of Biochemistry* **270**, 1458 (2003).

181. S.N. Sarcar and D.L. Miller: A specific, promoter-independent activity of T7 RNA polymerase suggests a general model for DNA/RNA editing in single subunit RNA Polymerases. *Scientific reports* **8** (2018).

182. E. Kierzek: The thermodynamic stability of RNA duplexes and hairpins containing N6-alkyladenosines and 2-methylthio-N6-alkyladenosines. *Nucleic Acids Research* **31**, 4472 (2003).

183. P. Gaspar, G. Moura, M.A.S. Santos and J.L. Oliveira: mRNA secondary structure optimization using a correlated stem–loop prediction. *Nucleic Acids Research* **41**, e73 (2013).

184. X. Mu, E. Greenwald, S. Ahmad and S. Hur: An origin of the immunogenicity of in vitro transcribed RNA. *Nucleic Acids Research* **46**, 5239 (2018).

185. M.Z. Wu, H. Asahara, G. Tzertzinis and B. Roy: Synthesis of low immunogenicity RNA with high-temperature in vitro transcription. *RNA* **26**, 345 (2020).

186. F.J. Triana-Alonso, M. Dabrowski, J. Wadzack and K.H. Nierhaus: Self-coded 3′-Extension of Run-off Transcripts Produces Aberrant Products during in Vitro

Transcription with T7 RNA Polymerase. *Journal of Biological Chemistry* **270**, 6298 (1995).

187. S.C. Devarkar, C. Wang, M.T. Miller, A. Ramanathan, F. Jiang, A.G. Khan, S.S. Patel and J. Marcotrigiano: Structural basis for m7G recognition and 2′-O-methyl discrimination in capped RNAs by the innate immune receptor RIG-I. *Proceedings of the National Academy of Sciences* **113**, 596 (2016).

188. Y.V. Svitkin, Y.M. Cheng, T. Chakraborty, V. Presnyak, M. John and N. Sonenberg: N1-methyl-pseudouridine in mRNA enhances translation through eIF2α-dependent and independent mechanisms by increasing ribosome density. *Nucleic Acids Research* **45**, 6023 (2017).

189. J.E. Lewis, J.M. Brameld, P. Hill, P. Barrett, F.J. Ebling and P.H. Jethwa: The use of a viral 2A sequence for the simultaneous over-expression of both the vgf gene and enhanced green fluorescent protein (eGFP) in vitro and in vivo. *Journal of neuroscience methods* **256**, 22 (2015).

190. J.M. Bakker, W.K. Bleeker and P.W. Parren: Therapeutic antibody gene transfer: an active approach to passive immunity. *Molecular therapy : the journal of the American Society of Gene Therapy* **10**, 411 (2004).

191. V.S. Efimova, L.V. Isaeva, A.A. Labudina, V.N. Tashlitsky, M.A. Rubtsov and L.A. Novikova: Polycistronic expression of the mitochondrial steroidogenic P450scc system in the HEK293T cell line. *Journal of cellular biochemistry* **120**, 3124 (2019).

192. M. Mathison, V.P. Singh, R.P. Gersch, M.O. Ramirez, A. Cooney, S.M. Kaminsky, M.J. Chiuchiolo, A. Nasser, J. Yang, R.G. Crystal and T.K. Rosengart: "Triplet" polycistronic vectors encoding Gata4, Mef2c, and Tbx5 enhances postinfarct ventricular functional improvement compared with singlet vectors. *The Journal of Thoracic and Cardiovascular Surgery* **148**, 1656 (2014).

193. S.K. Goparaju, K. Kohda, K. Ibata, A. Soma, Y. Nakatake, T. Akiyama, S. Wakabayashi, M. Matsushita, M. Sakota, H. Kimura, M. Yuzaki, S.B.H. Ko and M.S.H. Ko: Rapid differentiation of human pluripotent stem cells into functional neurons by mRNAs encoding transcription factors. *Scientific Reports* **7**, 42367 (2017).

194. Z. Liu, O. Chen, J.B.J. Wall, M. Zheng, Y. Zhou, L. Wang, H. Ruth Vaseghi, L. Qian and J. Liu: Systematic comparison of 2A peptides for cloning multi-genes in a polycistronic vector. *Scientific reports* **7** (2017).

195. A.A. Shaimardanova, K.V. Kitaeva, I.I. Abdrakhmanova, V.M. Chernov, C.S. Rutland, A.A. Rizvanov, D.S. Chulpanova and V.V. Solovyeva: Production and Application of Multicistronic Constructs for Various Human Disease Therapies. *Pharmaceutics* **11**, 580 (2019).

196. G.A. Luke and M.D. Ryan: Using the 2A Protein Coexpression System: Multicistronic 2A Vectors Expressing Gene(s) of Interest and Reporter Proteins, (Springer New York2018), pp. 31.

197. T. Nenasheva, T. Gerasimova, Y. Serdyuk, E. Grigor'eva, G. Kosmiadi, A. Nikolaev, E. Dashinimaev and I. Lyadova: Macrophages Derived From Human Induced Pluripotent Stem Cells Are Low-Activated "Naïve-Like" Cells Capable of Restricting Mycobacteria Growth. *Frontiers in immunology* **11**, 1016 (2020).

198. J.J. Gam, B. Diandreth, R.D. Jones, J. Huh and R. Weiss: A 'poly-transfection' method for rapid, one-pot characterization and optimization of genetic systems. *Nucleic Acids Research* **47**, e106 (2019).

199. T. Beissert, M. Perkovic, A. Vogel, S. Erbar, K.C. Walzer, T. Hempel, S. Brill, E. Haefner, R. Becker, Ö. Türeci and U. Sahin: A Trans-amplifying RNA Vaccine Strategy for Induction of Potent Protective Immunity. *Molecular Therapy* **28**, 119 (2020).

200. Z.S. Badieyan, T. Berezhanskyy, M. Utzinger, M.K. Aneja, D. Emrich, R. Erben, C. Schüler, P. Altpeter, M. Ferizi, G. Hasenpusch, C. Rudolph and C. Plank: Transcript-activated collagen matrix as sustained mRNA delivery system for bone regeneration. *Journal of controlled release : official journal of the Controlled Release Society* **239**, 137 (2016).

Appendix I

OPEN

mRNA Transfection-Induced Activation of Primary Human Monocytes and Macrophages: Dependence on Carrier System and Nucleotide Modification

Hanieh Moradian[1,2,3], Toralf Roch[1,4,5], Andreas Lendlein[1,2,3] & Manfred Gossen[1,2*]

Monocytes and macrophages are key players in maintaining immune homeostasis. Identifying strategies to manipulate their functions via gene delivery is thus of great interest for immunological research and biomedical applications. We set out to establish conditions for mRNA transfection in hard-to-transfect primary human monocytes and monocyte-derived macrophages due to the great potential of gene expression from *in vitro* transcribed mRNA for modulating cell phenotypes. mRNA doses, nucleotide modifications, and different carriers were systematically explored in order to optimize high mRNA transfer rates while minimizing cell stress and immune activation. We selected three commercially available mRNA transfection reagents including liposome and polymer-based formulations, covering different application spectra. Our results demonstrate that liposomal reagents can particularly combine high gene transfer rates with only moderate immune cell activation. For the latter, use of specific nucleotide modifications proved essential. In addition to improving efficacy of gene transfer, our findings address discrete aspects of innate immune activation using cytokine and surface marker expression, as well as cell viability as key readouts to judge overall transfection efficiency. The impact of this study goes beyond optimizing transfection conditions for immune cells, by providing a framework for assessing new gene carrier systems for monocyte and macrophage, tailored to specific applications.

Innate immune cells play an important role in response to pathological conditions and maintaining immune homeostasis[1]. Among them, monocytes and monocyte-derived macrophages have remarkable properties, including their immunomodulatory capacities. Monocytes with various distinct phenotypes are key players of early inflammation. During inflammation, monocytes can dynamically repolarize to different phenotypes in response to local signals, which is thought to be more efficient at resolving tissue homeostasis than the recruitment of other anti-inflammatory and pro-regenerative subsets of monocytes or macrophages[2–4].

Macrophages themselves have special functions such as phagocytosis of invading pathogens or apoptotic cells, antigen presentation to T cells, elimination of pathogens via releasing reactive oxygen species or proteolytic enzymes, and secretion of pro- or anti-inflammatory signaling molecules to recruit various types of other immune cells[5–9]. Elucidation and manipulation of monocyte and macrophage phenotypes is therefore essential to fully explore their role in immunoregulation. This will benefit not only basic immunological research but also clinical and translational studies[3,10,11].

For innate immune cell manipulation, transfections have been commonly used to introduce nucleic acids, such as plasmid DNA (pDNA) or small interfering RNA, to induce or inhibit the expression of a target protein,

[1]Institute of Biomaterial Science, Helmholtz-Zentrum Geesthacht, 14513, Teltow, Germany. [2]Berlin-Brandenburg Center for Regenerative Therapies (BCRT), 13353, Berlin, Germany. [3]Institute of Biochemistry and Biology, University of Potsdam, 14476, Potsdam, Germany. [4]Charité – Universitätsmedizin Berlin, corporate member of Freie Universität Berlin, Humboldt-Universität zu Berlin, and Berlin Institute of Health, Berlin-Brandenburg Center for Regenerative Therapies, Berlin, Germany. [5]Center for Translational Medicine, Medical Department I, Marien Hospital Herne, University Hospital of the Ruhr-University Bochum, Herne, Germany. *email: manfred.gossen@hzg.de
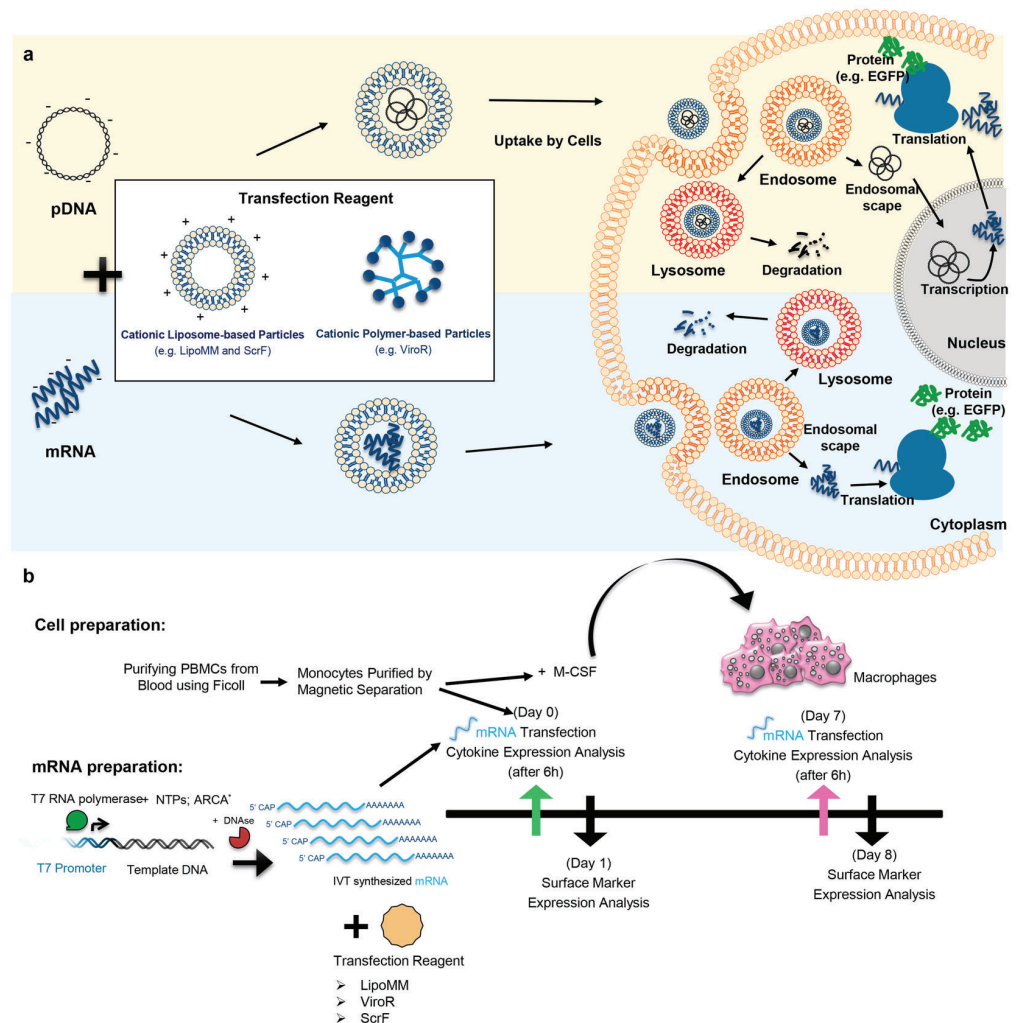
Figure 1. (**a**) Different paths to protein expression upon cells transfection with mRNA or pDNA (**b**) Experimental work flow to isolate and generate primary human monocytes and macrophages and to compare the transfection efficiency of mRNA transfection reagents. LipoMM: Lipofectamine MessengerMax, ScrF: Screen*Fect*, ViroR: Viromer RED, IVT-mRNA: in vitro transcribed mRNA, ARCA: anti–reverse cap analog, EGFP: enhanced green fluorescent protein.

respectively[12–14]. However, initial studies revealed that, particularly for macrophages, transfection is more challenging in comparison to most other primary mammalian cells[15]. The low transfection efficiency in monocytes/macrophages can be attributed to the following reasons. Firstly, there is a very limited chance for pDNA to freely reach the nucleus due to nuclear envelope breakdown during mitosis, since macrophages do not, or hardly, proliferate[16,17]. Secondly, these immune cells are equipped with pattern recognition receptors, which can detect nucleic acids as potential foreign and dangerous viral invaders, and initiate the inflammatory signaling cascade leading to pDNA degeneration or macrophage apoptosis[18]. Hence, finding a robust transfection approach to address these issues is highly demanded.

Transfection of messenger RNA (mRNA) is a promising alternative to pDNA or viral vector to achieve target protein expression, particularly in non-proliferative cells such as primary human cells[19,20]. One advantage of mRNA transfection is that there is neither the need for mRNA to enter the cell nucleus, nor the possibility to integrate into the host genomic DNA (Fig. 1a)[21]. Thus, this method can be a proper alternative for transfection of non-proliferative cells[22], including primary human macrophages and monocytes. Moreover, it will avoid genotoxicity issues associated with chromosomal insertion of DNA vectors in clinical gene transfer applications. In contrast to most pDNA transfections and viral transduction protocols, mRNA transfection will result in a transient, non-stable gene expression. However, transient expression is beneficial for several "hit-and-run" applications, including current differentiation protocols[23,24].

The mRNA gene delivery technology made significant progress after overcoming commonly known issues related to mRNA, such as susceptibility to degradation by RNases in surrounding media before reaching the

65

Features provided by the manufacturer	LipoMM	ViroR	ScrF
Material's chemistry	Lipid-based nanoparticle	Polymeric carrier, based on polycationic PEI core, highly substituted with hydrophobic and anionic side chains	Cationic thioether lipids, containing hydrophobic alkyl groups
Specific structural features	Cationic lipids optimized for mRNA delivery application;	Polymers mimicking viral (influenza hemagglutinin) biophysics	Biomimetic lipid-like molecules made by thiol-yne click chemistry
Tested cell types	Primary cell types such as neurons, fibroblast, hepatocytes and Keratinocytes, specifically tested for mRNA CRISPRs	Primary adherent and suspension cells including monocytes and macrophages and stem cells	Many different human and mouse cell lines such as HEK293, NIH3T3, RAW 264.7 and mouse embryonic stem cells (mESC)

Table 1. Characteristics of the three commercially available mRNA transfection reagents provided by the manufacturer. LipoMM: Lipofectamine MessengerMax, ScrF: Screen*Fect*, ViroR: Viromer RED.

target cell[25]. Many parameters of *in vitro* transcription technology have been evaluated and optimized to prevent mRNA degradation, improve translation efficiency, and reduce unspecific immunogenicity upon transfection[19].

Despite 5′ and 3′-end modifications mimicking natural mRNAs, in vitro transcribed mRNA (IVT-mRNA) can activate immune responses in transfected cells. This effect is often more dramatic for macrophages, which are highly specialized cells for defense against RNA-based viruses and are equipped with numerous receptors including pattern recognition receptors. Toll-like receptors (TLR), particularly endosomal TLR3, 7, and 8, can recognize single- and double-stranded nucleic acids[21]. Therefore, when passing through the endosome, transfected IVT-mRNA could be recognized by immune cells as foreign. However, the immune response can be significantly diminished by utilizing modified nucleotides, as was initially reported by Kariko *et al*. for pseudouridine (Ψ) and 5′-methyl cytidine[26].

The aim of this study was to set up a robust method for IVT-mRNA transfection in primary human monocytes and monocyte-derived macrophages, while minimizing pleiotropic effects, in particular immune cell activation. We tested three commercially available transfection reagents for mRNA delivery. These included liposomal and polymer-based formulations, as cationic lipid based carriers have different physicochemical properties such as size, shape, and chemical structure compared with polyplexes. These key features not only affect and determine the way they condense and transport their cargo, but also uptake mechanism and subsequent endosomal release, and eventually transfection efficiency. The effects of mRNA modification as well as mRNA concentrations were systematically investigated, using cell viability, transfection efficiency, and the monocyte and macrophage activation as critical readouts. The results of this study provide guidelines for choosing proper mRNA transfection carriers for monocytes and macrophages and highlights the need for not only focusing on gene transfer rates, but also for analyzing cell stress and activation in parallel.

Results

Experimental setup. In order to evaluate the effect of different mRNA transfection protocols on monocytes and macrophages, experiments were designed as follows. mRNAs were synthesized using the *in vitro* transcription method, with non-modified or modified nucleotides. Either of three commercially available mRNA transfection reagents, namely the liposomal reagents Lipofectamine MessengerMax (LipoMM) and Screen*Fect* mRNA (ScrF) as well as the polymeric reagent Viromer RED (ViroR) were compared for transfection efficiency; see also Table 1 provided in *Methods*. CD14 positive monocytes purified from peripheral blood mononuclear cells (PBMCs) using magnetic cell sorting, were immediately transfected. A fraction of the CD14 positive monocytes were differentiated into macrophages by cultivation for seven days in the presence of macrophage colony-stimulating factor (M-CSF) and transfected at day 7. Supernatants from monocyte and macrophage cultures were harvested 6 h post transfection and analyzed for the expression of tumor necrosis factor alpha (TNF-α) and interferon beta (IFN-β). One day after transfection, the reporter gene and the CD80 expression was analyzed by flow cytometry. The schematic overview of the experimental workflow is depicted in Fig. 1b.

Viability of monocytes and macrophages upon mRNA transfection. The forced introduction of nucleic acids in cells often causes substantial stress that might ultimately effect viability. Crucial parameters are type and purity of nucleic acid, the transfection protocol followed and the type of transfection reagent used[27]. The meaningful cell type-dependent optimization of transfection protocols requires that post-transfection phenotypes that are caused by the genetic payload-dependent alteration in the target cells' transcriptome can be distinguished from side effects of the chosen transfection method or the potential innate immune response of cells upon uptake of exogenous nucleic acids. To this end, we comparatively analysed primary human monocytes and macrophages, treated with different transfection reagents for the introduction of IVT-mRNA encoding enhanced green fluorescent protein (EGFP) to allow for single cell analysis of transfected and non-transfected cells. To address post transfection viability, cells were treated with 4′,6-Diamidino-2-Phenylindole, dihydrochloride (DAPI) immediately prior to the flow cytometric analysis to discriminate live from dead cells. To identify live single cells, a gating strategy as illustrated in Fig. S1 was applied. Cells were first discriminated from debris using forward versus side scatter (FSC vs. SSC) parameters (Fig. S1a). Then, aggregated cells were excluded using FSC-area (FSC-A) against FSC-height (FSC-H) (Fig. S1b) followed by identification of DAPI positive cells, which are considered as dead or apoptotic (Fig. S1c). Among live cells, the amount of EGFP positive cell populations was determined by using untransfected cells as gating control (Fig. S1d).
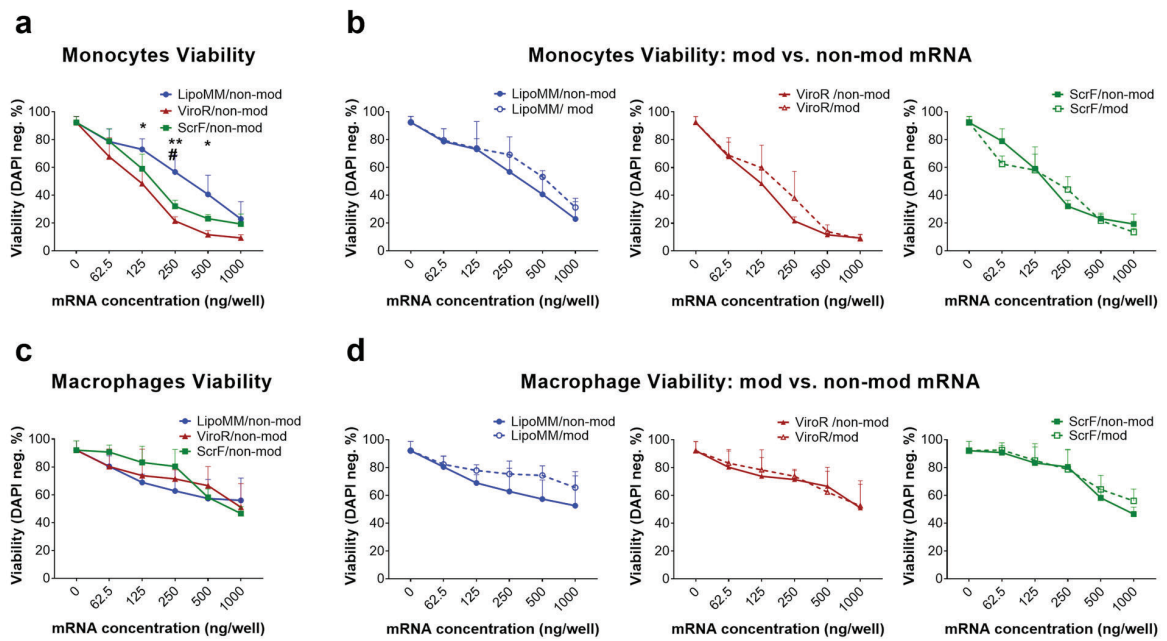
Figure 2. Viability of monocytes and macrophages after mRNA transfection with different mRNA transfection reagents; (**a**) Viability of monocytes transfected with non-modified mRNA using LipoMM (blue), ViroR (red), and ScrF (green); (**b**) monocytes viability after transfection with modified or non-modified mRNA using LipoMM, ViroR, and ScrF. (**c**) Evaluation of macrophages viability after transfection with non-modified mRNA comparing LipoMM, ViroR, and ScrF; viability of macrophages transfected with modified or non-modified mRNA by LipoMM, ViroR, and ScrF. (**d**) Values for no mRNA (0 ng/well) refer to untransfected cells throughout. Values are presented as mean ± standard deviation (SD), n = 3. Error bars indicate SD. Statistical differences in viability is depicted with * for LipoMM vs. ViroR, # for LipoMM vs. ScrF and + for ViroR vs. ScrF. *, #p < 0.05, **p < 0.01.

Monocyte viability was measured after transfection of the three chosen reagents complexed with either modified or non-modified IVT-mRNA. For all transfection reagents, viability decreased with increasing mRNA doses used. LipoMM resulted in significantly higher monocyte viability for most mRNA concentrations, as indicated (Fig. 2a). However, there was no difference between viability of monocytes transfected with ScrF and ViroR (Fig. 2a).

For the macrophage viability, no statistically significant difference between the different transfection reagents was observed when comparing within each dose or average of all doses (Fig. 2c).

The viability of monocytes and macrophages after transfection with mRNA specifically modified with pseudouridine and 5-methyl-cytidine was compared to their viability after transfection with non-modified mRNA for each transfection reagent. In most conditions modified mRNA fails to demonstrate a convincing decrease in cell death when compared to non-modified mRNA for both monocytes and macrophages (Fig. 2b,d), resulting in a lack of statistical significant difference. Surprisingly, monocytes seemed to be more vulnerable to increasing mRNA doses than macrophages, when comparing the overall decrease of viability between monocytes and macrophages (shown in Fig. 2a,c, respectively). For instance, the significant viability decrease was observed in monocytes at 250 ng/well for LipoMM, 62.5 ng/well for ViroR and 125 ng/well for ScrF; whereas, a significant drop in viability of macrophages was only seen above 500 ng/well for all transfection reagents.

Transfection efficiency in primary human monocytes and macrophages. EGFP was used as a reporter protein to monitor mRNAs transfection efficiency in monocytes and macrophages, which was initially visualized by fluorescent microscopy (Fig. 3a) and subsequently quantified by flow cytometry (Fig. 3b–f). A substantial number of EGFP expressing macrophages could be microscopically observed already for 125 ng mRNA per well, especially when the transfection was performed with LipoMM (Fig. 3a). The numbers of EGFP expressing macrophages after transfection with ViroR and ScrF were clearly lower in comparison to LipoMM. The use of modified mRNA seems to decrease the number of EGFP expressing macrophages, at least for ViroR and ScrF (Fig. 3a). Besides, morphology of transfected macrophages was evaluated using phase contrast microscopy, which indicated morphologically heterogeneous population of cells within various groups compared to untransfected and activated cells (Fig. S2). Moreover, non-modified mRNA resulted in higher EGFP intensity, when compared to modified mRNA for all three transfection reagents (Fig. 3b).

Quantification by flow cytometry over all mRNA doses confirmed a higher frequency of EGFP positive cells among macrophages transfected with mRNA complex with LipoMM comparing to ViroR and ScrF (Fig. 3b,e).
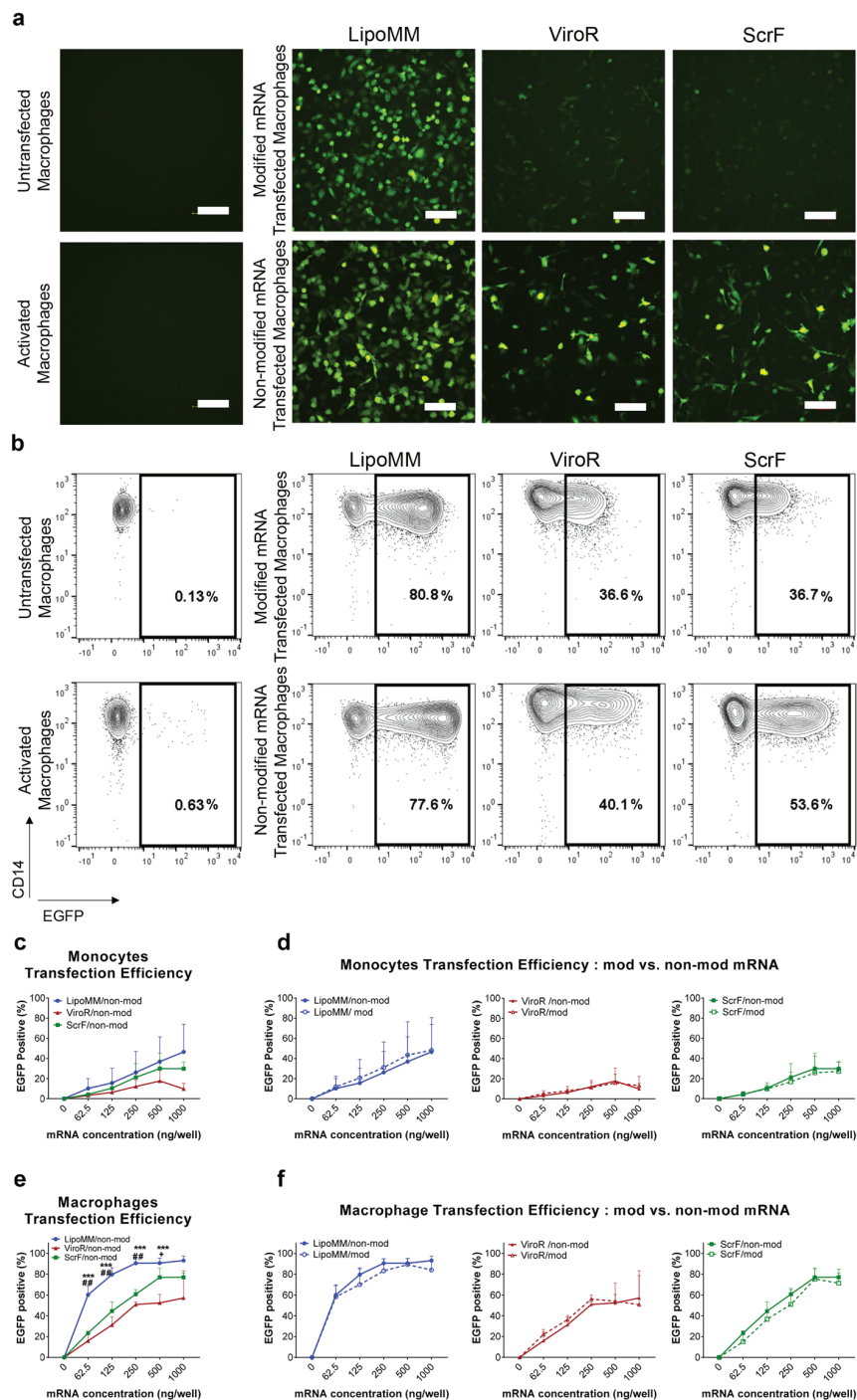
67

Figure 3. Transfection efficiency for monocytes and macrophages comparing LipoMM, ViroR, and ScrF; (**a**) Representative fluorescent microscopy images (bar = 100 μm) and (**b**) contour plots indicating EGFP expression of macrophages transfected with 125 ng/well of modified and non-modified mRNA via LipoMM, ViroR, and ScrF. (**c**) Quantification of EGFP positive cells as indicator of transfection efficiency for non-modified mRNA transfected monocytes and comparison of monocytes transfected with modified or non-modified mRNA using LipoMM, ViroR, and ScrF (**d**). The same comparison was performed for macrophages transfected with non-modified mRNA (**e**) and for macrophages transfected with modified or non-modified mRNA using LipoMM, ViroR, and ScrF (**f**). Values for no mRNA (0 ng/well) refer to untransfected cells throughout. "Activated" refers to cells treated with lipopolysaccharide (LPS) (2 μg·mL^{-1}) and interferon gamma (IFN-γ) (10 ng·mL^{-1}) for 24 h. Statistical differences in transfection efficiency is depicted with * for LipoMM vs. ViroR, # for LipoMM vs. ScrF and + for ViroR vs. ScrF. $^+$p < 0.05, ##p < 0.01, ***p < 0.001; Values are presented as mean ± SD, n = 3. Error bars indicate SD.

No statistical differences were observed when the transfection efficiency was compared for modified and non-modified mRNA (Fig. 3f).

To investigate the dose-dependence of the transfection efficiency for monocytes, the frequency of EGFP positive cells was determined after transfection with increasing amounts of mRNA. The flow cytometry quantification of EGFP expressing monocytes and macrophages revealed increasing transfection efficiency as measured by percentage of EGFP positive cells when increasing amounts of mRNA were applied to the cells. Non-modified mRNA transfection via LipoMM resulted in consistently highest efficiency for both types of immune cells, even more than 80% for macrophages, followed by ScrF and ViroR (Fig. 3c,e). As for the microscopic analysis, only minor differences between the use of modified versus non-modified mRNA was obvious for both monocytes and macrophages (Fig. 3d,f, respectively), at least when quantifying the percentage of EGFP positive cells (see above). Noteworthy, the mRNA dose/response mostly points at saturation effects, i.e. expression plateaued out at high mRNA doses. Overall, it is apparent that macrophages are more efficiently to transfect with mRNA when compared to monocytes.

Monocytes and macrophages activation. Activation of immune cells such as monocyte or macrophages is a natural process, in which cells acquire pro-inflammatory functions associated with the expression of characteristic cell surface molecules such as CD80 and releasing inflammatory mediators such as TNF-α. Monocytes and macrophages can be activated by lipopolysaccharides (LPS, also known as endotoxin), which can be further potentiated by interferon gamma (IFNγ)[28]. Cell stimulation also occurs in artificial *in vitro* culture settings, such as introduction of external synthetic nucleic acids. Here we investigated whether mRNA transfection can trigger monocyte and macrophage activation. Part of the cell activation by exogenous nucleic acids is based on antiviral response mechanisms of innate immune cells, resulting in the expression of antiviral response molecules, such as cytokine IFN-β. Accordingly, LPS + INF-γ-triggered activation was selected as positive control due to its capacity to induce CD80 and TNF-α expression. Cells treated with the three different transfection reagents were analysed for CD80 expression by flow cytometry. The level of CD80 expression of cells transfected with increasing amounts of modified and non-modified mRNA doses using the three different transfection reagents, LipoMM, ViroR, and ScrF, is illustrated as histograms for monocytes and macrophages (Fig. 4a,b). In general, higher amounts of mRNA resulted in increasing activation levels for all three transfection reagents. However, modified mRNAs triggered less CD80 expression in monocytes and macrophages compared to non-modified mRNA in all conditions (Fig. 4a,b).

Monocytes transfected with LipoMM induced the lowest activation compared to ViroR and ScrF (Fig. 4c). Whereas, the minimum CD80 expression was observed in macrophages transfected with ScrF (Fig. 4e). The polyplex transfection reagent, ViroR, turned out to elicit the highest monocyte and macrophage activation for all mRNA doses (Fig. 4c,e). For monocytes and macrophages, the results also indicated that mRNA modification resulted in substantially less cell CD80 expression when compared to non-modified mRNA (Fig. 4d,f). One exception was the low-level activation of macrophages transfected with ScrF (see above), which was similar for modified and non-modified mRNA (Fig. 4f). Comparing the slope of the CD80 dose/response in monocyte versus macrophages revealed that monocytes activation was more responsive to increasing mRNA doses than in macrophages (Fig. 4c,e).

When analyzed under the same transfection conditions for the secretion of TNF-α and IFN-β, both cell types overall responded to increasing concentrations of lipo-/polyplex in a dose-dependent manner (Fig. 5). However, while this activation was very modest for modified IVT-mRNA, the use of non-modified IVT-mRNA led to a dramatic increase in cytokine levels, up to two orders of magnitude.

Lastly, we addressed the question if the contact with, or uptake of carriers alone (i.e., without being complexed with mRNA) by cells might contribute to their activation. For most of the conditions analyzed, neither monocytes nor macrophages were activated by "transfection reagent-only", as assessed by CD80 expression and TNF-α secretion, and no effect on viability could be detected. Only for ScrF reagent added to monocytes, CD80 and TNF-α were slightly increased (Fig. 6). We noted a substantial, but transient acidification of the medium after addition of this transfection reagent, and monocytes might be particular sensitive to these conditions. Overall, increasing mRNA doses always increased cell activation both for monocytes and macrophages, particularly for non-modified mRNA.

Activation of macrophages transfected with mRNA coding mCherry vs. EGFP. Certain levels of cell stimulation persisted, despite reduced cell activation for modified mRNA, even for cells transfected with the lowest amount of mRNA for all three transfection reagents. Some studies attribute immune stimulation to the expression of EGFP protein[29–32]. To elucidate if EGFP protein contributes to cell activation, another fluorescent protein with substantially different amino acid sequence was selected. The homology value calculated is only 28.8%. To this end, macrophages were transfected with modified and non-modified mRNA coding for either EGFP or mCherry and the expression of CD80 and TNF-α were evaluated as the marker of cell activation. mCherry expression was validated using fluorescent microscopy (Fig. 7a) and flow cytometry analysis (Fig. 7b,c), which indicated higher mCherry intensity for non-modified mRNA compared with modified mRNA similar to what was observed for EGFP. However, there was no significant decrease in cell viability within different groups (Fig. 7d). The CD80 expression analyzed via flow cytometry illustrated no significant difference in activation of macrophages transfected with mRNA coding EGFP and mCherry within both lower and higher concentrations (Fig. 7e). Consistently, there was no significant difference in TNF-α expression of cells transfected with either of the two evaluated fluorescent proteins (Fig. 7f). Remarkably, the minimum level of CD80 expression and TNF-α secretion was observed for macrophages transfected with lower dose (62.5 ng) of modified mRNA coding EGFP (Fig. 7e,f).
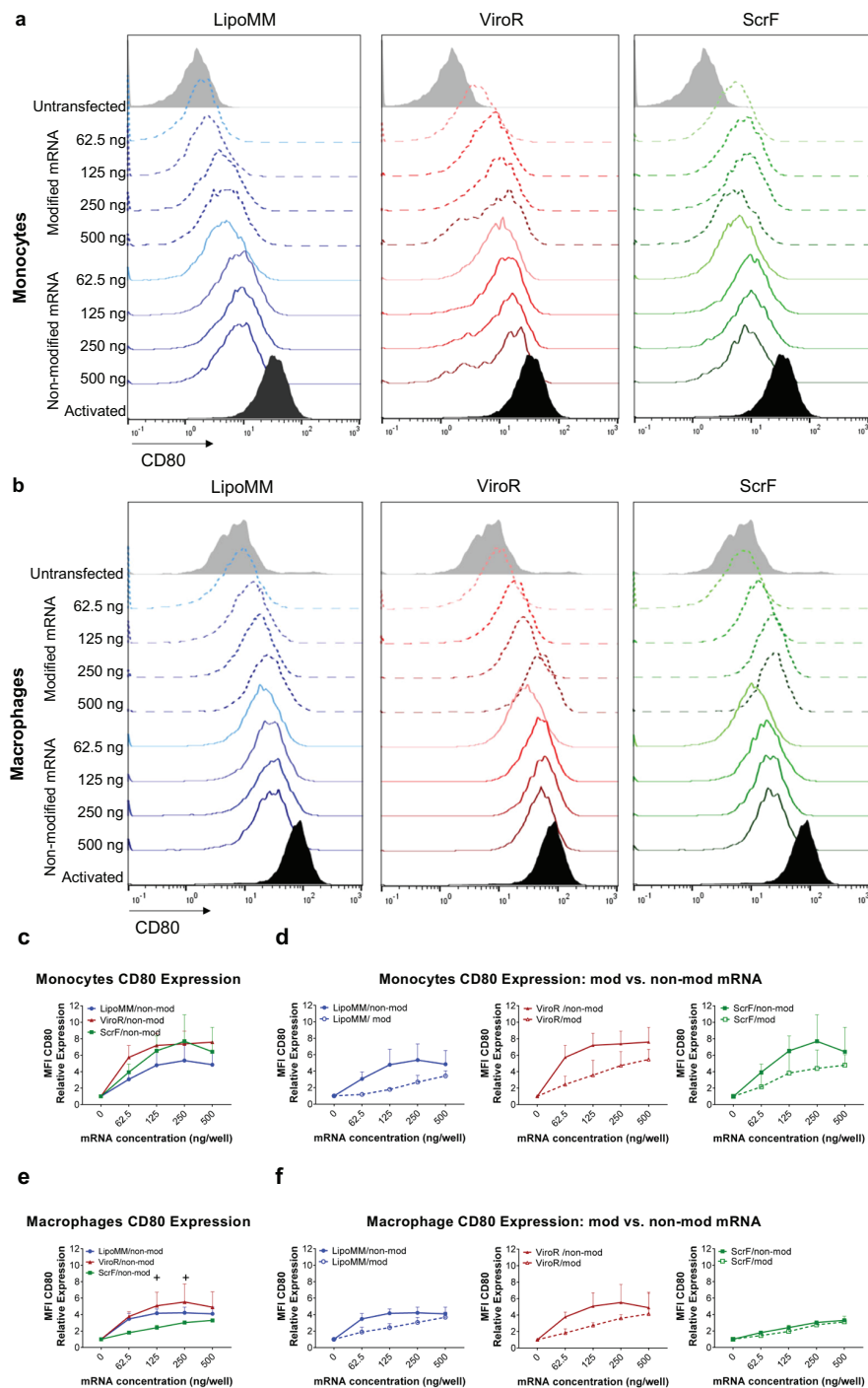
Figure 4. Activation of monocytes and macrophages assessed via CD80 expression; Histograms of CD80 expression in (**a**) monocytes and (**b**) macrophages transfected with modified (dashed lines) and non-modified mRNA (solid line) using LipoMM, ViroR, and ScrF. (**c**) Mean fluorescent intensity (MFI) of CD80 normalized to untransfected cells in monocytes transfected with non-modified mRNA using three transfection reagents. CD80 expression in monocytes transfected with either modified or non-modified mRNA using LipoMM, ViroR, and ScrF (**d**). The same assessment performed for macrophages to compare activation caused by three transfection methods (**e**), or modified versus non-modified mRNA transfected by LipoMM, ViroR and ScrF (**f**). Values for no mRNA (0 ng/well) refer to untransfected cells throughout. "Activated" refers to cells treated with LPS ($2 \, \mu g \cdot mL^{-1}$) and IFN-γ ($10 \, ng \cdot mL^{-1}$) for 24 h. Statistical differences in activation levels are depicted with + for ViroR vs. ScrF. $^+p < 0.05$, $^{**}p < 0.01$, $^{***}p < 0.001$; Values are presented as mean $\pm$ SD, n = 3. Error bars indicate SD.
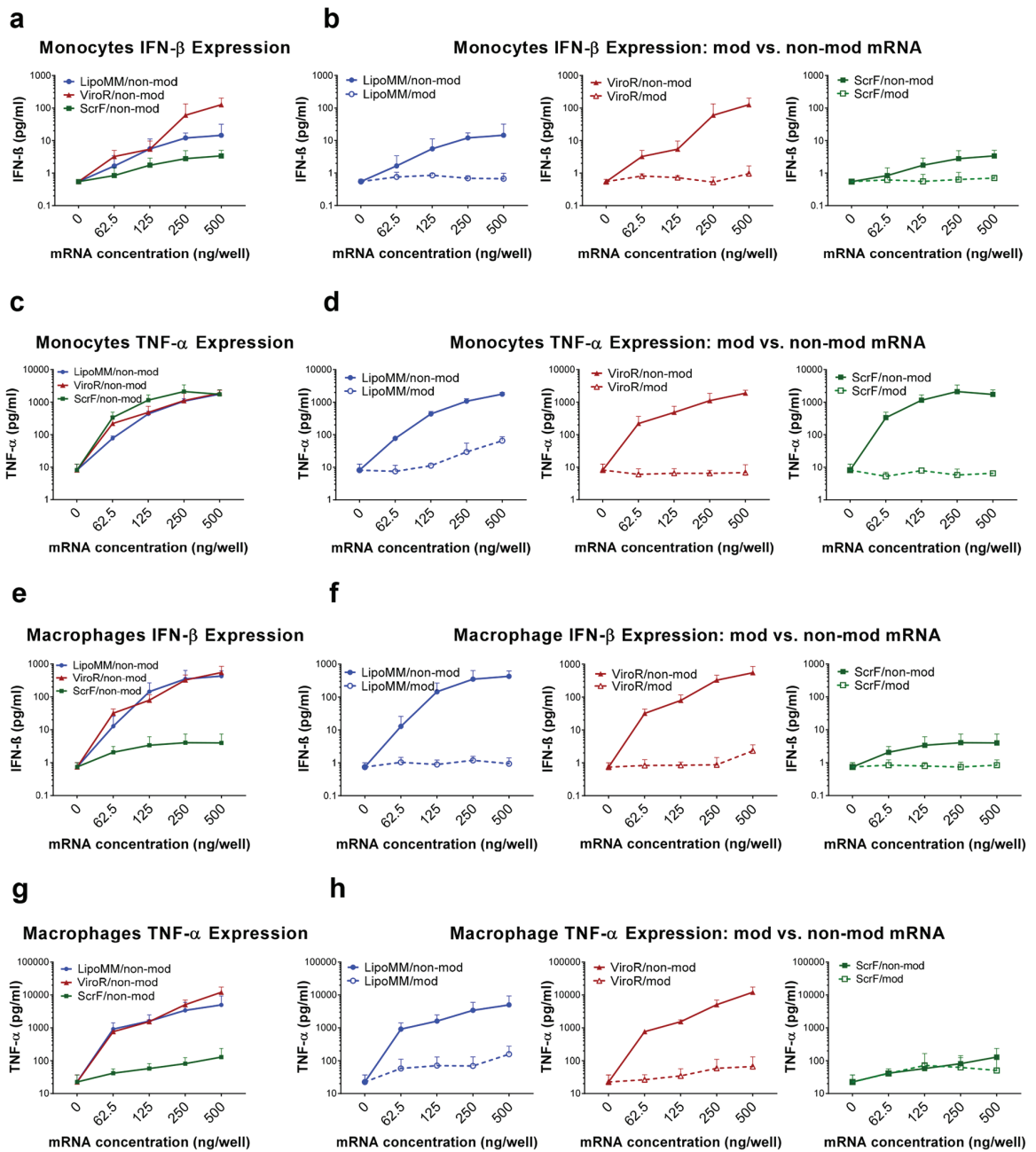
70

Figure 5. Evaluation of cytokine secretion in transfected monocytes and macrophages; Quantification of IFN-β secreted by monocytes transfected with non-modified mRNA using the three different transfection reagents (**a**) and comparison of IFN-β secretion in monocytes between modified (dashed lines) and non-modified mRNA (solid line) transfected by LipoMM, ViroR, and ScrF (**b**). Quantification of TNF-α secreted by monocytes transfected with non-modified mRNA using three transfection reagents (**c**) and comparison of TNF-α secretion in monocytes between modified (dashed lines) and non-modified mRNA (solid line) (**d**). The analogous assessment as shown in (**a,b**) for monocytes performed for macrophage IFN-β secretion secreted in response to the three transfection methods (**e,f**). The analogous assessment as shown in (**c,d**) for monocytes performed for macrophage TNF-α secretion induced via three transfection reagents (**g,h**). All cytokines were measured 6 h after transfection; Values for no mRNA (0 ng/well) refer to untransfected cells throughout. Values are presented as mean ± SD, n = 3. Error bars indicate SD.

Discussion

Developing transfection methods for manipulation of macrophage functions would be of utmost interest for basic as well as applied translational researches. In this regard, many studies have investigated different nucleic acid transfection strategies for macrophages, such as gene gun[33], nucleofection[14,34], magnetofection[35], and
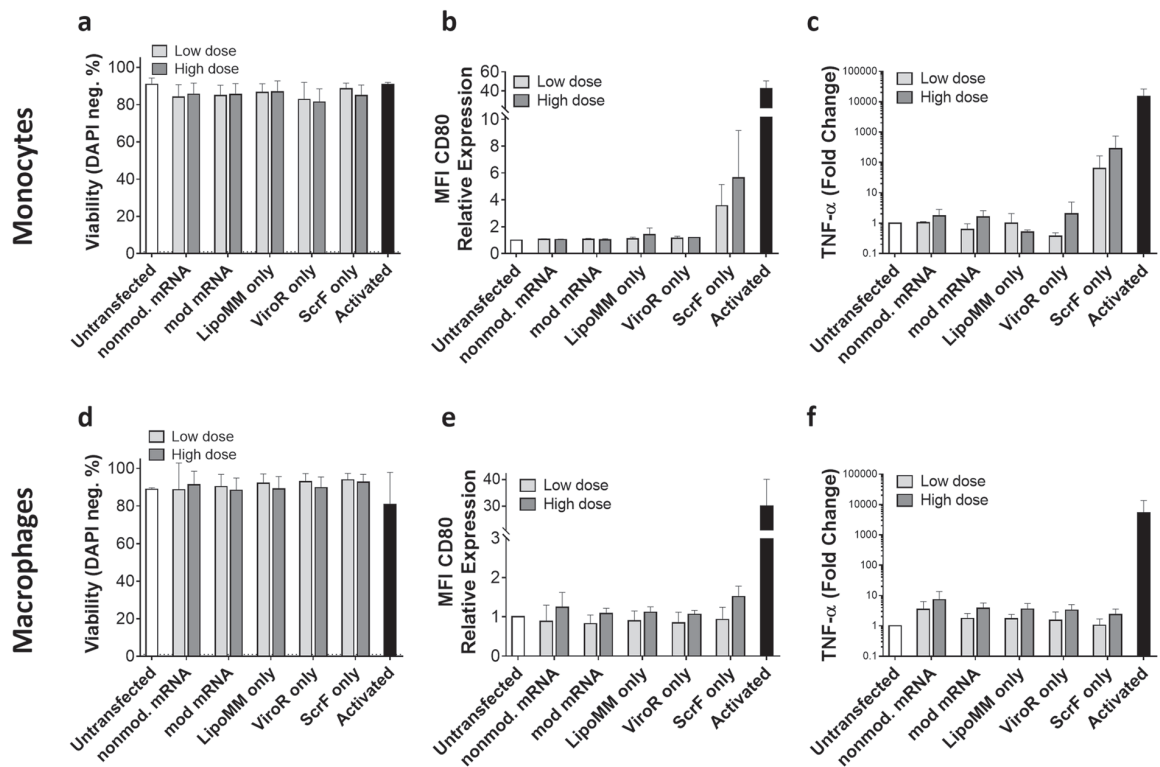
71

Figure 6. The effect of mRNA and carrier reagent only on viability (**a**), CD80 expression (**b**), and TNF-α secretion (**c**) in monocytes transfected with low dose equivalent to 62.5 ng/well and high dose equivalent to 250 ng/well mRNA condition. In the same way, viability (**d**), CD80 expression (**e**), and TNF-α secretion (**f**) measured in macrophages. Cells were evaluated 24 h after transfection. Values are presented as mean ± SD, n = 3. Error bars indicate SD.

lipofection[36,37]. However, all of these transfection methods have their limitations due to the resulting poor transfection efficiency, low cell survival, and high rates of immune stimulation of transfected cells[16,17].

Most of the existing knowledge about monocytes and macrophages comes from either mouse models or cell lines such as murine RAW 264.7 and human THP-1[38]. Neither of these cells represents human monocytes and macrophages properly. However, isolation and culture of primary human monocytes from blood and subsequent *in vitro* differentiation to macrophages is a valuable tool, providing a more precise model for studies focused on macrophages[13]. Thus, to develop a transfection method for primary human cells, which are more relevant for clinical applications, we investigated monocytes isolated from PBMCs and monocyte-derived macrophages.

In vitro transcribed mRNA was selected as cargo for this gene transfer study, as it promotes a high level but transient expression of transgenes and lacks genotoxicity. Despite the very high transfection efficiency for higher mRNA doses, up to 90% for macrophages transfected with LipoMM, cell viability under these conditions was low. However, we could achieve over 70% EGFP positive macrophages with no significant impact on their viability. In contrast to pDNA, this high transfection efficiency for the non-proliferative macrophages can at least be partially attributed to the fact that reaching to the cytoplasm is sufficient for mRNA to be expressed. pDNA has to either actively pass the nuclear envelope, or wait for its breakdown during mitosis, a process restricted to proliferating cells. This explanation is consistent with a former study, in which mRNA transfection resulted in over 45% of EGFP expressing cells using two different cell lines with chemically inhibited-proliferation and in non-dividing primary human neurons[22]. In a comparative study, Van De Parre *et al.* also reported a significant difference between mRNA and pDNA transfection efficiency for a murine macrophage cell line[39]. In another study, EGFP coding mRNA nanoparticles, made of Stemfect mRNA transfection reagent, were used for transfection of the JAWSII cell line, primary human and mouse dendritic cells (DCs). This resulted in over 97% transfection efficiency for the cell line, but only around 50% and 60% in human and mouse primary cells[40]. This great gap between the established cell line and the primary cells highlights the importance of using a model, which is more relevant for therapeutic and clinical applications.

Another advantage of using IVT-mRNA is that its *in vitro* production provides the opportunity to incorporate various nucleoside modifications to the transcribed mRNA, and to investigate the impact of these modifications along with non-modified mRNA. Among different modifications, we have chosen the substitution of cytidine and uridine with 5-methyl-cytidine and pseudouridine. Our results showed that the nucleotide modification initiated in general lower activation of monocytes and macrophages upon mRNA transfection in almost
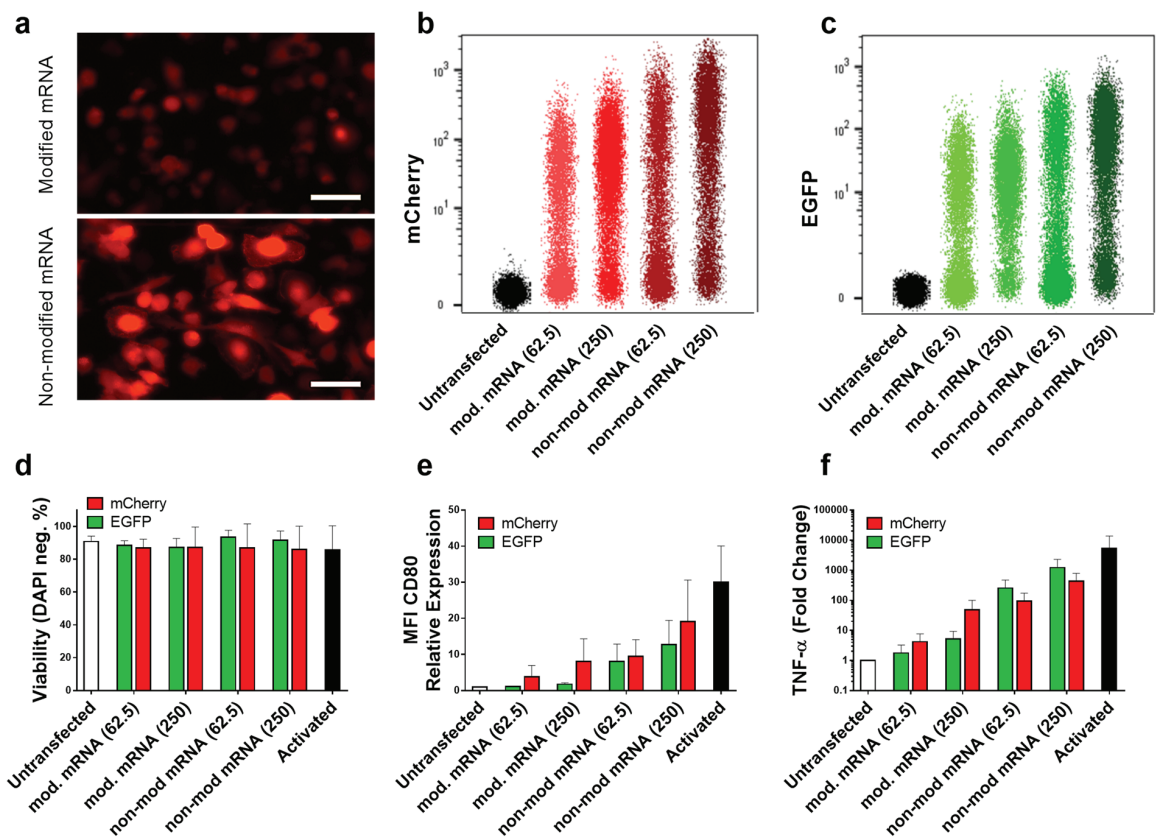
Figure 7. Macrophages transfected with modified or non-modified mRNA encoding for either EGFP or mCherry. mCherry expression was evaluated via fluorescent microscopy (**a**), and flow cytometry (**b**) which was measured in parallel with similar doses (62.5 and 250 ng/well) for EGFP (**c**). Viability of transfected cells was measured side by side (**d**), which shows no significant reduction compared with untransfected cells. Immune activation was assessed via CD80 expression normalized to untransfected cells (**e**) and TNF-α secretion also normalized to untransfected cells (**f**). No difference in CD80 expression was observed between EGFP and mCherry neither for modified nor for non-modified mRNA at lower dose (62.5 ng/well). All parameters have been measured 24 h after transfection. Values are presented as mean ± SD, n=3. Error bars indicate SD.

all different conditions when compared to non-modified mRNA. The extent of differential immune activation, non-modified vs. modified IVT-mRNA, depended on the chosen readout. Among activation markers, upregulation of CD80 was much less pronounced than that of TNF-α secretion. IFN-β secretion, as an antiviral response marker, was increased by up to two orders of magnitude when using non-modified IVT-mRNA compared to the modified RNA. While cell type and carrier system-dependent differences emerged, they did not consolidate to a clear picture pointing at either lipoplexes or polyplexes as preferred carriers for minimizing immune cell activation. A study by Kariko et al., upon evaluation of various modifications, concluded that complete substitution of non-modified nucleosides with 5-methyl-cytidine and pseudouridine, could remarkably reduce DCs cell activation[26]. These DCs were differentiated from primary-human monocytes, the same progenitor cells as for macrophages used in this study. Given the importance of using modified IVT-mRNA to dampen immune cell activation, it is not surprising that efforts continue to find better modifications as well as other approaches to improve the quality of IVT-mRNA[41]. For instance, in a more recent study, Vaidyanathan et al. screened various chemical modifications of 5′-CAP and nucleotides as well as transcript sequence optimization for expression of Cas9 protein, as a gene editing tool in CRISPR/Cas9 technology[42].

At least for the carrier systems and cell types analyzed here, cell activation triggered by intrinsic properties of transfection reagents alone seems to be minor. With one notable exception (ScrF for monocytes), the reagents in absence of mRNA neither decreased viability nor did they upregulate CD80 or TNF-α expression. However, it is noteworthy to point out the limitations of such controls, as "transfection reagent-only" differs in size, and other physical properties such as net charge of the particles, when compared to mRNA-containing lipo- or polyplexes.

The other important factor determining an efficient gene transfection is the type of carrier. Various non-viral gene delivery vehicles made of cationic polymers or lipids with different modifications have been developed[27,43]. However, beyond the transfection of established cell lines, only few of them achieved robust gene delivery in primary cells[22,44]. The number of successful gene transfer systems is even more limited, when delivery of specific cargo such as mRNA is demanded[45].

73

Optimized transfection protocols are often a compromise between different requirements, which do not necessarily correlate with each other, including transfection efficiency, viability, and absence of pleiotropic effects[46]. In that sense, LipoMM was distinguished for mRNA transfection of macrophages, in terms of higher transfection efficiency in most transfection conditions in comparison with the two others. This major difference in transfection efficiency could be due to the intrinsic different nature of these particles. Lipoplexes and polyplexes differ in physicochemical characteristics and therefore their function as nucleic acid carrier. Liposomal-based carriers consist of a hydrophilic cationic head group and a hydrophobic tail. The size ratio of these two groups determines the final structure of lipoplex particles upon electrostatic interaction with negatively charged nucleic acid molecules, which can be micellar, vesicle-like bilayer or multilamellar[47]. However, polyplexes can form branched spherical shape, or tubular structure depending of molecular weight, geometry of the cationic polymer, and number of primary amines available at polymer surface[47,48].

Another important carrier property, which can affect cellular uptake is the surface charge[49]. Lipoplexes are known to have overall positive charge even after complexation with nucleic acids[50], whereas the polyplex used in this study, ViroR, was reported to have overall neutral charge on the surface upon nucleic acid complexation due to its special chemical structure (information provided by supplier). Complexes with overall positive charge were reported to result in higher transfection efficiency, due to increase in cellular uptake mediated and augmented by initial electrostatic interaction with negatively charged cell membrane proteoglycans[48,51]. However, the disadvantage of having positive surface charge could be the potential aggregate formation in presence of negatively charged serum proteins. Endosomal release is the next important step, which is very crucial for a successful gene transfection. Lipoplexes can escape from endosome by fusion to endosomal membrane and subsequently release their cargo to cytoplasm, due to the presence of hydrophobic tail[47,48]. However, polyplexes cannot harness this mechanism, due to the lack of hydrophobic tail. Instead, the "proton sponge" effect is suggested and widely accepted mechanism to explain their endosomal escape[48]. Another critical step for polyplexes is the release of cargo from the carrier upon successful release to cytosolic space, which can be the limiting factor and hinder successful transfection in case of high molecular weight polycations with high charge density[52].

Fluorescent proteins have been widely used in gene transfection studies due to their convenient traceability with single cell resolution. Therefore, to ensure that the measured cell activation is primarily attributed to the mRNA-carrier complex and not specific to (over)expression of the chosen reporter protein, another fluorescent marker with different amino acid sequence, namely mCherry, was compared to EGFP. There was no consistent pattern of reporter-specific CD80 or TNF-α stimulation and, most importantly, no differences in viability when comparing EGFP with mCherry. In other words, our results suggest that the observed macrophage activation was not influenced by the type of reporter protein as has been speculated for EGFP, causing cell stimulation by itself in certain experimental settings[31].

In summary, we systematically investigated responses of primary human monocytes and monocyte-derived macrophages to three widely available mRNA transfection reagents as well as the necessity of mRNA modification. A crucial parameter in our study was the immune activation of cells, which was evaluated and considered as a key factor aside from cells viability and transfection efficiency. Overall, LipoMM turned out to be superior to ViroR and ScrF in terms of higher transfection efficiency and in most cases resulted in higher viability. With regard to immune cell activation we conclude that the use of non-modified IVT-mRNA is the only consistent parameter resulting in low-level activation. By contrast, no clear picture emerged in this study whether the use of lipoplexes or polyplexes would be of principle advantage. Preferences would have to be established depending on the specific cell type and actual reagent considered. Despite the success of lipoplex-based transfection reagents, the future perspective on exploiting mRNA technology in the biomedical and translational researches, like the emergence of transcript-activated matrixes (TAMs)[53], highlights the need for further development of IVT-mRNA polyplex nanoparticles. For instance, ViroR as a commercial polyplex was outperformed here with regard to cell viability and transfection efficiency by the widely used LipoMM, leaving room for further improvement of polyplex carriers, especially given their potential for *in vivo* delivery. Thus, the results presented in this study might serve as a blueprint for the evaluation of any new mRNA carrier system, in particular highlighting the need for a comprehensive evaluation of cellular immune response mechanism.

Methods

mRNA synthesis by *in vitro* transcription (IVT). A plasmid vector, pRNA2-(A)$_{128}$[54], was used as a template for *in vitro* transcription of mRNA coding EGFP. This plasmid contains a T7 promoter, 5′UTR, coding region for EGFP, tandem of human β-globin 3′-UTRs, and a 128-base polyadenine [poly(A)] sequence facilitating the generation of mRNA encoded with poly(A) tail without a post-transcriptional *in vitro* tailing reaction. The plasmids were first digested downstream of the poly(A) site using BspMI enzyme (New England Biolabs, Ipswich, MA). The digested plasmids were analysed and simultaneously purified by agarose gel electrophoreses and isolation of the IVT template band using a gel extraction kit (MN, Germany). The concentration of the purified fragment was measured using UV/Vis-spectroscopy (NanoDrop 1000 Spectrophotometer; PEQLAB). mRNAs were synthesized using a TranscriptAid T7 High Yield Transcription Kit (K0441, Thermo Scientific) following the manufacturer's instruction. The 5′ end of mRNA was modified co-transcriptionally with anti–reverse cap analog (ARCA) (Jena Bioscience, Germany)[55]. Chemically modified mRNAs were also generated by complete substitution of uridine and cytidine with 100 mM pseudouridine (Jena Bioscience, Germany) and 5-methyl-cytidine (Jena Bioscience, Germany), respectively. DEPC treated RNase free water and lithium chloride were added to the mRNA products to the final concentration of 2.5 M and the reaction was incubated at −20 °C overnight followed by centrifugation at 13000 g at 4 °C for 30 minutes. Further washing was done using 70 vol% cold ethanol, and final mRNA products were resuspended in UltraPure™ nuclease-free sterile water (Merck Millipore, Germany). All IVT-mRNAs were analysed by denaturing agarose gel electrophoresis for integrity (Fig. S3) and homogeneity and the concentration was determined photospectroscopically.

Preparation of primary human monocyte and monocyte-derived macrophages. PBMC were isolated from buffy coats (Deutsche Rote Kreuz, Berlin; ethics vote EA2/018/16; Charité University Medicine Berlin) using Ficoll (L6115, Biochrom, Germany) density gradient centrifugation. Monocytes were purified from PBMCs by negative selection using Monocyte Isolation Kit II (Miltenyi Biotec, Germany) according to the manufacturer's instruction. Monocytes express high levels of CD14[56]. Therefore, the purity of isolated monocytes was evaluated through CD14 expression, measured by flow cytometry (MACSQuant VYB, Miltenyi Biotec) using previously published protocol[57,58], which in most cases was at least 80%. Upon purification, cells were suspended in pre-warmed very low endotoxin (VLE) RPMI 1640 (FG 1415, Biochrom) supplemented with 10 vol% FBS (Biochrom) and were seeded in 24 well plates (TPP Techno Plastic Product AG, Switzerland) at a density of 5×10^5 cells per well. To avoid unspecific endotoxin mediated cell activation, all solutions used in the monocyte and macrophage assays were evaluated for endotoxin levels using EndoLISA® test (Hyglos, Germany) and only used when the amount of detected endotoxins was below 0.5 EU/mL. Monocytes were either used directly for transfection or further cultivated at 37 °C and 5 vol% CO_2 for 6–7 days in medium supplemented with 50 ng·mL^{-1} human M-CSF (Miltenyi Biotec) to generate monocyte-derived macrophages. The medium was changed every third day, upon washing vigorously with pre-warmed complete medium to remove non-adherent cells. Cells were cultured in antibiotic-free medium.

mRNA transfection using three different transfection reagents. The transfection of mRNA was performed using three commercially available transfection reagents including Lipofectamine MessengerMAX (Thermo scientific), Viromer RED (Lipocalyx, Germany), and ScreenFect mRNA (InCella, Germany), all of which are, according to the manufacturers, specifically formulated for mRNA transfection. To the extent available through the suppliers, physical and chemical characteristics as well as validated target cells are provided in Table 1.

A premixed concentrated solution containing carrier-mRNA complexes was prepared for each transfection reagent according to the detailed protocol describes as follows. MessengerMAX reagent was diluted in Opti-MEM medium (Gibco® by life technologies™, Germany) at 1:50 volume ratio, and incubated for 10 minutes at room temperature. The equal volume of diluted modified or non-modified IVT-mRNAs in Opti-MEM medium (4 ng·µL^{-1}) were subsequently added to MessengerMAX solution. LipoMM-mRNA complex mixtures were incubated for 5 minutes at room temperature and the corresponding volumes to deliver various mRNA doses (62.5, 125, 250, 500, 1000 ng per well) were added to each 24-well.

To prepare ViroR-mRNA polyplexes, mRNA was diluted in 225 µL of provided Viromer RED buffer at 11 ng·µL^{-1}. In another tube, a 0.75 µL droplet of Viromer® was placed on the tubes' wall and immediately mixed with 18 µl of buffer and vortexed for 5 seconds. The mRNA solution was then added to the diluted Viromer RED®, mixed swiftly, and incubated for 15 min at room temperature.

The ScrF-mRNA master solution was prepared as follows. The concentrated ScreenFect® mRNA was mixed with the provided dilution buffer (1:20 volume ratio) then combined immediately with the equal volume of mRNA diluted in the same buffer (8 ng·µL^{-1}). The resulting solution was mixed by pipetting thoroughly, and incubated for 20 min at room temperature to allow complex formation.

To transfect monocytes immediately after cell purification, upon formation of an mRNA-transfection reagent master mixes, the corresponding amount of mRNA complexes were added to the respective empty well (24-well plate) followed by adding 500 µl of cell suspension. Accordingly, at the end of the differentiation period at day 7, the medium was replaced with warm VLE RPMI supplemented with 10 vol% FBS. After 4 h, the proper amounts of transfection reagent-mRNA complexes were added dropwise to each well of monocyte-derived macrophages. As positive control for immune stimulation, LPS (2 µg·mL^{-1}) (Enzo life science, USA) and IFN-γ (10 ng·mL^{-1}) (Miltenyi Biotec) were added to the medium of untransfected cells.

Evaluation of transfection efficiency by fluorescent microscopy. To evaluate the EGFP expression of adherent human macrophages, cells were imaged 24 h after transfection, using a Nikon inverted microscope ELIPSE T*i*-U equipped with long-life mercury light source, Intensilight C-HGFI. The NIS-Elements imaging software package (version 4.51) was used to analyze microscopic images.

Measurement of cell viability, transfection efficiency, and activation of monocytes and macrophages by flow cytometry. Cells were harvested 24 h after transfection for further staining and analyzed by flow cytometry. Whereas monocytes, could be harvest by pipetting, macrophages had to be dissociated using TrypLE Select (Gibco® by life technologies™, Germany) according to manufacturer's instruction. To avoid unspecific antibody binding, cells were blocked by incubation with FcR Blocking Reagent (Miltenyi Biotec) for 10 min at 4 °C after washing with flow cytometry washing solution (PBS pH 7.2, BSA, EDTA). Subsequently, cells were stained with antibodies including anti-human CD14-PE-Vio770 (clone TÜK4) (Miltenyi Biotec), and CD80-PE (clone L307.4) (BD Pharmingen™, San Jose, USA) for 10 min at 4 °C using the recommended dilution factor 1:100 (5 µg·mL^{-1} final concentration). After a final washing step with cold flow cytometry washing solution, cells were acquired with MACSQuant VYB® (Miltenyi Biotec). DAPI at a final concentration of 1 µg·mL^{-1}, was added to each sample immediately prior to flow cytometric analysis, to discriminate DAPI-negative live cells from DAPI-positive dead cells. All flow cytometric data were analysed using FlowJo software V10.

Cytokine detection in monocyte and macrophage cell culture supernatants. Monocyte and macrophage culture supernatants were harvested and stored at −20 °C until further usage. The secretion of IFN-β and TNF-α was quantified in thawed supernatants using Bio-Plex® Multiplex Immunoassay System (BioRad, Geramny) according to the manufacturer's instructions. Briefly, to prepare the standard curves, 50 µL of the reconstituted cytokine standards were added to 150 µL culture medium (the same batch as samples were

collected) and eight 4-fold serial dilutions were made. Anti-cytokine coupled beads were diluted in assay buffer and $50\,\mu$L were added into each well of the plate. Plates were washed twice, before $50\,\mu$L of standard solution or sample supernatants were added. After incubation at 900 rpm for 30 min at room temperature, plates were washed three times with 1x washing buffer. The detection antibodies ($20 \times$ stock) were diluted in detection antibody diluent HB, and $25\,\mu$L were added into each well followed by an incubation at 900 rpm for 30 min at room temperature. After plates had been washed three times, $50\,\mu$L of PE conjugated streptavidin diluted 1:200 were added into each well and incubated at 900 rpm for 10 min at room temperature. After three final washing steps, beads were resuspended in $125\,\mu$L assay buffer, shaken at 900 rpm for 30 s and the plates were analyzed using the Bio-Plex® 200 system (BioRad, Germany).

Comparison of EGFP and mCherry in terms of macrophages activation. The PCR-amplified DNA fragment encoding mCherry was cloned into pRNA2-(A)$_{128}$. Briefly, EGFP coding sequence was replaced with mCherry by digestion of plasmid with *HindIII* and *NotI* restriction enzymes (New England Biolabs), and insertion of mCherry fragment in the vector. mRNA synthesis was performed using the new plasmid, pRNA2-(A)$_{128}$-mCherry, exactly as described for pRNA2-(A)128; see *Methods* section "mRNA synthesis by *in vitro* transcription". Macrophages were transfected with 62.5 ng and 250 ng mRNA coding EGFP or mCherry by Lipofectamine MessengerMAX (Thermo scientific). Moreover, the homology value of the two proteins amino acid sequence was calculated by NCBI online blast tool.

Statistics. Data are presented as means$\pm$ standard deviation (SD) of at least three independent experiments. Normally distributed data of multiple groups were statistically analysed by Two-Way ANOVA, Tukey's multiple comparison test using GraphPad Prism 7.00 (La Jolla, CA 92037, USA). Statistical significance is considered as $p < 0.05$.

Data availability
The datasets generated during and/or analysed during the current study are available from the corresponding author on reasonable request.

References
1. Zhou, D. *et al.* Macrophage polarization and function with emphasis on the evolving roles of coordinated regulation of cellular signaling pathways. *Cell Signal.* **26**, 192–197, https://doi.org/10.1016/j.cellsig.2013.11.004 (2014).
2. Mitchell, A. J., Roediger, B. & Weninger, W. Monocyte homeostasis and the plasticity of inflammatory monocytes. *Cell Immunol.* **291**, 22–31, https://doi.org/10.1016/j.cellimm.2014.05.010 (2014).
3. Ogle, M. E., Segar, C. E., Sridhar, S. & Botchwey, E. A. Monocytes and macrophages in tissue repair: Implications for immunoregenerative biomaterial design. *Exp. Biol. Med.* **241**, 1084–1097, https://doi.org/10.1177/1535370216650293 (2016).
4. Kratofil, R. M., Kubes, P. & Deniset, J. F. Monocyte Conversion During Inflammation and Injury. *Arterioscler. Thromb. Vasc. Biol.* **37**, 35–42, https://doi.org/10.1161/atvbaha.116.308198 (2017).
5. Anders, C. B., Lawton, T. M. W. & Ammons, M. C. B. Metabolic immunomodulation of macrophage functional plasticity in nonhealing wounds. *Curr. Opin. Infect. Dis.* **32**, 204–209, https://doi.org/10.1097/qco.0000000000000550 (2019).
6. Ginhoux, F. & Jung, S. Monocytes and macrophages: developmental pathways and tissue homeostasis. *Nat. Rev. Immunol.* **14**, 392–404, https://doi.org/10.1038/nri3671 (2014).
7. Varol, C., Mildner, A. & Jung, S. Macrophages: development and tissue specialization. *Annu. Rev. Immunol.* **33**, 643–675, https://doi.org/10.1146/annurev-immunol-032414-112220 (2015).
8. DeNardo, D. G. & Ruffell, B. Macrophages as regulators of tumour immunity and immunotherapy. *Nat. Rev. Immunol.* **19**, 369–382, https://doi.org/10.1038/s41577-019-0127-6 (2019).
9. Murray, P. J. Macrophage Polarization. *Annu. Rev. Physiol.* **79**, 541–566, https://doi.org/10.1146/annurev-physiol-022516-034339 (2017).
10. Brown, B. N., Ratner, B. D., Goodman, S. B., Amar, S. & Badylak, S. F. Macrophage polarization: an opportunity for improved outcomes in biomaterials and regenerative medicine. *Biomater.* **33**, 3792–3802, https://doi.org/10.1016/j.biomaterials.2012.02.034 (2012).
11. Kim, Y. K., Chen, E. Y. & Liu, W. F. Biomolecular strategies to modulate the macrophage response to implanted materials. *J. Mater. Chem. B* **4**, 1600–1609, https://doi.org/10.1039/C5TB01605C (2016).
12. Troegeler, A. *et al.* An efficient siRNA-mediated gene silencing in primary human monocytes, dendritic cells and macrophages. *Immunol. Cell Biol.* **92**, 699–708, https://doi.org/10.1038/icb.2014.39 (2014).
13. Warwick, C. A. & Usachev, Y. M. Culture, Transfection, and Immunocytochemical Analysis of Primary Macrophages. *Methods Mol. Biol.* **1554**, 161–173, https://doi.org/10.1007/978-1-4939-6759-9_9 (2017).
14. Scherer, O. *et al.* A procedure for efficient non-viral siRNA transfection of primary human monocytes using nucleofection. *J. Immunol. Methods* **422**, 118–124, https://doi.org/10.1016/j.jim.2015.04.007 (2015).
15. Keller, A. A., Maess, M. B., Schnoor, M., Scheiding, B. & Lorkowski, S. Transfecting Macrophages. *Methods Mol. Biol.* **1784**, 187–195, https://doi.org/10.1007/978-1-4939-7837-3_18 (2018).
16. Maess, M. B., Wittig, B. & Lorkowski, S. Highly efficient transfection of human THP-1 macrophages by nucleofection. *J Vis Exp*, e51960, https://doi.org/10.3791/51960 (2014).
17. Maess, M. B., Keller, A. A., Rennert, K., Mosig, A. & Lorkowski, S. Optimization of the transfection of human THP-1 macrophages by application of Nunc UpCell technology. *Anal. Biochem.* **479**, 40–42, https://doi.org/10.1016/j.ab.2014.12.023 (2015).
18. Zhang, X. & Mosser, D. M. Macrophage activation by endogenous danger signals. *J. Pathol.* **214**, 161–178, https://doi.org/10.1002/path.2284 (2008).
19. Oh, S. & Kessler, J. A. Design, Assembly, Production, and Transfection of Synthetic Modified mRNA. *Methods* **133**, 29–43, https://doi.org/10.1016/j.ymeth.2017.10.008 (2018).
20. Weissman, D. & Kariko, K. mRNA: Fulfilling the Promise of Gene Therapy. *Mol. Ther.* **23**, 1416–1417, https://doi.org/10.1038/mt.2015.138 (2015).
21. Sahin, U., Kariko, K. & Tureci, O. mRNA-based therapeutics–developing a new class of drugs. *Nat. Rev. Drug. Discov.* **13**, 759–780, https://doi.org/10.1038/nrd4278 (2014).

22. Zou, S., Scarfo, K., Nantz, M. H. & Hecker, J. G. Lipid-mediated delivery of RNA is more efficient than delivery of DNA in non-dividing cells. *Int. J. Pharm.* **389**, 232–243, https://doi.org/10.1016/j.ijpharm.2010.01.019 (2010).
23. Youn, H. & Chung, J. K. Modified mRNA as an alternative to plasmid DNA (pDNA) for transcript replacement and vaccination therapy. *Expert. Opin. Biol. Ther.* **15**, 1337–1348, https://doi.org/10.1517/14712598.2015.1057563 (2015).
24. Warren, L. *et al.* Highly efficient reprogramming to pluripotency and directed differentiation of human cells with synthetic modified mRNA. *Cell Stem Cell* **7**, 618–630, https://doi.org/10.1016/j.stem.2010.08.012 (2010).
25. Sergeeva, O. V., Koteliansky, V. E. & Zatsepin, T. S. mRNA-Based Therapeutics - Advances and Perspectives. *Biochem.* **81**, 709–722, https://doi.org/10.1134/s0006297916070075 (2016).
26. Kariko, K., Buckstein, M., Ni, H. & Weissman, D. Suppression of RNA recognition by Toll-like receptors: the impact of nucleoside modification and the evolutionary origin of RNA. *Immun.* **23**, 165–175, https://doi.org/10.1016/j.immuni.2005.06.008 (2005).
27. Kauffman, K. J., Webber, M. J. & Anderson, D. G. Materials for non-viral intracellular delivery of messenger RNA therapeutics. *J. Control. Rel.* **240**, 227–234, https://doi.org/10.1016/j.jconrel.2015.12.032 (2016).
28. Sansom, D. M., Manzotti, C. N. & Zheng, Y. What's the difference between CD80 and CD86? *Trends Immunol.* **24**, 314–319 (2003).
29. Beagles, K. E., Peterson, L., Zhang, X., Morris, J. & Kiem, H. P. Cyclosporine inhibits the development of green fluorescent protein (GFP)-specific immune responses after transplantation of GFP-expressing hematopoietic repopulating cells in dogs. *Hum. Gene Ther.* **16**, 725–733, https://doi.org/10.1089/hum.2005.16.725 (2005).
30. Koelsch, K. A., Wang, Y., Maier-Moore, J. S., Sawalha, A. H. & Wren, J. D. GFP affects human T cell activation and cytokine production following *in vitro* stimulation. *PLoS One* **8**, e50068, https://doi.org/10.1371/journal.pone.0050068 (2013).
31. Ansari, A. M. *et al.* Cellular GFP Toxicity and Immunogenicity: Potential Confounders in *in Vivo* Cell Tracking Experiments. *Stem Cell Rev.* **12**, 553–559, https://doi.org/10.1007/s12015-016-9670-8 (2016).
32. Gambotto, A. *et al.* Immunogenicity of enhanced green fluorescent protein (EGFP) in BALB/c mice: identification of an H2-Kd-restricted CTL epitope. *Gene Ther.* **7**, 2036–2040 (2000).
33. Burke, B., Sumner, S., Maitland, N. & Lewis, C. E. Macrophages in gene therapy: cellular delivery vehicles and *in vivo* targets. *J. Leukoc. Biol.* **72**, 417–428 (2002).
34. Siegert, I. *et al.* Electroporation of siRNA into mouse bone marrow-derived macrophages and dendritic cells. *Methods Mol. Biol.* **1121**, 111–119, https://doi.org/10.1007/978-1-4614-9632-8_9 (2014).
35. Huttinger, C. *et al.* Neoadjuvant gene delivery of feline granulocyte-macrophage colony-stimulating factor using magnetofection for the treatment of feline fibrosarcomas: a phase I trial. *J. Gene Med.* **10**, 655–667, https://doi.org/10.1002/jgm.1185 (2008).
36. Dokka, S., Toledo, D., Shi, X., Ye, J. & Rojanasakul, Y. High-efficiency gene transfection of macrophages by lipoplexes. *Int. J. Pharm.* **206**, 97–104 (2000).
37. Lai, Y., Xu, X., Zhu, Z. & Hua, Z. Highly efficient siRNA transfection in macrophages using apoptotic body-mimic Ca-PS lipopolyplex. *Int. J. Nanomed.* **13**, 6603–6623, https://doi.org/10.2147/ijn.s176991 (2018).
38. Schnoor, M. *et al.* Efficient non-viral transfection of THP-1 cells. *J. Immunol. Methods* **344**, 109–115, https://doi.org/10.1016/j.jim.2009.03.014 (2009).
39. Parre, V. D. *et al.* but not plasmid DNA is efficiently transfected in murine J774A.1 macrophages. *Biochem. Biophys. Res. Commun.* **327**, 356–360, https://doi.org/10.1016/j.bbrc.2004.12.027 (2005).
40. Phua, K. K., Leong, K. W. & Nair, S. K. Transfection efficiency and transgene expression kinetics of mRNA delivered in naked and nanoparticle format. *J. Control. Rel.* **166**, 227–233, https://doi.org/10.1016/j.jconrel.2012.12.029 (2013).
41. Kariko, K. *In vitro*-Transcribed mRNA Therapeutics: Out of the Shadows and Into the Spotlight. *Mol. Ther.* **27**, 691–692, https://doi.org/10.1016/j.ymthe.2019.03.009 (2019).
42. Vaidyanathan, S. *et al.* Uridine Depletion and Chemical Modification Increase Cas9 mRNA Activity and Reduce Immunogenicity without HPLC Purification. *Mol. Ther. Nucleic Acids* **12**, 530–542, https://doi.org/10.1016/j.omtn.2018.06.010 (2018).
43. Stanton, M. G. Current Status of Messenger RNA Delivery Systems. *Nucleic Acid. Ther.* **28**, 158–165, https://doi.org/10.1089/nat.2018.0726 (2018).
44. Lou, B., De Koker, S., Lau, C. Y. J., Hennink, W. E. & Mastrobattista, E. mRNA Polyplexes with Post-Conjugated GALA Peptides Efficiently Target, Transfect, and Activate Antigen Presenting Cells. *Bioconjug Chem.* **30**, 461–475, https://doi.org/10.1021/acs.bioconjchem.8b00524 (2019).
45. Kariko, K., Muramatsu, H., Keller, J. M. & Weissman, D. Increased erythropoiesis in mice injected with submicrogram quantities of pseudouridine-containing mRNA encoding erythropoietin. *Mol. Ther.* **20**, 948–953, https://doi.org/10.1038/mt.2012.7 (2012).
46. Goncalves, C., Akhter, S., Pichon, C. & Midoux, P. Intracellular Availability of pDNA and mRNA after Transfection: A Comparative Study among Polyplexes, Lipoplexes, and Lipopolyplexes. *Mol. Pharm.* **13**, 3153–3163, https://doi.org/10.1021/acs.molpharmaceut.6b00376 (2016).
47. Tros de Ilarduya, C., Sun, Y. & Duzgunes, N. Gene delivery by lipoplexes and polyplexes. *Eur. J. Pharm. Sci.* **40**, 159–170, https://doi.org/10.1016/j.ejps.2010.03.019 (2010).
48. Shende, P., Ture, N., Gaud, R. S. & Trotta, F. Lipid- and polymer-based plexes as therapeutic carriers for bioactive molecules. *Int. J. Pharm.* **558**, 250–260, https://doi.org/10.1016/j.ijpharm.2018.12.085 (2019).
49. Environ Toxicol ChemKettler, K., Veltman, K., van de Meent, D., van Wezel, A. & Hendriks, A. J. Cellular uptake of nanoparticles as determined by particle properties, experimental conditions, and cell type. *Env. Toxicol. Chem.* **33**, 481–492, https://doi.org/10.1002/etc.2470 (2014).
50. Ur Rehman, Z., Hoekstra, D. & Zuhorn, I. S. Mechanism of polyplex- and lipoplex-mediated delivery of nucleic acids: real-time visualization of transient membrane destabilization without endosomal lysis. *ACS nano* **7**, 3767–3777, https://doi.org/10.1021/nn3049494 (2013).
51. Resina, S., Prevot, P. & Thierry, A. R. Physico-chemical characteristics of lipoplexes influence cell uptake mechanisms and transfection efficacy. *PLoS One* **4**, e6058, https://doi.org/10.1371/journal.pone.0006058 (2009).
52. Elouahabi, A. & Ruysschaert, J. M. Formation and intracellular trafficking of lipoplexes and polyplexes. *Mol. Ther.* **11**, 336–347, https://doi.org/10.1016/j.ymthe.2004.12.006 (2005).
53. Balmayor, E. R. *et al.* Modified mRNA for BMP-2 in Combination with Biomaterials Serves as a Transcript-Activated Matrix for Effectively Inducing Osteogenic Pathways in Stem Cells. *Stem Cell Dev.* **26**, 25–34, https://doi.org/10.1089/scd.2016.0171 (2017).
54. Williams, D. J., Puhl, H. L. & Ikeda, S. R. A Simple, Highly Efficient Method for Heterologous Expression in Mammalian Primary Neurons Using Cationic Lipid-mediated mRNA Transfection. *Front. Neurosci.* **4**, 181, https://doi.org/10.3389/fnins.2010.00181 (2010).
55. Grudzien-Nogalska, E. *et al.* Synthesis of anti-reverse cap analogs (ARCAs) and their applications in mRNA translation and stability. *Methods Enzymol.* **431**, 203–227, https://doi.org/10.1016/s0076-6879(07)31011-2 (2007).
56. Naeim, F., Nagesh Rao, P., Song, S. X. & Phan, R. T. In *Atlas of Hematopathology (Second Edition)* (eds. Faramarz Naeim, P. Nagesh Rao, Sophie X. Song & Ryan T. Phan) 29–56 (Academic Press, 2018).
57. Roch, T. *et al.* Expression pattern analysis and activity determination of matrix metalloproteinase derived from human macrophage subsets. *Clin. Hemorheol. Microcirc.* **58**, 147–158, https://doi.org/10.3233/ch-141885 (2014).
58. Vijaya Bhaskar, T. B., Ma, N., Lendlein, A. & Roch, T. The interaction of human macrophage subsets with silicone as a biomaterial. *Clin. Hemorheol. Microcirc.* **61**, 119–133, https://doi.org/10.3233/ch-151991 (2015).

77

Author contributions

The manuscript has been read and approved by all authors. M.G., T.R. and H.M. conceived the study concept and designed experiments. H.M. performed most of the experiments and analysed the data. M.G., T.R. and H.M. evaluated and interpreted the data. H.M. drafted the manuscript. M.G., A.L. and T.R. revised manuscript. M.G. and A.L. supervised the study.

Competing interests

The authors declare no competing interests.

Additional information

Supplementary information is available for this paper at https://doi.org/10.1038/s41598-020-60506-4.

Correspondence and requests for materials should be addressed to M.G.

Reprints and permissions information is available at www.nature.com/reprints.

Publisher's note Springer Nature remains neutral with regard to jurisdictional claims in published maps and institutional affiliations.
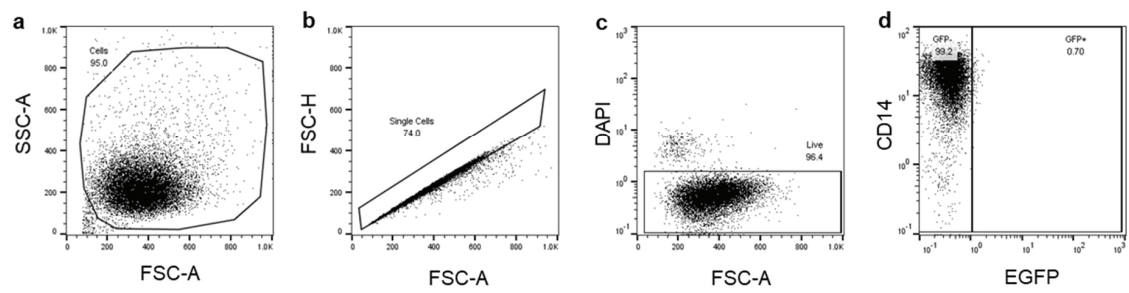
mRNA Transfection-Induced Activation of Primary Human Monocytes and Macrophages: Dependence on Carrier System and Nucleotide Modification

Hanieh Moradian[1, 2, 3], Toralf Roch[1,4,5], Andreas Lendlein[1, 2, 3], Manfred Gossen[1, 2, *]

1   Institute of Biomaterial Science, Helmholtz-Zentrum Geesthacht, 14513 Teltow, Germany
2   Berlin-Brandenburg Center for Regenerative Therapies (BCRT), 13353 Berlin, Germany
3   Institute of Biochemistry and Biology, University of Potsdam, 14476 Potsdam, Germany
4   Charité – Universitätsmedizin Berlin, corporate member of Freie Universität Berlin, Humboldt-Universität zu Berlin, and Berlin Institute of Health, Berlin-Brandenburg Center for Regenerative Therapies, Berlin, Germany
5   Center for Translational Medicine, Medical Department I, Marien Hospital Herne, University Hospital of the Ruhr-University Bochum, Herne, Germany.

* Corresponding Author, email address: manfred.gossen@hzg.de

Supplementary Figure 1. Gating strategy for flow cytometry data analysis; cells were discriminated from debris (**a**), followed by exclusion of aggregated cells (**b**). Discrimination of live and dead cells using DAPI as indicator for cell death (**c**), Identification of GFP expressing CD14 positive monocytes and macrophages (**d**)
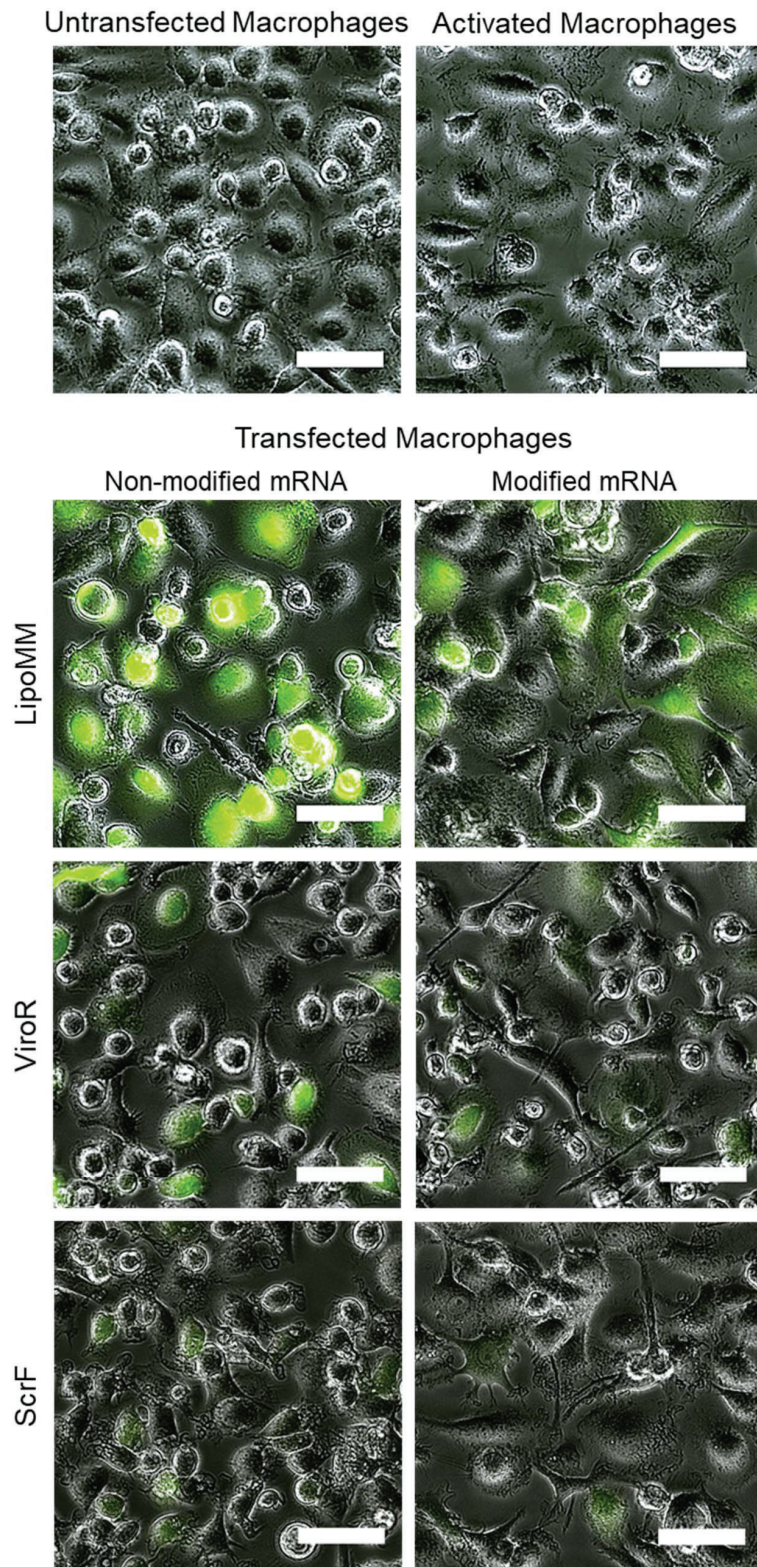
Supplementary Figure 2. Morphological analysis of Macrophages transfected with either modified or non-modified mRNA using three carrier reagents (125 ng/well). Phase contrast merged with EGFP fluorescent images show typical macrophage morphology for transfected as well as untransfected and activated (LPS+IFN-γ) cells (Scale bar=50 μm).
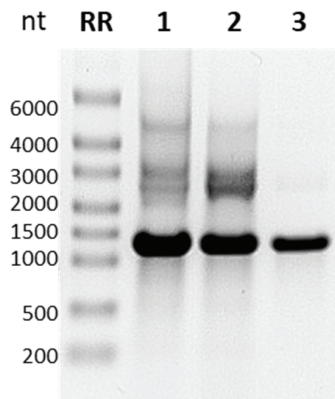
Supplementary Figure 3. Evaluation of IVT-mRNA integrity; mRNA product before (lane 1) and after (lane 2) treatment with DNase, as well as after purification using LiCl (lane 3) shows no residual plasmid template DNA or obvious degradation products. RiboRuler (RR; Thermo Scientific™) was used as size standard. The full-size gel (uncropped) is presented in Supplementary Figure 4.
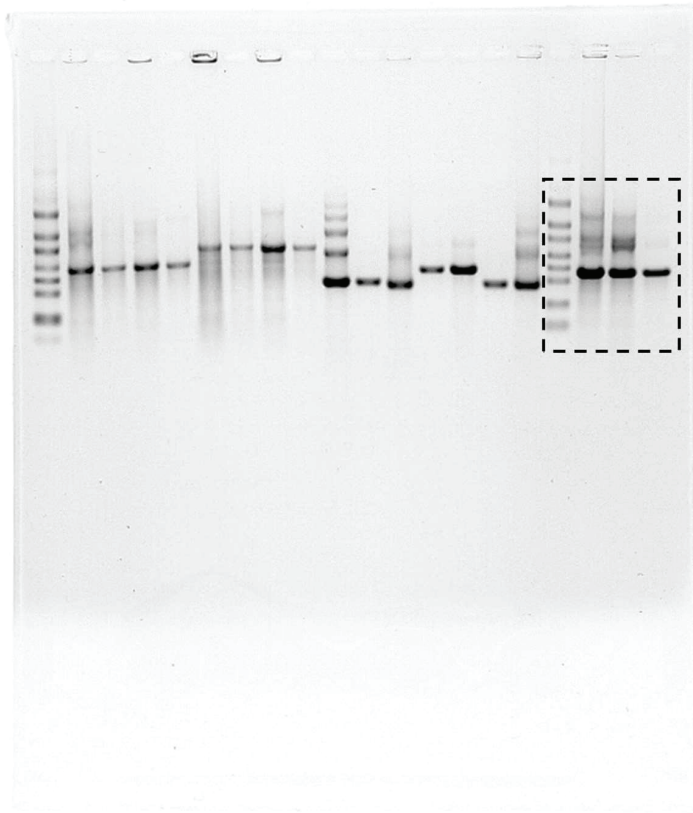
Supplementary figure 4. Area inside the dashed rectangle corresponds to cropped gel picture presented as Supplementary Figure 3. All other lanes are unrelated to this study.

Appendix II

Chemical modification of uridine modulates mRNA-mediated proinflammatory and antiviral response in primary human macrophages

Hanieh Moradian,[1,2,3] Toralf Roch,[4,5,6] Larissa Anthofer,[1,2] Andreas Lendlein,[1,2,3] and Manfred Gossen[1,2]

[1]Institute of Active Polymers, Helmholtz-Zentrum Hereon, Kantstr. 55, 14513 Teltow, Germany; [2]Berlin-Brandenburg Center for Regenerative Therapies (BCRT), Föhrerstr. 15, 13353 Berlin, Germany; [3]Institute of Biochemistry and Biology, University of Potsdam, Karl-Liebknecht-Str. 24-25, 14476 Potsdam, Germany; [4]Berlin Institute of Health at Charité – Universitätsmedizin Berlin, BIH Center for Regenerative Therapies (BCRT), Charitéplatz 1, 10117 Berlin, Germany; [5]Charité – Universitätsmedizin Berlin, Corporate Member of Freie Universität Berlin, Humboldt-Universität zu Berlin, Berlin Center for Advanced Therapies, Augustenburger Platz 1, 13353 Berlin, Germany; [6]Center for Translational Medicine, Immunology, and Transplantation, Medical Department I, Marien Hospital Herne, University Hospital of the Ruhr-University Bochum, Hölkeskampring 40, 44625 Herne, Germany

In vitro transcribed (IVT)-mRNA has been accepted as a promising therapeutic modality. Advances in facile and rapid production technologies make IVT-mRNA an appealing alternative to protein- or virus-based medicines. Robust expression levels, lack of genotoxicity, and their manageable immunogenicity benefit its clinical applicability. We postulated that innate immune responses of therapeutically relevant human cells can be tailored or abrogated by combinations of 5′-end and internal IVT-mRNA modifications. Using primary human macrophages as targets, our data show the particular importance of uridine modifications for IVT-mRNA performance. Among five nucleotide modification schemes tested, 5-methoxy-uridine outperformed other modifications up to 4-fold increased transgene expression, triggering moderate proinflammatory and non-detectable antiviral responses. Macrophage responses against IVT-mRNAs exhibiting high immunogenicity (e.g., pseudouridine) could be minimized upon HPLC purification. Conversely, 5′-end modifications had only modest effects on mRNA expression and immune responses. Our results revealed how the uptake of chemically modified IVT-mRNA impacts human macrophages, responding with distinct patterns of innate immune responses concomitant with increased transient transgene expression. We anticipate our findings are instrumental to predictively address specific cell responses required for a wide range of therapeutic applications from eliciting controlled immunogenicity in mRNA vaccines to, e.g., completely abrogating cell activation in protein replacement therapies.

INTRODUCTION

Growing demands for rapid, robust, and scalable production of therapeutics for disease prevention or treatment lead to remarkable advances in mRNA-based medicines over the past few years.[1–3] Lack of genotoxicity and facile production, as well as efficient intracellular delivery are advantages of mRNA therapeutics, when compared with preceding non-cellular, nucleic acids-based Advanced Therapy Medicinal Products such as recombinant viruses of DNA or recombinant protein-based medicines.[4,5] Clinical applications of mRNA include both, protein replacement therapies[6] and mRNA vaccines,[7,8] deployed not only for treatment of inherited and non-infectious acquired diseases such as cancer,[9] but also viral diseases, such as recently the severe acute respiratory syndrome coronavirus 2 (SARS-CoV-2).[10,11] The latter is a showcase example for the power of mRNA technology in tackling disease, outpacing other types of vaccines, with rather fast development from bench to market.[12]

Despite progress in mRNA production technology by *in vitro* transcription (IVT) via bacteriophage enzymes such as SP6, T3, and T7 RNA polymerases, potential immunogenicity of transcripts remains a major issue for some mRNA-based medicines.[5,13] The exogenous *in vitro* transcribed mRNAs (IVT-mRNA) can be recognized by various endosomal and cytosolic pattern recognition receptors (PRRs).[8] Examples are Toll-like receptor-7, and -8 (TLR-7, -8) and TLR-3,[14] sensing single- and double-stranded RNA (ssRNA and dsRNA), respectively. The latter can also be recognized by melanoma differentiation-associated protein 5 (MDA5)[15,16] and retinoic acid-inducible gene I (RIG-I), which are part of the RIG-I-like receptor family. Pathways activated by these PRRs induce production of cytokines, such as type I interferons (IFNs), tumor necrosis factor-α (TNF-α), interleukin (IL)-1β, and IL-6,[17] as well as upregulation of co-stimulatory molecules such as CD80, CD86, and CD40.[18] RIG-I also recognizes the 5′-triphosphate end of IVT-RNA, particularly those of dsRNA termini.[19] In addition, cell-autonomous mechanisms mediated by 2′–5′ oligoadenylate synthases (OAS), RNase L, or the
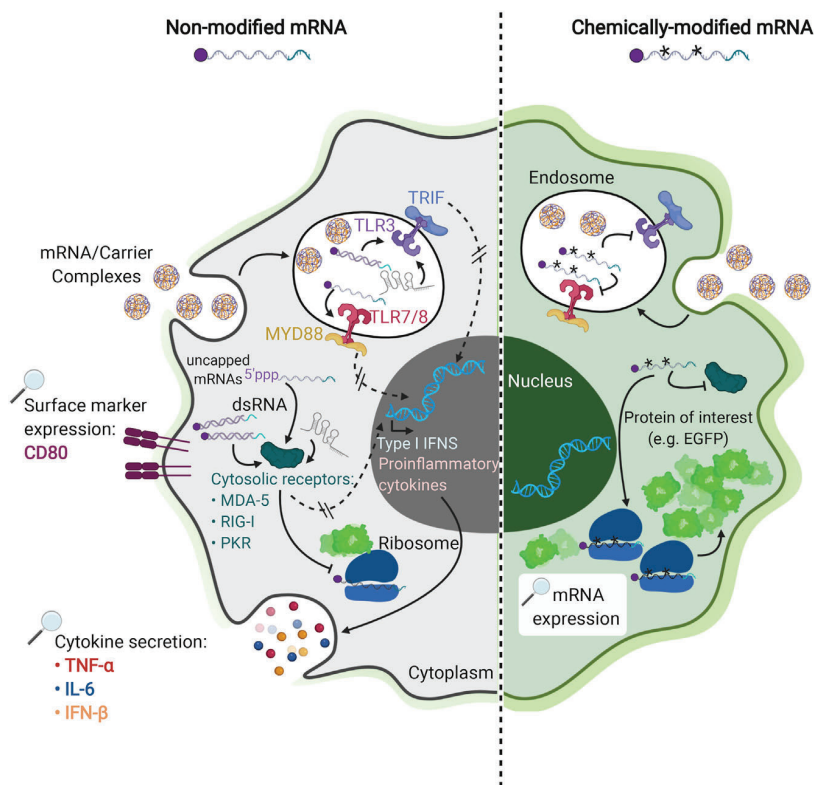
Figure 1. The effect of chemical modification of IVT-mRNA on potential cell response

Intracellular pathways of innate immune response in macrophages transfected with either non-modified (left) versus chemically modified IVT-mRNA (right). The elements labeled with magnifying glass are the actual readouts measured at the present study.

rophages reveals the pattern of cellular response, which could be harnessed to minimize or potentially abrogate the subsequent immune response (Figure 1). In a comprehensive side-by-side study, mRNA constructs with three distinct cap structures, with or without extra phosphatase treatment, were investigated in parallel with three different uridine modifications and one cytidine modification; see Figure 2 and Table S1 for details of mRNA synthesis process and chemistry, and Figure S1 for precise chemical formula of cap and nucleoside modifications. The quality and biological performance of chemically modified IVT-mRNAs upon transfection in macrophages were evaluated as key readouts. This was achieved by assessing changes in surface marker expression and the cytokine secretion patterns as indicators of antiviral and proinflammatory immune responses. Transfection efficiency and level of transgene expression were determined to rule out that the postulated effect of modifications, i.e., dampening of the innate immune response, should not reduce protein production. In fact, the highest possible level of expression from the administration of the lowest feasible dose of mRNA is desired, if not required, for most clinical applications, also under health economic considerations. Thus, our work provides guidelines to uncouple maximized IVT-mRNA-mediated protein production levels from immune activation that could be prohibitive for future translational applications.

IFN-induced, RNA-activated protein kinase R (PKR) can directly lead to RNA instability and inhibition of RNA expression.[20–22]

Previous studies suggested several approaches to abrogate or modulate unintended immune activation, such as chemical modification of either cap structures[23,24] or nucleotides,[23–27] optimization of pDNA template sequence,[23,28] and modification of IVT reaction conditions,[29,30] as well as extra purification steps to remove impurities, e.g., dsRNA by-products.[31,32] However, most of these strategies were evaluated either *in vitro*, using non-primary macrophage and monocyte cell lines such as RAW 264.7 or THP-1, respectively, or investigated *in vivo* by using mouse models.[33] Indeed, macrophages are of particular interest for this type of study. Here, we analyze the effects of IVT-mRNA transfection in primary human monocyte-derived macrophages, which are the first line of cellular defense due to their high phagocytosis capacity. We, therefore, consider this cell type to be of special relevance for clinical research, not only for its expected uptake of formulated IVT-mRNA even if not specifically targeted,[34] but also because of its considerable immune-modulatory capacity,[35,36] as well as its ability to initiate and modulate antiviral or anti-tumor T cell responses[37,38] as antigen-presenting cells,[39] and as a potential direct target in addressing macrophage-related diseases.[40]

We postulated that systematic analysis of different 5′-end and internal nucleotide modifications of IVT-mRNA transfected in human mac-

RESULTS
Study design
IVT-mRNAs with distinct chemical compositions were evaluated by agarose gel electrophoresis and dot blot analysis to determine transcript integrity and potential dsRNA by-products, respectively. Primary human macrophages were generated from blood-derived CD14+ monocytes. Macrophages (MΦs) were subsequently transfected with lipoplexes containing the chemically modified IVT-mRNAs. The fluorescent protein marker production was evaluated 24 h posttransfection by fluorescent microscopy and further quantified with flow cytometry. In parallel, immune response of transfected MΦs was assessed either by measurement of activation-induced cell surface molecules such as CD80, and by analyzing cytokine secretion patterns, which included TNF-α, IL-6, and IFN-β.
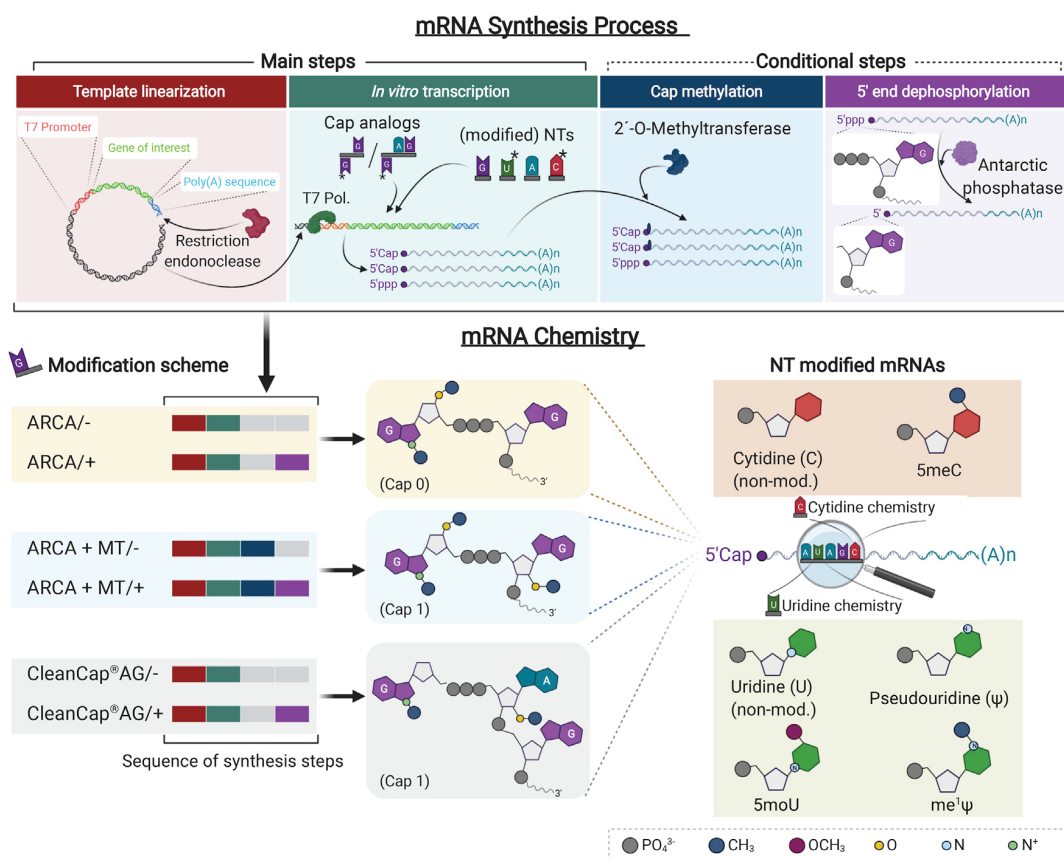
Figure 2. Overview of *in vitro* transcription process and chemical modifications of IVT-mRNA used in this study

Main steps, and conditional post-transcriptional treatments, which were only applied to samples with cap modifications, i.e., methylation and dephosphorylation, are illustrated at the top panel. Simplified chemistry of IVT-mRNA synthesized and utilized at this study with various cap and/or nucleotide modifications are depicted at the bottom panel. Sequence of synthesis steps applied for cap modified mRNAs are indicated as colored bars corresponding to each synthesis step. Phosphatase treatment step is further indicated with/− or/+ next to sample name. Chemical formula only indicate the main variations among nucleotides as well as cap structures. See Figure S1 for precise chemical formula of cap and nucleotide modifications, and Table S1 for detailed information on chemistry and synthesis process of each sample. pDNA, plasmid DNA; T7 Pol., T7 RNA polymerase; NTs, nucleotides; ARCA, anti-reverse cap analog; Ψ, pseudouridine; me^{1}Ψ, N^1-Methylpseudouridine; 5moU, 5-methoxy-uridine; 5meC, 5-methyl-cytidine.

Chemical modification of IVT-mRNA

Three variations of cap structure, including anti-reverse cap analogs (ARCA) as an example of Cap 0 structure, 2′-O-methylated ARCA (ARCA + MT), and CleanCap AG (CleanCap), as two examples of Cap 1 structure, were investigated side-by-side (Figure 2). Note that co-transcriptional integration of CleanCap requires a nucleotide change in T7 promoter at +1/+2 positions from "GG" to "AG"; see "Materials and methods: IVT-mRNA synthesis with various chemical modifications" for detailed explanation of the procedure.

Since none of the co-transcriptional cap modifications are entirely efficient in transcript capping, a fraction of uncapped IVT-mRNA could trigger immune response through their 5′-triphosphate end groups. Thus, to investigate the effect/necessity of 5′-triphosphate removal on overall biological performance of IVT-mRNA products,

both in terms of protein production level and immune stimulation, an extra phosphatase treatment was included for each of the three examined cap structures and evaluated in parallel.

To assess the importance of IVT-mRNA nucleotide modifications, non-modified IVT-mRNA was compared with uridine modifications, namely pseudouridine (Ψ), N1-methyl-pseudouridine (me^{1}Ψ), and 5-methoxyuridine (5moU), a cytidine modification 5-methylcy-tidine (5meC), as well as a combination of Ψ and 5meC (Ψ/5meC) (Table S1).

Of note, IVT-mRNA synthesized with the various cap structures for comparative analysis of the effect of 5′-end modifications were uniformly substituted with Ψ and 5meC. This combination of nucleotide modifications, which has been extensively analyzed in the past, is
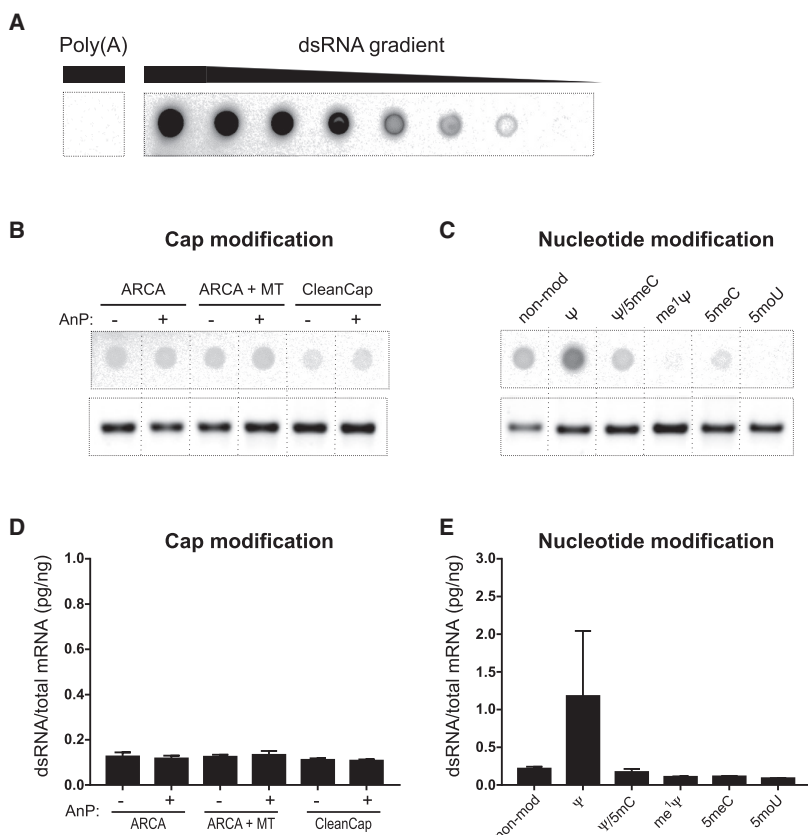
Figure 3. IVT-mRNA double strand content and integrity investigated by dot blot and agarose gel electrophoresis

(A) Poly(A) as ssRNA-negative control, and dsRNA positive control were blotted with the same amount as main samples (1,000 ng/dot), next to dsRNA gradient of 4-fold serial dilutions for generating a standard curve for subsequent quantifications and detected by a dsRNA-antibody. Representative dot blots of IVT-mRNAs with different (B) cap modifications, and (C) nucleotide modifications presented side-by-side with denatured agarose gel electrophoresis images of the same samples. Quantified dsRNA for IVT-mRNAs with various cap modifications (D) as well as (E) nucleotide modifications plotted as weight percent of dsRNA content (calculated according to positive control standard curve) to total mRNA amount blotted on membrane for each sample. Error bars indicate SEM for three independently synthesized IVT-mRNA batches blotted on the membrane in duplicates; see Figure S2 for uncropped membrane and the gel image. ARCA, anti-reverse cap analog; MT, methyl-transferase; AnP, Antarctic phosphatase; Ψ, pseudouridine; me$^1\Psi$, N^1-Methylpseudouridine; 5moU, 5-methoxy-uridine; 5meC, 5-methylcytidine.

known to reduce the immune response without its complete elimination,[41] and thus can serve as a baseline for analyzing further modifications. Conversely, for comparatively analyzing the effects of internal nucleotide modifications, we uniformly incorporated a 5′ ARCA as a standard cap structure in the synthesis of IVT-mRNAs.

Chemical modification of nucleotides, but not cap structure, affects dsRNA content of IVT-mRNA

Dot blot analysis was performed using the J2 dsRNA-specific antibody in order to evaluate the degree of dsRNA formation in the run-off transcripts, which is a major trigger of cellular anti-IVT-mRNA responses (Figure 3), as positive control serial dilutions of a dsRNA sample were used for validation and subsequent quantification (Figure 3A). Accordingly, the calculated values of dsRNA were normalized to the total amount of membrane-immobilized IVT-mRNA for each sample. Identical amounts of ssRNA were measured as negative control, and found to be non-detectable by the dsRNA-specific antibody, ruling out the interference of unspecific binding of J2 antibody in this experimental setup (Figure 3A).

No obvious differences were observed between signal intensities of IVT-mRNAs equipped with different cap structures, in the groups with or without 5′-end dephosphorylation (Figure 3B). This finding

was also proved quantitatively, with only minor variations in dsRNA content (Figure 3D). In contrast, IVT-mRNAs with ARCA as cap structure and various nucleotide modifications had a prominent effect on dsRNA content of IVT-mRNA products. Notably, the highest dsRNA content was found in non-modified IVT-mRNA, and Ψ-modified IVT-mRNA. However, the dsRNA signal was reduced by 5meC, and Ψ/5meC modifications of IVT-mRNAs. Interestingly, IVT-mRNA with other uridine modifications, i.e., me$^1\Psi$ and 5moU, resulted in the lowest number of dsRNA by-products (Figures 3C and 3E), underscoring overall impact of uridine on quality of transcripts. Moreover, the integrity of IVT-mRNA samples was evaluated with agarose gel electrophoresis (Figures 3B and 3C) to rule out correlation of detected dsRNA signal to presence of potential unknown side-products or possible degradation. Of note, similar patterns were consistently observed throughout IVT-mRNA samples of three independent syntheses.

Protein production level was substantially influenced by IVT-mRNA chemistry

Transfection efficiency and level of protein production were measured as key parameters to assess biological performance of IVT-mRNAs with distinct chemical modifications. IVT-mRNA coding enhanced GFP (EGFP) was transfected in primary human monocyte-derived macrophages in low dose (125 ng·mL^{-1}) and high dose (500 ng·mL^{-1}). The corresponding mRNA amounts for the two administrated doses were selected according to cell viability and immune activation as described in our earlier study.[41] IVT-mRNA expression was initially assessed qualitatively by fluorescent microscopy (Figures 4A and 4E), and quantified at single cell resolution by
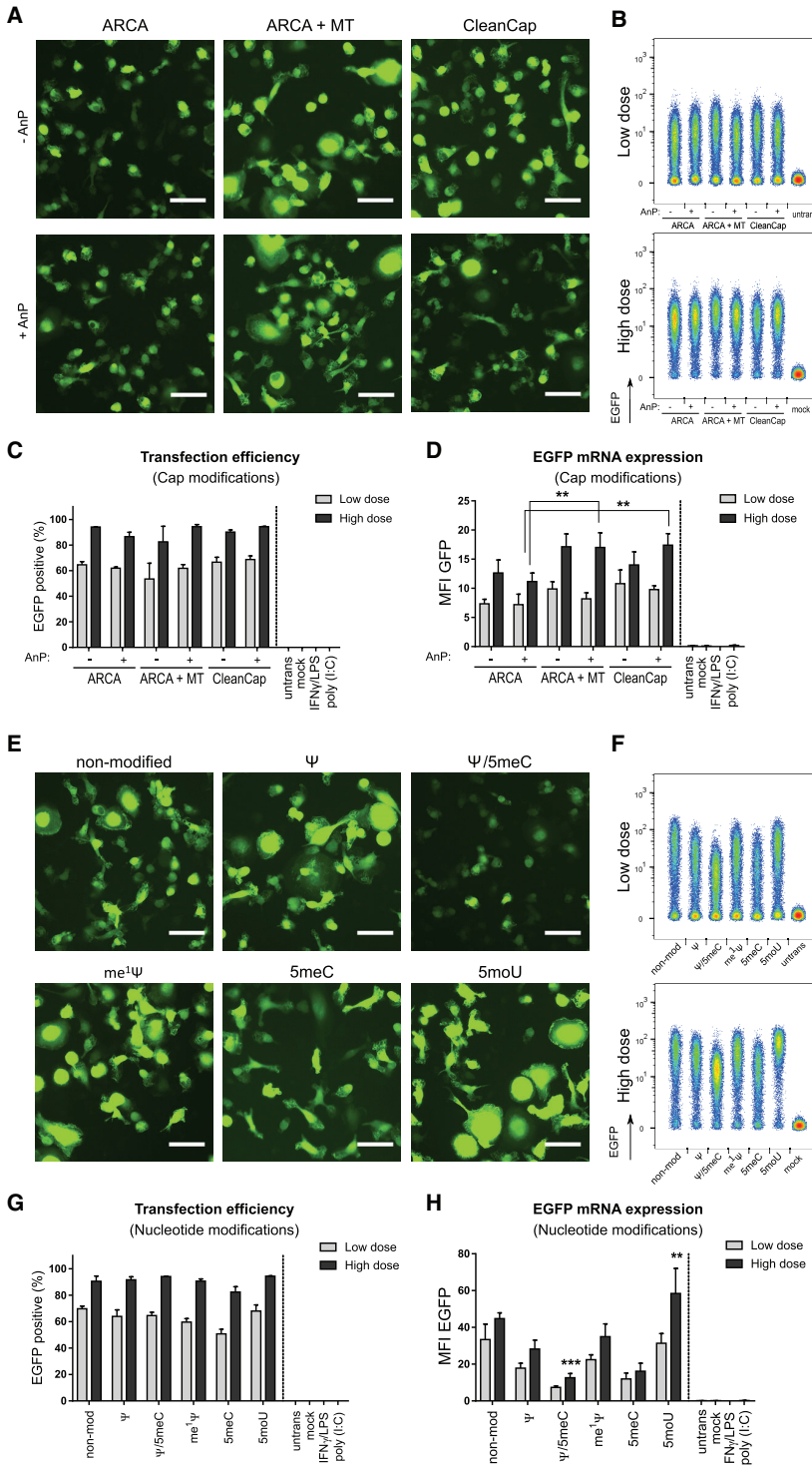
Figure 4. Transfection efficiency and EGFP mRNA expression level in macrophages transfected with IVT-mRNA with various cap and nucleotide modifications

(A) Representative fluorescent images and (B) flow cytometric density plots indicating EGFP expression in macrophages transfected with low dose and high dose of IVT-mRNA made of either Cap 0 (i.e., ARCA), or Cap 1 (i.e., ARCA + MT, and CleanCap) with and without phosphatase treatment. (C) Quantification of transfection efficiency, and (D) EGFP mRNA expression level in macrophages transfected with low doses and high doses of the different IVT-mRNAs with cap modifications. (E) Representative fluorescent images of macrophages transfected with low doses of IVT-mRNA composed of nucleotides with different chemical modifications. (F) Flow cytometric density plots indicating EGFP expression in macrophages transfected with low dose and high dose of IVT-mRNA with various nucleotide modifications. (G) Transfection efficiency and (H) EGFP mRNA expression level quantified by flow cytometry and plotted in terms of EGFP-positive cells percentage and MFI of EGFP signal among EGFP-positive cell populations, respectively. Poly(I:C) was also transfected in low dose (125 ng·mL^{-1}). For each condition 125 ng·mL^{-1} and 500 ng·mL^{-1} of IVT-mRNA were used for transfection referred here as low dose and high dose, respectively. Values are presented as mean ± SD. Error bars indicate SD of three independent experiments from three individual donors. Bar = 50 μm. Statistical differences are depicted with **p < 0.005, ***p < 0.001. ARCA, anti-reverse cap analog; MT, methyl-transferase; AnP, Antarctic phosphatase; Ψ, pseudouridine; me^{1}Ψ, N^1-Methylpseudouridine; 5moU, 5-methoxy-uridine; 5meC, 5-methyl-cytidine.

flow cytometry (Figures 4B–4D, 4F–4H). Modifications of the cap structure had only a slight impact on fluorescence intensity of macrophages transfected with either Cap 0 (ARCA) or Cap 1 (ARCA + MT or CleanCap) modified IVT-mRNAs (Figures 4A and 4B). In addition, no obvious differences in EGFP production from phosphatase-treated IVT-mRNAs, for any of the three examined cap structures could be observed (Figure 4A). No signal was detected for the untransfected controls (Figure S3). Moreover, flow cytometric assessment revealed substantial amounts of EGFP-producing MΦ with slight variations in EGFP production level after transfection with low as well as high doses of cap modified IVT-mRNA (Figure 4B). Transfection efficiency and EGFP mRNA expression was quantified as percent of EGFP-positive cells, and mean fluorescent intensity (MFI) of EGFP in positive cells, respectively (Figures 4C and 4D). Remarkably, the low and high IVT-mRNA doses led to a transfection efficiency of more than 60% and 80%, respectively. However, no significant differences were found between transfection efficiency of IVT-mRNAs with distinct cap modifications, neither at low dose nor at high dose (Figure 4C). When treated with phosphatase, the level of EGFP production was significantly higher for Cap 1 (i.e., ARCA + MT and CleanCap) compared with Cap 0 (i.e., ARCA) at high dose of mRNA (Figure 4D).

For IVT-mRNA with chemical modifications of nucleotides, non-modified as well as Ψ, me^{1}Ψ, and 5moU modified IVT-mRNAs led to the highest EGFP signal intensity, notably also at low dose of mRNA, whereas 5meC and its combination with Ψ resulted in the lowest EGFP synthesis in transfected MΦs, measured 24 h post transfection (Figure 4E). Different EGFP levels were consistently detected in MΦs transfected with various nucleotide modifications both at low dose and, more prominently, at high dose of IVT-mRNA (Figure 4F). Especially 5moU outperformed the other chemical modifications under the aspect of maximizing protein synthesis. While the number of EGFP-positive cells was not affected by different nucleotide modifications at low and high doses of mRNA (Figure 4G), the EGFP production level was substantially higher for 5moU, non-modified, and me^{1}Ψ IVT-mRNA, especially at high dose of mRNA (Figure 4H). The lowest levels of EGFP mRNA expression were consistently observed for Ψ/5meC modified IVT-mRNA (Figures 4E, 4F, and 4H). The results were consistent for different mRNA syntheses, since similar transfection efficiencies and EGFP intensities could be observed when one donor was treated with three independently prepared IVT-mRNA batches (Figure S4), which excluded a potential bias due to batch effects.

In addition to the quantitative assessment with flow cytometry and qualitative analysis with fluorescent microscopy, the resulting protein produced by IVT-RNA with different chemical modifications were evaluated using western blot analysis. In fact, it could be confirmed that intact EGFP protein was produced for all chemically modified IVT-mRNA with no sign of other unspecific side products (Figure S5).

Nucleotide chemical modifications of IVT-mRNA modulate CD80 in transfected MΦs already at low doses

Unintended cellular stress, and immune responses elicited by IVT-mRNA upon transfection are critical issues, which could lead to com-plete inhibition of protein production machinery and eventually result in cell death. Analysis of co-stimulatory surface molecules, such as CD80, was found to be a valuable readout for evaluating the activation of transfected MΦs.[41] Thus, CD80 production was measured by flow cytometry and compared within different IVT-mRNA modifications (Figure 5). Macrophage treatment with IFNγ/lipopolysaccharide (LPS) resulted in a substantial upregulation of CD80, whereas poly(I:C) induced only little amounts of CD80. Interestingly, the CD80 levels on cells transfected with low dose of IVT-mRNA remained unchanged, irrespective of cap modifications, whereas noticeable CD80 upregulations were detected at the high-dose conditions (Figure 5A). Quantification of the results revealed that phosphatase treatment consistently reduced these elevated CD80 levels for all three examined cap structures (Figure 5B).

Nucleotide modification of IVT-mRNA, on the other hand, resulted in pronounced differences in CD80 level both at low dose, and more dramatically at high dose of IVT-mRNA transfected MΦs, clearly recognizable by comparison of histograms with negative and positive controls (Figure 5C). Maximum level of CD80 was related to non-modified and 5meC-modified IVT-mRNA, when compared quantitatively (Figure 5D). While Ψ modification resulted in high CD80 production levels, combined Ψ and 5meC modifications resulted in substantial reduction of IVT-mRNA induced CD80 production levels (Figure 5D). Other uridine modifications including me^{1}Ψ or 5moU led to no changes in CD80 production in relation to untransfected MΦs when transfected at low dose of IVT-mRNA, and only a slight increase at high dose (Figure 5D).

The downstream effect of IVT-mRNA-induced immune response on cell viability was investigated by measurement of DAPI-negative cells via flow cytometry. Interestingly, MΦs that were producing a higher level of CD80, such as high dose of ARCA + MT in cap modified IVT-mRNA and non-modified, Ψ, and 5meC-modified IVT-mRNAs, were observed to have a low level of cell viability (Figure S6).

Chemical modifications of IVT-mRNA influenced both proinflammatory and antiviral cytokines secretion by transfected MΦs

To evaluate the immune activation of MΦs, secretion of TNF-α, IL-6, and IFN-β was measured at 6 h and 24 h posttransfection, throughout all cap modifications (Figure 6), as well as nucleotide modifications (Figure 7). There were no significant differences between TNF-α and IL-6 secretion from MΦs transfected with Cap 0 structure (i.e., ARCA) and Cap 1 structures (i.e., ARCA + MT, or CleanCap) 6 h after transfection (Figures 6A and 6C). This applies for low dose and most of high doses of IVT-mRNA, in particular when absolute cytokine levels are considered in relation to the LPS positive control. However, after 24 h, Cap 1 structures induced higher levels of TNF-α and IL-6 compared with Cap 0 at high dose of mRNA (Figures 6B and 6D). Noteworthy, phosphatase-treated IVT-mRNAs elicited less TNF-α and IL-6 secretion at high dose of IVT-mRNA, consistently for all cap structures, when compared with untreated IVT-mRNA of the same cap formula
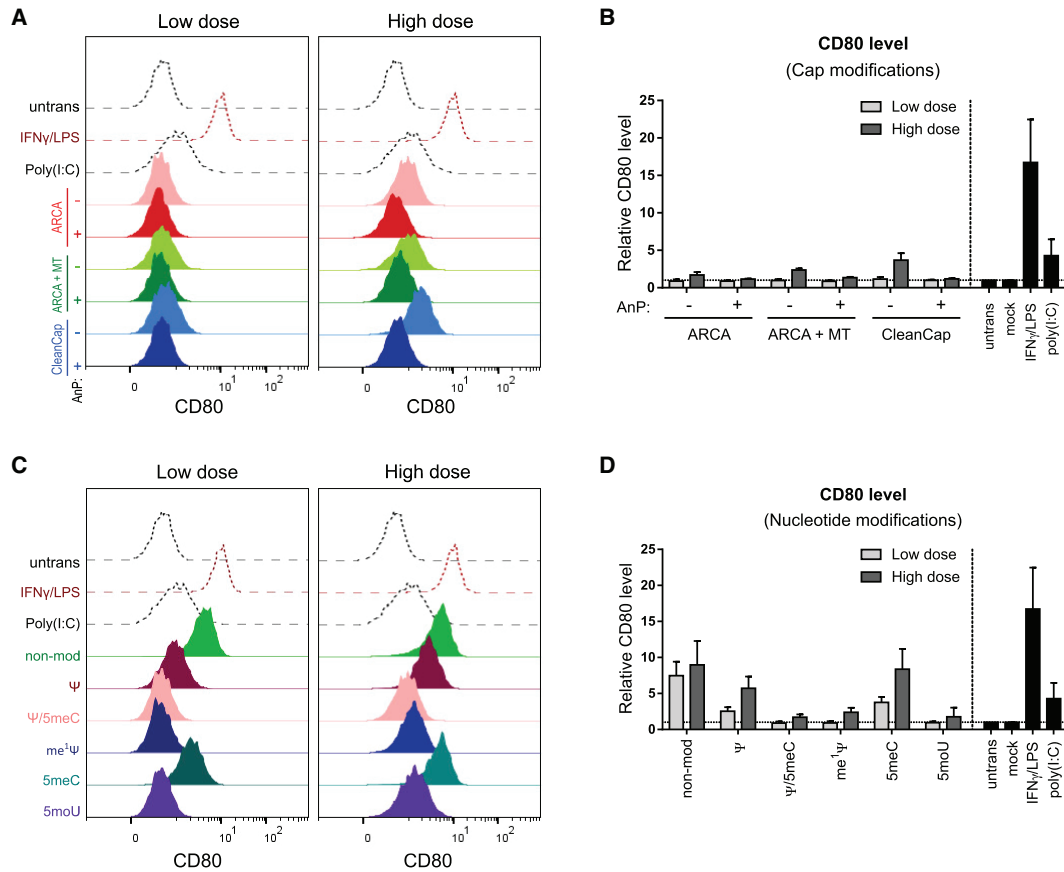
Figure 5. Evaluation of CD80 expression in macrophages, in response to IVT-mRNA transfection with different chemistry

Staggered histogram of CD80 levels in macrophages transfected with low doses and high doses of IVT-mRNA with various cap modifications (A), as well as nucleotide modifications (C) along with untransfected, poly(I:C), the dsRNA positive control transfected in low dose, and activated macrophages. Activated cells were treated with LPS/IFN-γ. MFI of CD80 normalized to untransfected cells is indicated for macrophages transfected with low doses and high doses of mRNA with different cap modifications (B) and nucleotide modifications (D). Mock transfection refers to carrier (i.e., LipoMM) without mRNA. For each condition 125 ng·mL^{-1} and 500 ng·mL^{-1} of IVT-mRNA were used for transfection, referred here as low dose and high dose, respectively. Expression was measured 24 h after transfection. Values are presented as mean ± SD. Error bars indicate SD of three independent experiments from three individual donors (n = 3). ARCA, anti-reverse cap analog; MT, methyl-transferase; AnP, Antarctic phosphatase; Ψ, pseudouridine; me^{1}Ψ, N^1-Methylpseudouridine; 5moU, 5-methoxy-uridine; 5meC, 5-methyl-cytidine.

(Figures 6A–6D). Similar patterns were observed for IFN-β, as enhanced IFN-β secretion was detected for Cap 1 compared with Cap 0 (Figures 6E and 6F). While there were no remarkable differences between various cap structures with and without phosphatase treatment at 6 h post transfection (Figure 6E), phosphatase treatment led to substantial decrease in IFN-β secretion, particularly noticeable for CleanCap by secretion of IFN-β almost identical to untransfected MΦs (Figures 6E and 6F) and unexpected for this cap structure given the reported high incorporation efficacy (data provided by manufacturer).

Nucleotide modifications had a profound effect on cytokine secretion (Figure 7). Non-modified nucleotides persistently resulted in the highest level of TNF-α, IL-6, and IFN-β, similar to corresponding positive controls, both at low and high doses of IVT-mRNA (Fig-

ure 7). IVT-mRNA modified only with Ψ or 5meC resulted in significantly high levels of TNF-α and IL-6 secretion at 6 h and more drastically at 24 h upon transfection, both at low and high doses of mRNA when compared with untransfected MΦs (Figures 7A–7D). However, transfection-induced cytokine secretion was significantly reduced, but not abolished, when the combination of the two modifications, i.e., Ψ/5meC, was applied together (Figures 7A–7D). Uridine substitution with me^{1}Ψ led to a significant reduction of TNF-α (Figures 7A and 7B) and IL-6 (Figures 7C and 7D) secretion at low dose, and high dose of IVT-mRNA, when compared with unmodified mRNA. In contrast, 5moU IVT-mRNA outperformed other modifications by completely preventing TNF-α and IL-6 induction, even at high doses of IVT-mRNA when measured at 6 h (Figures 7A and 7C) and 24 h (Figures 7B and 7D). Consistently, IFN-β secretion was found to be minimal for the 5moU modification (Figures 7E and 7F), whereas
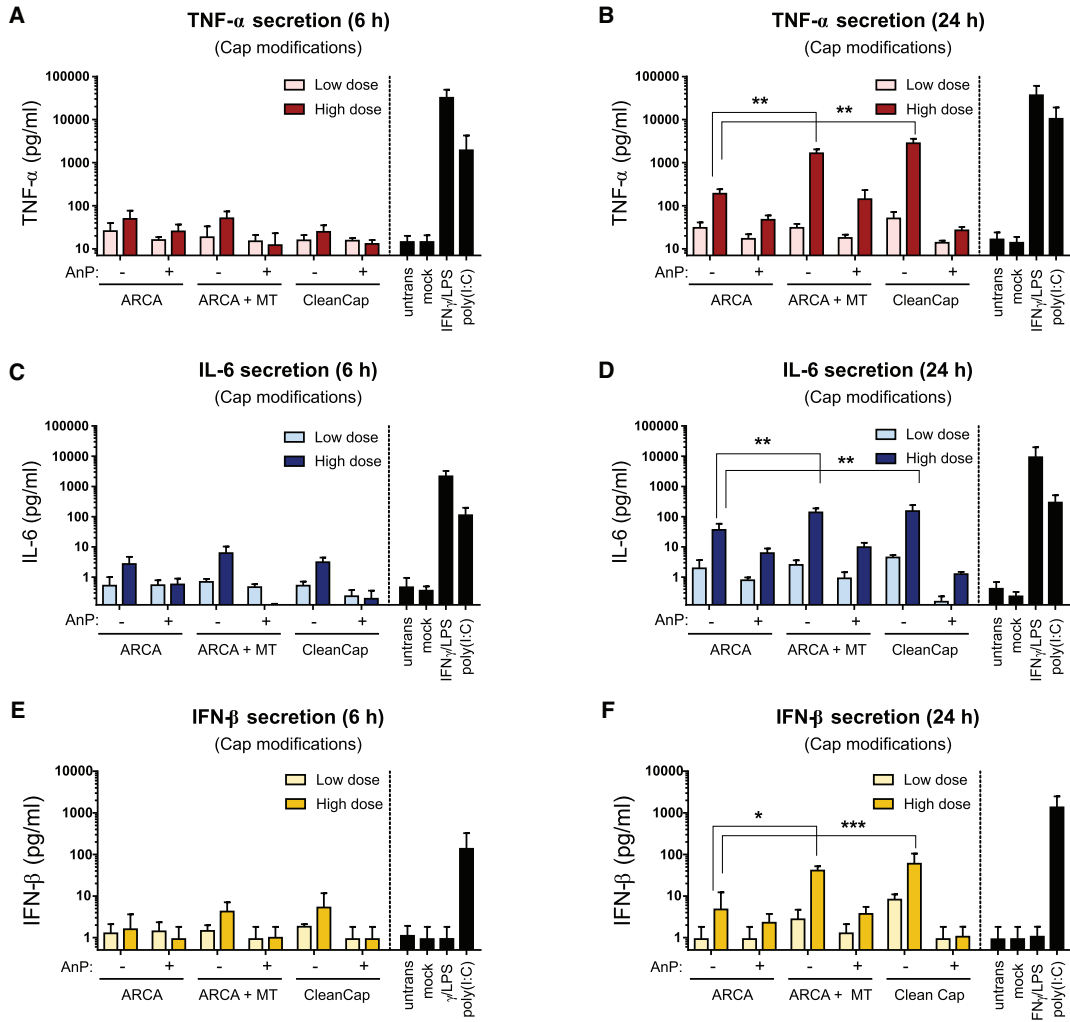
Figure 6. Cytokine secretion by macrophages transfected with cap modified IVT-mRNA

TNF-α secretion was measured (A) 6 h and (B) 24 h after transfection with low doses and high doses of IVT-mRNA. IL-6 secretion was quantified (C) 6 h and (D) 24 h post transfection. IFN-β secretion was evaluated (E) 6 h and (F) 24 h upon transfection. Mock transfection refers to carrier (i.e., LipoMM) without mRNA. Poly(I:C) was also transfected in low dose as positive control. For each condition, 125 ng·mL^{-1} and 500 ng·mL^{-1} of IVT-mRNA were used for transfection, referred here as low dose and high dose, respectively. Values are presented as mean ± SD. Error bars indicate SD of three independent experiments from three individual donors. Statistical differences are depicted with *$p < 0.05$, **$p < 0.005$, ***$p < 0.001$. Error bars indicate SD. ARCA, anti-reverse cap analog; MT, methyl-transferase; AnP, Antarctic phosphatase.

non-modified, Ψ-, 5meC-modified IVT-mRNA resulted in the highest level of antiviral response. While Ψ/5meC and me^{1}Ψ modifications were beneficial in reduction of IFN-β secretion both at low and high doses of IVT-mRNA at 6 h (Figure 7E), they failed to completely overcome the IFN-β production at high dose of mRNA when measured at 24 h. Overall, 5moU-modified IVT-mRNA was found to induce only minimal levels of cytokine secretion, in most cases similar to untransfected MΦs (Figure 7).

To ensure that the observed effects were not specific to the sequence of EGFP, an IVT-mRNA coding for another protein,

i.e., mCherry, with a different nucleotide sequence was evaluated for four selected nucleotide modification conditions. The transfection efficiency, as well as level of mRNA expression revealed the same pattern of differences as observed for EGFP (Figure S7A). The immune activation was measured 24 h post transfection in terms of CD80 expression and IFN-β secretion. When plotted side-by-side to EGFP transfected macrophages, no remarkable difference was identified (Figures S7B and S7C). This result was consistent with dsRNA content of mCherry IVT-mRNA samples evaluated by dot blot (Figure S8).
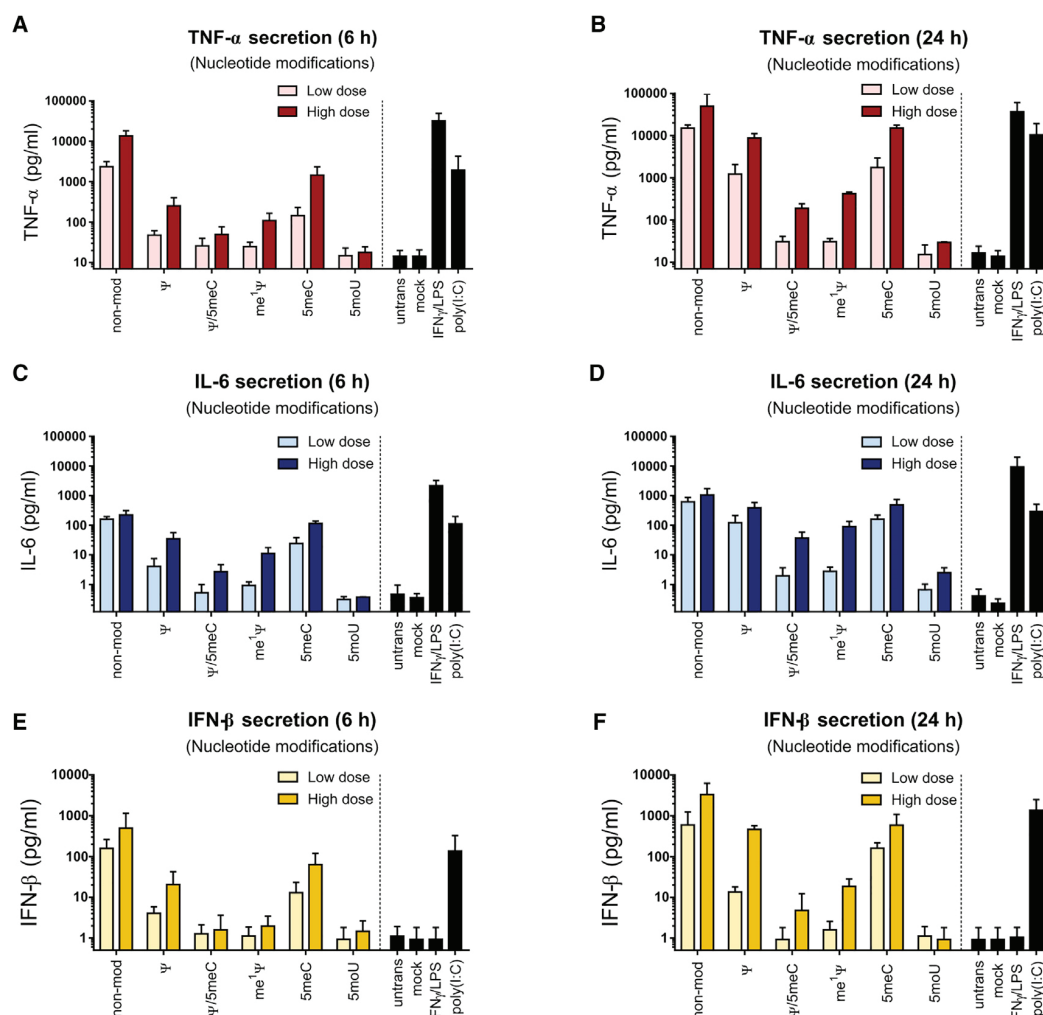
Figure 7. Cytokine secretion in macrophages transfected with IVT-mRNA with various nucleotide modifications

TNF-α secretion was measured (A) 6 h and (B) 24 h after transfection with low doses and high doses of different IVT-mRNA formula. IL-6 secretion was quantified (C) 6 h and (D) 24 h after transfection. IFN-β secretion was investigated (E) 6 h and (F) 24 h upon transfection. Mock transfection refers to carrier (i.e., LipoMM) without mRNA. Poly(I:C) was also transfected in low-dose positive control. For each condition, 125 ng·mL^{-1} and 500 ng·mL^{-1} of IVT-mRNA were used for transfection, referred here as low dose and high dose, respectively. Values are presented as mean ± SD. Error bars indicate SD of three independent experiments from three individual donors (n = 3). Ψ, pseudouridine; me^{1}Ψ, N^1-Methylpseudouridine; 5moU, 5-methoxy-uridine; 5meC, 5-methyl-cytidine.
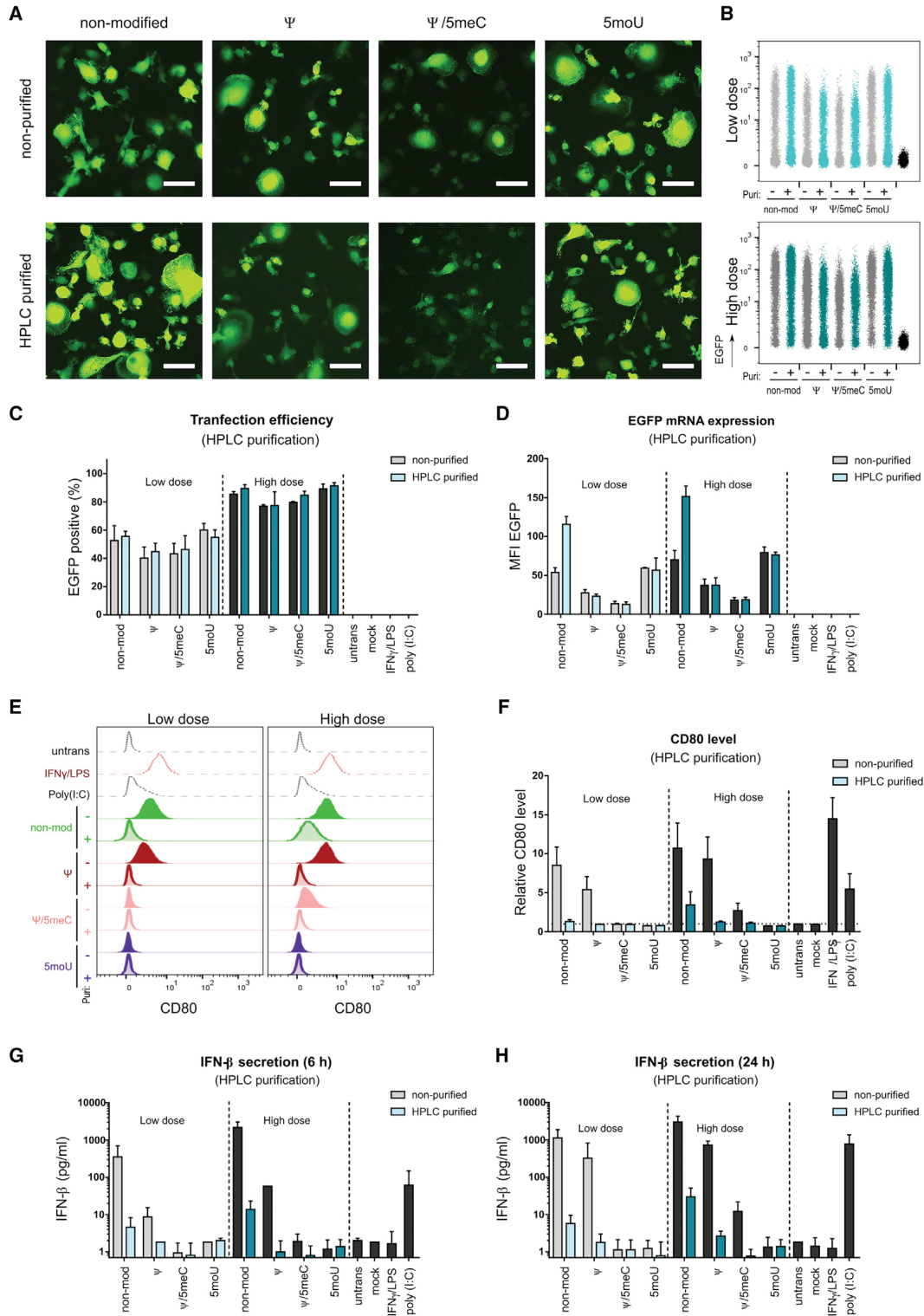
Effect of HPLC purification on MΦ immune response triggered upon transfection of IVT-mRNA

While we have shown so far that immune responses due to delivery of synthesized mRNAs can be minimized if not abrogated by the proper choice of modified nucleotides, we also addressed the possibility of avoiding macrophage activation by an additional HPLC-purification step even for otherwise immunogenic IVT-mRNA chemistry, as previously described for other cell types.[31] The elimination of impurities and dsRNA by preparative chromatography, also proved by dot blot (Figure S8C), barely effected transfection efficiency and levels of transgene expression (Figures 8A–8E) in a series of experiments analogous to those presented in Figure 4. The only exception was the

2-fold increase in EGFP MFI for non-modified IVT-mRNA. By contrast, for IVT-mRNAs that were highly immunogenic in the un-purified stage, i.e., non-modified and Ψ-modified, cell activation measured both by CD80 levels (Figure 8F) and IFN-β production (Figures 8G and 8H) was largely reduced, confirming the efficacy of this technique in elimination of immune-stimulatory mRNA specimens and contaminants.

DISCUSSION

We investigated the effect of systematically varied IVT-mRNA chemistry, including various cap structures as well as nucleotide modifications in human monocyte-derived macrophages, analyzing transgene

A
non-modified Ψ Ψ/5meC 5moU

non-purified

HPLC purified

B

Low dose

High dose

EGFP

Puri: - + - + - + - +
non-mod Ψ Ψ/5meC 5moU

C

Tranfection efficiency
(HPLC purification)

EGFP positive (%)

Low dose   High dose

non-mod Ψ Ψ/5meC 5moU non-mod Ψ Ψ/5meC 5moU untrans mock IFNγ/LPS poly (I:C)

☐ non-purified ☐ HPLC purified

D

EGFP mRNA expression
(HPLC purification)

MFI EGFP

Low dose   High dose

non-mod Ψ Ψ/5meC 5moU non-mod Ψ Ψ/5meC 5moU untrans mock IFNγ/LPS poly (I:C)

☐ non-purified ☐ HPLC purified

E

Low dose   High dose

untrans
IFNγ/LPS
Poly(I:C)
non-mod - +
Ψ - +
Ψ/5meC - +
5moU - +

Puri:

CD80   CD80

F

CD80 level
(HPLC purification)

Relative CD80 level

Low dose   High dose

non-mod Ψ Ψ/5meC 5moU non-mod Ψ Ψ/5meC 5moU untrans mock IFN /LPS poly (I:C)

☐ non-purified ☐ HPLC purified

G

IFN-β secretion (6 h)
(HPLC purification)

IFN-β (pg/ml)

Low dose   High dose

non-mod Ψ Ψ/5meC 5moU non-mod Ψ Ψ/5meC 5moU untrans mock IFNγ/LPS poly (I:C)

☐ non-purified ☐ HPLC purified

H

IFN-β secretion (24 h)
(HPLC purification)

IFN-β (pg/ml)

Low dose   High dose

non-mod Ψ Ψ/5meC 5moU non-mod Ψ Ψ/5meC 5moU untrans mock IFNγ/LPS poly (I:C)

☐ non-purified ☐ HPLC purified

(legend on next page)

expression and activation of these primary cells. Being equipped with numerous sensors/receptors against a variety of pathogen-associated molecular patterns, macrophages play a pivotal role in innate immune response and can initiate adaptive immunity. Consequently, evaluation of their behavior is of high relevance for development of new therapeutics, such as mRNA vaccines. When compared with variations of cap structure, modification of nucleotides had the more pronounced effect on macrophages as identified by transgene expression levels and immunogenicity (Figure S9). While these biological responses could neither be attributed to differences in mRNA integrity nor potential unintended side-products of the T7-mediated *in vitro* transcription process, we found a partial correlation to the dsRNA content of transcripts, bringing up the necessity for extra purification steps. In fact, HPLC purification led to the reduction of dsRNA content and subsequently reduced the immunogenicity of the IVT-mRNA.

Given the sometimes striking effects of IVT-mRNA purification steps on both transgene expression and cell activation, this issue deserves further attention, as evidenced by recent research. In line with our findings, Karikó et al. reported a direct correlation between dsRNA content of non-modified and Ψ-modified and Ψ/5meC-modified mRNA and type I IFN response of transfected dendritic cells.[31] However, elimination of dsRNA by HPLC alone was not sufficient for complete evasion of innate immune response, drawing attention to other aspects of IVT-mRNA, which could be involved in induction of immune activation.[29] Last, as a note of caution in considering a direct quantitative connection between dsRNA content and immune activation, we want to point out that the J2 antibody test used by us and some of the studies mentioned, to the best of our knowledge has not been rigorously validated to exclusively respond to dsRNA structures, irrespective of chemical modifications of the target transcripts.

Despite a high degree of similarity and functional equivalence, IVT-mRNA molecules can be distinguished from endogenous mRNA through differences in their chemical compositions and distinct trafficking routes. Therefore, many studies have been conducted to mimic intrinsic mRNA chemistry, such as the cap structure. Considering the fact that Cap 1 structure is more prevalent in higher eukary-

otes than Cap 0,[42,43] in an *in vivo* study Vaidyanathan et al. investigated the immune stimulation and functional protein production by IVT-mRNA made of Cap 0 and Cap 1 structure, along with three other approaches, but did not find striking differences in their functionality and immunogenicity.[23] Likewise, we also found no remarkable differences in proinflammatory and antiviral responses in primary macrophages, as well as level of protein production between Cap 0- and Cap 1-modified IVT-mRNA. Our observation is also in agreement with a previous study,[43] where no differences in RIG-I-mediated immune activation was reported between ssRNA samples with Cap 0 versus a 2′-O-methylated cap, i.e., a Cap 1 structure. However, when cap modifications were examined and compared in dsRNA samples, Cap 1 was superior to Cap 0 in inhibition of RIG-I pathway.[43] In our experimental setting, a modest decrease of innate immune response with almost no detectable change in protein production level was observed for phosphatase-treated IVT-mRNAs. Notably, the dampening of immune response upon dephosphorylation was slightly more pronounced, when high doses of IVT-mRNA were applied.

In order to evaluate the impact of nucleotide chemical modifications on corresponding IVT-mRNA expression level and immune response, macrophages were transfected with low and high doses of IVT-mRNA in side-by-side experiments. Our results revealed that modification of IVT-mRNA with Ψ led to high level of protein production, but concurrently induced high levels of IFN-β, TNF-α, and IL-6 secretion. In line with these results, a previous study suggested an enhanced immunogenicity for Ψ-modified mRNA, which was correlated to dsRNA mediated-MDA5 stimulation.[16] The combination of Ψ and 5meC modifications, however, was effective in the reduction of IVT-mRNA immunogenicity. This finding is in agreement with previous reports by others[31] and us,[41] where we observed similar pattern throughout different doses, also when examined with different types of carriers such as polyplexes.[41]

Reduced protein expression observed for Ψ/5meC and 5meC-modified mRNA might be attributed to cell-autonomous immunity, which can be mediated by dsRNA interacting with PKR. Following activation by dsRNA or viral RNA, PKR monomers are phosphorylated and dimerize to form the active enzyme.[44] Dimerized PKR can

Figure 8. HPLC purification increases protein expression and ameliorates immune activation of macrophages
(A) Representative fluorescent images transfected with low dose of non-purified and HPLC-purified IVT-mRNAs comparing non-modified mRNA with Ψ-, Ψ/5meC-, and 5moU-modified mRNA. (B) Flow cytometric density plots indicating EGFP expression in macrophages transfected with low dose (top) and high dose (bottom) of IVT-mRNA comparing non-modified mRNA with Ψ-, Ψ/5meC-, and 5moU-modified and non-purified (gray color) versus HPLC-purified (blue color) conditions. (C) Transfection efficiency and (D) EGFP mRNA expression level quantified by flow cytometry and plotted as percentage and MFI of EGFP-positive cells, respectively. (E) Staggered histogram of CD80 levels in macrophages transfected with low doses (left) and high doses (right) of IVT-mRNA comparing non-modified mRNA with Ψ-, Ψ/5meC-, and 5moU-modified and non-purified with HPLC-purified samples. Untransfected, poly(I:C)-treated, and LPS/IFN-γ-activated macrophages served as negative, positive, and high control, respectively. (F) MFI of CD80 normalized to untransfected cells for macrophages transfected with low doses and high doses of non-purified versus HPLC-purified IVT-mRNAs comparing non-modified mRNA with Ψ-, Ψ/5meC-, and 5moU-modified IVT-mRNAs. Mock transfection refers to carrier (i.e., LipoMM) without mRNA. (G, H) IFN-β secretion after (G) 6 h and (H) 24 h upon transfection with low doses and high doses of non-purified versus HPLC-purified IVT-mRNAs comparing non-modified mRNA with Ψ-, Ψ/5meC-, and 5moU-modified IVT-mRNAs. Mock transfection refers to carrier (i.e., LipoMM) without mRNA. Untransfected, poly(I:C)-treated, and LPS/IFN-γ-activated macrophages served as negative, positive, and high control, respectively. For each condition, 125 ng·mL^{-1} and 500 ng·mL^{-1} of IVT-mRNA were used for transfection, referred here as low dose and high dose, respectively. Values are presented as mean ± SD. Error bars indicate SD of three independent experiments from three individual donors. Bar = 50 μm.

phosphorylate eIF2α, leading to translation inhibition. Consistently, Anderson et al. reported enhanced activation of PKR in a cell-free *in vitro* system for Ψ-modified IVT-mRNA compared with non-modified transcripts.[45] OAS can also be activated by dsRNA to poly-merize ATP into oligomers of adenosine, which can specifically activate RNaseL that, in turn, mediates RNA degradation. OAS can be induced by type I IFNs. We found IFN-β production elevated by non-modified, Ψ-modified and 5meC-modified mRNA, but only for 5meC-modified mRNA a reduced mRNA expression was observed, indicating that PKR or OAS pathways could be activated by this modification. However, HPLC purification of 5meC-modified mRNA completely abolished the IFN-β secretion, while the EGFP expression remained at low level, indicating that interferon-induced cell-autologous mRNA decay pathways are not responsible for the reduced translation.[31]

Chemical modifications of uridine, including me[1]Ψ, and 5moU out-performed others in terms of augmenting mRNA expression level, as well as substantially reducing both antiviral and proinflammatory cytokine secretion. In particular, 5moU-modified IVT-mRNA led to almost complete evasion of IFN-β secretion, a result that even extended to high-dose IVT-mRNA transfection. This finding is in line with an earlier report, where in an *in vivo* experimental setup a similar pattern of reduced activation was reported for 5moU, when compared with unmodified and other uridine and cytidine chemical modifications.[23] Another study by Nelson and colleagues also sug-gested that me[1]Ψ modification of IVT-mRNA reduced, but not eliminated the expression of inflammatory chemokine, CXCL-10, produced by transfected primary human monocyte-derived macro-phages. However, when this modification was combined with an extra purification step using reversed-phase high-performance liquid chro-matography (RP-HPLC), it resulted in the pronounced inhibition of innate immune response to background level, examined both *in vitro* and *in vivo*.[29] Both of the recently developed mRNA-based SARS-CoV-2 vaccines that are on the market as of the beginning of 2021 rely on me[1]Ψ-modified IVT-mRNA formulated in lipid-based nano-particles,[10,46] where the moderate activation of the immune system is often intended. However, our study demonstrates that, at least for macrophages, the immune reaction can be reduced almost to background levels without employing sophisticated extra purifica-tion steps, only by using 5moU modification of IVT-mRNA, thus facilitating potential applications that require minimal immune stimulation.

We observed that nucleotide modifications of IVT-mRNA with me[1]Ψ and 5moU increased yield of protein production. This was in line with a previous report that attributed the enhanced expression level of me[1]Ψ-modified IVT-mRNA to increased ribosome loading density and higher ribosomal recycling rate compared with mRNA containing canonical uridine in cell-free translation systems.[47] Other studies, however, attribute high mRNA expression to reduced inhib-itory effects of cell-autonomous antiviral defense mechanism medi-ated by PKR or OAS leading to mRNA decay or translation inhibi-tion.[16] Noteworthy, we found that the pattern in immune activation

observed between the nucleotide modifications tested were not dose-sensitive. However, variations of protein synthesis were more obvious upon transfecting low IVT-mRNA doses and deviation of immune response at high doses of IVT-mRNA.

Elucidation of the mechanisms involved in modulation of immune response by chemical modification of nucleotides, in particular uri-dine, were the subject of previous studies that can be summarized as follows: (1) transcripts containing modified nucleotides were re-ported to have less binding affinity to endosomal ssRNA sensors TLR7/8[25,27,48]; (2) several studies reported that the incorporation of modified nucleotides in transcripts results in less mRNA sensor acti-vation as shown for cytosolic, RIG-I,[43] MDA5,[16] and TLR-3 [18,27], with subsequent reduction of type I IFN and proinflammatory cytokines secretion, as well as reduction of PKR activity resulting in increased translation[24]; (3) nucleotide modifications can reduce unspecific pro-moter-independent activities of T7 RNA polymerase during the IVT process, like synthesis of long dsRNA by-products[16]; and last, (4) reduction of dsRNA potency in receptor stimulation.[49]

Conclusion

In the present study, we investigated the effects of different cap and nucleotide modifications of IVT-mRNA upon macrophage transfec-tion. The different modifications and/or treatments of the transcripts' 5′-end had only modest consequences for protein expression and macrophage activation. Intriguingly, the use of nucleotide modifica-tions had a major impact on the overall biological performance of the IVT-mRNAs. Chemical modification of uridine, in particular 5moU showed the highest levels of protein production with negligible induction of inflammatory macrophage responses. While most envis-aged therapeutic applications of IVT-mRNA will profit from the highest possible protein yield per transcript delivered, such applica-tions, ranging from protein replacement, expression of tumor anti-gens, or "classical" vaccination strategies, have distinct requirements for eliciting inflammatory responses, both quantitatively and qualita-tively. Thus, while further experiments are required to elucidate mo-lecular mechanisms corresponding to each specific modification, this study should motivate consideration of human macrophages as a mediator of custom-tailored mRNA-induced inflammatory reactions for the intended therapeutic application.

MATERIALS AND METHODS
IVT-mRNA synthesis with various chemical modifications
Synthesis of mRNA was performed via *in vitro* transcription by T7 RNA polymerase in two groups to introduce chemical modifications to cap structures and nucleotides described in detail as follows; also see Figure 2, and Table S1 for more information about chemical composition and overview of synthesis process.

1) Template linearization

The plasmid DNA (pDNA) vector, pRNA2-(A)$_{128}$[50] was utilized as template for synthesis of mRNAs with ARCA as cap structure. It con-sists of a standard T7 promoter, a short 5′-UTR containing a Kozak

sequence, an EGFP coding region, and a head-to-tail duplicated human β-globin 3′-UTR followed by a 128-base-pair (bp) polyadenine [poly(A)] sequence.

A modified version of this plasmid comprised the features (mentioned above) aside from an altered T7 promoter transcriptional start site by changing from "GG" to "AG". In this way, the standard promoter sequence 5′-TAATACGACTCACTATA<u>GG</u>-3′ is changed to 5′-TAATACGACTCACTATA<u>AG</u>-3′, in order to accommodate integration of CleanCap AG as cap structure.

pDNA templates were linearized with BspMI restriction enzyme (New England Biolabs, Frankfurt, Germany), and purified by adding 0.05 volume of 3 M sodium acetate (Thermo Fisher Scientific, Darmstadt, Germany), 0.1 volume of 0.5 M EDTA (Thermo Fisher Scientific) and 2 volumes 100% EtOH (Carl Roth, Karlsruhe, Germany). Upon incubation at −20°C for 1 h, samples were centrifuged at 14,000 × g at 4°C for 30 min. The resulting DNA pellets were air-dried and resuspended in UltraPure nuclease-free sterile water (Merck Millipore, Darmstadt, Germany) for downstream experiments.

2) T7-mediated *in vitro* transcription

mRNAs were synthesized using TranscriptAid T7 High Yield Transcription Kit (Thermo Fisher Scientific) according to the manufacturer's instructions. Cap modified mRNAs were synthesized by co-transcriptional incorporation of either ARCA (Jena Bioscience, Jena, Germany) as a dinucleotide Cap 0, or CleanCap AG (TriLink, San Diego, CA) as a trinucleotide Cap 1 analog, at final concentrations of 5 mM. In both cases, IVT-mRNAs were also chemically modified by complete substitution of uridine and cytidine with pseudouridine (Ψ) (Jena Bioscience) and 5-methyl-cytidine (5meC) (Jena Bioscience).

mRNAs with chemical modification of nucleotides were synthesized with complete substitution of either uridine or cytidine with corresponding modified nucleotides. Hereby, uridine is fully substituted either by Ψ, N1-methyl-pseudouridine (me^{1}Ψ) (Jena Bioscience) or 5-methoxy-uridine (5moU) (Jena Bioscience); cytidine is fully substituted by 5meC. In addition, in one case, uridine and cytidine were modified by supplying a combination of Ψ and 5meC. All nucleotides were used at final concentration of 5 mM in the transcription reaction, except GTP, which was decreased to 1.5 mM to increase capping efficiency. The 5′-end of these IVT-mRNAs was determined co-transcriptionally by ARCA incorporation. IVT-mRNAs were purified using lithium chloride and resuspended in UltraPure nuclease-free sterile water supplemented with 0.1 mM EDTA.

3) Cap methylation

In order to generate Cap 1 from ARCA-capped mRNA, IVT products were purified with RNeasy kit (Qiagen, Hilden, Germany), denatured at 65°C for 5 min, treated with mRNA Cap 2′-O-methyl-transferase (5 U/μg) (M0366S) (New England Biolabs) in 1x capping buffer and

0.2 mM S-adenosylmethionine (SAM) for 1 h at 37°C, and then repurified by using a RNeasy kit.

4) 5′-end dephosphorylation

Dephosphorylation of the 5′-end of potentially uncapped IVT-mRNAs was performed by treatment with 1 U/μg Antarctic phosphatase (M0289L) (New England Biolabs) in 1x Antarctic phosphatase buffer. All transcripts were purified from reaction mixture by overnight incubation at −20°C in lithium chloride solution (Thermo Fisher Scientific) at final concentration of 2.8 M. Upon centrifugation at 14,000 × g at 4°C for 30 min, IVT-mRNA products were washed with 70% EtOH, and the air-dried pellets were then resuspended in UltraPure nuclease-free sterile water containing 0.1 mM EDTA.

IVT-mRNA purification with HPLC
Four of the mRNAs with different nucleotide chemistries were purified by HPLC using 7.8 × 50 mm alkylated non-porous polystyrene-divinylbenzene (PS-DVB)-based RNASep Prep RNA purification column (ADS Biotech, Hillington Park, Glasgow). WAVE Optimized Buffer A contained 0.1 M triethylammonium acetate in water (ADS Biotech), and WAVE Optimized Buffer B, composed of 0.1 M TEAA in 25% Acetonitrile (ADS Biotech), were used as the buffer system throughout. The purification was done according to the previously published protocol.[31] The collected fractions were desalted via Amicon Ultra-15 centrifugal filter unit (30 K membrane) (Merck Millipore), and the mRNA samples were subsequently recovered from fractions using overnight precipitation by 1:10 vol NaOAc and 1 vol isopropanol and glycogen (Roche).

IVT-mRNA characterization
The concentrations of IVT-mRNAs were determined using UV/Vis-spectroscopy (NanoDrop 1000 Spectrophotometer; Peqlab, Erlangen, Germany) and integrity of transcripts was analyzed by denaturing agarose gel electrophoresis.

Measurement of dsRNA by dot blot assay
The dsRNA content of synthesized IVT-mRNAs was analyzed by dot plot assay according to the previously published protocol in Baiersdörfer et al.[32] Briefly, IVT-mRNA samples were blotted on a super-charged nylon membrane (GE Healthcare Life Science, Freiburg, Germany) using a 96-well bio-dot silicon gasket (Bio-Rad, Munich, Germany), at concentration of 1,000 ng per dot. In parallel, 1:4 serial dilutions of 142-bp dsRNA positive control (Jena Bioscience), were blotted on the same membrane, starting at 1,000 ng as the highest concentration. Besides, 1,000 ng of single-stranded polyadenylic acid (poly(A)) (Sigma-Aldrich, Hamburg, Germany) was blotted side-by-side as negative control. After loading of the samples, the membrane was air-dried and blocked in 5% (w/v) blotting grade non-fat dry milk (Bio-Rad) in 1x Tris-buffered saline with Tween 20 (TBS-T) buffer (Cell Signaling Technology, Leiden, Netherlands) at room temperature (RT) for 1 h. The membrane was incubated with 15 mL 1:5,000 diluted dsRNA-specific monoclonal antibody

(mAb) J2 (English & Scientific Consulting, Szirák, Hungary) in 1% (w/v) blotting grade non-fat dried milk at 4°C overnight on a rocker shaker. The membrane was washed three times with 30 mL 1x TBS-T, and incubated with 15 mL 1:2,500 diluted horseradish peroxidase (HRP)-conjugated goat anti-mouse immunoglobulin G (IgG) (Thermo Fisher Scientific) in 1% (w/v) blotting grade non-fat dry milk at RT for 1 h. Upon washing three times with 30 mL 1x TBS-T, the membrane was treated with 0.1 mL/cm enhanced chemiluminescence (ECL) western blotting detection reagent (GE Healthcare Life Science) in the dark and immediately analyzed using a ChemiDoc MP imaging system (Bio-Rad). For comparison of different samples, signal intensities were measured by corresponding densitometry software, Image Lab (Bio-Rad), using volume tools. The dsRNA content of samples was interpolated using dsRNA positive control standard curve, then normalized to the total amount of mRNA loaded per dot, i.e., 1,000 ng, and eventually presented as dsRNA/total mRNA % (w/w).

In vitro culture of primary human macrophages

Primary human macrophages were differentiated from monocytes, according to the protocol reported previously.[41] In brief, monocytes were purified from buffy coat-derived peripheral blood mononuclear cells (Deutsches Rotes Kreuz, Berlin, Germany; ethics vote EA2/018/16; Charité University Medicine Berlin, Berlin, Germany), by magnetic sorting using the Monocyte Isolation Kit II (Miltenyi Biotec, Bergisch Gladbach, Germany) according to the manufacturer's instruction. CD14-positive monocytes were subsequently cultured in very low endotoxin (VLE) RPMI 1640 (PAN-Biotech, Aidenbach, Germany), supplemented with 10% (v/v) fetal bovine serum (FBS) (Sigma-Aldrich), and 50 ng/mL human macrophage colony stimulating factor (Miltenyi Biotec) at 37°C in an atmosphere with 5 vol % CO_2 for 7 days, with medium change at day 3. Upon differentiation, macrophages were cultured in VLE RPMI, only supplemented with 10% (v/v) FBS for subsequent experiments.

IVT-mRNA transfection

The transfection experiment was performed by complexing IVT-mRNA with Lipofectamine MessengerMAX (LipoMM) (Thermo Fisher Scientific) reagent as follows: LipoMM reagent was diluted in Opti-MEM reduced serum medium (Thermo Fisher Scientific) at a 1:50 volume ratio, and incubated for 10 min at RT. The resulting solution was then mixed with equal volume of Opti-MEM containing 4 ng/μL of IVT-mRNA. Complexed IVT-mRNAs were briefly vortexed and incubated for 10 min at RT. The corresponding volumes to deliver 125 ng and 500 ng IVT-mRNA per 1 mL of cell culture medium were added drop-wise to each well, referred to as low dose and high dose, respectively, throughout all experiments. Macrophages were transfected with poly(I:C) (125 ng/mL), mimicking dsRNA as positive control. Besides, transfection reagent mixed with Opti-MEM without addition of IVT-mRNA was considered as mock negative control. Untransfected cells treated with 2 μg/mL LPS (Enzo Life Sciences) and 10 ng/mL IFN-γ (Miltenyi Biotec) served as positive control for innate immune response. Macrophages were imaged with inverted microscope ELIPSE T*i*-U equipped pE-300lite LED light source (Nikon, Düsseldorf, Germany) 24 h after transfection, and images were analyzed with NIS-Elements imaging software, version 4.51 (Nikon). Of note, to avoid unintended cell activation due to potential endotoxin contamination, all reagents used for IVT-mRNA synthesis as well as cell isolation and cell culture mediums were purchased as very low endotoxin and/or endotoxin-free grade. Besides, IVT-mRNA batches were regularly tested for endotoxin level using EndoLISA assay according to guidance for industry pyrogen and endotoxins testing from the Food and Drug Administration (FDA), and consistently proved to be endotoxin-free (EU < 0.05).

Evaluation of IVT-mRNA expression and CD80 expression with flow cytometry

At 24 h post transfection, macrophages were harvested by scraping, then washed with cold autoMACS running buffer (Miltenyi Biotec). Cells were incubated with FcR blocking reagent (Miltenyi Biotec) for 10 min at 4°C, to avoid unspecific antibody binding. Upon washing, cells were stained with CD80-PE (clone L307.4) (BD Bioscience, Heidelberg, Germany) antibody with dilution factor 1:100 (5 μg/mL final concentration) at 4°C for 10 min. After a final washing step, cells were analyzed with MACSQuant VYB (Miltenyi Biotec). For live-dead discrimination, DAPI, at a final concentration of 1 μg/mL, was added to each sample immediately before measurement. All flow cytometric data were analyzed by FlowJo software V10 using the previously established gating strategy.[41] Briefly, cells were initially identified from debris by gating on forward versus side scatter area (FSC-A versus SSC-A) dot plots, followed by exclusion of aggregated cells using forward scatter area against height (FSC-A versus FSC-H). DAPI-negative cells were identified as live cells. EGFP-positive cell populations were determined among live single cells, by gating with respect to untransfected negative controls.

Cytokine measurements

Macrophage culture media were collected at 6 h and 24 h post transfection, centrifuged at $1,000 \times g$ at 4°C for 15 min to remove possible cell debris, and the supernatants were preserved at −20°C until downstream measurements. Concentrations of cytokines were measured by Bio-Plex immunoassay (Bio-Rad) using Bio-Plex standards including Pro Human Cytokine Screening Group 1 (171D50001; Bio-Rad) for TNF-α and IL-6, and Pro Human Inflammation Panel 1 (171DL0001) (Bio-Rad) for IFN-β, according to corresponding manufacturers protocol. Briefly, 50 μL of 1x magnetic beads conjugated with capture antibody were added to each well of the 96-well assay plate, and washed twice with 1x wash buffer (Bio-Rad) in a Bio-Plex Pro II wash station (Bio-Rad). Subsequently, 50 μL of a dilution series of reconstituted cytokine standards and sample supernatants were added to prewashed beads and incubated on a shaker at 900 rpm at RT for either 30 min or 1 h, depending on the assay type. The plates were washed three times with 1x wash buffer, and then incubated with 1x biotinylated detection antibodies on a shaker at 900 rpm at RT for 30 min. Upon three times washing, 1x PE-conjugated streptavidin was added to each well and plates were incubated at 900 rpm at RT for 10 min. After three last washing steps,

beads were resuspended in 125 μL assay buffer, shaken at 900 rpm for 30 s and measured by Bio-Plex 200 System (Bio-Rad).

Statistics and software

Data were statistically analyzed using Prism 7.00 software (GraphPad, San Diego, CA). All data are presented as means ± standard deviation (SD) of at least three independent experiments. two-way ANOVA test was performed for multiple comparisons between different groups with a 95% confidence interval. Statistical significance was considered as $p < 0.05$.

Figures 1 and 2 created with BioRender.com.

SUPPLEMENTAL INFORMATION

Supplemental information can be found online at https://doi.org/10.1016/j.omtn.2022.01.004.

AUTHOR CONTRIBUTIONS

M.G., H.M., and T.R. conceptualized the study; M.G., H.M., and T.R. developed the methodology; H.M., and L.A. performed study investigation; H.M. wrote the original draft; M.G., T.R., and A.L. reviewed and edited the manuscript; M.G. and A.L. acquired the funding; M.G. and A.L. acquired the resources; M.G. and A.L. supervised the study.

DECLARATION OF INTERESTS

The authors declare no competing interests.

REFERENCES

1. Sahin, U., Karikó, K., and Türeci, Ö. (2014). mRNA-based therapeutics–developing a new class of drugs. Nat. Rev. Drug Discov. 13, 759–780.

2. Sergeeva, O.V., Koteliansky, V.E., and Zatsepin, T.S. (2016). mRNA-based therapeutics - advances and perspectives. Biochemistry 81, 709–722.

3. Coutinho, M.F., Matos, L., Santos, J.I., and Alves, S. (2019). RNA therapeutics: how far have we gone? Adv. Exp. Med. Biol. 1157, 133–177.

4. Weissman, D. (2015). mRNA transcript therapy. Expert Rev. Vaccin. 14, 265–281.

5. Meng, Z., O'Keeffe-Ahern, J., Lyu, J., Pierucci, L., Zhou, D., and Wang, W. (2017). A new developing class of gene delivery: messenger RNA-based therapeutics. Biomater. Sci. 5, 2381–2392.

6. Magadum, A., Kaur, K., and Zangi, L. (2019). mRNA-based protein replacement therapy for the heart. Mol. Ther. 27, 785–793.

7. Pardi, N., Hogan, M.J., Porter, F.W., and Weissman, D. (2018). mRNA vaccines — a new era in vaccinology. Nat. Rev. Drug Discov. 17, 261–279.

8. Linares-Fernández, S., Lacroix, C., Exposito, J.Y., and Verrier, B. (2020). Tailoring mRNA vaccine to balance innate/adaptive immune response. Trends Mol. Med. 26, 311–323.

9. Reinhard, K., Rengstl, B., Oehm, P., Michel, K., Billmeier, A., Hayduk, N., Klein, O., Kuna, K., Ouchan, Y., Wöll, S., et al. (2020). An RNA vaccine drives expansion and efficacy of claudin-CAR-T cells against solid tumors. Science 367, 446–453.

10. Corbett, K.S., Edwards, D.K., Leist, S.R., Abiona, O.M., Boyoglu-Barnum, S., Gillespie, R.A., Himansu, S., Schäfer, A., Ziwawo, C.T., DiPiazza, A.T., et al. (2020). SARS-CoV-2 mRNA vaccine design enabled by prototype pathogen preparedness. Nature 586, 567–571.

11. Moradian, H., Lendlein, A., and Gossen, M. (2020). Strategies for simultaneous and successive delivery of RNA. J. Mol. Med. (Berl) 98, 1767–1779.

12. Mulligan, M.J., Lyke, K.E., Kitchin, N., Absalon, J., Gurtman, A., Lockhart, S., Neuzil, K., Raabe, V., Bailey, R., Swanson, K.A., et al. (2020). Phase I/II study of COVID-19 RNA vaccine BNT162b1 in adults. Nature 586, 589–593.

13. Blanchard, E.L., Loomis, K.H., Bhosle, S.M., Vanover, D., Baumhof, P., Pitard, B., Zurla, C., and Santangelo, P.J. (2019). Proximity ligation assays for in situ detection of innate immune activation: focus on in vitro-transcribed mRNA. Mol. Ther. Nucleic Acids 14, 52–66.

14. Kawai, T., and Akira, S. (2008). Toll-like receptor and RIG-1-like receptor signaling. Ann. New York Acad. Sci. 1143, 1–20.

15. Züst, R., Cervantes-Barragan, L., Habjan, M., Maier, R., Neuman, B.W., Ziebuhr, J., Szretter, K.J., Baker, S.C., Barchet, W., Diamond, M.S., et al. (2011). Ribose 2'-O-methylation provides a molecular signature for the distinction of self and non-self mRNA dependent on the RNA sensor Mda5. Nat. Immunol. 12, 137–143.

16. Mu, X., Greenwald, E., Ahmad, S., and Hur, S. (2018). An origin of the immunogenicity of in vitro transcribed RNA. Nucleic Acids Res. 46, 5239–5249.

17. Devoldere, J., Dewitte, H., De Smedt, S.C., and Remaut, K. (2016). Evading innate immunity in nonviral mRNA delivery: don't shoot the messenger. Drug Discov. Today 21, 11–25.

18. Akira, S., and Takeda, K. (2004). Toll-like receptor signalling. Nat. Rev. Immunol. 4, 499–511.

19. Hornung, V., Ellegast, J., Kim, S., Brzózka, K., Jung, A., Kato, H., Poeck, H., Akira, S., Conzelmann, K.K., Schlee, M., et al. (2006). 5'-Triphosphate RNA is the ligand for RIG-I. Science 314, 994–997.

20. Macmicking, J.D. (2012). Interferon-inducible effector mechanisms in cell-autonomous immunity. Nat. Rev. Immunol. 12, 367–382.

21. Lemaire, P.A., Anderson, E., Lary, J., and Cole, J.L. (2008). Mechanism of PKR activation by dsRNA. J. Mol. Biol. 381, 351–360.

22. Eley, H.L., Russell, S.T., and Tisdale, M.J. (2010). Mechanism of activation of dsRNA-dependent protein kinase (PKR) in muscle atrophy. Cell Signal. 22, 783–790.

23. Vaidyanathan, S., Azizian, K.T., Haque, A., Henderson, J.M., Hendel, A., Shore, S., Antony, J.S., Hogrefe, R.I., Kormann, M.S.D., Porteus, M.H., et al. (2018). Uridine depletion and chemical modification increase Cas9 mRNA activity and reduce immunogenicity without HPLC purification. Mol. Ther. Nucleic Acids 12, 530–542.

24. Nallagatla, S.R., and Bevilacqua, P.C. (2008). Nucleoside modifications modulate activation of the protein kinase PKR in an RNA structure-specific manner. RNA 14, 1201–1213.

25. Karikó, K., Buckstein, M., Ni, H., and Weissman, D. (2005). Suppression of RNA recognition by Toll-like receptors: the impact of nucleoside modification and the evolutionary origin of RNA. Immunity 23, 165–175.

26. Karikó, K., Muramatsu, H., Welsh, F.A., Ludwig, J., Kato, H., Akira, S., and Weissman, D. (2008). Incorporation of pseudouridine into mRNA yields superior nonimmunogenic vector with increased translational capacity and biological stability. Mol. Ther. 16, 1833–1840.

27. Kormann, M.S., Hasenpusch, G., Aneja, M.K., Nica, G., Flemmer, A.W., Herber-Jonat, S., Huppmann, M., Mays, L.E., Illenyi, M., Schams, A., et al. (2011). Expression of therapeutic proteins after delivery of chemically modified mRNA in mice. Nat. Biotechnol. 29, 154–157.

28. Feyrer, H., Munteanu, R., Baronti, L., and Petzold, K. (2020). One-pot production of RNA in high yield and purity through cleaving tandem transcripts. Molecules 25, 1142.

98

29. Nelson, J., Sorensen, E.W., Mintri, S., Rabideau, A.E., Zheng, W., Besin, G., Khatwani, N., Su, S.V., Miracco, E.J., Issa, W.J., et al. (2020). Impact of mRNA chemistry and manufacturing process on innate immune activation. Sci. Adv. 6, eaaz6893.

30. Wu, M.Z., Asahara, H., Tzertzinis, G., and Roy, B. (2020). Synthesis of low immunogenicity RNA with high-temperature in vitro transcription. RNA 26, 345–360.

31. Karikó, K., Muramatsu, H., Ludwig, J., and Weissman, D. (2011). Generating the optimal mRNA for therapy: HPLC purification eliminates immune activation and improves translation of nucleoside-modified, protein-encoding mRNA. Nucleic Acids Res. 39, e142.

32. Baiersdörfer, M., Boros, G., Muramatsu, H., Mahiny, A., Vlatkovic, I., Sahin, U., and Karikó, K. (2019). A facile method for the removal of dsRNA contaminant from in vitro-transcribed mRNA. Mol. Ther. Nucleic Acids 15, 26–35.

33. Xu, Y., Huang, L., Kirschman, J.L., Vanover, D.A., Tiwari, P.M., Santangelo, P.J., Shen, X., and Russell, D.G. (2019). Exploitation of synthetic mRNA to drive immune effector cell recruitment and functional reprogramming in vivo. J. Immunol. 202, 608–617.

34. Ponzoni, M., Pastorino, F., Di Paolo, D., Perri, P., and Brignole, C. (2018). Targeting macrophages as a potential therapeutic intervention: impact on inflammatory diseases and cancer. Int. J. Mol. Sci. 19, 1953.

35. Navegantes, K.C., de Souza Gomes, R., Pereira, P.A.T., Czaikoski, P.G., Azevedo, C.H.M., and Monteiro, M.C. (2017). Immune modulation of some autoimmune diseases: the critical role of macrophages and neutrophils in the innate and adaptive immunity. J. Transl. Med. 15, 36.

36. Ackermann, M., Dragon, A.C., and Lachmann, N. (2020). The immune-modulatory properties of iPSC-derived antigen-presenting cells. Transfus. Med. Hemother 47, 444–453.

37. Guerriero, J.L. (2019). Macrophages: their untold story in T cell activation and function. Int. Rev. Cell Mol. Biol. 342, 73–93.

38. Merkley, S.D., Chock, C.J., Yang, X.O., Harris, J., and Castillo, E.F. (2018). Modulating T cell responses via autophagy: the intrinsic influence controlling the function of both antigen-presenting cells and T cells. Front. Immunol. 9, 2914.

39. Hume, D.A. (2008). Macrophages as APC and the dendritic cell myth. J. Immunol. 181, 5829.

40. Scharenberg, S.G., Poletto, E., Lucot, K.L., Colella, P., Sheikali, A., Montine, T.J., Porteus, M.H., and Gomez-Ospina, N. (2020). Engineering monocyte/macrophage−specific glucocerebrosidase expression in human hematopoietic stem cells using genome editing. Nat. Commun. 11, 3327.

41. Moradian, H., Roch, T., Lendlein, A., and Gossen, M. (2020). mRNA transfection-induced activation of primary human monocytes and macrophages: dependence on carrier system and nucleotide modification. Sci. Rep. 10, 4181.

42. Schuberth-Wagner, C., Ludwig, J., Bruder, A.K., Herzner, A.M., Zillinger, T., Goldeck, M., Schmidt, T., Schmid-Burgk, J.L., Kerber, R., Wolter, S., et al. (2015). A conserved histidine in the RNA sensor RIG-I controls immune tolerance to N1-2'O-methylated self RNA. Immunity 43, 41–51.

43. Devarkar, S.C., Wang, C., Miller, M.T., Ramanathan, A., Jiang, F., Khan, A.G., Patel, S.S., and Marcotrigiano, J. (2016). Structural basis for m7G recognition and 2'-O-methyl discrimination in capped RNAs by the innate immune receptor RIG-I. Proc. Natl. Acad. Sci. U S A. 113, 596–601.

44. Nanduri, S., Carpick, B.W., Yang, Y., Williams, B.R.G., and Qin, J. (1998). Structure of the double-stranded RNA-binding domain of the protein kinase PKR reveals the molecular basis of its dsRNA-mediated activation. EMBO J. 17, 5458–5465.

45. Anderson, B.R., Muramatsu, H., Nallagatla, S.R., Bevilacqua, P.C., Sansing, L.H., Weissman, D., and Karikó, K. (2010). Incorporation of pseudouridine into mRNA enhances translation by diminishing PKR activation. Nucleic Acids Res. 38, 5884–5892.

46. Sahin, U., Muik, A., Derhovanessian, E., Vogler, I., Kranz, L.M., Vormehr, M., Baum, A., Pascal, K., Quandt, J., Maurus, D., et al. (2020). COVID-19 vaccine BNT162b1 elicits human antibody and TH1 T cell responses. Nature 586, 594–599.

47. Svitkin, Y.V., Cheng, Y.M., Chakraborty, T., Presnyak, V., John, M., and Sonenberg, N. (2017). N1-methyl-pseudouridine in mRNA enhances translation through eIF2α-dependent and independent mechanisms by increasing ribosome density. Nucleic Acids Res. 45, 6023–6036.

48. Freund, I., Eigenbrod, T., Helm, M., and Dalpke, A.H. (2019). RNA modifications modulate activation of innate toll-like receptors. Genes 10, 92.

49. Durbin, A.F., Wang, C., Marcotrigiano, J., and Gehrke, L. (2016). RNAs containing modified nucleotides fail to trigger RIG-I conformational changes for innate immune signaling. mBio 7:e00833-16.

50. Williams, D.J., Puhl, H.L., and Ikeda, S.R. (2010). A simple, highly efficient method for heterologous expression in mammalian primary neurons using cationic lipid-mediated mRNA transfection. Front. Neurosci. 4, 181.

99

Supplemental information

Chemical modification of uridine modulates

mRNA-mediated proinflammatory and antiviral

response in primary human macrophages

Hanieh Moradian, Toralf Roch, Larissa Anthofer, Andreas Lendlein, and Manfred Gossen

Supporting Information for

Chemical modification of uridine modulates mRNA-mediated proinflammatory and antiviral response in primary human macrophages

Hanieh Moradian[1, 2, 3], Toralf Roch[4, 5,6], Larissa Anthofer[1, 2], Andreas Lendlein[1, 2, 3], Manfred Gossen[1, 2, 1]

1   Institute of Active Polymers, Helmholtz-Zentrum Hereon, Kantstr. 55, 14513 Teltow, Germany
2   Berlin-Brandenburg Center for Regenerative Therapies (BCRT), Föhrerstr. 15, 13353 Berlin, Germany
3   Institute of Biochemistry and Biology, University of Potsdam, Karl-Liebknecht-Str. 24-25, 14476 Potsdam, Germany
4   Berlin Institute of Health at Charité – Universitätsmedizin Berlin, BIH Center for Regenerative Therapies (BCRT), Charitéplatz 1, 10117 Berlin, Germany
5   Charité – Universitätsmedizin Berlin, Corporate Member of Freie Universität Berlin, Humboldt-Universität zu Berlin, Berlin Center for Advanced Therapies, Augustenburger Platz 1, 13353 Berlin, Germany
6   Center for Translational Medicine, Immunology, and Transplantation, Medical Department I, Marien Hospital Herne, University Hospital of the Ruhr-University Bochum, Hölkeskampring 40, 44625 Herne, Germany
* Corresponding Author, email address: manfred.gossen@hereon.de

---

[1] Corresponding author: Dr. Manfred Gossen, Institute of Active Polymers and Berlin-Brandenburg Center for Regenerative Therapies, Helmholtz-Zentrum Hereon, Kantstr. 55, 14513 Teltow, Germany. Tel.: +49 (0) 30 450539-491; Fax: +49 (0)30 450539-991; E-mail: manfred.gossen@hereon.de.
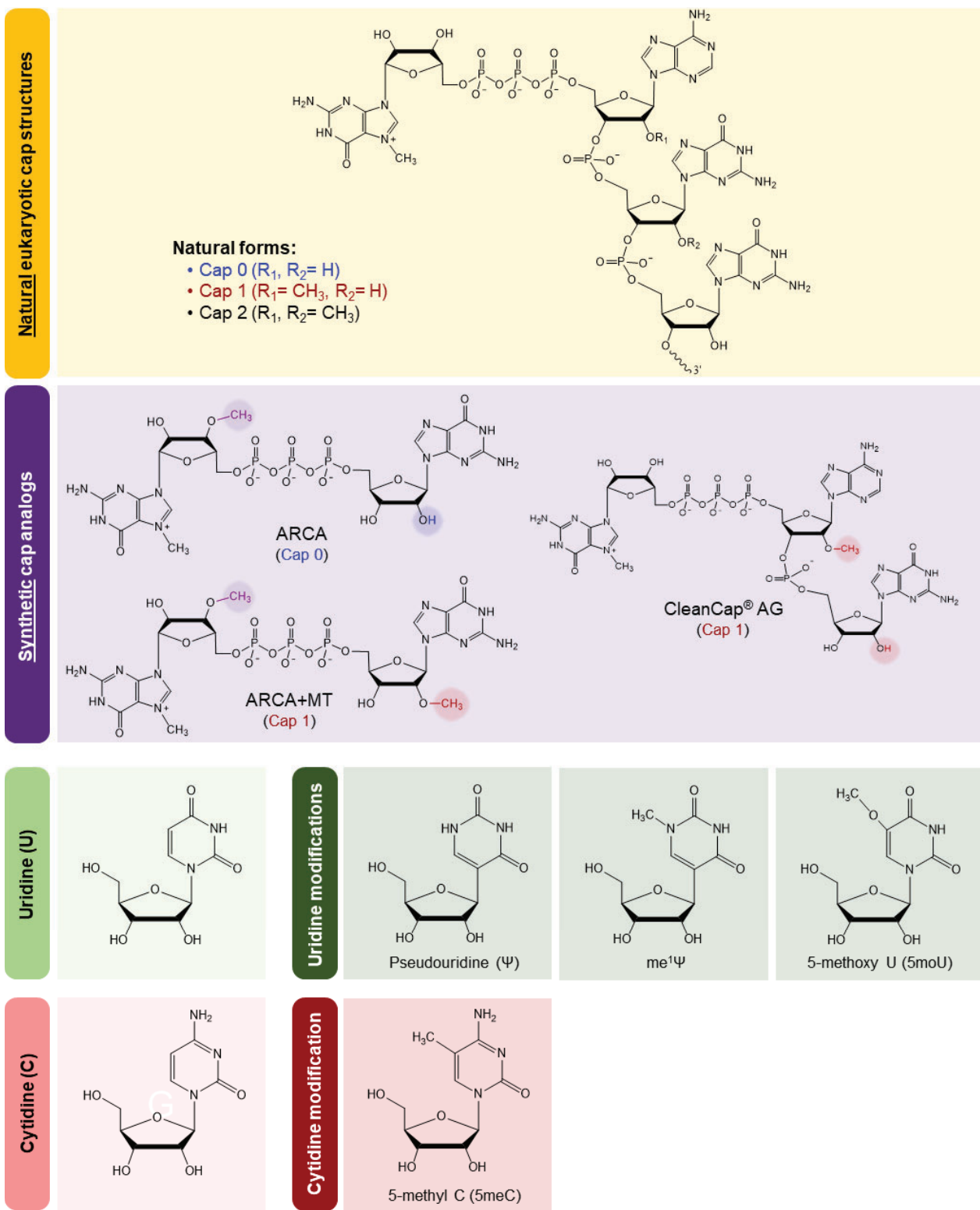
1

Figure S1. The upper panel (yellow box) depicts the chemical formula of naturally occurring eukaryotic cap structures in context of mRNA modification including Cap 0, Cap 1 and Cap 2 forms. Synthetic anti-reverse cap analogs used as initiator of *in vitro* mRNA synthesis process in form of dinucleotide ARCA, with and without extra methylation (Cap 0 vs. Cap 1), and trinucleotide CleanCap®AG, methylated at first adenosine (Cap1) (purple box). The changes of cap analogs compared to the natural cap are highlighted. The lower panels depict original and modified uridine and cytidine nucleoside implemented in this study; (ARCA: anti-reverse cap analogue, MT: methyl-transferase, Ψ: pseudouridine, me^{1}Ψ: N^1-Methylpseudouridine, 5moU: 5-methoxy-uridine, 5meC: 5-methyl-cytidine)
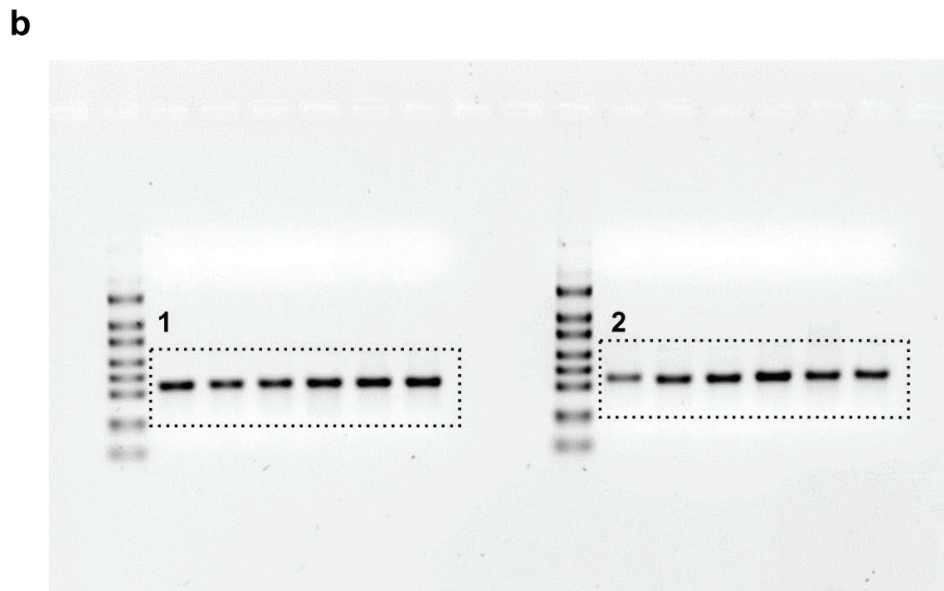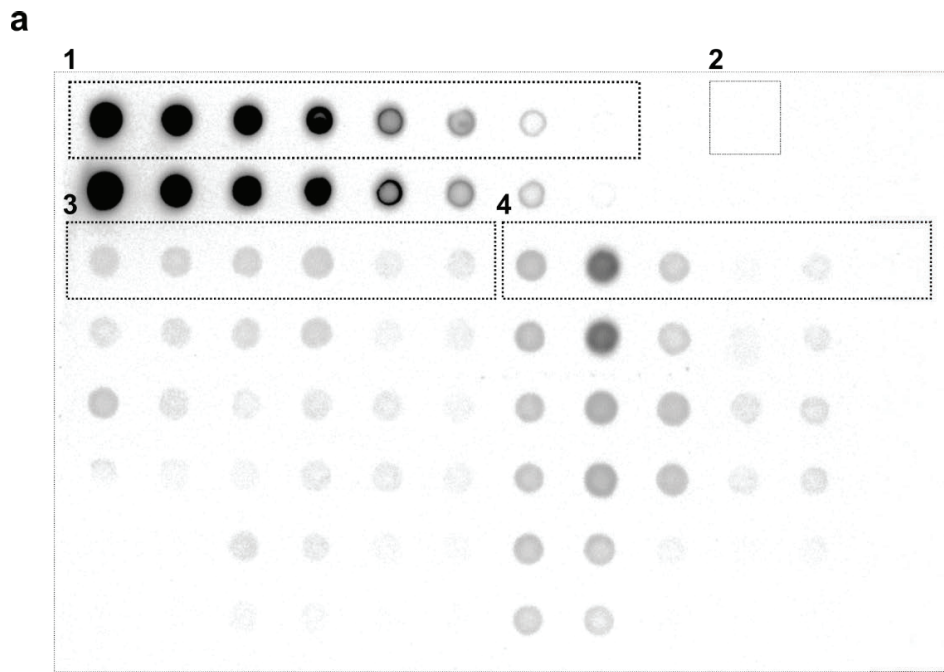
2

Figure S2. The uncropped image of **(a)** a dot blot membrane and **(b)** an agarose gel. **(a)** The dotted frames on dot blot correspond to samples as follows; 1) dsRNA standard series, 2) ssRNA as negative control, 3) cap modified IVT-mRNAs, 4) nucleotide modified IVT-mRNAs; all of which are presented in figure 3a-c. **(b)** The dotted frames on the agarose gel image correspond to 1) cap modified and 2) nucleotide modified IVT-mRNAs presented in figure 3b, c.
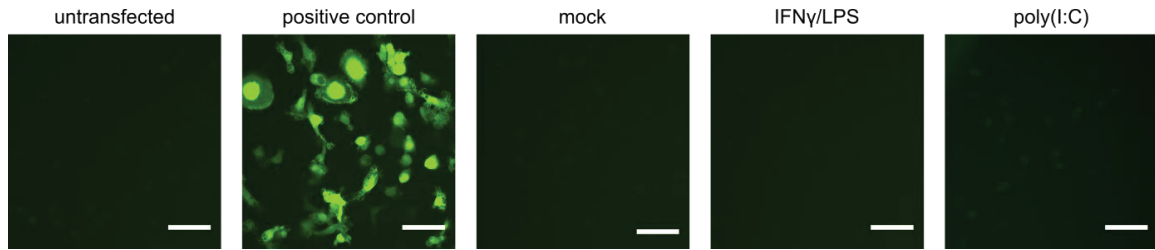
Figure S3. Fluorescent images of control samples, including untransfected, EGFP transfected positive control, mock transfected (LipoMM only), IFNγ/LPS treated as proinflammatory immune response positive control and poly(I:C) transfected macrophages as dsRNA-induced antiviral response positive control. Scale bar= 50 μm.
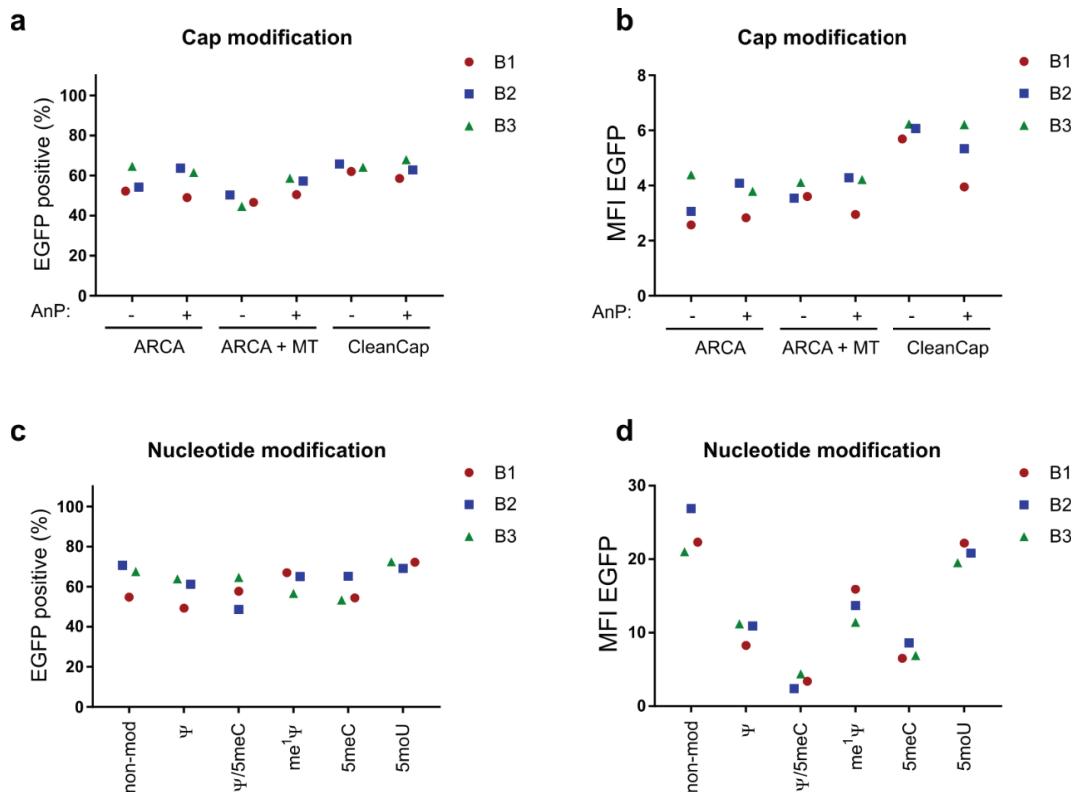

Figure S4. Evaluation of batch effects by comparison of three independently synthesized IVT-mRNA batches within the same donor; comparison of **(a)** transfection efficiency and **(b)** level of EGFP production between three batches of IVT-mRNA (B1-B3), with cap modification. Macrophages transfected IVT-mRNA with distinct nucleotide modification were evaluated in terms of **(c)** transfection efficiency and **(d)** level of EGFP production throughout three IVT-mRNA batches. (ARCA: anti-reverse cap analogue, MT:methyl-transferase, AnP: Antarctic phosphatase, Ψ: pseudouridine, me^{1}Ψ: N^1-Methylpseudouridine, 5moU: 5-methoxy-uridine, 5meC: 5-methyl-cytidine)
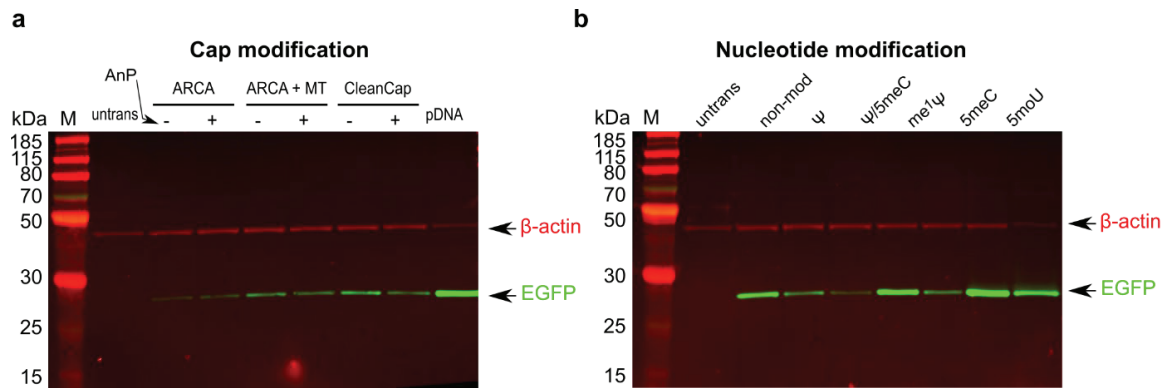
Figure S5. Protein expression evaluated by western blot analyses for macrophages transfected with either **(a)** cap modified or **(b)** nucleotide modified IVT-mRNA (ARCA: anti-reverse cap analogue, MT:methyl-transferase, AnP: Antarctic phosphatase, Ψ: pseudouridine, me^{1}Ψ: N^1-Methylpseudouridine, 5moU: 5-methoxy-uridine, 5meC: 5-methyl-cytidine)
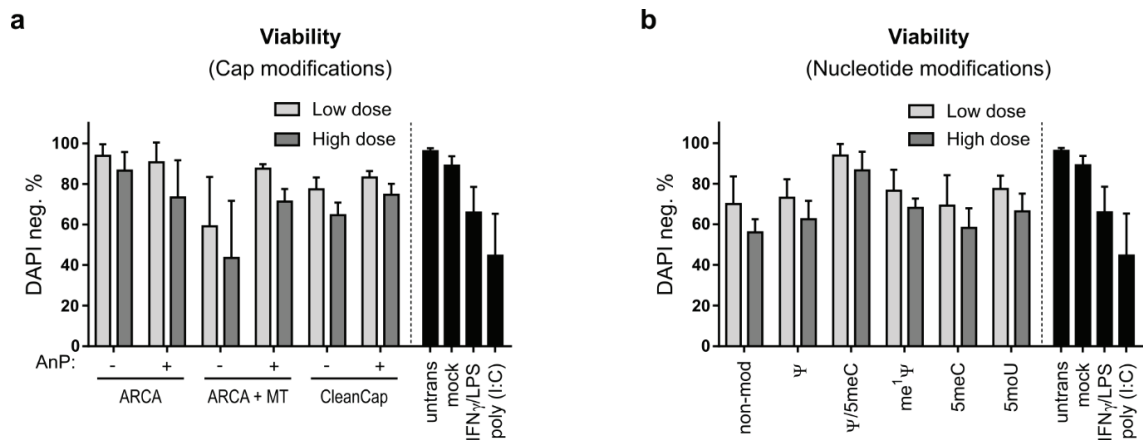

Figure S6. Viability of macrophages transfected with low dose and high dose of IVT-mRNA with chemical modification of either **(a)** cap structure or **(b)** nucleotides, evaluated by determining the percentage of DAPI-negative cells. Values are presented as mean ± SD, n = 3. (ARCA: anti-reverse cap analogue, MT: methyl-transferase, AnP: Antarctic phosphatase, Ψ: pseudouridine, me^{1}Ψ: N^1-Methylpseudouridine, 5moU: 5-methoxy-uridine, 5meC: 5-methyl-cytidine)
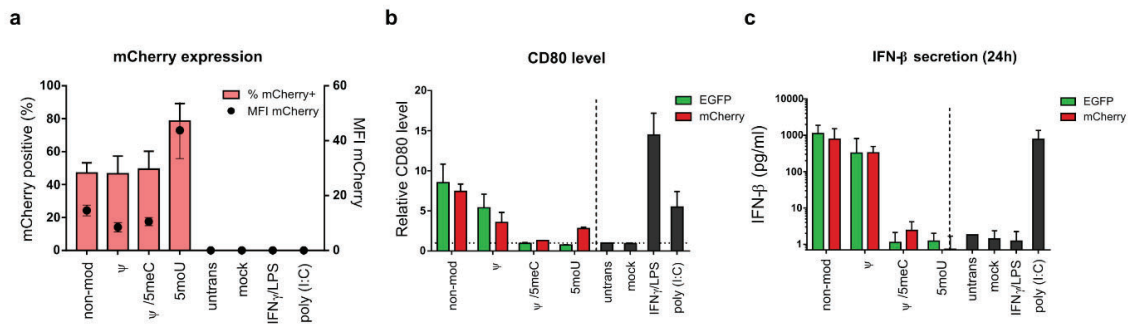
5

Figure S7. Macrophage response to transfection of mRNA coding for mCherry and EGFP with different nucleotide modification. (a) Transfection efficiency (bar graph, left axis), and mRNA expression level quantified by percentage of mCherry positive cells and mean fluorescent intensity of mCherry, respectively, (scattered dots, right axis), quantified using flow cytometry, 24 h post transfection. Comparison of CD80 level (b) and IFN-β secretion (c) by macrophages after IVT-mRNA transfection enconding for mCherry or EGFP with different nucleotide modifications, both measured 24 h after transfection. mCherry IVT-mRNA was transfected in low dose, i.e. 125 ng·mL^{-1}. Untransfected, poly(I:C)-treated, and LPS/IFN-γ-activated macrophages served as negative, positive and high control, respectively. Values are presented as mean ± SD. Error bars indicate SD of three independent experiments from three individual donors.
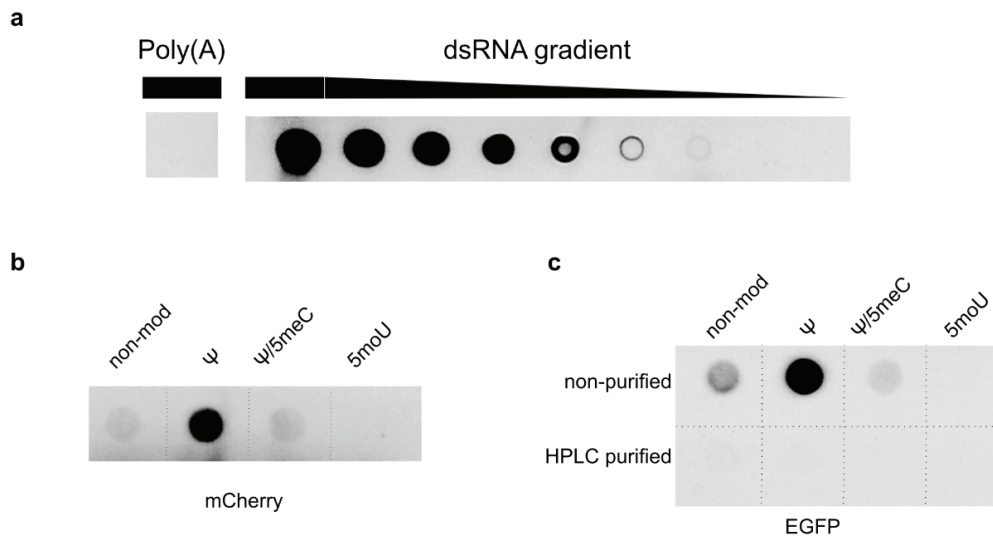

Figure S8. dsRNA detection by J2 antibody comparing non-purified with HPLC-purified IVT-mRNAs **(a)** Poly(A) as ssRNA negative control, and dsRNA positive control were blotted with the same amount as main samples (1000 ng/dot), dsRNA was 4-fold serial diluted (from left to right). **(b)** dsRNA content of mCherry encoding IVT-mRNA modified with different nucleotide modifications evaluated by J2 antibody binding. **(c)** Representative dot blots of EGFP encoding IVT-mRNAs with different nucleotide modifications comparing non-purified (top) versus HPLC-purified (bottom) samples. (Ψ: pseudouridine, 5moU: 5-methoxy-uridine, 5meC: 5-methyl-cytidine)
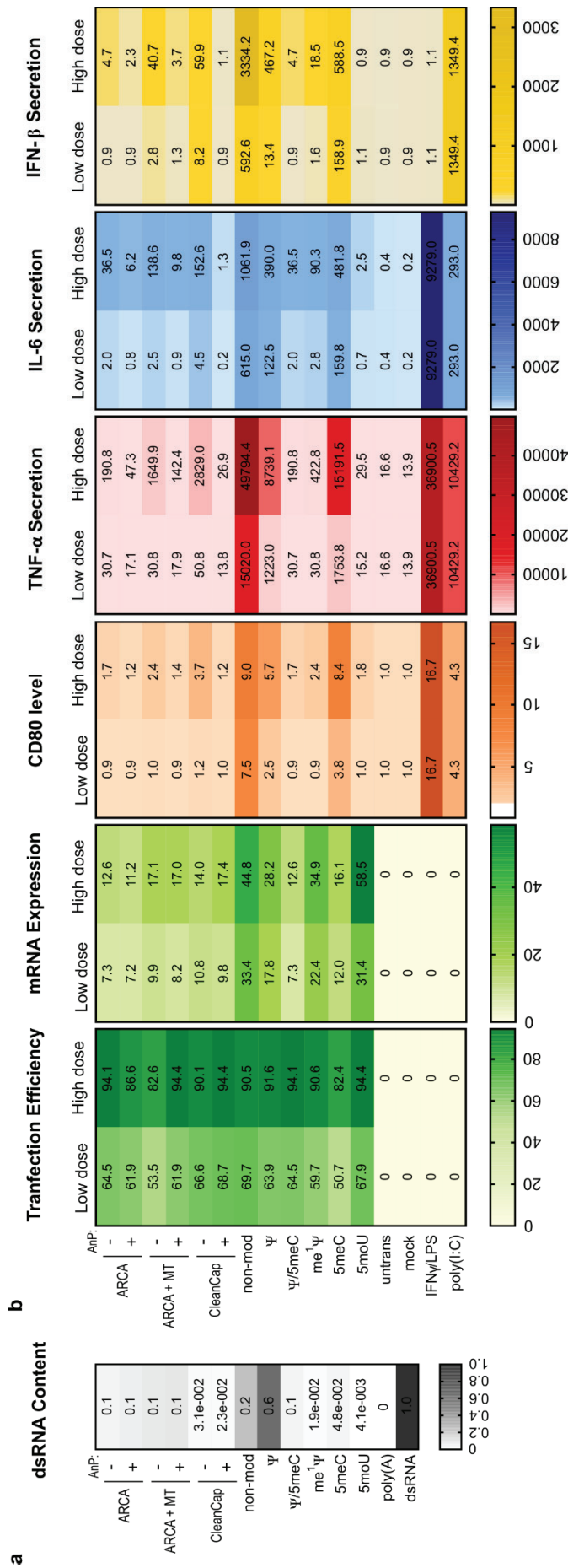
a

dsRNA Content

	AnP	dsRNA Content
ARCA	−	0.1
ARCA	+	0.1
ARCA + MT	−	0.1
ARCA + MT	+	0.1
CleanCap	−	3.1e-002
CleanCap	+	2.3e-002
non-mod		0.2
Ψ		0.6
Ψ/5meC		0.1
me¹Ψ		1.9e-002
5meC		4.8e-002
5moU		4.1e-003
poly(A)		0
dsRNA		1.0

b

	AnP	Transfection Efficiency Low dose	High dose	mRNA Expression Low dose	High dose	CD80 level Low dose	High dose	TNF-α Secretion Low dose	High dose	IL-6 Secretion Low dose	High dose	IFN-β Secretion Low dose	High dose
ARCA	−	64.5	94.1	7.3	12.6	0.9	1.7	30.7	190.8	2.0	36.5	0.9	4.7
ARCA	+	61.9	86.6	7.2	11.2	0.9	1.2	17.1	47.3	0.8	6.2	0.9	2.3
ARCA + MT	−	53.5	82.6	9.9	17.1	1.0	2.4	30.8	1649.9	2.5	138.6	2.8	40.7
ARCA + MT	+	61.9	94.4	8.2	17.0	0.9	1.4	17.9	142.4	0.9	9.8	1.3	3.7
CleanCap	−	66.6	90.1	10.8	14.0	1.2	3.7	50.8	2829.0	4.5	152.6	8.2	59.9
CleanCap	+	68.7	94.4	9.8	17.4	1.0	1.2	13.8	26.9	0.2	1.3	0.9	1.1
non-mod		69.7	90.5	33.4	44.8	7.5	9.0	15020.0	49794.4	615.0	1061.9	592.6	3334.2
Ψ		63.9	91.6	17.8	28.2	2.5	5.7	1223.0	8739.1	122.5	390.0	13.4	467.2
Ψ/5meC		64.5	94.1	7.3	12.6	0.9	1.7	30.7	190.8	2.0	36.5	0.9	4.7
me¹Ψ		59.7	90.6	22.4	34.9	0.9	2.4	30.8	422.8	2.8	90.3	1.6	18.5
5meC		50.7	82.4	12.0	16.1	3.8	8.4	1753.8	15191.5	159.8	481.8	158.9	588.5
5moU		67.9	94.4	31.4	58.5	1.0	1.8	15.2	29.5	0.7	2.5	1.1	0.9
untrans		0	0	0	0	1.0	1.0	16.6	16.6	0.4	0.4	0.9	0.9
mock		0	0	0	0	1.0	1.0	13.9	13.9	0.2	0.2	0.9	0.9
IFNγ/LPS		0	0	0	0	16.7	16.7	36900.5	36900.5	9279.0	9279.0	1.1	1.1
poly(I:C)		0	0	0	0	4.3	4.3	10429.2	10429.2	293.0	293.0	1349.4	1349.4

Figure S9. Overview of the properties and performance of IVT-mRNA with different cap and nucleotide modifications in terms of dsRNA content, protein expression, and inflammatory responses of transfected macrophages illustrated as heat map graphs. **(a)** dsRNA content, **(b)** (from left to right) transfection efficiency in percentage of EGFP positive cells, mRNA expression level measured by mean fluorescent intensity (MFI) of EGFP signal, and relative CD80 surface marker expression indicating the inflammatory responses, normalized MFI measured 24 h after transfection. The cytokine secretion measured 24 h after transfection is presented as concentration (pg·mL^{-1}) of TNF-α, IL-6 and IFN-β. Untransfected, poly(I:C)-treated, and LPS/IFN γ-activated macrophages served as negative, positive and high control, respectively.

Table S1. Chemical modifications and process of preparation of IVT-mRNAs synthesized

	Sample ID	Chemical composition		Post-transcriptional modifications	
		Cap structure (type)	Nucleotides	2'-O-Methyltransferase treatment	Phosphatase treatment
Cap modified IVT-mRNA	ARCA/-	ARCA (Cap 0)	Ψ/5meC/A/G	-	-
	ARCA/+	ARCA (Cap 0)	Ψ/5meC/A/G	-	+
	ARCA+MT/-	ARCA (Cap 1)	Ψ/5meC/A/G	+	-
	ARCA+MT/+	ARCA (Cap 1)	Ψ/5meC/A/G	+	+
	CleanCap/-	CleanCap AG (Cap 1)	Ψ/5meC/A/G	-	-
	CleanCap/+	CleanCap AG (Cap 1)	Ψ/5meC/A/G	-	+
Nucleotide modified IVT-mRNA	non-mod	ARCA (Cap 0)	U/C/A/G	-	-
	Ψ	ARCA (Cap 0)	Ψ/C/A/G	-	-
	me^{1}Ψ	ARCA (Cap 0)	me^{1}Ψ/C/A/G	-	-
	5meC	ARCA (Cap 0)	U/5meC/A/G	-	-
	5moU	ARCA (Cap 0)	5moU/C/A/G	-	-
	Ψ/5meC (2nt. mod.)	ARCA (Cap 0)	Ψ/5meC/A/G	-	-

Sample ID refers to abbreviations which was used in text throughout. (ARCA: anti-reverse cap analogue, MT: methyl-transferase, Ψ: pseudouridine, me^{1}Ψ: N^1-Methylpseudouridine, 5moU: 5-methoxy-uridine, 5meC: 5-methyl-cytidine, 2nt. mod: two nucleotides were modified)

8

Appendix III

MRS Communications

Research Letter

Check for updates

Co-delivery of genes can be confounded by bicistronic vector design

Hanieh Moradian [ID] **,** Institute of Active Polymers, Helmholtz-Zentrum Hereon, 14513 Teltow, Germany; Berlin-Brandenburg Center for Regenerative Therapies (BCRT), 13353 Berlin, Germany; Institute of Biochemistry and Biology, University of Potsdam, 14476 Potsdam, Germany
Manfred Gossen [ID] **,** Institute of Active Polymers, Helmholtz-Zentrum Hereon, 14513 Teltow, Germany; Berlin-Brandenburg Center for Regenerative Therapies (BCRT), 13353 Berlin, Germany
Andreas Lendlein [ID] **,** Institute of Active Polymers, Helmholtz-Zentrum Hereon, 14513 Teltow, Germany; Berlin-Brandenburg Center for Regenerative Therapies (BCRT), 13353 Berlin, Germany; Institute of Biochemistry and Biology, University of Potsdam, 14476 Potsdam, Germany

Address all correspondence to Andreas Lendlein at **lendlein@uni-potsdam.de**

Abstract

Maximizing the efficiency of nanocarrier-mediated co-delivery of genes for co-expression in the same cell is critical for many applications. Strategies to maximize co-delivery of nucleic acids (NA) focused largely on carrier systems, with little attention towards payload composition itself. Here, we investigated the effects of different payload designs: co-delivery of two individual "monocistronic" NAs versus a single bicistronic NA comprising two genes separated by a 2A self-cleavage site. Unexpectedly, co-delivery via the monocistronic design resulted in a higher percentage of co-expressing cells, while predictive co-expression via the bicistronic design remained elusive. Our results will aid the application-dependent selection of the optimal methodology for co-delivery of genes.

Introduction

Delivery of recombinant nucleic acids (NA) into cells is an essential process in gene therapy[1] as well as genetic engineering for basic research.[2] Robust delivery systems typically consist of polymeric or liposomal nanocarriers with physically bound RNA or DNA, including therapeutic NAs,[3,4] but also vaccines,[5] as highlighted by the response to the recent SARS-CoV-2 global outbreak.[6] The NA payload depends on the requirements of the application, which in many cases demand expression of multiple transgenes. To rapidly identify expression via live cell imaging, target transgene can be coupled with a fluorescence reporter gene, also facilitating subsequent cell sorting.[7,8] When production of large multisubunit proteins like antibodies is aimed, multiple genes coding for different subunits must be simultaneously delivered to the same cell.[9] The same applies for the expression of enzyme complexes.[10] Also (re)programming cells fate requires combinatorial expression of transcription factors.[11–13] This includes the dedifferentiation of somatic cells into induced pluripotent stem cells (iPSCs),[14] or the transdifferentiation to another somatic cell lineage.[15] Genome editing by CRISPR/Cas9 technology even requires delivery of three NA types including a guide RNA (gRNA), a gene (mRNA/pDNA) coding Cas9 protein, and optionally the DNA donor for targeting are crucial to successfully perform.[7,16]

There are various strategies to achieve simultaneous delivery of multiple NAs, and thus co-synthesis of multiple proteins in the same cell, including (i) incorporation of multiple transcription units within the same vector,[17,18] (ii) fusion of genes,[19] (iii) introduction of internal translation initiation sites such as internal ribosome entry sites (IRES),[20] (iv)

inserting enzyme-dependent cleavage sites in polyproteins,[21] and (v) enzyme-independent (apparent) self-cleavage sites between genes.[22,23] The first method is only applicable for gene delivery via plasmid DNA (pDNA), but not messenger RNA (mRNA). Moreover, the introduction of post-translational enzymatic cleavage sites is restricted to co-localization of enzyme and protein. Therefore, cap-independent internal initiation sites, e.g. IRES, and enzyme-independent (apparent) self-cleavage peptides such as 2A peptides gained considerable popularity, both result in multi-gene expression within a single cassette, also referred to as "multicistronic" genes. When encountering 2A sequences, ribosomes skip the formation of the peptide bond between glycine and proline amino acids of the 2A peptide, only to continue with translation of the second gene. Thus, in theory, this vector design should inherently result in a 1:1 molar stoichiometry of the two nascent polypeptide chains, while the equilibrium of the proteins in question might diverge. In any case, connecting genes on the NA level by 2A peptides encoding sequences should guarantee the co-synthesis of either of the proteins in a transfected cell, and was reported to result in reliable co-expression when evaluated empirically.[24] Of note, while the multicistronic approach ensures equimolar representation of the genes in question, the effective intracellular concentration of the encoded proteins may differ substantially, especially due to differences in protein stability. Alternatively, two distinct monocistronic genes could be packaged within the same carrier, and being taken up and co-expressed by the same cell.[25,26]

The aim of this study was to find the most reliable and robust gene co-delivery approach for simultaneous production of two proteins in the same cell, by comparing two commonly

used strategies including delivery of a "bicistronic" gene versus co-delivery of two distinct "monocistronic" genes. We hypothesized that co-expression of two transgenes directly coupled by 2A-design should be most efficient to ensure predictable synthesis of both the corresponding proteins in a cell, due to the inherently equivalent molar ratio of the two genes encoded in the same open reading frame, as one transcription unit with continuous ribosomal protein synthesis. This notion was empirically investigated by systematic side-by-side comparison of cells either transfected with nucleic acid comprising of two genes separated by a 2A peptide, or co-transfected with two separate nucleic acids as a control (Fig. 1). These experiments were initially performed by direct comparison of equimass versus equimolar ratio of the two genes, as only possible and reasonable for the monocistronic approach and evaluated by transfection of in vitro transcribed mRNA (IVT-mRNA) as payload, followed up by equimass ratio analysis only. The latter was also investigated by implementing pDNA as genetic payload for a selected set of experiments. Given that the initial quantitative co-expression via the 2A approach was confounded, we further evaluated the effect of the size of the first gene on co-expression rates and the potential cell-type specificity of this effect. Establishing effective methods for co-expression of multiple transgenes could be beneficial in addressing complex gene delivery studies.

Materials and methods
Design of pDNA vectors
pRNA2-(A)128 plasmid DNA vector comprising a CMV promoter, a T7 promoter, a short intron-less 5'-untranslated region (UTR) with Kozak sequence, enhanced green fluorescent protein (EGFP) coding region (or other open reading frames in case of pRNA2-derivatives used in this study), a head-to-tail duplicated human β-globin 3′-UTR providing increased transcript stability, followed by a homopolymeric 128-base polyadenine stretch (for use as a template in the IVT reaction and a poly(A) signal (for direct use of the plasmid in DNA transfections); all as described previously[27] (Figure S1). Thus, identical pRNA2 constructs and their derivatives are dual-use for IVT-mRNA and pDNA applications. In order to induce simultaneous expression of two genes upon cellular (co-)delivery, DNA templates were designed according to two different approaches described as follows:

(i) **Monocistronic genes** comprised of only one gene in a single cassette (Figure S1 left panel). Enhanced green fluorescent protein (EGFP) coding region in pRNA2-(A)$_{128}$ vector mentioned above was replaced with one of the following genes: red fluorescent protein (mCherry), interleukin 13 (IL13), or Krueppel-like factor 4 (KLF4), to generate pRNA2-(A)$_{128}$-mCherry, pRNA2-(A)$_{128}$-IL13, or pRNA2-(A)$_{128}$-KLF4, respectively.

(ii) **Bicistronic genes** consist of two genes in the same cassette separated by a 2A peptide sequence (Fig. 1, upper panel, Fig. S1, right panel). Among different existing 2A peptide sequences, the P2A peptide was selected in this study, due to superior performance as reported previously.[28] Consequently, the three above-mentioned genes, i.e. mCherry, IL13 and KLF4 coding genes, were coupled with EGFP expressing sequence in a single vector, separated by a P2A peptide containing amino acid sequence of GSGATNFSLLKQAGDVEENPGPKL. The resulting vectors were referred to as pRNA2-(A)$_{128}$-mCherry-2A-EGFP, pRNA2-(A)$_{128}$-IL13-2A-EGFP, and pRNA2-(A)$_{128}$-KLF4-2A-EGFP, respectively.

mRNA synthesis by in vitro transcription
Monocistronic and bicistronic mRNAs were individually synthesized by in vitro transcription using the above-mentioned pDNAs. mRNAs were synthesized according to our previously published protocol.[29] Briefly, plasmid vectors were linearized with BspMI restriction enzyme (New England Biolabs, Germany), and precipitated using a salt mixture including 0.05 Vol 3 M sodium acetate (Thermo Fisher Scientific, Germany), in presence of 0.1 Vol 0.5 M ethylenediaminetetraacetic acid (EDTA) (Thermo Fisher Scientific), and 2 Vol 100% EtOH (Carl Roth, Karlsruhe, Germany). Subsequently, mRNAs were synthesized using TranscriptAid T7 High Yield Transcription Kit (Thermo Fisher Scientific) according to the manufacturer's instruction. Of note, the 5′ end of IVT-mRNA was co-transcriptionally modified with anti–reverse cap analog (ARCA) (Jena Bioscience, Germany). For transfection of macrophages, chemically modified IVT-mRNAs coding for mCherry, EGFP and mCherry-2A-EGFP were prepared by complete substitution of uridine and cytidine with pseudouridine (Jena Bioscience) and 5-methylcytidine (Jena Bioscience), respectively. IVT-mRNAs were purified using lithium chloride precipitation and resuspended in UltraPure™ nuclease-free sterile water (Merck Millipore, Germany) supplemented with 0.1 mM EDTA. The concentration of IVT-mRNA products was determined by UV/Vis-spectroscopy (NanoDrop 1000 Spectrophotometer; Peqlab, Germany). Moreover, the quality/integrity of transcripts were assessed by denaturing agarose gel electrophoresis.

Transfection of IVT-mRNA
Lipofectamine MessengerMAX (LipoMM; Thermo Fisher Scientific), a commercially available, lipoplex-forming reagent optimized for RNA transfections, was selected as a reagent for delivery of IVT-mRNAs. The IVT-mRNA/LipoMM complexes, required for co-delivery/co-transfection of monocistronic genes (MonoCis (CoTF)) or delivery of a bicistronic 2A peptide-comprising gene (BiCis (2A-P)), were prepared as follows; MessengerMAX reagent was diluted 1:50 (vol) in 125 μL Opti-MEM reduced serum medium (Thermo Fisher Scientific), and incubated for 10 min at RT. The resulting solution was added to the equal volume of Opti-mem containing
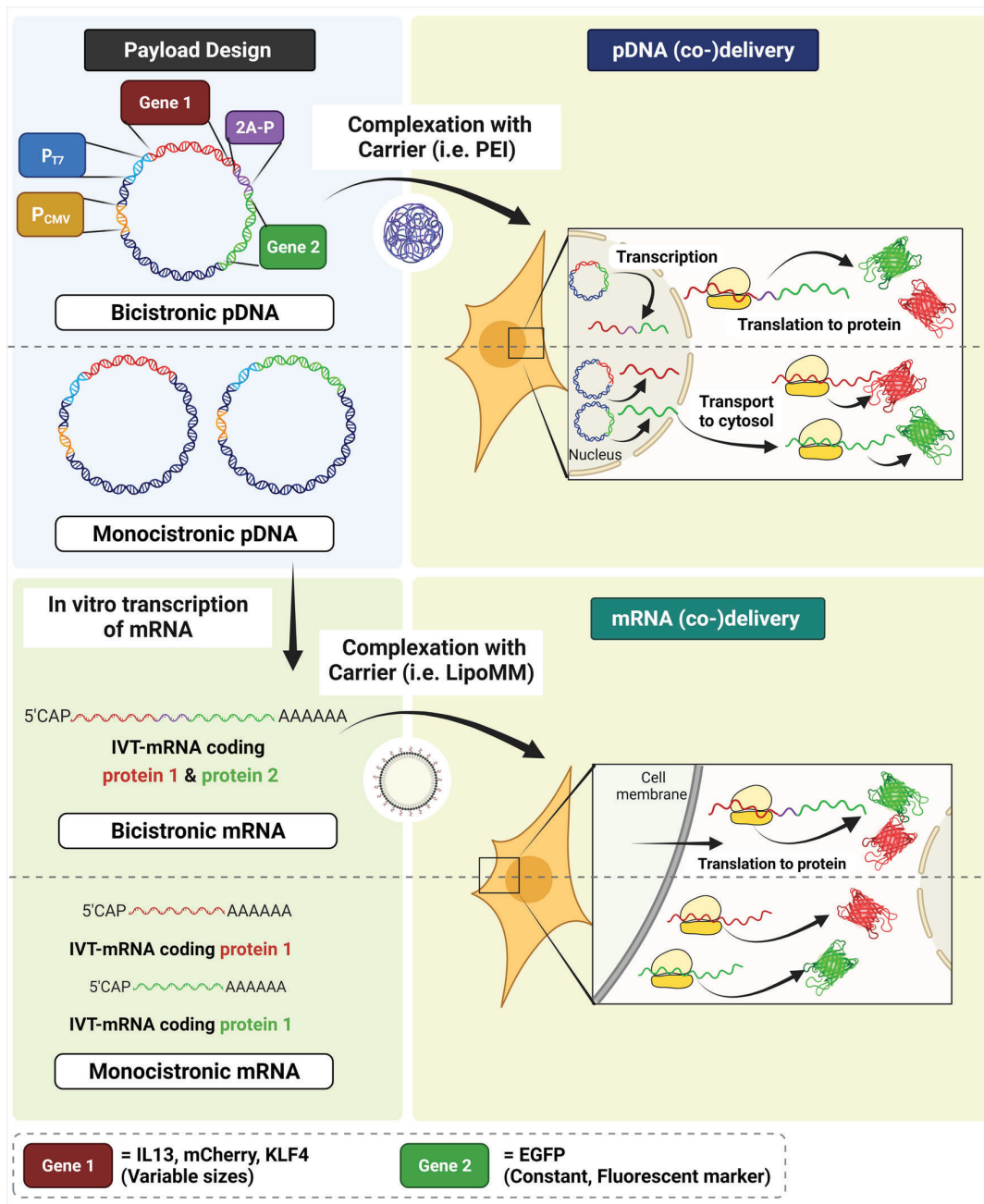
110

Figure 1. Schematic representation of the study design to achieve nucleic acid-directed co- production of target proteins in individual cells. Plasmid DNA was directly (co-)delivered to cells using an established carrier system (i.e. PEI) (upper panel) or used as a template to IVT-mRNA, followed by (co-)delivery of IVT-mRNA by LipoMM to cells (lower panel). The former requires nucleus entry and transcription to mRNA, whereas in the latter case IVT-mRNA is, upon cellular uptake and endosomal escape, instantly translated to protein in the cytoplasm (not illustrated here). In both cases, however, mRNA is the ultimate entity, which is processed by ribosomes as a blueprint for protein synthesis. The two distinct payload designs, namely monocistronic and bicistronic nucleic acid refer to two genes integrated within one continuous open reading frame, and different IVT-mRNAs co-formulated together in a single carrier type (e.g., lipoplex or polyplex) in a statistical fashion, respectively. Three different genes with distinct sizes were assessed as the first gene, while keeping EGFP as a fluorescent marker constantly as the second gene. The order of representation does not reflect the experimental sequence. (Illustration created by BioRender.com).

defined amount of IVT-mRNA, individually or in mixture in case of co-transfection; see Table S1 for the precise amounts of IVT-mRNA used for equimass versus equimolar experiment when following the monocistronic approach. Briefly, for equal mass transfections either 500 ng of the respective BiCis IVT-mRNA or 250 ng of each of the 2 MonoCis IVT-mRNAs, as indicated, were used. For equal mole transfections the number of molecules for each of the MonoCis IVT-mRNA was equivalent to the molar amounts of 500 ng of the respective BiCis mRNA (Table S1). The monocistronic EGFP encoding IVT-mRNA (length: 1253 nts; i.e. 500 ng/well equals 1.24 pmol/well of 12-well plate) was used as a reference point throughout. For the transfection of cells in 6-well plates in case of equimass experiments, 1 μg IVT-mRNA, i. e. 1 μg bicistronic IVT-mRNA, or 500 ng from each of the two different IVT-mRNAs (MonoCis) premixed together (equal mass approach), or 1 μg combined total of the KLF4 and EGFP IVT-mRNA in the indicated ratios for the equal mole approach was used to prepare BiCis (2A-P), and MonoCis (CoTF) complexes, respectively. The mixture was briefly vortexed and incubated for 5 min at RT. Subsequently, the transfection complexes containing 1 μg IVT-mRNA in overall 250 μL Optimem were added to each well of HeLa (ATCC; CCl-2) cells in a 6-well plate format. HeLa cells were pre-seeded at a density of $3.00E+05$ cells per well of 6-well plates, in high glucose DMEM, supplemented with GlutaMAX™, pyruvate (Gibco, Germany), 10 vol% FBS (Biochrom, Germany) and 1 U·mL^{-1} Penicillin–Streptomycin (Gibco, Germany), 24 h before transfection with IVT-mRNA.

Quantitative analysis of cells with flow cytometry

Cells were harvested at above specified time points with TrypLE Select (Thermo Fisher Scientific). Upon washing with cold flow cytometry washing solution (Miltenyi Biotec, Germany), cells were analyzed with a MACSQuant VYB® flow cytometer (Miltenyi Biotec, Germany).

Production of non-fluorescent protein, e.g. KLF4, was detected by immunocytochemistry, using eBioscience ™ Foxp3 /transcription factor staining buffer set (Thermo Fisher Scientific), according to manufacturer's instruction. The KLF4 protein was subsequently stained with recombinant Alexa Fluor® 647 anti-KLF4 antibody (Abcam, Germany). Cells were measured by MACSQuant VYB® flow cytometer. All flow cytometric data were analyzed with FlowJo software V10.

Statistics

Data are presented as means ± standard deviation (SD) of at least three independent experiments. In case of primary human macrophages, three independent experiments were performed using cells derived from three different donors. Data were statistically analyzed via Prism 7.00 software (GraphPad, USA).

Results and discussion
Study design

The reliability of two methods differing in payload design was investigated in a series of side-by-side experiments. Two separate monocistronic genes were co-transfected in the first approach, whereas a single bicistronic gene coding both proteins in a single cassette, separated by a 2A peptide was delivered in the second approach. Herein, the former is referred to as "MonoCis (CoTF)", while the latter is named "BiCis (2A-P)" throughout all experiments. As we previously validated the reliability of MonoCis (CoTF) approach,[26] this condition was mainly included as reference and control to determine the performance of BiCis (2A-P) method. Throughout this study a fluorescent marker protein, i.e. enhanced green fluorescent protein (EGFP) was selected as the second protein, in order to enable facile and prompt monitoring of gene expression, investigated by fluorescent microscopy and quantified via flow cytometry. Experiments were designed to evaluate the effect of several parameters including cell type, NA identity (RNA vs. DNA) and size of the first gene on co-expression rate. The molecular weights of nucleic acids and also the respective genes implemented in this study are summarized in Table I. Addressing the latter parameter was spurred by our initial, unexpected observation, where inconsistent patterns of co-expression were monitored at single cell resolution for the BiCis (2A-P) approach.

Size of first gene does not correlate with co-expression rate

As one possible explanation we investigated the effect of first gene's size on co-expression rate of two genes, as well as expression level of the second gene. Three different IVT-mRNAs coding for IL13, mCherry (mCh), and KLF4 were selected, exemplifying the small (1/2 X), medium (1 X), and large (2 X) sizes, respectively, when compared to the size of the second gene, i.e. EGFP (G) (Table I, Fig. 2(a)). Note that for IL13 and KLF4 the choice of these genes was solely based on their size, not a potential biological function. These genes were either placed in position 1 upstream of EGFP in a single cassette, represented as BiCis (2A-P) (Fig. 2(a), left panel), or co-packaged as separate units each with EGFP within the same complex, named MonoCis (CoTF) (Fig. 2(a), right panel).

Given an identical mass of different IVT-mRNAs, those with smaller size correspond to larger numbers of molecules compared to that of larger size. Thus, a series of preliminary experiments with equal mass as well as equal moles were performed, to identify the reliable experimental set-up, and to avoid any potential misinterpretation of EGFP expression. The percent of EGFP positive cells and intensity of EGFP signal were measured by flow cytometry in side-by-side experiments, and presented for each condition (Fig. 2(b), (c)). The results demonstrated that the observed reduction of co-expression rate for a large gene in position 1 is not caused by its underrepresentation in terms of molar concentration when following an

112

Table I. Characteristics of the genes investigated in this study.

Gene Name	Description/function	Molecular Weight of pDNA vector (kDa)	Molecular Weight of IVT-mRNA (kDa)	Molecular weight of ORF[a] pDNA (kDa)	Molecular weight of ORF[a] mRNA (kDa)
EGFP	MonoCis/fluorescent marker	3201	401	444	231
IL13	MonoCis/control for small size gene	2979	286	271	141
mCherry	MonoCis/fluorescent marker/control for medium size gene	3165	382	439	228
KLF4	MonoCis/control for large size gene	3590	603	873	453
IL13-2A-EGFP	BiCis/co-expression of a gene with marker	3467	539	760	394
mCherry-2A-EGFP	BiCis/co-expression of a gene with marker	3634	625	927	481
KLF4-2A-EGFP	BiCis/co-expression of a gene with marker	4077	855	1370	711

[a]*ORF* open reading frame.

equal mass co-transfection protocol (Fig. 2b). Thus, for the subsequent experiments, the equal mass method was implemented throughout. The corresponding molar amounts for each condition is presented in Table S2.

The expression level of EGFP in HeLa cells transfected with either of these approaches was evaluated by fluorescent microscopy (Fig. 2(d)). No consistent pattern of variation in EGFP intensity was observed with respect to the size of the first gene, in cells transfected with BiCis (2A-P) IVT-mRNAs. While mCh/G resulted in higher EGFP expression than IL13/G, extremely only a strongly diminished signal was detected for KLF4/G (Fig. 2d, upper panel). However, MonoCis (CoTF) consistently led to a higher EGFP expression when compared to the BiCis (2A-P) approach (Fig. 2d, lower panel).

The co-expression rate as well as expression of the first protein were evaluated by flow cytometry (Fig. 2e-h). Data suggested no differences in percent of double positive cell population between cells transfected with mCh/G via two distinct methods. Unexpectedly, however, MonoCis (CoTF) was superior to BiCis (2A-P) in cells transfected with KLF4/G in terms of co-expression rate (Fig. 2g). When analyzed individually, there were no differences in production level of the first protein, namely mCh and KLF4 in mCh/G and KLF4/G transfected cells, respectively, between BiCis (2A-P) and MonoCis (CoTF) methods (Fig. 2f & h, left panel). However, as mentioned above, level of second protein production in the BiCis (2A-P) approach was remarkably lower compared to the MonoCis (CoTF) for KLF4/G (Fig. 2h, right panel).
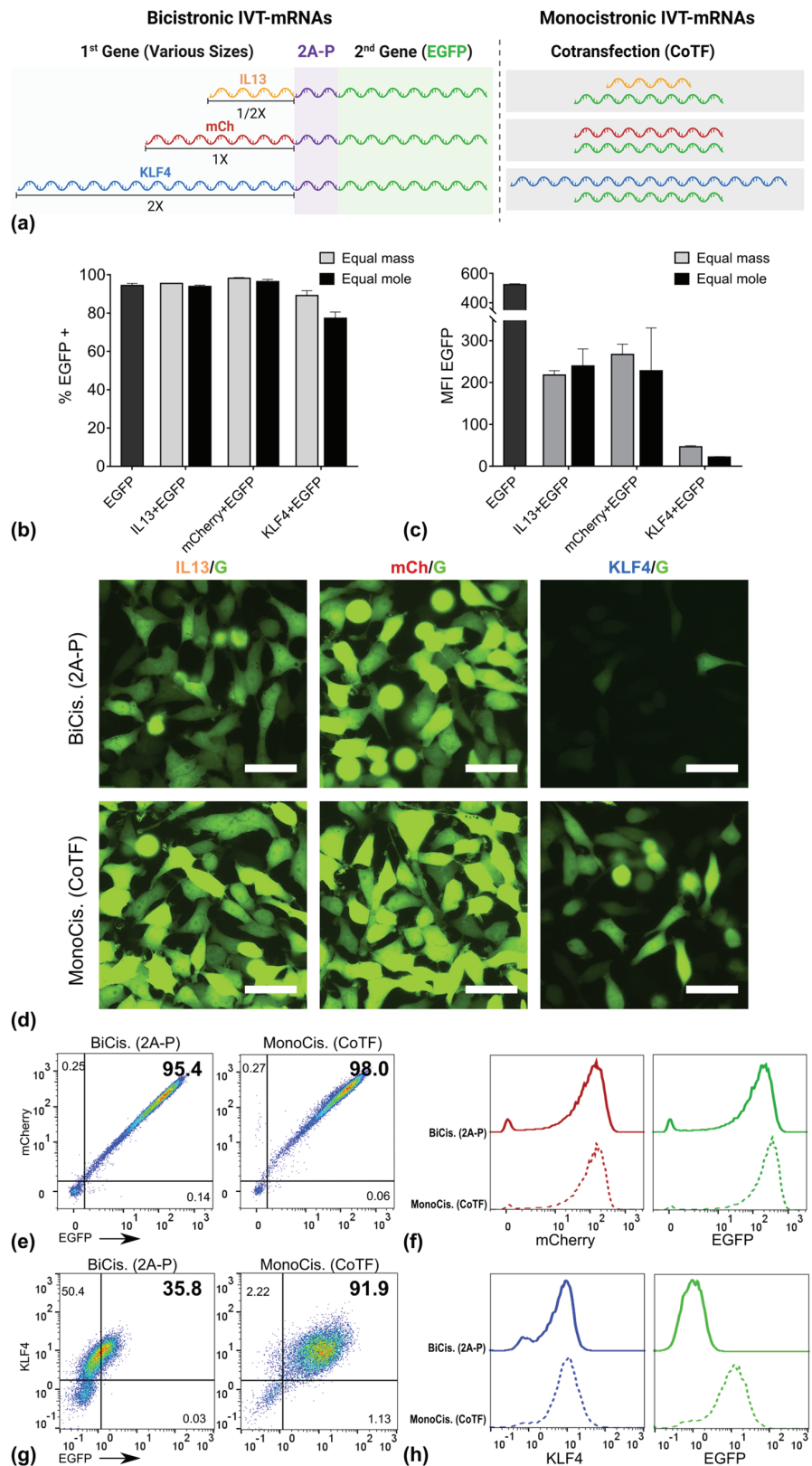
The EGFP expression quantified with flow cytometry (Fig. 3a), both in terms of percent of EGFP positive cells (Fig. 3a, middle panel), and intensity of EGFP signal representing level of expression within population of EGFP positive cells (Fig. 3a, right panel) was remarkably lower in BiCis (2A-P) compared to MonoCis (CoTF) for all three sizes. In particular, the minimum level of expression corresponded to KLF4/G both for MonoCis (CoTF), and more dramatically for BiCis (2A-P) methods (Fig. 3a, left panel).

Since the IVT-mRNA coding for KLF4 is almost twice as large as EGFP coding IVT-mRNA, the co-transfection with the MonoCis approach was also evaluated with ratios other than 1:1 (1:1.5), specifically 9:1 (6:1) and 1:9 (1:13.6), referring to KLF4: EGFP IVT-mRNA mass ratio (values in parenthesis referring to the molar ratio). Expression of both proteins were subsequently measured and plotted for each condition (Figure S3). Transfection of cells with MonoCis (CoTF) approach consistently led to higher percent of double positive cells, particularly remarkable also when the lowest ratio (i.e. 9:1) of EGFP was delivered (Figure S3).

These findings are consistent with previous report by Liu et al.[12], where they also found puzzling patterns of second protein production, examined for different types of 2A peptides in multicistronic genes. While originally analyzing the efficacy of different 2A sequences, they also observed striking differences of EGFP expression in multicistronic reprogramming vectors, when placed in different positions relative to the other genes.[12] The lower expression of second gene could potentially be attributed to detachment of ribosomes from messenger RNA, upon translation of first protein, as suggested by Shaimardanova et al.[30]. This was consistent with our observations, where no changes were detected in production of first protein, along with diminished production of second protein, particularly noticeable in KLF4/G transfected cells.

To investigate whether the differences observed between the two methods depend on the target cell-type, primary human monocyte-derived macrophages were transfected with mCh/G via both BiCis (2A-P) and MonoCis (CoTF) methods. Transfected macrophages were analyzed 24 h post-transfection for expression of the fluorescence marker proteins via fluorescent microscopy (Figure S4a), as well as flow cytometry (Figure S4b-f). There was no obvious difference between macrophages transfected with either method in terms of expression of mCherry and EGFP, as shown in individual channels (Figure S4a, left and middle panel), and merged fluorescent images (Figure S4a, right panel). However, when quantified

Figure 2. Impact of size ratio of the first gene to the second gene on the co-expression of two genes. (a) schematic overview of constructs, which were used and compared in parallel, IL13 with half size of EGFP as the small, mCherry with similar size to EGFP as medium, and KLF4 with almost double size of EGFP as large constructs were delivered together with EGFP either in one cassette with 2A-P as self-cleavage site, or co-delivered. For the monocistronic approach the percentage of EGFP positive population (b) and intensity of EGFP signal (mean fluorescent intensity) (c) reflecting the EGFP expression were quantified using flow cytometric evaluation of cells. Corresponding data for the bicistronic approach are provided in Figure S2. (d) Fluorescent images of HeLa cells transfected with any of the three genes with different sizes with two different approaches. Percent of double positive cells shown in form of dot plots (e), as well as expression level of the first protein (mCherry) and second protein (EGFP) compared between the two methods (f). Similarly, percent of double positive cells (g) and evaluation of protein production for KLF4 as first protein and EGFP as second protein and (h), both measured via immunocytochemistry (ICC) and flow cytometry. Numbers indicated within dot plots represent % of cells inside the corresponding gate. Error bars indicate SD for three independently performed experiments. Scale bar = 50 μm. See Table S1 for precise numbers describing equimass versus equimolar transfection, corresponding to each method.

114

IVT-mRNA transfection

pDNA transfection
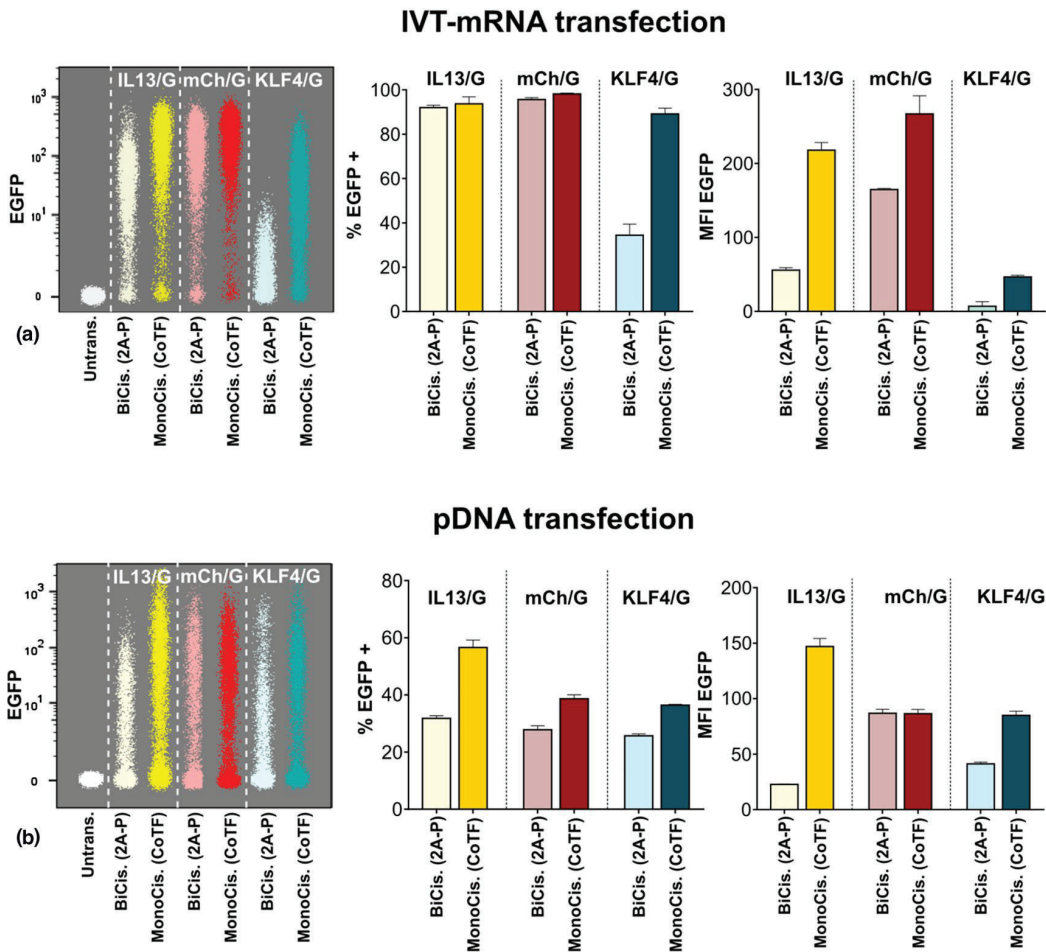
Figure 3. Quantification of transgene expression in BiCis versus MonoCis configuration. (a) Flow cytometric analysis of HeLa cells transfected with IVT-mRNA via the two methods; Left panel: Merged dot plot of cells expressing EGFP evaluated by flow cytometry. Middle panel: The percentage of EGFP positive cells. Right panel: The level of EGFP expression quantified from flow cytometry data. (b) Side-by-side comparison of EGFP expression in HeLa cells transfected by transgene-encoding plasmid DNA; Left panel: Merged dot plot of different genes expressed in HeLa cells measured by flow cytometry. Middle panel: Transfection efficiency indicated as percent of EGFP positive cells. Right panel: The level of transgene expression quantified by mean fluorescent intensity of EGFP signal. Cells were analyzed 24 h after IVT-mRNA transfection, and 48 h after pDNA transfection. Values are presented as mean ± SD, $n = 3$. Error bars indicate SD.

with flow cytometry, the production level of both proteins was slightly lower in macrophages transfected with BiCis (2A-P) compared to MonoCis (CoTF) approach (Figure S4c, e, f). The co-expression rate, i.e. percent of double positive cells, were consistently lower for BiCis (2A-P) compared to MonoCis (CoTF) approach (Figure S4b, d). These findings argue against a cell-type dependence of co-expression patterns according to the approach chosen. However, the consistent differences between the two methods were interestingly more pronounced in primary cells than in established cell line, e.g. HeLa cells, which emphasized the importance of selection of proper payload design to achieve a reliable co-expression.

Plasmid DNA transfection results in 2nd gene expression pattern similar to mRNA transfections

Next, we asked whether the differences observed between cells transfected with the two methods based on various payload design were exclusive to IVT-mRNA or could it be generalized to other nucleic acid entities, in particular plasmid DNA (pDNA) used in this study. Similar to IVT-mRNA, bicistronic pDNA was comprised of both genes at the same plasmid separated by 2A peptide, whereas monocistronic pDNA coding for each gene had to be co-delivered. The experiments were performed by using equimass transfection

of pDNA (Table S2). The level of second protein production in HeLa cells was measured using flow cytometry as the key readout (Fig. 3b). Interestingly, no correlation was identified between size of first gene and the expression of the second gene coding EGFP, as indicated by side-by-side comparison of pDNA samples with increasing size of the first gene, i.e. IL3/G, mCh/G, and KLF4/G, respectively (Fig. 3b, left panel). Transfection efficiency determined as percent of EGFP positive cells (Fig. 3b, middle panel), and level of protein production quantified and defined as mean fluorescent intensity (MFI) of EGFP signal (Fig. 3b, right panel) were compared in cells transfected with pDNA. Data suggested that BiCis (2A-P) consistently resulted in lower transfection efficiency and protein production level of the second protein, when compared to MonoCis (CoTF) approach (Fig. 3b). Overall, comparison of data between pDNA transfection (Fig. 3b) with IVT-mRNA transfection (Fig. 3a) revealed that the differences observed between two methods is not dependent on the chemical identity of the chosen NA nor its biophysical properties, i.e. linear with relaxed topology for IVT-mRNA as compared to circular, supercoiled pDNA. However, the extent to which the expression differs is more pronounced for IVT-mRNA transfection; See left panels in Fig. 3a& b.

Conclusions

We implemented two methods for simultaneous delivery of two distinct genes based on different payload compositions. A systematic comparison of a bicistronic gene coding for two proteins separated by a 2A peptide sequence side-by-side with the co-delivery of two separate genes revealed that the latter is the more reliable approach. While a bicistronic design will lead to a one-to-one stoichiometry of templates for protein synthesis independent of formulation and uptake route, experimental evidence on the level of proteins actually synthesized argued against this notion. Moreover, none of the envisaged and examined parameters including the first protein's size, cell-type, or nucleic acid identity (IVT-mRNA vs. pDNA) had a determining role on co-expression rates. In contrast, co-delivery of two monocistronic genes consistently resulted in robust expression of the second protein, proved to be true throughout all tested conditions with different gene sizes, for both IVT-mRNA and pDNA, among different cell-types. As the underlying mechanisms contributing to the observed erratic performance of the 2A peptide remain to be solved, we can only speculate about potential effects of nucleic acid sequence and the corresponding secondary structure of mRNA around the 2A peptide, or the conformation of first nascent protein on tendency of ribosomes whether to continue translation of the second protein or to disengage from the mRNA and thus stop translation. In any case, it is obvious that the 2A sequence can affect protein-synthesizing ribosomes in a way that it impedes on their scheduled translation path.

Author contributions

HM conceived the study concept and designed experiments. HM performed all of the experiments and analyzed the data. HM, MG and AL evaluated and interpreted the data. HM and MG drafted the manuscript. AL critically revised the manuscript. MG and AL supervised the study. The manuscript has been read and approved by all authors.

Data availability

The datasets generated during and/or analysed during the current study are available from the corresponding author on reasonable request.

Declarations

Conflict of interest

All authors declare that they have no conflict of interest.

116

Supplementary Information

The online version contains supplementary material available at https://doi.org/10.1557/s43579-021-00128-7.

References

1. G. Both, I. Alexander, S. Fletcher, T.J. Nicolson, J.E. Rasko, S.D. Wilton, G. Symonds, Gene therapy: therapeutic applications and relevance to pathology. Pathology **43**, 642 (2011)
2. O. Krämer, S. Klausing, T. Noll, Methods in mammalian cell line engineering: from random mutagenesis to sequence-specific approaches. Appl. Microbiol. Biotechnol. **88**, 425 (2010)
3. I. Lostalé-Seijo, J. Montenegro, Synthetic materials at the forefront of gene delivery. Nat. Rev. Chem. **2**, 258 (2018)
4. Y.K. Sung, S.W. Kim, Recent advances in the development of gene delivery systems. Biomater. Res. **23**, 8 (2019)
5. N. Pardi, M.J. Hogan, F.W. Porter, D. Weissman, mRNA vaccines—a new era in vaccinology. Nat. Rev. Drug Discov. **17**, 261 (2018)
6. G. Forni, A. Mantovani, G. Forni, A. Mantovani, L. Moretta, R. Rappuoli, G. Rezza, A. Bagnasco, G. Barsacchi, G. Bussolati, M. Cacciari, P. Cappuccinelli, E. Cheli, R. Guarini, M.L. Bacci, M. Mancini, C. Marcuzzo, M.C. Morrone, G. Parisi, G. Pasquino, C. Patrono, A.Q. Curzio, G. Remuzzi, A. Roncaglia, S. Schiaffino, P. Vineis and R. on behalf of the Covid-19 Commission of Accademia Nazionale dei Lincei, COVID-19 vaccines: where we stand and challenges ahead. *Cell Death Differ.* **28**, 626 (2021).
7. K. Duda, L.A. Lonowski, M. Kofoed-Nielsen, A. Ibarra, C.M. Delay, Q. Kang, Z. Yang, S.M. Pruett-Miller, E.P. Bennett, H.H. Wandall, G.D. Davis, S.H. Hansen, M. Frödin, High-efficiency genome editing via 2A-coupled co-expression of fluorescent proteins and zinc finger nucleases or CRISPR/Cas9 nickase pairs. Nucleic Acids Res. **42**, 84 (2014)
8. J.E. Lewis, J.M. Brameld, P. Hill, P. Barrett, F.J. Ebling, P.H. Jethwa, The use of a viral 2A sequence for the simultaneous over-expression of both the vgf gene and enhanced green fluorescent protein (eGFP) in vitro and in vivo. J. Neurosci. Methods **256**, 22 (2015)
9. J.M. Bakker, W.K. Bleeker, P.W. Parren, Therapeutic antibody gene transfer: an active approach to passive immunity. Mol. Ther. **10**, 411 (2004)
10. V.S. Efimova, L.V. Isaeva, A.A. Labudina, V.N. Tashlitsky, M.A. Rubtsov, L.A. Novikova, Polycistronic expression of the mitochondrial steroidogenic P450scc system in the HEK293T cell line. J. Cell. Biochem. **120**, 3124 (2019)
11. S.K. Goparaju, K. Kohda, K. Ibata, A. Soma, Y. Nakatake, T. Akiyama, S. Wakabayashi, M. Matsushita, M. Sakota, H. Kimura, M. Yuzaki, S.B.H. Ko, M.S.H. Ko, Rapid differentiation of human pluripotent stem cells into functional neurons by mRNAs encoding transcription factors. Sci. Rep. **7**, 42367 (2017)
12. Z. Liu, O. Chen, J.B.J. Wall, M. Zheng, Y. Zhou, L. Wang, H. Ruth Vaseghi, L. Qian, J. Liu, Systematic comparison of 2A peptides for cloning multigenes in a polycistronic vector. Sci. Rep. **7**, 2193 (2017)
13. M. Mathison, V.P. Singh, R.P. Gersch, M.O. Ramirez, A. Cooney, S.M. Kaminsky, M.J. Chiuchiolo, A. Nasser, J. Yang, R.G. Crystal, T.K. Rosengart, "Triplet" polycistronic vectors encoding Gata4, Mef2c, and Tbx5 enhances postinfarct ventricular functional improvement compared with singlet vectors. J. Thorac. Cardiovasc. Surg. **148**, 1656 (2014)
14. L. Shao, W.-S. Wu, Gene-delivery systems for iPS cell generation. Expert Opin. Biol. Ther. **10**, 231 (2010)
15. A.M. Kabadi, P.I. Thakore, C.M. Vockley, D.G. Ousterout, T.M. Gibson, F. Guilak, T.E. Reddy, C.A. Gersbach, Enhanced MyoD-induced transdifferentiation to a myogenic lineage by fusion to a potent transactivation domain. ACS Synth. Biol. **4**, 689 (2015)
16. J. Liu, J. Chang, Y. Jiang, X. Meng, T. Sun, L. Mao, Q. Xu, M. Wang, Fast and efficient CRISPR/Cas9 genome editing in vivo enabled by bioreducible lipid and messenger RNA nanoparticles. Adv. Mater. **31**, 1902575 (2019)
17. J.A. Curtin, A.P. Dane, A. Swanson, I.E. Alexander, S.L. Ginn, Bidirectional promoter interference between two widely used internal heterologous promoters in a late-generation lentiviral construct. Gene Ther. **15**, 384 (2008)
18. J. Tian, S.T. Andreadis, Independent and high-level dual-gene expression in adult stem-progenitor cells from a single lentiviral vector. Gene Ther. **16**, 874 (2009)
19. S.Y. Chen, C. Zani, Y. Khouri, W.A. Marasco, Design of a genetic immunotoxin to eliminate toxin immunogenicity. Gene Ther. **2**, 116 (1995)
20. H.Y. Chan, X. Xing, P. Kraus, S.P. Yap, P. Ng, S.L. Lim, T. Lufkin, Comparison of IRES and F2A-based locus-specific multicistronic expression in stable mouse lines. PLoS ONE **6**, 28885 (2011)
21. A.F. Sequeira, J. Turchetto, N.J. Saez, F. Peysson, L. Ramond, Y. Duhoo, M. Blémont, V.O. Fernandes, L.T. Gama, L.M.A. Ferreira, C.I.P.I. Guerreiro, N. Gilles, H. Darbon, C.M.G.A. Fontes, R. Vincentelli, Gene design, fusion technology and TEV cleavage conditions influence the purification of oxidized disulphide-rich venom peptides in *Escherichia coli*. Microb. Cell Fact. **16**, 4 (2017)
22. A.L. Szymczak, D.A. Vignali, Development of 2A peptide-based strategies in the design of multicistronic vectors. Expert Opin. Biol. Ther. **5**, 627 (2005)
23. G.A. Luke, M.D. Ryan, Using the 2A protein coexpression system: multicistronic 2A vectors expressing gene(s) of interest and reporter proteins. Methods Mol. Biol. **1755**, 31 (2018)
24. R.W. Daniels, A.J. Rossano, G.T. Macleod, B. Ganetzky, Expression of multiple transgenes from a single construct using viral 2A peptides in Drosophila. PLoS ONE **9**, 100637 (2014)
25. J.J. Gam, B. DiAndreth, R.D. Jones, J. Huh, R. Weiss, A "poly-transfection" method for rapid, one-pot characterization and optimization of genetic systems. Nucleic Acids Res. **47**, e106 (2019)
26. H. Moradian, A. Lendlein, M. Gossen, Strategies for simultaneous and successive delivery of RNA. J. Mol. Med. **98**, 1767 (2020)
27. D.J. Williams, H.L. Puhl, S.R. Ikeda, A. Simple, Highly efficient method for heterologous expression in mammalian primary neurons using cationic lipid-mediated mRNA transfection. Front. Neurosci. **4**, 181 (2010)
28. Y. Wang, F. Wang, R. Wang, P. Zhao, Q. Xia, 2A self-cleaving peptide-based multi-gene expression system in the silkworm Bombyx mori. Sci. Rep. **5**, 16273 (2015)
29. H. Moradian, T. Roch, A. Lendlein, M. Gossen, mRNA transfection-induced activation of primary human monocytes and macrophages: dependence on carrier system and nucleotide modification. Sci. Rep. **10**, 4181 (2020)
30. A.A. Shaimardanova, K.V. Kitaeva, I.I. Abdrakhmanova, V.M. Chernov, C.S. Rutland, A.A. Rizvanov, D.S. Chulpanova, V.V. Solovyeva, Production and application of multicistronic constructs for various human disease therapies. Pharmaceutics **11**, 580 (2019)

117

Co-delivery of genes can be confounded by bicistronic vector design

Hanieh Moradian[1, 2, 3], Manfred Gossen[1, 2], Andreas Lendlein[1, 2, 3,*]

1   Institute of Active Polymers, Helmholtz-Zentrum Hereon, 14513 Teltow, Germany
2   Berlin-Brandenburg Center for Regenerative Therapies (BCRT), 13353 Berlin, Germany
3   Institute of Biochemistry and Biology, University of Potsdam, 14476 Potsdam, Germany

* Corresponding Author, email address: lendlein@uni-potsdam.de

A) Supplementary Materials and Methods

Transfection of macrophages with IVT-mRNA

mCherry, EGFP and mCherry-2A-EGFP coding mRNAs were also examined in primary human macrophages. Macrophages were differentiated *in vitro* from monocytes purified from buffy coat-derived peripheral blood mononuclear cells (PBMCs) (Deutsche Rote Kreuz, Berlin; ethics vote EA2/018/16; Charité University Medicine Berlin) as previously described [1]. Macrophages were transfected with complexes containing chemically modified IVT-mRNAs. Respective volumes of the above prepared complexes were transferred to each well to deliver 125 ng/mL mRNA in cell culture medium. Macrophages were transfected at a density of 2.00E+06 cells per well of 6 well plates in 2 mL very low endotoxin (VLE) RPMI medium (Biochrom) supplemented with 10 vol% FBS.

Transfection of plasmid DNA (pDNA)

Being equipped with a CMV promoter, the pDNA templates were also directly transfected into HeLa cells. Plasmids were complexed and delivered via transfection-grade 25 kDa linear polyethylenimine (PEI) (Polyscience, Germany), a commercially available, polyplex-forming transfection reagent routinely used for delivery of plasmid DNAs, according to a previously published protocol [2]. Briefly, 2 µg pDNA diluted in 50 µL of 150 mM NaCl was combined with 7.5 mM PEI at nitrogen/phosphate (N/P) molar ratio of 20. pDNA solution was prepared either with 2 µg of single bicistronic pDNA or by pre-mixing 1 µg from each of two monocistronic pDNAs, referred to as BiCis (2A-P) and MonoCis (CoTF) transfection, respectively. The resulting mixture containing 2 µg pDNA was vortexed for 30 sec, and incubated for 10 min at RT for complex formation and then added dropwise to each well. HeLa cells were pre-seeded at a density of 2.50E+05 cells per well of 6-well plates 24 h before transfection.

Evaluation of cells with fluorescent microscopy

To evaluate fluorescent proteins production, cells were imaged with an inverted microscope ELIPSE Ti-U (Nikon) equipped with a mercury light source, Intensilight C-HGFI, and single-band filter sets; EGFP-BP filter (466/40, 525/50 nm), or TRITC filter (562/40, 641/75 nm) (Semrock, Germany). Images were acquired 24 and 48 h after cells transfection with IVT-mRNA or pDNA, respectively. All images were analyzed with NIS-Elements imaging software, version 4.51 (Nikon).

2

B) Supplementary Data

Monocistronic pDNA Vector   **Bicistronic pDNA Vector**
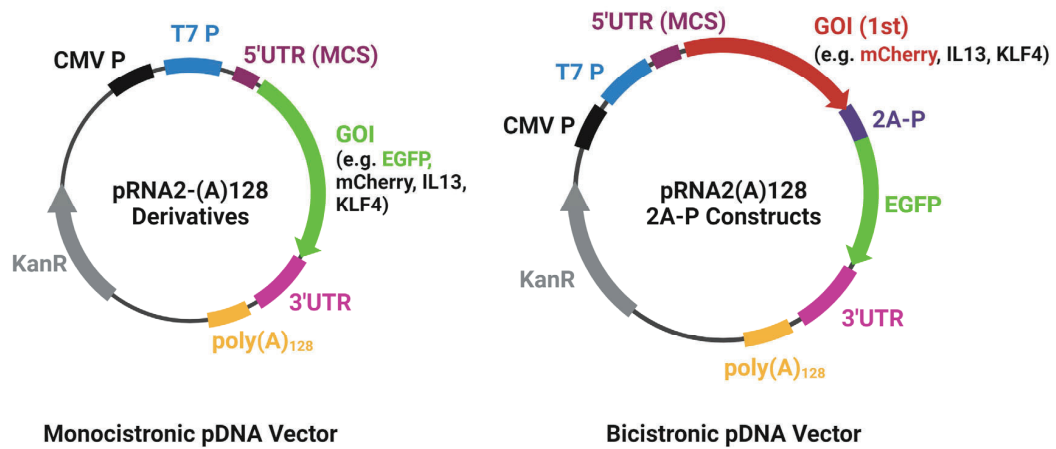
Figure S1. Maps of plasmids used either as template for *in vitro* transcription of mRNA or directly transfected into cells. Both have common features such as a CMV promoter, a T7 promoter, multiple cloning sites (MCS) in the 5'UTR, a head-to-tail duplicated human β-globin 3'-UTR, and a stretch of 128 Adenines, named poly(A)128, to ensure the co-transcriptional addition of a poly(A) tail. Kanamycin resistance was also a common feature in both plasmids used for clonal selection. Monocistronic pDNA vectors encompass one position for the gene of interest, e.g. EGFP, mCherry, KLF4, and IL-13 (left panel), whereas bicistronic pDNA templates consist of two genes in a single open reading frame separated by a 2A peptide sequence (2A-P) [3].
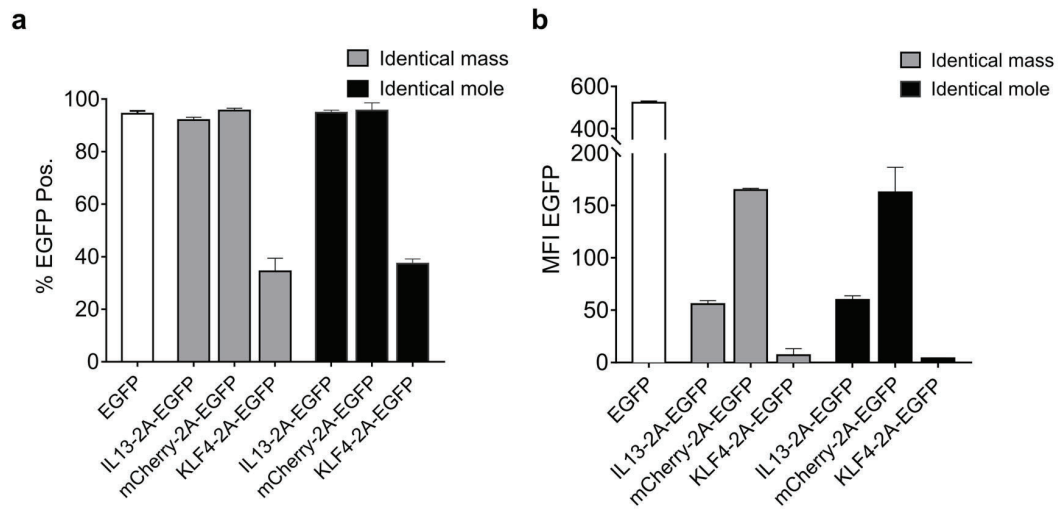
Figures S2. The percentage of EGFP positive population (a) and intensity of EGFP signal (mean fluorescent intensity) (b) reflecting the EGFP expression were quantified using flow cytometric evaluation of cells for transfection of bicistronic 2A constructs, provided in comparison to the results from monocistronic co-transfection according to the figure 2b, and c, respectively.
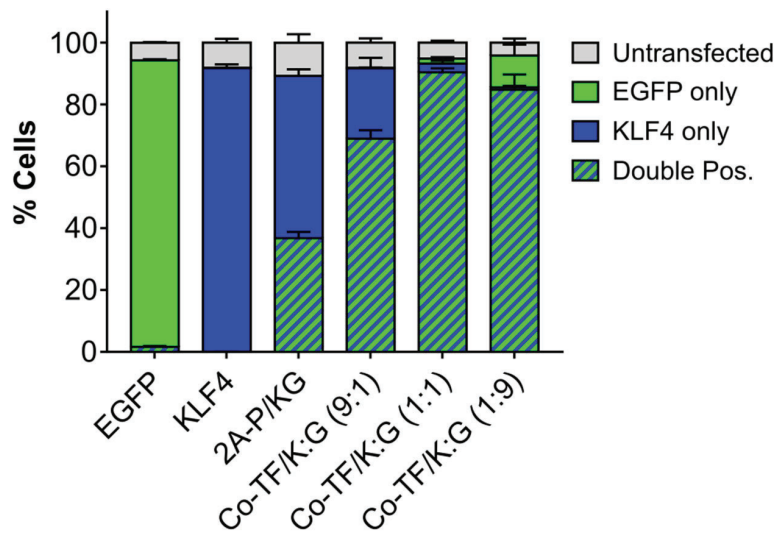
Figure S3. Distribution of transgene expression patterns plotted upon individual transfections, 2A-P, and CoTF of Hela cells with KLF4 and EGFP encoding IVT mRNA by flow cytometric evaluation. Error bars indicate SD for three independently performed experiments.
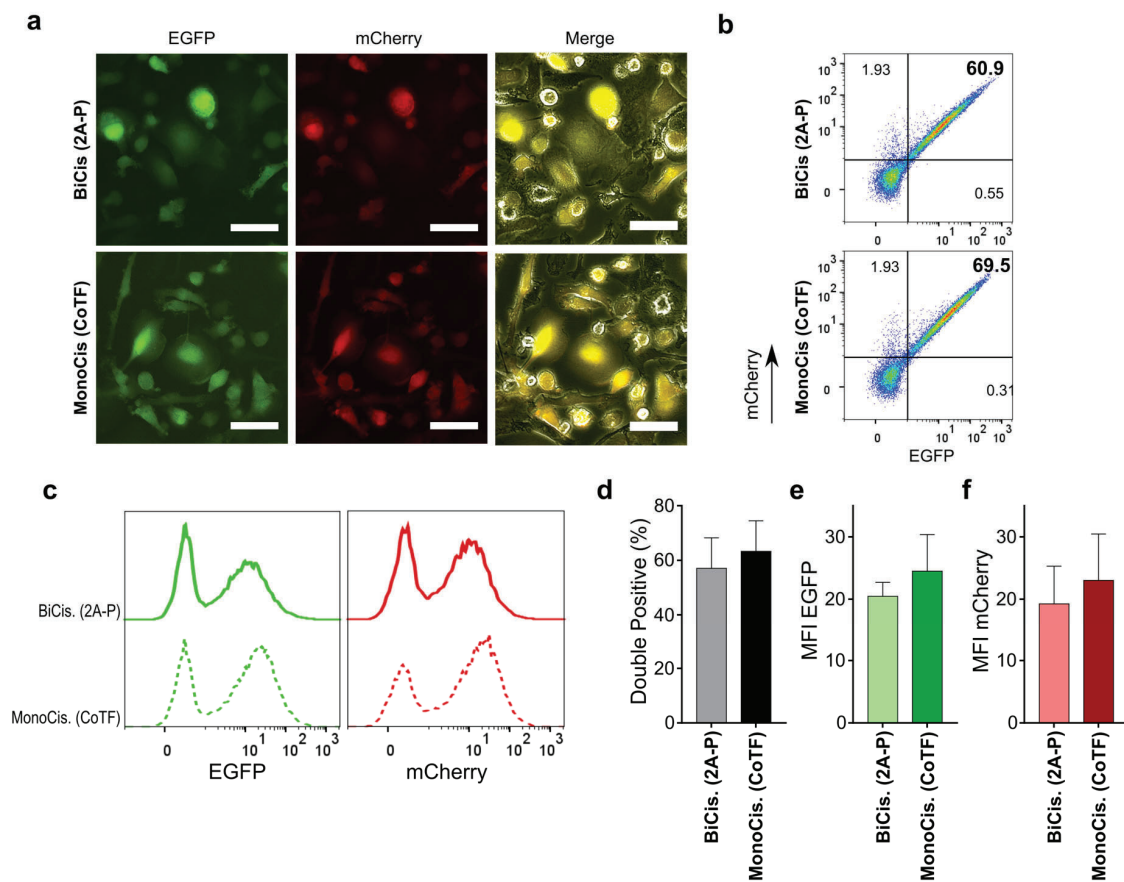
Figure S4. Macrophages transfected with mCherry-2A-EGFP or co-transfected with separate mCherry and EGFP coding IVT-mRNA. (a) Fluorescent images presented in EGFP channel (left panel), mCherry channel (middle panel) as well as merged with phase contrast (right panel). **(b)** Density plots of mCherry-2A-EGFP (upper graph) and mCherry co-transfected with EGFP (lower graph). **(c)** Overlaid histograms of EGFP and mCherry to compare the fluorescence intensity of the transfected cells, solid lines represent the BiCis and dashed lines correlate to MonoCis transfection. **(d)** Percent of double positive cells, **(e)** mean fluorescent intensity (MFI) of EGFP signal and **(f)** mCherry signal are plotted and compared within the two groups; Values are presented as mean ± SD, n≥3, from independent donors each. Numbers indicated within dot plots represent % of cells inside the corresponding gate. Scale bar = 50 μm.

Table S1. The equimass versus equimolar experiment with IVT-mRNA

Payload design	Experiment	Genes	Total mass (ng)	Amont of 1st gene mass (mole)	Amont of 2nd gene (EGFP) mass (mole)
MonoCis (co-transfection)	**Equal mass**	IL13+EGFP	500	**250 ng** (0.873 pmol)	**250 ng** (0.612 pmol)
		mCherry + EGFP	500	**250 ng** (0.6525 pmol)	**250 ng** (0.612 pmol)
		KLF4 + EGFP	500	**250 ng** (0.4135 pmol)	**250 ng** (0.612 pmol)
	Equal mole	IL13+EGFP	636.7	265 ng **(0.925 pmol)**	371.7 ng **(0.925 pmol)**
		mCherry + EGFP	625.7	305.4 ng **(0.797 pmol)**	320.3 ng **(0.797 pmol)**
		KLF4 + EGFP	586.8	352.5 ng **(0.583 pmol)**	234.3 ng **(0.583 pmol)**
BiCis (transfection)	**Identical mole (to standard)**	IL13-2A-EGFP	670.6	1.241 pmol	
		mCherry-2A-EGFP	778.4	1.241 pmol	
		KLF4-2A-EGFP	1064.0	1.241 pmol	
	Identical mass (to standard)	IL13-2A-EGFP	500	**0.925 pmol**	
		mCherry-2A-EGFP	500	**0.797 pmol**	
		KLF4-2A-EGFP	500	**0.583 pmol**	

*The standard transfection condition (reference point): **500ng ≈ 1.241pmol** mRNA per well of 12-well plate.

7

Table S2. The molar amounts of genes, which were used in equimass experiments.

		Gene	Mass amount (ng)	Molecular size (nts/bps)	Molar amount (pmol)
mRNA	MonoCis	IL13 (1st gene)	500	891	1.746
		mCherry (1st gene)	500	1192	1.305
		KLF4 (1st gene)	500	1881	0.827
		EGFP (2nd gene)	500	1250	1.224
	BiCis	IL13-2A-EGFP	1000	1681	1.850
		mCherry-2A-EGFP	1000	1951	1.594
		KLF4-2A-EGFP	1000	2668	1.166
pDNA	MonoCis	IL13 (1st gene)	1000	4821	0.336
		mCherry (1st gene)	1000	5122	0.316
		KLF4 (1st gene)	1000	5811	0.278
		EGFP (2nd gene)	1000	5180	0.312
	BiCis	IL13-2A-EGFP	2000	5611	0.577
		mCherry-2A-EGFP	2000	5881	0.550
		KLF4-2A-EGFP	2000	6598	0.491

8

Reference

1. H. Moradian, T. Roch, A. Lendlein and M. Gossen: mRNA Transfection-Induced Activation of Primary Human Monocytes and Macrophages: Dependence on Carrier System and Nucleotide Modification. *Sci Rep* **10**, 4181 (2020).
2. H. Moradian, A. Lendlein and M. Gossen: Strategies for simultaneous and successive delivery of RNA. *J Mol Med (Berl)* **98**, 1767 (2020).
3. D.J. Williams, H.L. Puhl and S.R. Ikeda: A Simple, Highly Efficient Method for Heterologous Expression in Mammalian Primary Neurons Using Cationic Lipid-mediated mRNA Transfection. *Front Neurosci* **4**, 181 (2010).

Appendix IV

JMolMed

ORIGINAL ARTICLE

Check for updates

Strategies for simultaneous and successive delivery of RNA

Hanieh Moradian[1,2,3] · Andreas Lendlein[1,2,3] · Manfred Gossen[1,2]

Abstract

Advanced non-viral gene delivery experiments often require co-delivery of multiple nucleic acids. Therefore, the availability of reliable and robust co-transfection methods and defined selection criteria for their use in, e.g., expression of multimeric proteins or mixed RNA/DNA delivery is of utmost importance. Here, we investigated different co- and successive transfection approaches, with particular focus on in vitro transcribed messenger RNA (IVT-mRNA). Expression levels and patterns of two fluorescent protein reporters were determined, using different IVT-mRNA doses, carriers, and cell types. Quantitative parameters determining the efficiency of co-delivery were analyzed for IVT-mRNAs premixed before nanocarrier formation (integrated co-transfection) and when simultaneously transfecting cells with separately formed nanocarriers (parallel co-transfection), which resulted in a much higher level of expression heterogeneity for the two reporters. Successive delivery of mRNA revealed a lower transfection efficiency in the second transfection round. All these differences proved to be more pronounced for low mRNA doses. Concurrent delivery of siRNA with mRNA also indicated the highest co-transfection efficiency for integrated method. However, the maximum efficacy was shown for successive delivery, due to the kinetically different peak output for the two discretely operating entities. Our findings provide guidance for selection of the co-delivery method best suited to accommodate experimental requirements, highlighting in particular the nucleic acid dose-response dependence on co-delivery on the single-cell level.

Keywords Integrated co-transfection · Parallel co-transfection · Successive transfection · Co-expression · In vitro synthesized mRNA · Transfection methods

Introduction

Delivery of genes and other functional nucleic acids as a powerful tool for basic research [1–3], in biomedical/therapeutic applications and biotechnology [4–7], has been practiced intensely for decades. Corresponding methods have been constantly advanced [8–11], facilitating efficient cellular delivery of different types of nucleic acids such as plasmid DNA (pDNA), small interfering RNA (siRNA), small hairpin RNA (shRNA), and, more recently, single-guide RNA (sgRNA) as well as in vitro transcribed messenger RNA (IVT-mRNA) [9, 12–15]. For numerous applications, the simultaneous delivery of more than a single nucleic acid is advantageous or even mandatory. This includes co-delivery of multiple nucleic acids of the same type [16], multiple types of nucleic acids [14, 17], and a nucleic acid coordinated with another entity such as drug [18, 19] or protein [20]. Robust reliable co-delivery methods are, therefore, of critical importance in many gene transfer studies. Only few of these studies, however, focused on the applied co-delivery strategies and analyzed their impact on study's outcomes, particularly for IVT-mRNA. Exemplary applications are the parallel transient overexpression of genes when

✉ Manfred Gossen
manfred.gossen@hzg.de

1 Institute of Biomaterial Science, Helmholtz-Zentrum Geesthacht, Kantstr. 55, 14513 Teltow, Germany

2 Berlin-Brandenburg Center for Regenerative Therapies (BCRT), 13353 Berlin, Germany

3 Institute of Biochemistry and Biology, University of Potsdam, 14476 Potsdam, Germany

⌂ Springer

required to analyze a given biological problem or even to realize the functional expression of the desired protein in the first place, e.g., as in the case of antibodies [21]. The coordinated knock-down (e.g., via siRNAs) and overexpression of related proteins are other instances [17, 22]. The co-transfection of traceable markers, mostly genes encoding fluorescent proteins, has been widely used to track, in particular on the single-cell level, the delivery of the gene of interest in a given study, as well as direct monitoring of gene transfer via in vivo imaging set up [23]. Placing two distinct functional entities described in these scenarios on separate vectors provides a level of experimental flexibility, which is difficult to achieve when combining them in a single vector. In some cases, however, the latter would not be possible, as delivery has to be performed at different time points, in order to coordinate peak expression of all transfected entities, which can kinetically vary from one nucleic acid type to the other [14].

Given this necessity for nucleic acid co-delivery in wide range of studies, and to fill this gap of crucial information, in this study, we investigated various strategies for co-delivery of nucleic acids, with a particular focus on IVT-mRNA. The aim of this study was to provide quantitative data to support proper choice of co-transfection methods and of experimental conditions within those methods. In this regard, we have investigated various co-delivery methods for simultaneous transfection, including "integrated co-transfection" (iCoTF) (Fig. 1a), "parallel co-transfection" (pCoTF) (Fig. 1b), as well as "successive transfection" (sTF) (Fig. 1c). The key readout was to determine heterogeneity and distribution of cells co-expressing both marker genes when using these methods in a dose-response manner (Fig. 1d). These studies were initiated in macrophages, which are a prime subject of our current research [24] and subsequently pursued in a cell line that is more readily available for routine transfection when compared with cells that had to be isolated and differentiated from primary human blood cells, at the cost of considerable time, effort, and resources. Co-transfection rates of IVT-mRNA in these cells were systematically investigated for different IVT-mRNA concentrations. In addition, various types of carriers, i.e., lipid- and polymeric-based carrier, were included to compare the different transfection methods. To further evaluate our concept, co-delivery and successive delivery of IVT-mRNA with another entity, i.e., siRNA with completely different properties and action mechanisms, was investigated. The findings of this study provide guidance to select the most effective method, depending on the specific experimental demands by identifying several critical criteria, of both, qualitative and quantitative nature.

Materials and methods

In vitro transcription of mRNA

Synthesis of mRNA coding enhanced green fluorescent protein (EGFP) and mCherry was performed via in vitro transcription, according to a previously published protocol [24]. Briefly, plasmid vectors, pRNA2-(A)$_{128}$ [25], encoding EGFP, and pRNA2-(A)$_{128}$-mCherry [24], both comprising a T7 promoter, 5′-UTR, the coding region for the respective fluorescent protein, head-to-tail duplicated human β-globin 3′-UTR, and followed by a 128-base polyadenine [poly(A)] sequence were linearized and purified by agarose gel electrophoreses using a gel extraction kit (Macherey-Nagel (MN), Germany). mRNAs were subsequently synthesized using a TranscriptAid T7 High Yield Transcription Kit (Thermo Fisher Scientific, Germany) following the manufacturer's instruction. The 5' end of IVT-mRNA was modified co-transcriptionally with anti-reverse cap analog (ARCA) (Jena Bioscience, Germany) [26]. Chemically modified IVT-mRNAs were generated by complete substitution of uridine and cytidine with 100 mM pseudouridine (Jena Bioscience, Germany) and 5-methylcytidine (m5C) (Jena Bioscience, Germany), respectively. IVT-mRNA was purified using lithium chloride precipitation and resuspended in UltraPure™ nuclease-free sterile water (Merck Millipore, Germany) containing 0.1 mM EDTA. The concentration of IVT-synthesized mRNAs was determined using a UV/Vis-spectrometer (NanoDrop 1000 Spectrophotometer; Peqlab, Germany) and further analyzed by denaturing agarose gel electrophoresis for integrity.

### Preparation of primary human monocyte-derived macrophages

Macrophages were derived from primary human monocytes as previously described [24]. Briefly, monocytes were purified from peripheral blood mononuclear cells (PBMC) isolated from buffy coats (Deutsche Rote Kreuz, Berlin; ethics vote EA2/018/16; Charité University Medicine Berlin) by negative selection using the Monocyte Isolation Kit II (Miltenyi Biotec, Germany) according to the manufacturer's instruction. Purified cells were cultured in very low endotoxin (VLE) RPMI 1640 (Biochrom, Germany), supplemented with 10 vol% FBS (Sigma, Germany) and 50 ng mL^{-1} human macrophage colony stimulating factor (M-CSF) (Miltenyi Biotec, Germany) at 37 °C and 5 vol% CO_2 for 6–7 days, with medium changes every third day. At the end of the differentiation period at day 7, the medium was replaced with warm VLE RPMI supplemented only with 10 vol% FBS.

Co-delivery of mRNA to primary human macrophages

Macrophages were transfected using chemically modified IVT-mRNAs in combination with Lipofectamine MessengerMAX (LipoMM; Thermo Fisher Scientific, Germany). Co-delivery was performed as follows:

(a) Integrated co-transfection

Fig. 1 Schematic overview of different transfection methods: integrated co-transfection **a** refers to mixing different IVT-mRNAs prior to complexation with carrier, whereas in parallel co-transfections **b**, IVT-mRNAs are complexed in particles and added to cells separately, and in successive transfections **c**, cells are transfected with two types of IVT-mRNA with a 24-h interval. **d** Cellular uptake of different ratios of the two types of mRNA (vertical axis) and of different doses of both IVT-mRNAs (horizontal axis) results in different color distribution and intensity and can be used as a key readout for this study
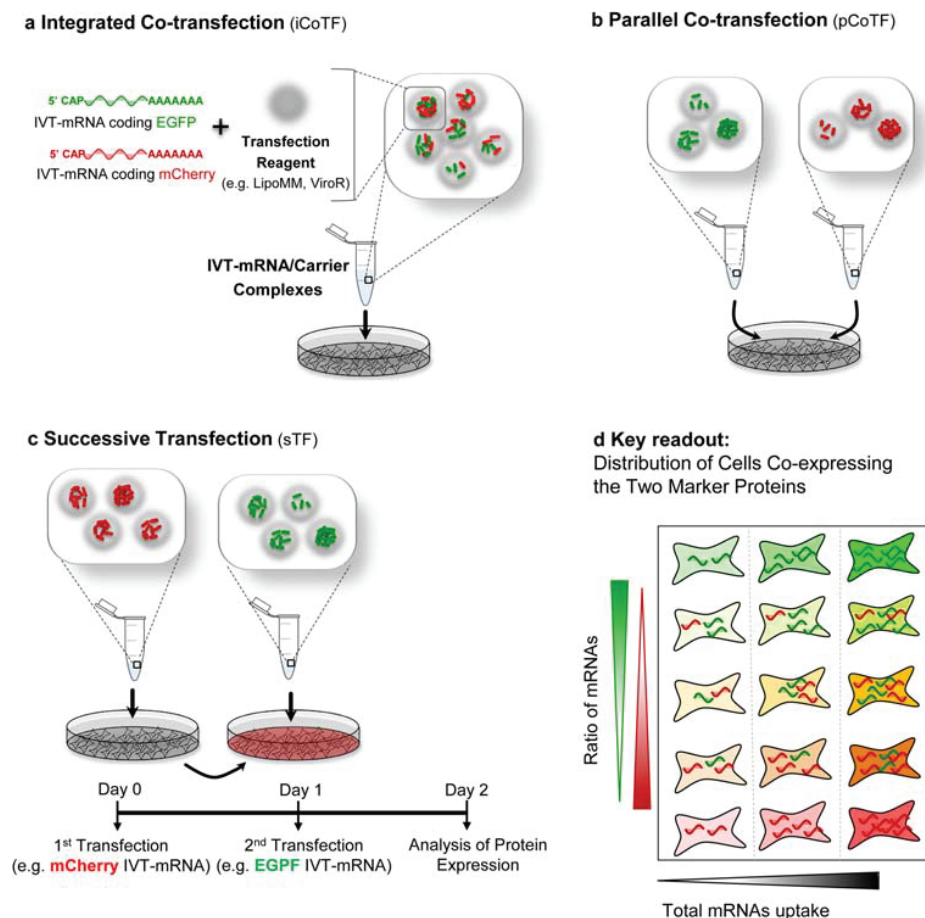
MessengerMAX reagent was diluted in Opti-MEM medium (Gibco, Germany) at 1:50 volume ratio and incubated for 10 min at RT. The resulting solution was added to the equal volume of premixed EGFP and mCherry mRNAs diluted in Opti-MEM medium to a final mRNA concentration of 4 ng μL^{-1} (Fig. 1a).

b   Parallel co-transfection

The diluted MessengerMAX reagent was divided in two equal parts, each was separately added to the equal volume of either EGFP or mCherry mRNA solutions (Fig. 1b). The LipoMM-mRNA mixtures were briefly vortexed and incubated for 5 min at RT for complex formation. Respective volumes of the co-transfection mixtures were transferred to each well to deliver the final mRNA concentrations equal to 12.5, 40, 125, and 250 ng mL^{-1} in cell culture medium. Cells were analyzed for fluorescent protein expression 24 h after transfection. Viability of cells was evaluated via 4′,6-diamidine-2′-phenylindole dihydrochloride (DAPI) staining, and quantified via flow cytometry, considering DAPI-negative cells as live cells. For the transfection conditions, chosen viability was above 95% throughout.

Macrophages transfected with mRNA only or carrier only did not show any discernible fluorescent signal nor a reduction in viability, as previously shown by us [24].

In both conditions, cells were transfected in 6-well plate format, with a density of 2.00E + 06 cells per well in 2 mL complete RPMI medium.

Co-delivery of mRNA to HeLa cells via a lipid- or a polymeric-based carrier

HeLa (ATCC; CCl-2) cells were seeded at a density of 3.00E + 05 cells per well in 6-well plates, in high glucose DMEM, supplemented with GlutaMAX™, pyruvate (Gibco, Germany), 10 vol% FBS (Biochrom, Germany), and 1 U mL^{-1} penicillin-streptomycin (Gibco, Germany), 24 h before transfection. LipoMM-mRNA co-transfection mixtures (both for iCoTF and pCoTF) were prepared exactly as described in the previous section; see "Co-delivery of mRNA to primary human macrophages" aside from using non-modified mRNAs.

A polymeric-based transfection reagent was also investigated by using Viromer RED (ViroR; Lipocalyx, Germany).

To prepare ViroR-mRNA complexes for iCoTF, equal amounts of EGFP and mCherry non-modified mRNAs were diluted in 318 μL of the provided ViroR buffer at final concentration of 11 ng μL^{-1}. In another tube, 1.25 μL of Viromer® reagent was placed on the tubes' wall and immediately mixed with 30 μL of the dilution buffer and vortexed for 5 s. The buffer containing premixed IVT-mRNAs was then added to the diluted Viromer® solution, mixed swiftly, and incubated for 15 min at RT. In parallel, two individually prepared mRNA solutions of EGFP or mCherry in 160 μL dilution buffer were separately mixed with 15 μL of diluted ViroR for pCoTF.

Corresponding volumes of the co-transfection mixture were transferred to each well of 24-well plate to deliver final IVT-mRNA concentration of 660, 330, 110, and 33 ng mL^{-1} in 500 μL culture medium, for both lipid-based and polymeric-based transfection reagents. Cells were further evaluated by fluorescent microscopy and flow cytometry 24 h after transfection.

To evaluate HeLa cell viability, cells were seeded in 96-well plate at a density of 1.40E + 04 cells per well, 24 h prior to transfection. Subsequently, transfection was performed with either the highest, i.e., 660 ng mL^{-1} or the lowest, i.e., 33 ng mL^{-1}, concentrations of mRNA in 100 μL medium per well. Mock transfection was done by addition of carrier only to the corresponding wells. The viability assay was performed 24 h upon cell transfection using Cell Titer® 96 AQ$_{ueous}$ Non-Radioactive MTS Assay (Promega, Germany), according to manufacturer's instruction. Briefly, 20 μL of MTS mixture (MTS solution mixed with PMS solution at ratio of 20:1) was added to each well and incubated for 3 h at 37 °C. Cells were treated with 100 μL of 1 mM CuCl$_2$ as positive control, i.e., maximum cell death. The plates were protected from light at all steps. Absorbance was measured at wavelength of 490 nm using a SpectraMax M5 microplate reader (Molecular Devices, San Jose, CA).

Co-delivery of plasmid DNA (pDNA) in HeLa cells

Plasmids were transfected using a transfection grade 25 kDa linear polyethylenimine (PEI) (Polyscience, Warrington, PA). To prepare the co-transfection mixture, PEI was dissolved in 150 mM NaCl solution to a final concentration of 2.4 mM. The diluted PEI solution was either added entirely to the equal volume of premixed pDNA solution in 150 mM NaCl (40 ng μL^{-1}) for iCoTF or splitted and mixed separately with each of the two pDNAs, for pCoTF. The resulting mixture was vortexed for 30 s and incubated for 10 min at RT for complex formation. HeLa cells, pre-seeded 24 h before transfection at a density of 2.50E + 05 cells per well of 6-well plates in 2 mL culture medium, were transfected with 1320, 660, 220, and 66 ng μL^{-1} of pDNAs and analyzed for gene expression 48 h after transfection.

Successive delivery of IVT-mRNA

HeLa cells were seeded at a density of 8.00E + 04 cells per well of 12-well plates in 1 mL culture medium, 24 h before first transfection. Non-modified IVT-mRNA coding mCherry was initially transfected via LipoMM in various doses (660, 330, 110, 33 ng μL^{-1}), according to previously described protocol at day 0; see "Co-delivery of mRNA to primary human macrophages" section. Cells were transfected for the second time with identical doses of mRNA coding EGFP at day 1. Cells were evaluated for fluorescent protein expression at day 2.

Co-delivery versus successive delivery of siRNA and IVT-mRNA

HeLa cells stably expressing a destabilized EGFP in a homogenous fashion [27] were seeded at a density of 3.00E + 04 cells per well of 24-well plates, in 500 μL complete DMEM medium (10 vol% FBS, no antibiotics), 24 h before transfection. Co-transfection conditions for simultaneous or successive delivery of siRNA and non-modified IVT-mRNA are outlined in Fig. 2. The preparation procedure is described as follows. To prepare iCoTF mixture, LipoMM reagent was diluted in Opti-MEM medium at 1:50 volume ratio and incubated for 10 min at RT. A premixed solution of IVT-mRNA coding mCherry (200 ng) and 20 pmol Stealth™ RNAi EGFP reporter control (Invitrogen, Germany) in Opti-MEM medium was added to the diluted LipoMM solution at 1:1 volume ratio, mixed well, and incubated for 5 min at RT for complex formation. Similarly prepared LipoMM solution was added separately to each of IVT-mRNA or Stealth™ RNAi solutions for pCoTF. Lipofectamine 2000 (Lipo2000; Thermo Fisher Scientific, Germany) was exclusively used for Stealth™ RNAi delivery in pCoTF-SR as well as all successive transfections, according to manufacturer's protocol; see Fig. 2. Briefly, Lipo2000 was diluted at 1:50 volume ratio in Opti-MEM medium and incubated for 5 min at RT. Twenty picomole of Stealth™ RNAi EGFP reporter control or the negative control was diluted in equal volume of Opti-MEM medium, mixed with Lipo2000 solution, and incubated for 20 min at RT for complex formation. A single transfection mixture of LipoMM-IVT-mRNA coding mCherry was prepared as outlined above and added either simultaneous with Lipo2000-siRNA mixture at day 0 or upon siRNA transfection at days 1 and 2 for pCoTF-SR, sTF-d1, and sTF-d2, respectively. Medium was changed 4 h after transfection for all conditions.

Evaluation of transfection efficiency by fluorescent microscopy

To evaluate the fluorescent proteins (EGFP and mCherry) expression, cells were imaged via a Nikon inverted microscope ELIPSE Ti-U equipped with long-life mercury light source, Intensilight C-HGFI, with single-band filter sets,

Conditions selected for transfection			Experiments performed for each condition			
Annotation	Transfection Reagent		Day 0	Day 1	Day 2	Day 3
	mRNA	siRNA				
Negative Control	-	Lipo2000	Transfection with Neg. control siRNA*	FCA	FCA	FCA
Integrated Co-transfection (iCoTF)	LipoMM	LipoMM	Transfection with a pre-mixture of mRNA and siRNA*	FCA	FCA	FCA
Parallel Co-transfection (pCoTF)	LipoMM	LipoMM	Transfection with mRNA and siRNA separately*	FCA	FCA	FCA
Parallel Co-transfection- Separate reagents (pCoTF-SR)	LipoMM	Lipo2000	Transfection with mRNA and siRNA separately*	FCA	FCA	FCA
Successive Transfection Day 1 (sTF-d1)	LipoMM	Lipo2000	Transfection with siRNA only*	Transfection with mRNA*	FCA	FCA
Successive Transfection Day 2 (sTF-d2)	LipoMM	Lipo2000	Transfection with siRNA only*	-	Transfection with mRNA*	FCA

* Medium was changed 4 hours after transfection.

Fig. 2 Design of experiments and description of transfection conditions for co-delivery of IVT-mRNA and siRNA; (FCA, flow cytometry analysis; LipoMM, Lipofectamine MessengerMax; Lipo2000, Lipofectamine 2000)

Semrock filter GFP-BP (466/40, 525/50 nm) for green fluorescence, or Semrock filter TRITC (562/40, 641/75 nm) for red fluorescence (mCherry) observations. The NIS-Elements imaging software package (version 4.51) and Image J software were utilized to analyze microscopic images.

Quantitative analysis of transfection efficiency by flow cytometry

Cells were harvested at previously specified time points by TrypLE Select (Gibco, Germany) according to manufacturer's instruction. Upon washing with cold flow cytometry washing solution (PBS pH 7.2, BSA, EDTA), cells were analyzed with a MACSQuant VYB® flow cytometer (Miltenyi Biotec, Germany). All flow cytometric data were analyzed with FlowJo software V10.

Statistics

Data are presented as means ± standard deviation (SD) of at least three independent experiments. Multiple comparison t test was performed via a GraphPad Prism 7.00 (La Jolla, CA 92037, USA). Statistical significance (alpha) was defined as 0.05.

Results

Co-delivery of IVT-mRNA in primary human monocyte-derived macrophages

Two different methods were investigated for IVT-mRNA delivery in monocyte-derived primary human macrophages. For

iCoTF, lipoplexes were prepared by premixing of EGFP and mCherry IVT-mRNAs before adding to the transfection reagent, whereas for pCoTF, the independently formed complexes were added to the same well (Fig. 1a, b). To evaluate the co-transfection efficiency for each method in dependence of the delivered mRNA doses, percentage of double-positive cells and intensity of reporter genes expression were recorded via fluorescent microscopy and quantified via flow cytometry.

There was an obvious difference in transfection patterns in macrophages transfected with two co-delivery methods even for high mRNA dose (125 ng mL^{-1}) as shown in Fig. 3a. The difference was also remarkable on single-cell level, presented as density plots in Fig. 3b, with iCoTF resulting in almost all of the transfected cells equally expressing both marker genes at the same level. In contrast, pCoTF results in heterogeneous population of cells expressing different levels of each reporter gene, observed as different color spectrum in merged fluorescent image (Fig. 3a) and the wide distribution of cells within double-positive gate (Fig. 3b). pCoTF also resulted in slightly higher level of fluorescent protein expression compared with iCoTF, measured via mean fluorescent intensity (MFI) of the peak on the adjacent histograms. Decreasing mRNA doses, however, drastically reduced the rates of the double-positive cells transfected with pCoTF method (ca. 50-fold) and compared with a moderate decrease (ca. 7-fold) with iCoTF (Fig. 3c).

IVT-mRNA Co-delivery methods: cell type and carrier dependence

The results obtained for macrophages in the course of ongoing studies [24] were repeated in HeLa cells to analyze whether or

Fig. 3 Simultaneous transfection of macrophages with EGFP and mCherry coding IVT-mRNA with two different strategies. Fluorescent microscopy images (bar = 50 μm) **a** and flow cytometric density plots **b** depicting the fraction of double-positive cells in integrated versus parallel co-transfected macrophages for an mRNA dose of 125 ng mL^{-1}. Analogous measurements were performed for cells transfected with various mRNA doses **c**. All experiments were performed using a liposomal carrier (LipoMM); multiple comparison t test revealed significant difference between iCoTF and pCoTF for all evaluated mRNA doses ($p <$ 0.05). No fluorescent signal-/double-positive event was observed for untransfected macrophages. Values are presented as mean ± SD, $n \geq 3$. Error bars indicate SD. (iCoTF, integrated co-transfection; pCoTF, parallel co-transfection)
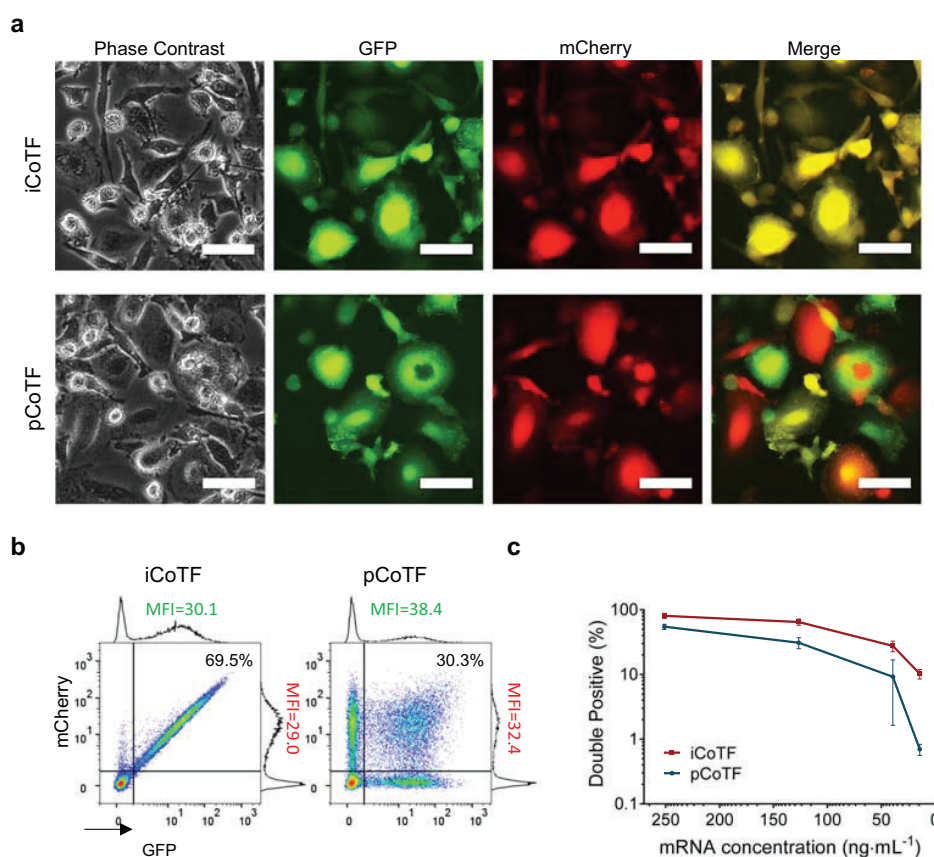
not the initial observations for the co-transfection experiments were limited to a specific cell type and also were extended by testing different carrier types. To this end, different doses of IVT-mRNAs coding mCherry and EGFP were co-transfected in HeLa cells using an example of a liposomal (LipoMM) and a polymeric (ViroR) gene carrier in side-by-side experiments. The encapsulation efficiency of each carrier system was evaluated for different carrier to mRNA ratios, as explained in "Supplementary Methods." The ratios carrier/mRNA used throughout the experiments shown revealed more than 95% encapsulation efficiency for LipoMM and more than 87% for ViroR, both of which confirms the successful entrapment of mRNA within carrier (Supplementary Fig. 1). Moreover, the physicochemical properties, i.e., size and zeta potential measurement of particles prepared with different types of mRNA (EGFP and mCherry), were measured (Supplementary Table 1). Comparison of different particles revealed no significant differences between carrier complexes prepared with different types of mRNA both for LipoMM and ViroR.

The fluorescent images showed that regardless of the type of carrier, iCoTF always resulted in higher percentage of cells expressing both EGFP and mCherry. Noteworthy, the overall expression levels were higher in LipoMM than for ViroR for both fluorescent proteins, as depicted in Fig. 4a, b.

Evaluation of the co-delivery rates at single-cell level by flow cytometry indicated the similar diagonal pattern for iCoTF and a rather wide distribution within double-positive cells for pCoTF mediated by both LipoMM and ViroR. The direct comparison of these two strategies revealed that the rates of double-positive cells are higher for integrated than for parallel co-transfection (Fig. 4c, d), particularly notable when lower doses of mRNA were transfected (Fig. 4e, f). There are no indications that these effects are either cell type or carrier dependent.

Cell viability measurement was performed using MTS assay. There was no significant difference between viability of cells transfected with iCoTF and pCoTF methods at the lowest and highest concentration of mRNA. Besides, mock transfection, i.e., cells transfected with transfection reagents only, and mRNA only had no significant impact on cell viability (Supplementary Fig. 2).

For comparison, HeLa cells were also transfected with the template plasmids used in IVT. This is possible as both fluorescent protein encoding plasmids contain a strong CMV promoter, allowing DNA-directed transgene expression. Linear PEI was chosen as a well-established carrier for pDNA transfection. As shown in Fig. 5, comparative analysis of the two co-delivery strategies for pDNA resulted in transfection patterns similar to those observed for IVT-mRNA.

Fig. 4 Comparison of IVT-mRNA co-delivery using liposomal and polymeric carriers in HeLa cells. Fluorescent microscopy images of HeLa cells co-transfected with non-modified IVT-mRNA coding mCherry and EGFP (330 ng mL^{-1}) with LipoMM **a** and ViroR **b** (bar = 100 μm). Density plots of integrated versus parallel co-transfection for high mRNA doses (330 ng mL^{-1}; upper panels) and low mRNA doses (33 ng mL^{-1}; lower panels) for HeLa cells transfected with LipoMM **c** and ViroR **d**. Percent of double-positive cells plotted against descending mRNA concentrations compared within two various co-transfection approaches both for LipoMM **e** and ViroR **f**. Multiple comparison t test revealed significant difference between iCoTF and pCoTF for all evaluated mRNA doses for both LipoMM and ViroR ($p <$ 0.05). No fluorescent signal-/ double-positive event was observed for untransfected and mock-transfected HeLa cells, i.e., cells treated with carrier only, as well as mRNA only. Values are presented as mean ± SD, $n \geq 3$. Error bars indicate SD. (iCoTF, integrated co-transfection; pCoTF, parallel co-transfection)
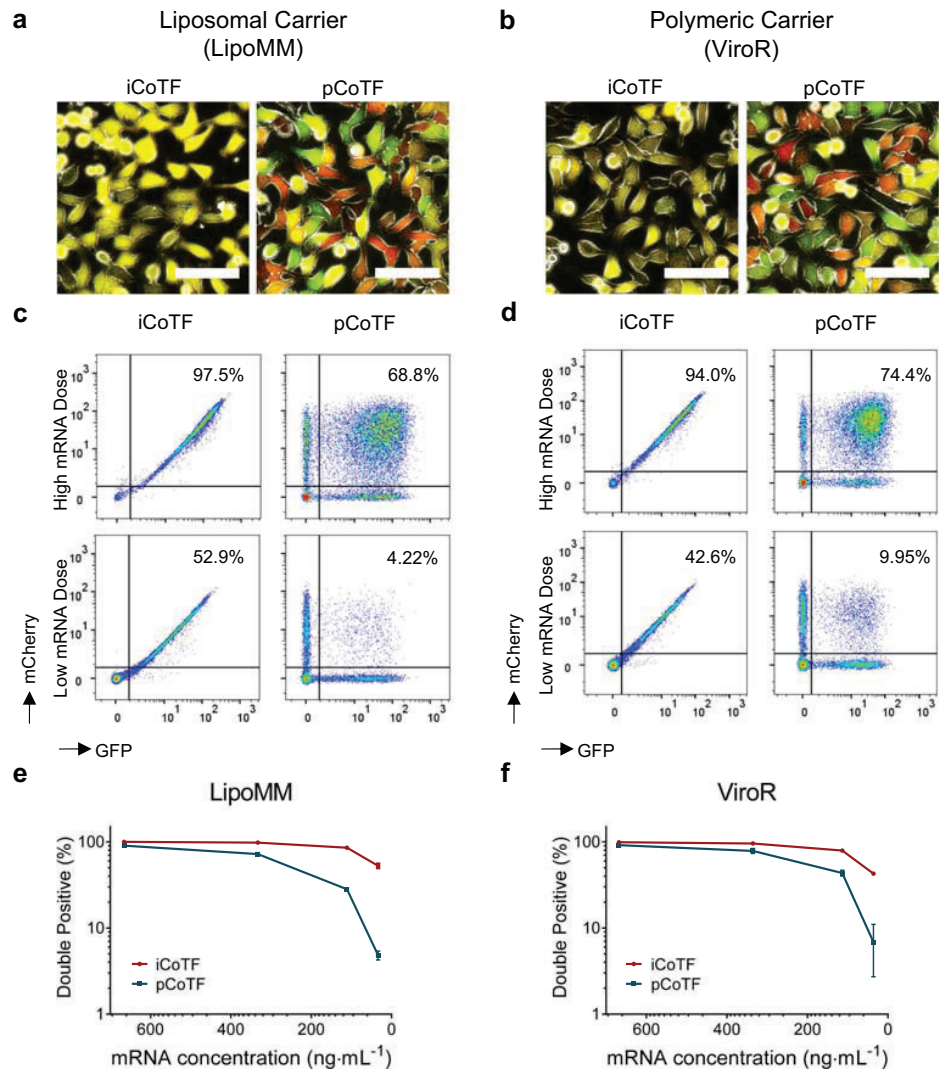
Successive delivery of IVT-mRNA

In order to create and investigate a model for successive transfection of IVT-mRNA, HeLa cells were transfected in separate steps as depicted in Fig. 1c. There was a clear difference in both transfection efficiency and fluorescent protein intensity between the first and the second transfection, which resulted in a remarkable heterogeneity in expression patterns of the two transgenes, particularly noticeable in merged fluorescent image (Fig. 6a). Interestingly, the overall ratio of double-positive to single-positive cells was very similar to what was observed earlier for parallel co-transfection; however, the ratio of the two single-positive cell populations was substantially different, when analyzed via flow cytometric density plots (compare Figs. 4c to 6b).

Despite the high transfection rates for mCherry (95 ± 1.2%), the first fluorescent protein, only 81.4 ± 4.1% of cells were positive for the EGFP reporter transfected second (Fig. 6b, c). Interestingly, those cells not transfected in the 1st round appeared to be more resistant to the 2nd round of transfection when compared with those already successfully transfected. Both effects in combination resulted in the example given in Fig. 6b in about 6-fold more mCherry+/EGFP- cells when compared with cells only positive for EGFP; for overall quantification, see also Fig. 6d. At decreasing doses of IVT-mRNA, this effect was even more pronounced due to the increased percentage of 1st round-negative cells. A quantitative evaluation is also provided in Table 1. The same IVT-mRNAs (identical batches) were also transfected in control experiments in a reverse order, i.e., EGFP first and subsequently mCherry. This allowed us to rule out that the observed bias resulted from quality differences in the IVT-mRNA preparations. Results are shown in Supplementary Fig. 3, underpinning that the order of transfection is decisive.
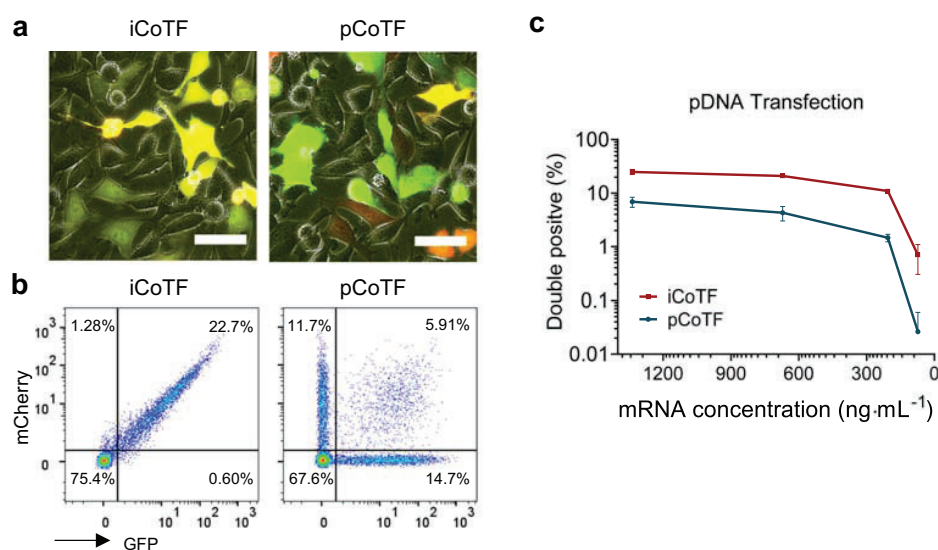
🖄 Springer

Fig. 5 Comparison of integrated and parallel co-transfection approaches for pDNA delivery in HeLa cells using PEI; fluorescence microscopy images illustrating EGFP and mCherry channel merged with phase contrast (bar =50 μm) **a**, flow cytometric density plots **b**, and percent of double-positive cells plotted against descending pDNA concentrations **c**; multiple comparison t test revealed significant difference between iCoTF and pCoTF for all evaluated pDNA doses ($p < 0.05$). No fluorescent signal-/double-positive event was observed for untransfected HeLa cells. Values are presented as mean $\pm$ SD, $n \geq 3$. Error bars indicate SD. (iCoTF, integrated co-transfection, pCoTF, parallel co-transfection)

Co-delivery versus successive delivery of siRNA and IVT-mRNA

The co-delivery of distinct types of nucleic acids, here siRNA and mRNA, was exemplary evaluated for the different transfection strategies described here, using fluorescent proteins as proxy readouts. A cell line stable expressing EGFP with nearly 100% expression penetrance [27] was transfected simultaneously with a siRNA knocking down the endogenous fluorescent EGFP and introducing a mCherry IVT-mRNA as a transfection marker.

Various strategies for simultaneous or successive delivery of siRNA and IVT-mRNA were studied and compared in side-by-side experiments. The goal was not only to achieve the highest percent of cells transfected with both siRNA and mRNA but also to achieve respective maximum efficiencies. This is of particular importance due to the kinetically different highest effectiveness of these two distinct entities, i.e., about 24 h for mRNA expression versus 60–72 h for siRNA knockdown. Therefore, three strategies, namely, "integrated co-transfection," "parallel co-transfection," and "parallel co-transfection-SR" were selected for simultaneous delivery. Both RNAs were transfected with LipoMM in the first two methods, whereas in the third approach, mRNA was transfected with LipoMM and siRNA with Lipo2000. In parallel, "successive transfection-d1"and "successive transfection-d2" were done, in which mRNA was transfected 1 day or 2 days after siRNA transfection, respectively (Fig. 2).

A substantial difference was observed in mCherry expression level at day 3, when different co-delivery methods were compared. Precisely, the maximum level of mCherry expression in transfected cells when analyzed microscopically was correlated to sTF-d1 and sTF-d2. There were few EGFP+ cells in parallel and successive transfected cells (Supplementary Fig. 4). iCoTF and sTF-d1 resulted in the highest percent of EGFP⁻mCherry⁺ cells' population (Fig. 7a, c). When investigated over the course of 3 days, the same pattern was observed consistently for different groups compared in terms of mCherry⁺ versus EGFP⁺ within each day (Fig. 7b). However, the highest EGFP knock-down was detected for sTF-d1 and iCoTF with the smallest EGFP-positive population (Fig. 7c) as well as the lowest EGFP intensity (Fig. 7d).

The kinetics of EGFP knock-down was tracked over 3 days indicating a minimal EGFP intensity over days 2 and 3 (Fig. 7d). Nevertheless, a slight increase was noticeable at day 3, when compared with histograms of the same samples at day 2 (Fig. 7d, left panel). Within each day, the lowest EGFP expression was correlated to the iCoTF and the sTF-d1 among all samples (Fig. 7d).

The kinetic study of mCherry over 3 days was depicted either as mean fluorescent intensity (MFI) of mCherry plots or as histograms (Fig. 7d, right panel). At day 1, the maximum mCherry intensity was observed for pCoTF and pCoTF-SR but not iCoTF. The same pattern of the highest mCherry intensity for pCoTF was also observed at day 2 and interestingly for sTF-d1 and sTF-d2 at day 3 (Fig. 7d, middle panel). As expected, the correlation between two transgenes at single-cell level decreased drastically for sTF-d2 (Fig. 7). Overall, the results of this experiment for co-delivery of two distinct entities such as siRNA and IVT-mRNA demonstrate that there is
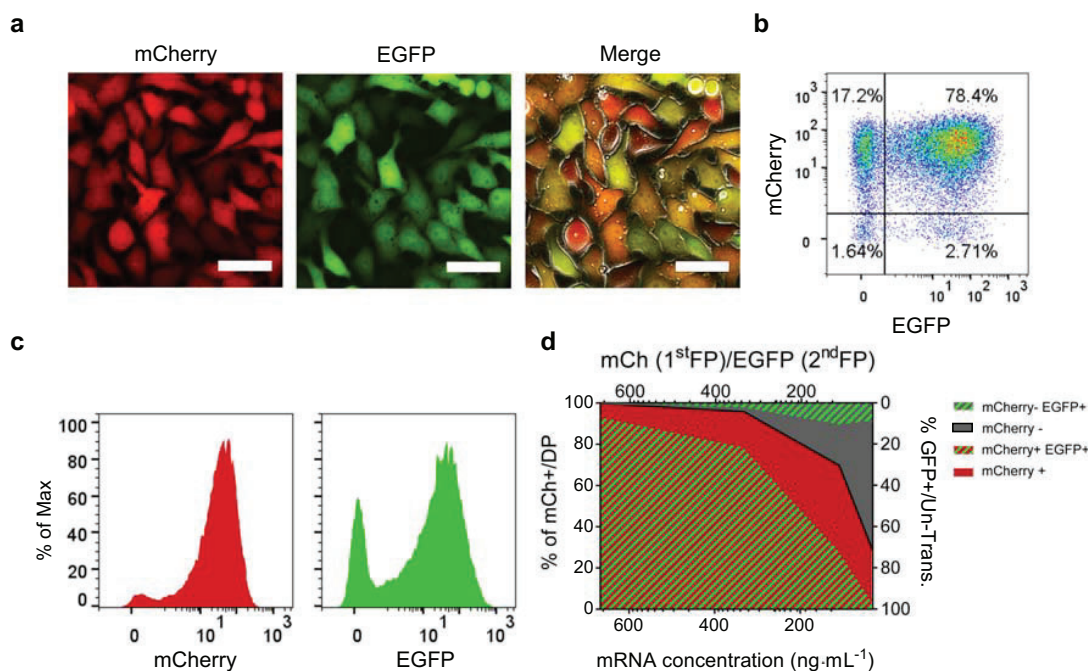
Fig. 6 Successive transfection of IVT-mRNA in HeLa cells with LipoMM; fluorescent images depicted as single fluorescence channels (left, middle), as well as merged with phase contrast in the right panel (bar =50 μm) **a**, flow cytometric analysis of cells via density plots **b**, and histograms of mCherry and EGFP **c**; summary of different populations' frequencies plotted for cells which were sequentially transfected with various mRNA doses **d**; no fluorescent signal was observed for untransfected and mock-transfected (carrier only) HeLa cells. Values are presented as mean, $n \geq 3$

no superior approach per se, but decisions on the transfection strategy have to be made according to the specific experimental demands. For instance, if co-transfection efficiency for both entities is the main interest, iCoTF is recommended. In contrast, when the reasonable rates of knock-down concurrent with the highest overexpression level (intensity) are primarily desired, here, sTF-d2 is the method of choice.

Discussion

Comparison of integrated versus parallel co-transfection methods for simultaneous co-delivery of IVT-mRNA coding for spectrally distinct fluorescent proteins was investigated. Our findings show remarkable differences in rates of co-transfected cells and the level of reporter gene expression between the two methods. Specifically, integrated co-transfection of mRNA resulted in almost identical expression levels of the two proteins in a given transfected cell, whereas parallel co-transfection led to heterogeneous population of cells in terms of transgene expression even within double-positive cells population. This effect was strongly dose dependent; in other words, the differences between these approaches were more pronounced for low mRNA doses. Thus, integrated co-transfection could be the method of choice, especially when low amounts of nucleic acid are required, or as suggested by Xie et al., in case of restricted transfection efficiency [28]. Besides, they reported that only the integrated and parallel co-transfection methods significantly affected the results,

Table 1 Quantitative evaluation of IVT-mRNA transfection

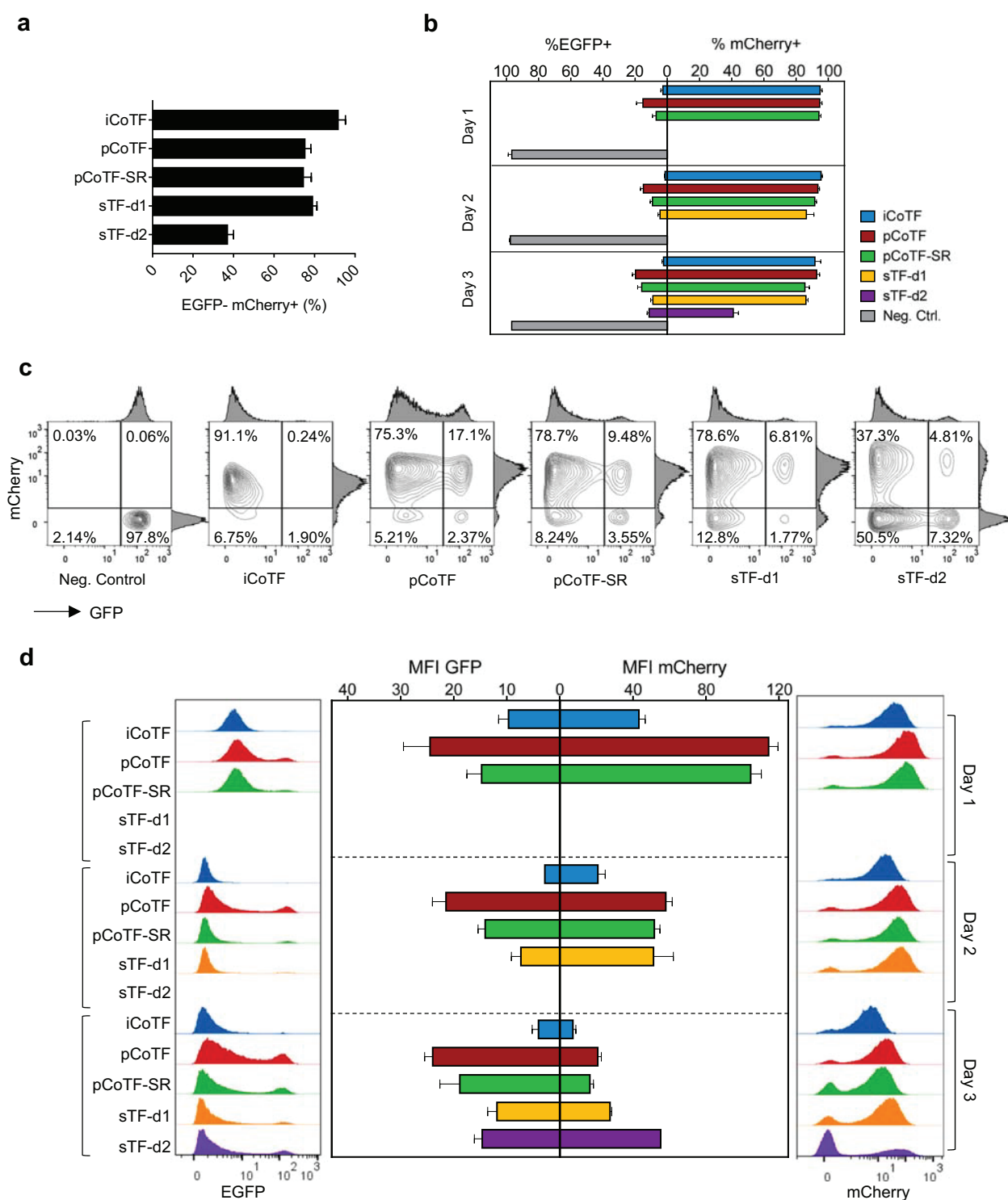| mRNA concentration (ng mL^{-1})	1st transfection	2nd transfection		
	% mCherry+ (of total cells)	% EGFP+ (of total cells)	% EGFP+ within mCherry+	% EGFP+ within mCherry-
660	99.8 ± 0.1	93.6 ± 2.3	93.8 ± 2.2	Not reported
330	95.7 ± 1.2	81.4 ± 4.1	82.3 ± 3.9	61.0 ± 2.5
110	69.7 ± 0.5	39.9 ± 6.1	41.8 ± 6.2	35.4 ± 6.2
33	28.4 ± 1.1	13.4 ± 0.5	15.4 ± 0.7	12.5 ± 0.8

Fig. 7 Co-delivery versus successive delivery of siRNA and IVT-mRNA in d2EGFP HeLa cells transfected with different conditions (see Fig. 2 for more detailed information) evaluated by flow cytometry; **a** percent of EGFP⁻mCherry⁺ cells plotted for comparison within different groups, **b** kinetic of mCherry expression (percent of mCherry⁺ cells) as well as EGFP knock-down (reduction in percent of EGFP+ cells) for different conditions over 3 days, **c** density plots along with adjacent histograms of cells at day 3, **d** kinetic of EGFP knock-down level depicted as EGFP mean fluorescent intensity (MFI) in parallel with mCherry expression level (MFI calculated for mCherry⁺ cells) indicated for different methods over 3 days (middle panel) shown side by side with EGFP (left panel) and mCherry (right panel) histograms; values are presented as mean $\pm$ SD, $n \geq$ 3. Error bars indicate SD

but not the other process parameters such as cell density and ratio between two transgenes [28].

Explanations for the striking differences between iCoTF and pCoTF in their ability to mediate a high proportion of cells simultaneously taking up two (or more) distinct nucleic acids as observed by us and others [2, 28–30] can be readily explained by considering either the number of cargo-loaded nanoparticles taken up by a given cell or the number of nucleic acid molecules per carrier unit. For the latter, high numbers of nucleic acid molecules per nanoparticle are expected to attenuate the expression heterogeneity when simultaneously delivering, e.g., two distinct nucleic acids. Provided that these are loaded on the carrier in the same efficiency, a high number of nucleic acids delivered per particle virtually ensure that even with a low number of particles taken up by the cell, both nucleic acid species would be present. It should be noted here that the decisive numbers in quantifying any such effect are not the numbers of nucleic acids per particle as measured directly in analytical settings but rather the number of those nucleic acids functionally delivered in the cell. In this respect, mRNAs should be a preferred model of research, as compared with pDNA as they do not have to overcome the barrier of the nuclear membrane and would be functionally available directly in the cytoplasm, minimizing the number of unknowns in such calculations. A similar consideration applies for the number of carriers taken up per cell; high numbers are expected to attenuate heterogeneity, also in the case of pCoTF. In order to provide an exemplary idea about the absolute numbers involved, one can reasonably estimate the number of mRNA molecules per cell based on the average number of 350 IVT-mRNA molecules per lipoplex particle, given by Leonhardt and colleagues, and considering the number of particles which is taken up by each cell. Using advanced microscopic methods, a maximum of 15 lipoplex particles were observed in each transfected cell for a relatively high dose of mRNA (1 μg mL^{-1}) [31]. These numbers have successfully been used to model especially kinetic aspects of mRNA delivery, from carrier uptake to protein expression [31–34].

The observed difference in expression heterogeneity between the iCoTF and pCoTF strategy was independent of the carrier system used, i.e. lipoplex or polyplex. However, given their diverging—and still controversial—intracellular trafficking routes and cargo release mechanisms [29, 35, 36], there might be ways to tailor carriers to accommodate task for co-delivery in a more directional manner, e.g., for polymeric carriers by controlling their size and cargo density [35–37].

The notable heterogeneity of co-transfected cells limits the utility of parallel co-transfection method in addressing scientific or technological questions, where the co-expression of two proteins (or regulatory RNA) in the same cell is mandatory. For other applications, though, such a heterogeneity is instrumental and can be exploited accordingly. One elegant example is the recent application of the simultaneous transfection of multiple plasmids, analogous to our parallel co-transfection, referred to as "poly-transfection method" by Gam and colleagues [30]. In their study, the resulting heterogeneity in the expression of transfected genes was analyzed on the single-cell level for the fast and efficient characterization and optimization of synthetic genetic systems and circuits [38–40]. Functional relevance of the integrated co-transfection method has been addressed in a study by Mendia et al., suggesting the highest cartilage matrix deposition secreted by integrated co-transfected human chondrocytes expressing both IGF-I and SOX9 [41].

For several applications, delivery of two nucleic acids to the same cells has to be successive over time. Examples are experimental settings, where expression of the first nucleic acid is prerequisite for the proper and/or effective function of the second nucleic acid. To mimic such a scenario, the successive delivery of mRNA coding mCherry followed by mRNA coding EGFP was evaluated. Results indicated that overall transfection efficiency was lower for the second than for the first transfection. A closer analysis of the fluorescent patterns revealed that the initially transfected cells had a higher probability for re-transfection when compared with those cells that were not transfected in the first round. One can speculate that this is the result of a functional heterogeneity in the cell population, rendering a subtraction of cells more resistant to nucleic acid uptake. This finding is of particular interest for studies where frequent transfection of cells is required or cannot be avoided. One example would be the repeated transfection of mRNAs coding transcription factors used for reprogramming of human fibroblasts and other differentiated cells to pluripotent stem cells [42, 43]. In another study, Michel et al. have investigated repeated co-transfection of EGFP and B18R mRNA in fibroblasts. They found that the presence of B18R significantly increased protein expression and in contrast reduced interferon expression over repeated transfection of cells [44]. Differential expression kinetics mediated by successive transfection could also be used to gain mechanistic biological insights. In this respect, Fan et al. elucidated the pharmacology of receptors and suggested that the interaction between the two parts of a receptor occurred constitutively if co-transfected, but not when expression was temporally separated, so they concluded that the mechanism of hetero-oligomers formation was likely co-translational [45].

Aside from some limitations, parallel co-delivery and successive delivery provide most flexibility for delivery of two nucleic acid entities with distinct properties. For instance, when dealing with complex gene networks, overexpression of one or even several genes needs to be concurrent with knock-down of other genes. Mimicking such conditions, by comparison of different co-transfection methods for co-delivery of siRNA along with IVT-mRNA, suggested that integrated co-transfection resulted in the highest rates of mCherry overexpression and EGFP knock-down, despite the low mCherry intensity at day 3. In parallel co-transfection, however, the knock-down efficiency

was rather low, which proved that there is not necessarily a formulation for a carrier which is optimal for different types of cargos. In this particular case, when transfected with Lipo2000, siRNA was more efficiently delivered for EGFP knock-down. This finding is consistent with a study by Miller et al., in which they reported that co-delivery of single-guide RNA (sgRNA) with 100 nucleotides and Cas9 mRNA with 4500 nucleotides was most effective both for in vitro and in vivo CRISPR/Cas gene editing, when separate zwitterionic amino lipids with distinct features were administrated. Moreover, by evaluation of successive delivery of sgRNA and siRNA, they have suggested kinetically different maximum effect for two entities due to their various functional mechanisms, supporting the need for sequential delivery [14]. In another recent study, reprogramming of primary human fibroblasts to iPSCs was efficiently performed by successive transfection of miRNA and mRNA [17].

In summary, the quantitative measurements of the co-transfection rates on the single-cell level in our study revealed the extent to which outcomes depend on the delivery scheme and strategy followed. The results emphasize the notion that efficient co-delivery protocols have to be designed on a one-by-one case. Our findings can serve as a guideline for future researches for selecting the appropriate co-delivery method matched to key experimental requirements according to the specific biological questions to be addressed. Moreover, the quantitative evaluation of complex patterns of cell transfection resulting from the different approaches can support studies directed towards predictive modeling of the transfection process, including the identification of chemical and physical carrier criteria to be implemented for the most efficient cargo loading to ensure co-delivery of nucleic acids.

Compliance with ethical standards

Competing interests The authors declare that they have no competing interests.

Declarations Peripheral blood mononuclear cells (PBMC) isolated from buffy coats; Deutsche Rote Kreuz, Berlin; ethics vote EA2/018/16; Charité University Medicine Berlin.

References

1. Goncalves C, Akhter S, Pichon C, Midoux P (2016) Intracellular availability of pDNA and mRNA after transfection: a comparative study among polyplexes, lipoplexes, and lipopolyplexes. Mol Pharm 13(9):3153–3163
2. Schwake G, Youssef S, Kuhr J-T, Gude S, David MP, Mendoza E, Frey E, Rädler JO (2010) Predictive modeling of non-viral gene transfer. Biotechnol Bioeng 105(4):805–813
3. Wong ASL, Choi GCG, Cheng AA, Purcell O, Lu TK (2015) Massively parallel high-order combinatorial genetics in human cells. Nat Biotechnol 33(9):952–961
4. Umrath F, Steinle H, Weber M, Wendel HP, Reinert S, Alexander D, Avci-Adali M (2019) Generation of iPSCs from jaw periosteal cells using self-replicating RNA. Int J Mol Sci 20(7). https://doi.org/10.3390/ijms20071648
5. Bhise NS, Shmueli RB, Gonzalez J, Green JJ (2012) A novel assay for quantifying the number of plasmids encapsulated by polymer nanoparticles. Small 8(3):367–373
6. Ghodasara A, Voigt CA (2017) Balancing gene expression without library construction via a reusable sRNA pool. Nucleic Acids Res 45(13):8116–8127
7. Pascolo S (2015) The messenger's great message for vaccination. Exp Rev Vaccines 14(2):153–156
8. Baba M, Itaka K, Kondo K, Yamasoba T, Kataoka K (2015) Treatment of neurological disorders by introducing mRNA in vivo using polyplex nanomicelles. J Control Release : Off J Control Rel Soc 201:41–48
9. Deering RP, Kommareddy S, Ulmer JB, Brito LA, Geall AJ (2014) Nucleic acid vaccines: prospects for non-viral delivery of mRNA vaccines. Exp Opin Drug Deliv 11(6):885–899
10. Zhao M, Li M, Zhang Z, Gong T, Sun X (2016) Induction of HIV-1 gag specific immune responses by cationic micelles mediated delivery of gag mRNA. Drug Deliv 23(7):2596–2607
11. Akulich KA, Andreev DE, Terenin IM, Smirnova VV, Anisimova AS, Makeeva DS, Arkhipova VI, Stolboushkina EA, Garber MB, Prokofjeva MM, Spirin PV, Prassolov VS, Shatsky IN, Dmitriev SE (2016) Four translation initiation pathways employed by the leaderless mRNA in eukaryotes. Sci Rep 6:37905
12. Uchida S, Kataoka K (2019) Design concepts of polyplex micelles for in vivo therapeutic delivery of plasmid DNA and messenger RNA. J Biomed Mater Res A 107(5):978–990

13. Li B, Zhang X, Dong Y (2019) Nanoscale platforms for messenger RNA delivery. Wiley Interdisc Rev Nanomed Nanobiotechnol 11(2):e1530

14. Miller JB, Zhang S, Kos P, Xiong H, Zhou K, Perelman SS, Zhu H, Siegwart DJ (2017) Non-viral CRISPR/Cas gene editing in vitro and in vivo enabled by synthetic nanoparticle co-delivery of Cas9 mRNA and sgRNA. Angew Chem Int Ed Eng 56(4):1059–1063

15. Toro Cabrera G, Mueller C (2016) Design of shRNA and miRNA for delivery to the CNS. Methods Mol Biol (Clifton, NJ) 1382:67–80

16. Shen Y, Qiao H, Fan Q, Zhang S, Tang T (2015) Potentiated osteoinductivity via cotransfection with BMP-2 and VEGF genes in microencapsulated C2C12 Cells. Biomed Res Int 2015:435253–435210

17. Kogut I, McCarthy SM, Pavlova M, Astling DP, Chen X, Jakimenko A, Jones KL, Getahun A, Cambier JC, Pasmooij AMG, Jonkman MF, Roop DR, Bilousova G (2018) High-efficiency RNA-based reprogramming of human primary fibroblasts. Nat Commun 9(1):745

18. Chowdhury N, Vhora I, Patel K, Doddapaneni R, Mondal A, Singh M (2017) Liposomes co-loaded with 6-phosphofructo-2-kinase/fructose-2, 6-biphosphatase 3 (PFKFB3) shRNA plasmid and docetaxel for the treatment of non-small cell lung cancer. Pharm Res 34(11):2371–2384

19. Ye C, Pan B, Xu H, Zhao Z, Shen J, Lu J, Yu R, Liu H (2019) Co-delivery of GOLPH3 siRNA and gefitinib by cationic lipid-PLGA nanoparticles improves EGFR-targeted therapy for glioma. J Mol Med 97(11):1575–1588

20. Kwissa M, Lindblad EB, Schirmbeck R, Reimann J (2003) Codelivery of a DNA vaccine and a protein vaccine with aluminum phosphate stimulates a potent and multivalent immune response. J Mol Med 81(8):502–510

21. Rybakova Y, Kowalski PS, Huang Y, Gonzalez JT, Heartlein MW, DeRosa F, Delcassian D, Anderson DG (2019) mRNA delivery for therapeutic anti-HER2 antibody expression in vivo. Mol Ther: J Am Soc Gene Ther 27(8):1415–1423

22. Dong Y, Dorkin JR, Wang W, Chang PH, Webber MJ, Tang BC, Yang J, Abutbul-Ionita I, Danino D, DeRosa F, Heartlein M, Langer R, Anderson DG (2016) Poly(glycoamidoamine) brushes formulated nanomaterials for systemic siRNA and mRNA delivery in vivo. Nano Lett 16(2):842–848

23. Oberli MA, Reichmuth AM, Dorkin JR, Mitchell MJ, Fenton OS, Jaklenec A, Anderson DG, Langer R, Blankschtein D (2017) Lipid nanoparticle assisted mRNA delivery for potent cancer immunotherapy. Nano Lett 17(3):1326–1335

24. Moradian H, Roch T, Lendlein A, Gossen M (2020) mRNA transfection-induced activation of primary human monocytes and macrophages: dependence on carrier system and nucleotide modification. Sci Rep 10(1):4181–4181

25. Williams DJ, Puhl HL, Ikeda SR (2010) A simple, highly efficient method for heterologous expression in mammalian primary neurons using cationic lipid-mediated mRNA transfection. Front Neurosci 4:181

26. Grudzien-Nogalska E, Stepinski J, Jemielity J, Zuberek J, Stolarski R, Rhoads RE, Darzynkiewicz E (2007) Synthesis of anti-reverse cap analogs (ARCAs) and their applications in mRNA translation and stability. Methods Enzymol 431:203–227

27. Wang W, Balk M, Deng Z, Wischke C, Gossen M, Behl M, Ma N, Lendlein A (2016) Engineering biodegradable micelles of polyethylenimine-based amphiphilic block copolymers for efficient DNA and siRNA delivery. J Control Release : Off J Control Rel Soc 242:71–79

28. Xie ZL, Shao SL, Lv JW, Wang CH, Yuan CZ, Zhang WW, Xu XJ (2011) Co-transfection and tandem transfection of HEK293A cells for overexpression and RNAi experiments. Cell Biol Int 35(3):187–192

29. ur Rehman Z, Hoekstra D, Zuhorn IS (2013) Mechanism of polyplex- and lipoplex-mediated delivery of nucleic acids: real-time visualization of transient membrane destabilization without endosomal lysis. ACS Nano 7(5):3767–3777

30. Gam JJ, DiAndreth B, Jones RD, Huh J, Weiss R (2019) A 'polytransfection' method for rapid, one-pot characterization and optimization of genetic systems. Nucleic Acids Res 47(18):e106–e106

31. Leonhardt C, Schwake G, Stögbauer TR, Rappl S, Kuhr JT, Ligon TS, Rädler JO (2014) Single-cell mRNA transfection studies: delivery, kinetics and statistics by numbers. Nanomedicine 10(4):679–688

32. Ligon TS, Leonhardt C, Rädler JO (2014) Multi-level kinetic model of mRNA delivery via transfection of lipoplexes. PLoS One 9(9): e107148

33. Fröhlich F, Reiser A, Fink L, Woschée D, Ligon T, Theis FJ, Rädler JO, Hasenauer J (2019) Multi-experiment nonlinear mixed effect modeling of single-cell translation kinetics after transfection. NPJ Syst Biol Appl 5:1

34. Reiser A, Woschée D, Mehrotra N, Krzysztoń R, Strey HH, Rädler JO (2019) Correlation of mRNA delivery timing and protein expression in lipid-based transfection. Integr Biol: Quant Biosci Nano Macro 11(9):362–371

35. Kowalski PS, Rudra A, Miao L, Anderson DG (2019) Delivering the messenger: advances in technologies for therapeutic mRNA delivery. Mol Ther: J Am Soc Gene Ther 27(4):710–728

36. Ulkoski D, Bak A, Wilson JT, Krishnamurthy VR (2019) Recent advances in polymeric materials for the delivery of RNA therapeutics. Exp Opin Drug Deliv 16(11):1149–1167

37. Wadhwa A, Aljabbari A, Lokras A, Foged C, Thakur A (2020) Opportunities and challenges in the delivery of mRNA-based vaccines. Pharmaceutics 12(2). https://doi.org/10.3390/pharmaceutics12020102

38. Davidsohn N, Beal J, Kiani S, Adler A, Yaman F, Li Y, Xie Z, Weiss R (2015) Accurate predictions of genetic circuit behavior from part characterization and modular composition. ACS Synth Biol 4(6):673–681

39. Guye P, Li Y, Wroblewska L, Duportet X, Weiss R (2013) Rapid, modular and reliable construction of complex mammalian gene circuits. Nucleic Acids Res 41(16):e156–e156

40. Li Y, Jiang Y, Chen H, Liao W, Li Z, Weiss R, Xie Z (2015) Modular construction of mammalian gene circuits using TALE transcriptional repressors. Nat Chem Biol 11(3):207–213

41. Simental-Mendia M, Lara-Arias J, Alvarez-Lozano E, Said-Fernandez S, Soto-Dominguez A, Padilla-Rivas GR, Martinez-Rodriguez HG (2015) Cotransfected human chondrocytes: over-expression of IGF-I and SOX9 enhances the synthesis of cartilage matrix components collagen-II and glycosaminoglycans. Braz J Med Biol Res 48(12):1063–1070

42. Yakubov E, Rechavi G, Rozenblatt S, Givol D (2010) Reprogramming of human fibroblasts to pluripotent stem cells using mRNA of four transcription factors. Biochem Biophys Res Commun 394(1):189–193

43. Warren L, Manos PD, Ahfeldt T, Loh Y-H, Li H, Lau F, Ebina W, Mandal PK, Smith ZD, Meissner A, Daley GQ, Brack AS, Collins JJ, Cowan C, Schlaeger TM, Rossi DJ (2010) Highly efficient reprogramming to pluripotency and directed differentiation of human cells with synthetic modified mRNA. Cell Stem Cell 7(5):618–630

44. Michel T, Golombek S, Steinle H, Hann L, Velic A, Macek B, Krajewski S, Schlensak C, Wendel HP, Avci-Adali M (2019) Efficient reduction of synthetic mRNA induced immune activation by simultaneous delivery of B18R encoding mRNA. J Biol Eng 13:40

45. Fan T, Varghese G, Nguyen T, Tse R, O'Dowd BF, George SR (2005) A role for the distal carboxyl tails in generating the novel pharmacology and G protein activation profile of mu and delta opioid receptor hetero-oligomers. J Biol Chem 280(46):38478–38488

Springer

Strategies for Simultaneous and Successive Delivery of RNA

Hanieh Moradian[1, 2, 3], Andreas Lendlein[1, 2, 3], Manfred Gossen[1, 2, *]

1   Institute of Biomaterial Science, Helmholtz-Zentrum Geesthacht, 14513 Teltow, Germany
2   Berlin-Brandenburg Center for Regenerative Therapies (BCRT), 13353 Berlin, Germany
3   Institute of Biochemistry and Biology, University of Potsdam, Potsdam, Germany

* Corresponding Author, email address: manfred.gossen@hzg.de

A) Supplementary Materials and Methods

Evaluation of Encapsulation Efficiency

mRNA/carrier complexes were prepared as described in "Materials and Methods; Co-delivery of mRNA to HeLa cells via a lipid- or a polymeric-based carrier", using EGFP mRNA. The protocol for quantification of encapsulation efficiency is adapted from [1]. Different ratios of transfection reagent/mRNA (v/w) were tested, keeping mRNA concentration constant. Upon formation of complexes, samples were diluted in 1x TE assay buffer (10 mM Tris-HCl, 1 mM EDTA, pH 7.5) to reach an equal amount of mRNA for all samples in 100 µL of buffer. Subsequently, 100 µL of 200-fold diluted Quant-iT RiboGreen RNA reagent (ThermoFisher Scientific, Germany) was added to all samples. In parallel, equal volume of the same samples were dissociated by incubation with 5 µL of either 10% Triton X-100 for LipoMM complexes, or heparin solution (5mg·mL^{-1} in TE buffer) for ViroR complexes. Samples were incubated for 20 min at 37 °C in the dark. TE buffer only was used as blank. Fluorescence was measured using a Tecan Infinite 200 PRO plate reader with an excitation wavelength of 485 nm and emission wavelength of 535 nm. The percent of encapsulation efficiency was determined using the following formula:

$$\{ (\ [E(Diss.S) - E(B)] - [E(S) - E(B)]\ ) / [E(Diss.S) - E(B)] \} \times 100$$

E(Diss.S) refers to emission of dissociated samples, i.e. total mRNA, E(S) describes emission of main samples, i.e. free mRNA in solution, and E(B) represents emission of blank at 535 nm. All samples were prepared as individually prepared triplicates.

Measurement of Physicochemical Properties of mRNA/carrier Complexes

The mRNA/carrier complexes, i.e. lipoplexes for LipoMM as well as polyplexes for ViroR, were evaluated in terms of size and zeta potential as two key physicochemical features. In order to elucidate the impact of mRNA type on final particles features, complexes were prepared with distinct types of mRNA, i.e. mRNA coding EGFP as well as mRNA coding mCherry. The size, polydispersity index (PDI) and zeta potential of complexes was determined by dynamic light scattering (DLS) via a ZetasizerNano from SZ instruments (Malvern Instruments, Herrenberg, Germany). Samples were diluted in 10 mM HEPES buffer with 1:4 and 1:10 dilution factor for LipoMM, and ViroR, respectively. The measurements were performed at 25 °C in disposable cuvettes.
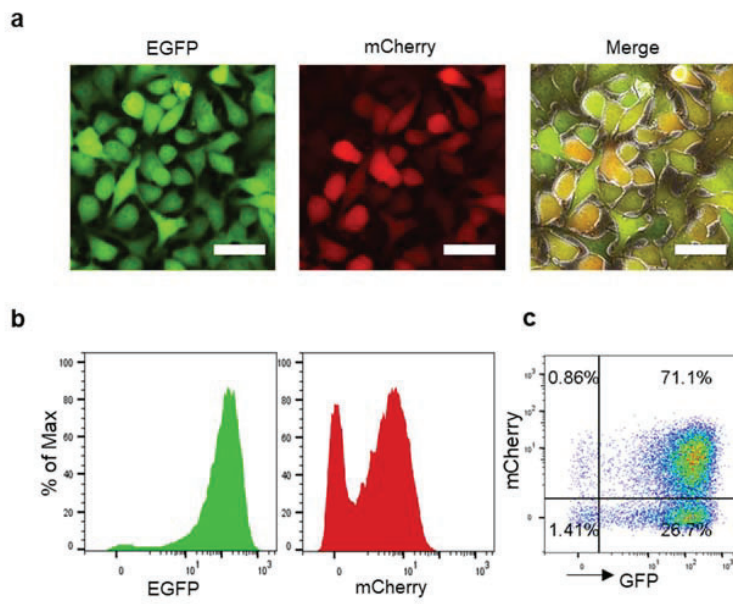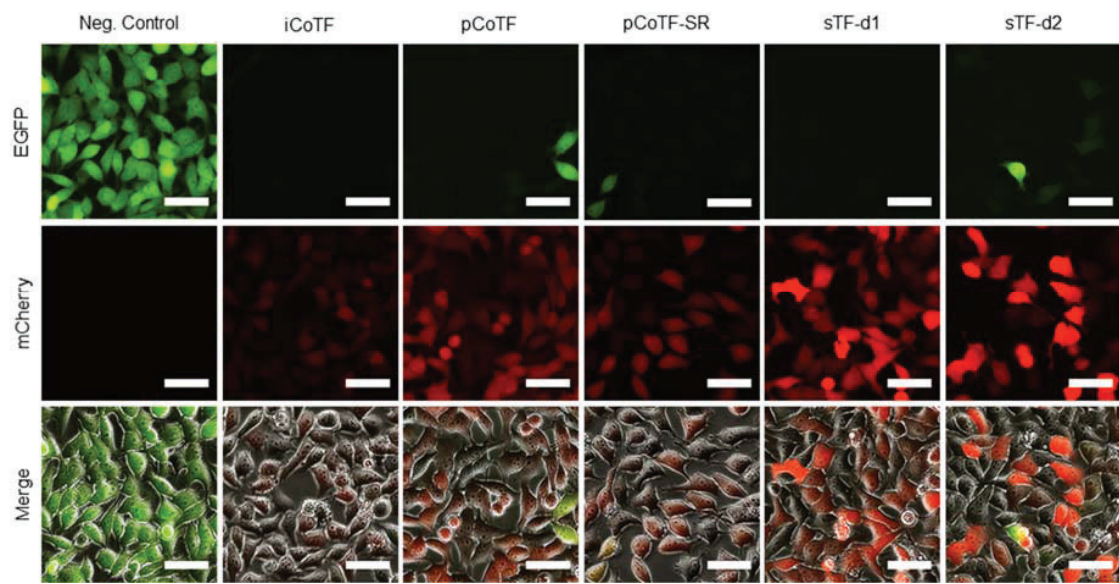
B) Supplementary Data
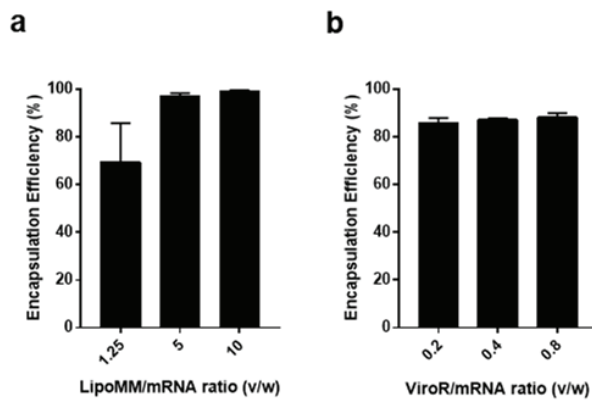
Supplementary Fig. 1 Encapsulation efficiency for carrier systems used for mRNA delivery **a** Lipofectamine messenger max (LipoMM) and **b** Viromer Red (ViroR). Three carrier/mRNA ratios were tested for both LipoMM and ViroR ($\mu l \cdot \mu g^{-1}$). The middle ratio transfection reagent/mRNA is that used throughout the transfection experiments. Values are presented as mean ± SD, n=3. Error bars indicate SD.

MTS Viability Assay
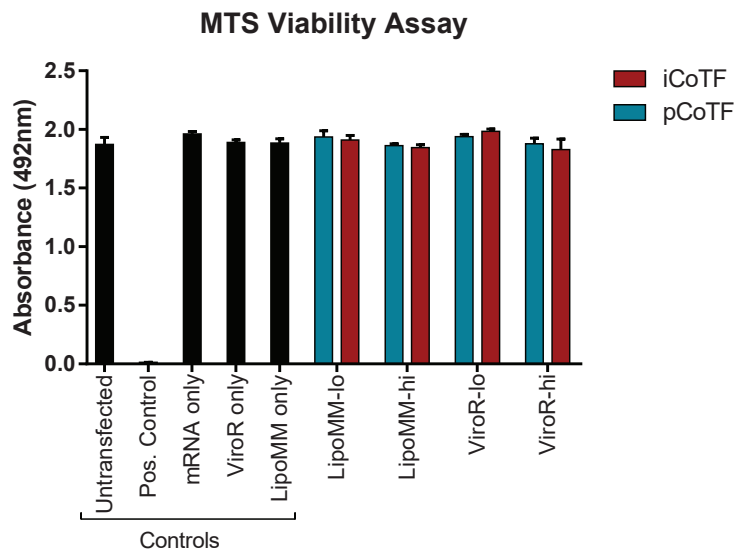
Supplementary Fig. 2 Viability assay measured with MTS assay, no significant differences were observed between the two co-delivery methods, i.e. iCoTF and pCoTF, neither for low nor for high mRNA doses (p>0.05). Values are presented as mean ± SD, n≥3. Error bars indicate SD. (iCoTF: integrated co-transfection, pCoTF: parallel co-transfection)

Supplementary Fig. 3 Successive transfection of IVT-mRNAs; cells were transfected with EGFP at first step and with mCherry mRNA at day 1 and were analyzed at day 2 **a-c**. Fluorescent images depicted as single channels and merged with phase contrast (bar =50 µm) **a**, flow cytometric analysis of cells; histograms of EGFP and mCherry **b** and density plot **c**.

Supplementary Fig. 4 Co-delivery versus successive of siRNA and IVT-mRNA in d2EGFP Hela cells; various methods evaluated by fluorescent microscopy imaging (bar =50 µm).

Supplementary Table 1. Particle size and zeta potential of the two carrier systems complexed with either EGFP or mCherry mRNA. Multiple comparison tests have shown no significant statistical difference between size and zeta values for complexes prepared with different mRNA types for each carrier type, i.e. p-values were greater than 0.05 for all cases.

Sample Name	Particle size		Zeta potential
	d (nm) ± SD	PDI ± SD	(mV) ± SD
LipoMM/ EGFP	515,90 ± 64,06	0,70 ± 0,14	-0,24 ± 0,27
LipoMM/ mCherry	497,94 ± 28,41	0,53 ± 0,10	-0,02 ± 0,09
ViroR/ EGFP	517,79 ± 40,97	0,11 ± 0,07	-0,09 ± 0,16
ViroR/ mCherry	511,93 ± 58,75	0,16 ± 0,07	-0,08 ± 0,51

References

1. Li B, Dong Y (2017) Preparation and Optimization of Lipid-Like Nanoparticles for mRNA Delivery. Methods in Molecular Biology (Clifton, NJ) 1632:207-217. doi:10.1007/978-1-4939-7138-1_13

8

Appendix V: List of publications and conference contributions

Publications

1. **H. Moradian,** T. Roch, A. Lendlein and M. Gossen: Chemical modification of uridine modulates mRNA-mediated proinflammatory and antiviral response in primary human macrophages. Molecular Therapy - Nucleic Acids 27, 854–869 (2022).
2. **H. Moradian**, M. Gossen and A. Lendlein: Co-delivery of genes can be confounded by bicistronic vector design. MRS Communications (2022).
3. **H. Moradian**, A. Lendlein and M. Gossen: Strategies for simultaneous and successive delivery of RNA. *Journal of Molecular Medicine* 98, 1767 (2020).
4. **H. Moradian**, T. Roch, A. Lendlein and M. Gossen: mRNA Transfection-Induced Activation of Primary Human Monocytes and Macrophages: Dependence on Carrier System and Nucleotide Modification. *Scientific reports* 10 (2020).
5. **H. Moradian**, H. Keshvari, H. Fasehee, R. Dinarvand and S. Faghihi: Combining NT3-overexpressing MSCs and PLGA microcarriers for brain tissue engineering: A potential tool for treatment of Parkinson's disease. *Materials science & engineering. C, Materials for biological applications* 76, 934 (2017).
6. **H. Moradian**, H. Fasehee, H. Keshvari and S. Faghihi: Poly(ethyleneimine) functionalized carbon nanotubes as efficient nano-vector for transfecting mesenchymal stem cells. *Colloids and surfaces. B, Biointerfaces* 122, 115 (2014).

Conference contributions

1. Oral presentation: **Hanieh Moradian**, Andreas Lendlein, Manfred Gossen: Nucleic Acid Co-Delivery: How to modulate protein co-expression by formulation of payload. *MRS Virtual Meeting – Beyond Nano-Challenges and Opportunities in Drug Delivery*, USA, 17-23 April 2021. (Best oral presentation award)
2. Oral presentation: **Hanieh Moradian**, Andreas Lendlein, Manfred Gossen: Effect of Nucleotide Chemistry on Expression of In Vitro Transcribed mRNA. *MRS Virtual Meeting – Beyond Nano-Challenges and Opportunities in Drug Delivery*, USA, 17-23 April 2021.
3. Poster presentation: **Hanieh Moradian**, Andreas Lendlein, Manfred Gossen : Co-transfection Strategies for In Vitro Transcribed mRNA. *Polydays*, Berlin, Germany, 11 – 13 September 2019.
4. Poster presentation: **Hanieh Moradian**, Andreas Lendlein, Manfred Gossen : Co-transfection Strategies for *In Vitro* Transcribed mRNA. *Advanced functional polymers for medicine (AFPM)*, Aalto University, Finland, 5-7 July 2019.